VOLUME 84 NO. ST6
OCTOBER 1958

JOURNAL of the

Structural Division

PROCEEDINGS OF THE

AMERICAN SOCIETY OF CIVIL ENGINEERS

BASIC REQUIREMENTS FOR MANUSCRIPTS

This Journal represents an effort by the Society to deliver information to the reader with the greatest possible speed. To this end the material herein has none of the usual editing required in more formal publications.

Original papers and discussions of current papers should be submitted to the Manager of Technical Publications, ASCE. Authors should indicate the technical division to which the paper should be referred. The final date on which a discussion should reach the Society is given as a footnote with each paper. Those who are planning to submit material will expedite the review and publication procedures by complying with the following basic requirements:

1. Titles should have a length not exceeding 50 characters and spaces.

2. A 50-word summary should accompany the paper.

3. The manuscript (a ribbon copy and two copies) should be double-spaced on one side of 8½-in. by 11-in. paper. Papers that were originally prepared for oral presentation must be rewritten into the third person before being submitted.

4. The author's full name, Society membership grade, and footnote reference stating present employment should appear on the first page of the paper.

5. Mathematics are reproduced directly from the copy that is submitted. Because of this, it is necessary that capital letters be drawn, in black ink, ⅛-in. high (with all other symbols and characters in the proportions dictated by standard drafting practice) and that no line of mathematics be longer than 6½-in. Ribbon copies of typed equations may be used but they will be proportionately smaller on the printed version.

6. Tables should be typed (ribbon copies) on one side of 8½-in. by 11-in. paper with a 6½-in. by 10½-in. invisible frame. Small tables should be grouped within this frame. Specific reference and explanation should be made in the text for each table.

7. Illustrations should be drawn in black ink on one side of 8½-in. by 11-in. paper within an invisible frame that measures 6½-in. by 10½-in.; the caption should also be included within the frame. Because illustrations will be reduced to 69% of the original size, the capital letters should be ⅛-in. high. Photographs should be submitted as glossy prints in a size that is less than 6½-in. by 10½-in. Explanations and descriptions should be made within the text for each illustration.

8. Papers should average about 12,000 words in length and should be no longer than 18,000 words. As an approximation, each full page of typed text, table, or illustration is the equivalent of 300 words.

Further information concerning the preparation of technical papers is contained in the "Technical Publications Handbook" which can be obtained from the Society.

Reprints from this Journal may be made on condition that the full title of the paper, name of author, page reference (or paper number), and date of publication by the Society are given. The Society is not responsible for any statement made or opinion expressed in its publications.

This Journal is published monthly by the American Society of Civil Engineers. Publication office is at 2500 South State Street, Ann Arbor, Michigan. Editorial and General Offices are at 33 West 39 Street, New York 18, New York. $4.00 of a member's dues are applied as a subscription to this Journal. Second-class postage paid at Ann Arbor, Michigan.

Journal of the
STRUCTURAL DIVISION
Proceedings of the American Society of Civil Engineers

STRUCTURAL DIVISION
EXECUTIVE COMMITTEE
Leo H. Corning, Chairman; George S. Vincent, Vice-Chairman;
Robert D. Dewell; Elmer K. Timby; Myle J. Holley, Jr., Secretary

COMMITTEE ON PUBLICATIONS
Nathan W. Morgan, Chairman; Mace H. Bell; Gerald F. Borrmann;
Edwin S. Elcock; Kurt H. Gerstle; Wayne C. Lewis; Alfred L. Parme;
Henry G. Schlitt; Philip A. Upp

CONTENTS

October, 1958

Papers

Number

Digital Computation for Stiffness Matrix Analysis
by J. S. Archer 1814

Numerical Solution for Interconnected Bridge Girders
by Henry Malter 1815

Generalization of the Successive Approximations Method
by Panagiotis D. Moliotis 1816

Golden Gate Bridge Vibration Studies
by George S. Vincent 1817

Concrete Beams and Columns with Bundled Reinforcement
by N. W. Hanson and Hans Reiffenstuhl 1818

Matric Formulation of Slope-Deflection Equations
by Chu-Kia Wang 1819

Equivalent Systems for the Deflection of Variable Stiffness Members
by D. G. Fertis and E. C. Zobel 1820

Amplification of Stress and Displacement in Guyed Towers
by Robert S. Rowe 1821

Discussion 1827

Copyright 1958 by the American Society of Civil Engineers.

Paper 1814 October, 1958 ST 6

Journal of the
STRUCTURAL DIVISION
Proceedings of the American Society of Civil Engineers

DIGITAL COMPUTATION FOR STIFFNESS MATRIX ANALYSIS

J. S. Archer[1] J.M. ASCE
(Proc. Paper 1814)

ABSTRACT

A matrix method is described for the static stress and normal mode analysis of highly indeterminate structures on large scale digital computers. The application of the technique to the analysis of basic types of Civil Engineering structures is discussed. A simple building frame problem is solved for stresses and deflections.

SUMMARY

The stiffness matrix method of structural analysis has been coded for use on high speed digital computers by several investigators. This technique has proved to be very successful for the analysis of highly indeterminate aircraft structures. It is here proposed that the same technique be used for the analysis of Civil Engineering structures on high speed digital computers. This may be accomplished through the development of similar digital computer programs or through the midification of digital computer programs now available.

INTRODUCTION

Scope

This paper contains an energy development of the basic theory for the Stiffness Matrix Method of structural analysis. It is shown that the method is particularly adaptable to a systematic analysis of any structure which may be described as a composition of simple structural elements, such as beams and plates.

Note: Discussion open until March 1, 1959. To extend the closing date one month, a written request must be filed with the Executive Secretary, ASCE. Paper 1814 is part of the copyrighted Journal of the Structural Engineering Division, Proceedings of the American Society of Civil Engineers, Vol. 84, No. ST 6, October, 1958.

1. Project Structures Engr., Convair, General Dynamics Corp., Fort Worth, Tex.

The present application of the technique to the analysis of aircraft structures at Convair, Fort Worth, Texas and at Convair, San Diego, California is described. The application of the technique to the analysis of Civil Engineering structures is also discussed. An example is given for a Civil Engineering structure to illustrate how the procedure works in a typical case. Finally some suggestions are given for a practical method of developing a similar procedure for individual needs.

History

The stiffness matrix type of structural analysis was discussed in 1944 in a paper by G. Kron,(1) Consulting Engineer, General Electric Company, Schenectady, N. Y. No practical application of the technique using digital computers was reported until December 1951 by H. U. Schuerch,(2) formerly associated with Convair, San Diego, California. S. Levy, now associated with the General Electric Company, carried out an investigation,(3) of the stiffness matrix procedure which was published in July 1953. G. Best and M. P. Keating, of Convair, Fort Worth, Texas, described the technique based upon their experience with the IBM 701 in a report,(4) dated September 1953. D. Williams, of the Royal Aircraft Establishment, England, prepared a very comprehensive paper,(5) on the subject which was published in June 1954. The technique of using matrix algebra for the analysis of aircraft structures has been taught at MIT by Prof. R. L. Bisplinghoff for several years. His text was first published in 1955.(6)

The author first made use of the stiffness matrix technique at MIT in the analysis of a load frame for dynamic tests on reinforced concrete and brick walls. The analysis was coded and solved on the WHIRLWIND Computer in 1954 and 1955. After coming to Convair, Fort Worth, Texas, in 1955 the author worked with G. Best to improve the IBM 701 analysis. The analysis has since been recoded for use on the IBM 704.

Theory

Let U represent the strain energy stored within a structure which is loaded by the forces p_1, p_2, ----, p_i, ----, p_η. The temperature of the material remains constant and the supports are rigid. Applying Castigliano's Theorem of Structure Equilibrium (Theorem I) one obtains;

$$p_i = \partial U / \partial \delta_i \tag{1}$$

where δ_i is the deflection of the point of application of the load p_i in the direction of p_i.

If the strain energy is evaluated in terms of the loads p_i acting upon the structure we may expand Equation (1) as follows:

$$p_i = \partial U / \partial \delta_i = \sum_j (\partial U / \partial p_j)(\partial p_j / \partial \delta_i) \tag{2}$$

If one assumes that the structure is elastic then Castigliano's Theorem for Linear Structures (Theorem II) may be applied.

$$\delta_j = \partial U / \partial p_j \tag{3}$$

Substituting Equation (3) into Equation (2),

$$p_i = \sum_j \delta_j \left(\partial p_j / \partial \delta_i \right) \tag{4}$$

The partial derivative $\partial p_j / \partial \delta_i$ represents the force developed at point j due to a unit deflection of point i, all other points remaining fixed. This force is represented by the symbol s_{ji}. The subscript j represents the point at which the force acts and the subscript i the point at which the unit deflection is imposed. With this substitution Equation (4) becomes:

$$p_i = \sum_j \delta_j s_{ji} \tag{5}$$

From Betti's Law or the generalized Maxwells' Law of Reciprocal Deflections we obtain the relation

$$s_{ji} = s_{ij} \tag{6}$$

and hence

$$p_i = \sum_j \delta_j s_{ij} \tag{7}$$

Writing Equation (7) in its expanded form

$$p_i = s_{i1} \delta_1 + s_{i2} \delta_2 + \cdots + s_{ij} \delta_j + \cdots + s_{in} \delta_n \tag{8}$$

It is evident from the expanded form that Equation (7) is a superposition equation expressing the total load at point i as the sum of the loads developed by each deflection component δ_j acting by itself. Each portion of Equation (7) describes an independent component of the structural behavior. The components may represent translation or rotation. The total number of components is the number of degrees of freedom which the idealized structure possesses.

Using matrix algebra notation, Equation (7) may be rewritten as

$$p = S \delta \tag{9}$$

where p is a vector or column matrix made up of the load components $p_1, p_2, \ldots, p_i, \ldots, p_n$. δ is a vector made up of the deflection components $\delta_1, \delta_2, \ldots, \delta_i, \ldots, \delta_n$. S is a square matrix consisting of an ordered array of the stiffness influence coefficients s_{ij} of Equation (7). Matrix S is called

the stiffness matrix of the structure. In the expanded form Equation (9) appears as follows:

$$\begin{Bmatrix} p_1 \\ p_2 \\ p_i \\ p_n \end{Bmatrix} = \begin{bmatrix} s_{11} & s_{12} & \cdots & s_{1j} & \cdots & s_{1n} \\ s_{21} & s_{22} & & s_{2j} & & s_{2n} \\ s_{i1} & s_{i2} & & s_{ij} & & s_{in} \\ s_{n1} & s_{n2} & \cdots & s_{nj} & \cdots & s_{nn} \end{bmatrix} \begin{Bmatrix} \delta_1 \\ \delta_2 \\ \delta_j \\ \delta_n \end{Bmatrix} \tag{10}$$

Equation (9) may be manipulated similar to an ordinary algebraic equation. For instance it may be solved for the deflections by premultiplying both sides of the equation by the inverse of the stiffness matrix S.

$$\delta = S^{-1} p = F p \tag{11}$$

The inverse of the stiffness matrix is represented by the symbol F and is called the flexibility influence coefficient matrix. It is composed of an ordered array of the flexibility influence coefficients f_{ij}. In the expanded form it appears as follows:

$$\begin{Bmatrix} \delta_1 \\ \delta_2 \\ \vdots \\ \delta_i \\ \vdots \\ \delta_n \end{Bmatrix} = \begin{bmatrix} f_{11} & f_{12} & \cdots & f_{1j} & \cdots & f_{1n} \\ f_{21} & f_{22} & \cdots & f_{2j} & \cdots & f_{2n} \\ \vdots & \vdots & & \vdots & & \vdots \\ f_{i1} & f_{i2} & \cdots & f_{ij} & \cdots & f_{in} \\ \vdots & \vdots & & \vdots & & \vdots \\ f_{n1} & f_{n2} & \cdots & f_{nj} & \cdots & f_{nn} \end{bmatrix} \begin{Bmatrix} p_1 \\ p_2 \\ \vdots \\ p_j \\ \vdots \\ p_n \end{Bmatrix} \tag{12}$$

In the typical problem Equation (11) must be constructed and solved for the deflections in terms of the loads. The direct determination of the coefficients f_{ij} of Equation (11) is difficult and impractical for a large indeterminate structure. However, the coefficients s_{ij} of Equation (9) are readily calculated. The usual procedure is thus, to compute the stiffness matrix coefficients directly from the known properties of the individual elements of the idealized structure. The coefficients of the flexibility matrix are obtained through the mathematical operation of inverting the stiffness matrix.

After the deflections of the structure are found the stresses developed in the structure may be determined. This is accomplished by using the stiffness matrix of the individual elements of the structure. Using computed deflections and equations of the same type as Equation (9) the internal loads on individual portions of the structure are readily obtained. Having obtained the internal forces on the individual elements, the structures engineer can readily compute the stresses in the structure.

INDIVIDUAL ELEMENT STIFFNESS MATRIX

(a) Beam Segment

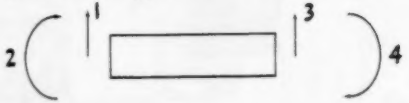

$$S \equiv \begin{bmatrix} S_{11} & S_{12} & S_{13} & S_{14} \\ S_{21} & S_{22} & S_{23} & S_{24} \\ S_{31} & S_{32} & S_{33} & S_{34} \\ S_{41} & S_{42} & S_{43} & S_{44} \end{bmatrix}$$

(b) Torque Tube

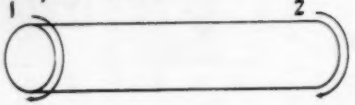

$$S \equiv \begin{bmatrix} S_{11} & S_{12} \\ S_{21} & S_{22} \end{bmatrix}$$

(c) Torque Box

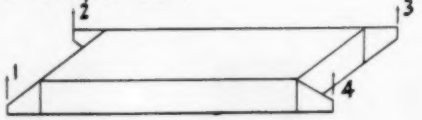

$$S \equiv \begin{bmatrix} S_{11} & S_{12} & S_{13} & S_{14} \\ S_{21} & S_{22} & S_{23} & S_{24} \\ S_{31} & S_{32} & S_{33} & S_{34} \\ S_{41} & S_{42} & S_{43} & S_{44} \end{bmatrix}$$

(d) Concentrated Spring

$$S \equiv \begin{bmatrix} S_{11} & S_{12} \\ S_{21} & S_{22} \end{bmatrix}$$

STIFFNESS MATRIX PROCEDURE

(a) Compute Stiffness Matrices For Individual Structural Elements.

(b) Assemble Stiffness Matrix for Complete Structure

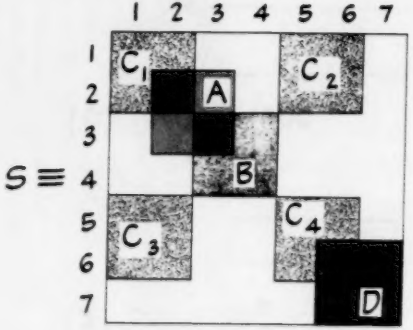

(c) Compute $F = S^{-1}$

(d) Compute $\delta = F \times p$

(e) Compute Internal Forces on Individual Elements

$$\begin{Bmatrix} p_{2A} \\ p_{3A} \end{Bmatrix} = [A] \begin{Bmatrix} \delta_2 \\ \delta_3 \end{Bmatrix}; \quad \begin{Bmatrix} p_{3B} \\ p_{4B} \end{Bmatrix} = [B] \begin{Bmatrix} \delta_3 \\ \delta_4 \end{Bmatrix};$$

$$\begin{Bmatrix} p_{1C} \\ p_{2C} \\ p_{5C} \\ p_{6C} \end{Bmatrix} = [C] \begin{Bmatrix} \delta_1 \\ \delta_2 \\ \delta_5 \\ \delta_6 \end{Bmatrix}; \quad \begin{Bmatrix} p_{6D} \\ p_{7D} \end{Bmatrix} = [D] \begin{Bmatrix} \delta_6 \\ \delta_7 \end{Bmatrix}$$

Present Applications

IBM 701

Structural analyses have been performed on the IBM 701 at Convair, Fort Worth, Texas, for structures having up to 106 independent coordinates. The structures analyzed were idealized as a group of interconnected structural elements. These elements consisted of beams, torque tubes, torque boxes, and concentrated springs (See Figure 1). The procedure followed for a typical stress analysis was as follows (See Figure 2):

a) Compute the stiffness matrices for the individual structural elements. Store on magnetic tape.
b) Assemble the stiffness matrix for the complete structure by bringing together the coefficients for all structural elements and adding corresponding coefficients. Individual coordinate identification numbers were indispensible for keeping the coefficients in order.
c) Invert the stiffness matrix to obtain the flexibility matrix for the structure.
d) Compute the deflections by determining the matrix product of the applied load vector and the flexibility matrix.
e) Compute the internal forces on the individual structural elements by computing the product of the appropriate deflections with the stiffness matrices for the individual structural elements.

The largest problems, of order 106, were found to require a total of four hours to assemble the stiffness matrix and eight hours to invert in order to obtain the flexibility matrix. Double precision arithmetic was used in this operation. Each stress calculation for a given load condition was obtained in an additional one and a half hours of computing time. Smaller problems were solved in considerably less time.

The analysis of beam elements was performed considering bending deformation only. A linear variation in moment of inertia from one end of a beam to the other was assumed.

In addition to the stress analyses, normal mode analyses were successfully performed. In such an analysis the natural frequencies and normal mode shapes were computed by an iteration technique.

IBM 704

The IBM 704 is much faster and has a larger high speed storage capacity than the IBM 701, therefore, a substantial savings in time can be realized by its use. Experience indicates that a matrix representing 100 independent coordinates can be assembled in one and inverted in three hours.

At Convair, Fort Worth, the IBM 704 program incorporated the following additions and refinements to the aforementioned IBM 701 program:

a) Shear deformation is included in the analysis of beams.
b) Effect of tapering flanges is computed.
c) Rectangular structural plates may be analyzed using a lattice analogy representation.
d) Beam moments of inertia are automatically computed if desired.
e) Length of beams and their directions are determined by the computer from basic geometric input.

Remington Rand 1103

Convair, San Diego, California, has coded the stiffness matrix structural analysis on the Remington Rand 1103. This computer is comparable to the IBM 701. The sizes of the problems worked by San Diego were in general smaller than those worked by Fort Worth. However the speed with which a given problem could be worked was greater than for the IBM 701.

Others

English aircraft literature contains many articles regarding the application of the stiffness matrix structural analysis, one of which has been cited.(5) It can reasonably be concluded, therefore, that this technique has been coded on English high speed digital computers.

Application to Civil Engineering Structures

Indeterminate Trusses

One of the most common Civil Engineering structures is the bridge truss. Such a structure could easily be analyzed by the stiffness matrix technique. However, the analysis of a determinate truss problem is quite simple and would hardly be worthwhile to analyze on a high speed digital computer. This is not always the case in the design of an indeterminate truss.

Consider the truss pictured in Figure 3. The distortion and loads on such a structure can be described by two orthogonal displacements at each joint. Hence the analysis of this structure would require a matrix of order 17, for its solution. If a secondary stress analysis is required this may be obtained simultaneously with the primary analysis. However, a rotation displacement at each joint must be represented requiring a matrix of order 27 for its solution as shown in Figure 4. The stress analysis of such a structure would give the forces in all members and the deflections of all joints of the structure. For a structure of this type the order of the matrix is generally much greater than the degree to which the structure in indeterminate.

Building Frames

Consider the simple building bent illustrated in Figure 5. The distortion of this structure is completely defined by the five coordinates illustrated: one rotation at each joint and one displacement at the roof level.

A more complicated broken story bent is illustrated in Figure 6. Even in this case, however, only twelve coordinates are necessary.

It is evident from these examples that the analysis of building frames could be accomplished to advantage using the stiffness matrix technique of analysis. If three dimensional frames are to be analyzed the torsion of the building could be included, as well as axial deformation of the columns.

The computed answer in this type of problem gives the rotation and translation of each end of the columns and beams, and the moments in the members.

Miscellaneous Structures

Consider the arch rib illustrated in Figure 7. The arch structure may be represented by a series of straight beam segments between the load points.

INDETERMINATE TRUSS ANALYSIS

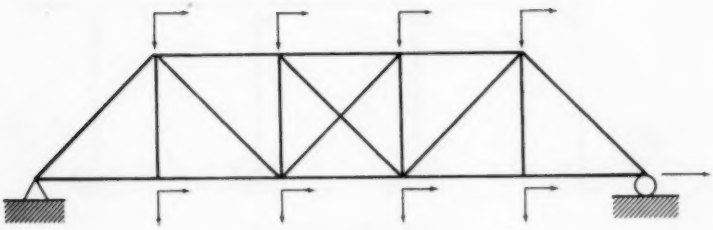

PRIMARY STRESS ANALYSIS

FIG. 3

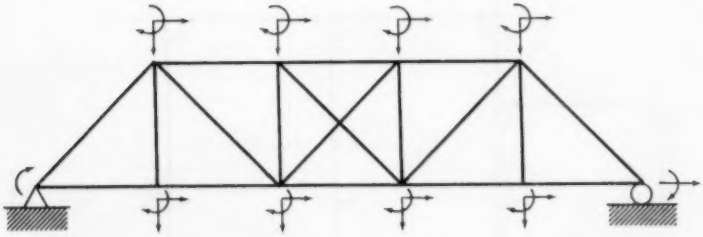

PRIMARY AND SECONDARY STRESS ANALYSIS

FIG. 4

BUILDING FRAME ANALYSIS

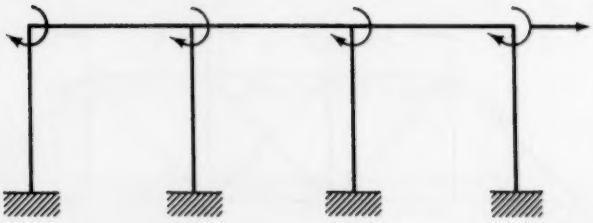

SIMPLE BUILDING FRAME

FIG. 5

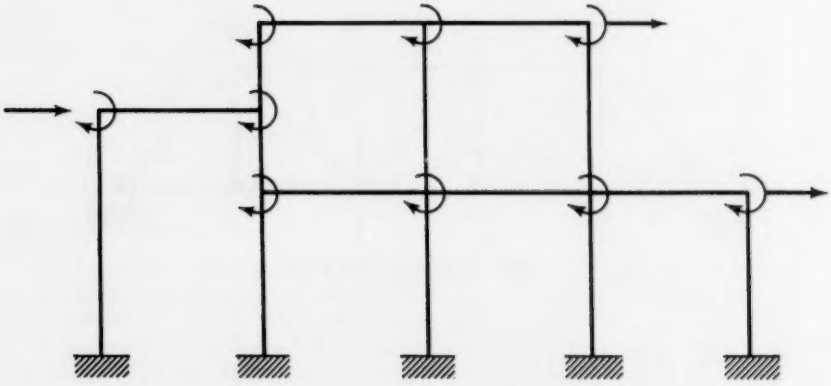

BROKEN STORY BUILDING FRAME

FIG. 6

ARCH RIB ANALYSIS

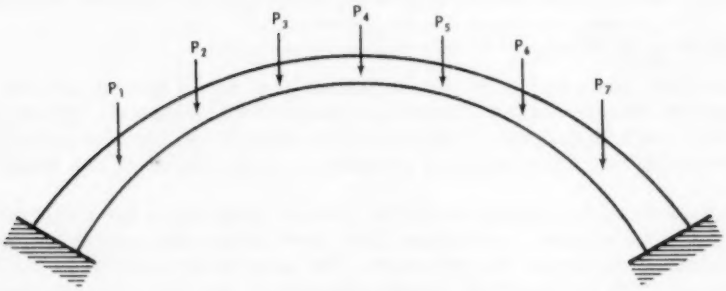

SIMPLE ARCH RIB

FIG. 7

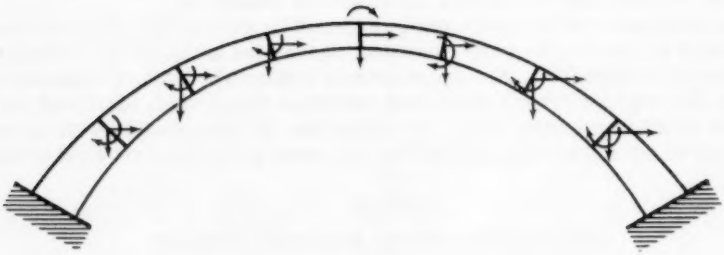

SEGMENTED ARCH RIB

FIG. 8

The distortion and loading of the structure may then be represented by the system of coordinates illustrated in Figure 8. Twenty one coordinates are required for a stiffness matrix analysis. Moments, shears, and axial thrusts may be computed at each end of each segment.

The stiffness matrix technique may be used to advantage in the analysis of arch dams, suspension bridges and towers. The analysis of shell type structures by the stiffness matrix method should be particularly advantageous. A stiffness matrix analysis on high speed computers would make it practical to analyze shells subjected to complex asymmetrical air load distributions.

Natural Mode Analysis

Most Civil Engineering structures are not analyzed to determine their response to dynamic forces. There are possibly two exceptions. First, the structure which is analyzed to determine the effect of earthquakes upon it and second, the structure which is designed to resist the effect of a bomb blast.

In either case, the calculation of the dynamic response of the structure to a transient load is easily performed if one first obtains the natural frequencies and mode shapes for the structure. The mode shape analysis is easily carried out using the flexibility matrix obtained for the deflection calculation. An iterative technique which converges on the lowest mode has given the best results.

Example

The building frame illustrated in Figure 9 has been analyzed on the IBM 704 for the load condition shown. The input geometry, stiffness, and load data was placed on 5 punched data cards. The load and deflection coordinates used for the stiffness matrix are illustrated in Figure 10.

The stiffness matrix illustrated in Figure 11a and the flexibility matrix illustrated in Figure 11b were computed, assembled and printed in about four minutes on the IBM 704. The deflections in Figure 12a and the stresses in Figure 12b obtained for the given load condition required an additional two minutes of IBM computing time. A comparison of these results with the answers given by Wilbur and Norris[7] to the same problem show good agreement.

RECOMMENDATIONS AND CONCLUSIONS

A major drawback to the application of high speed digital computers is the initial difficulty of getting a given type of problem set up and coded. This operation is expensive because it requires trained coding personnel and generally an expert in the field in which the problem will be used.

If the problem is large it will require a considerable effort for checkout to the point where the program is operational. Therefore, the use of a digital computer can only be justified if several problems are to be solved, or if the problem can only be solved using the computer.

Several alternatives are available to surmount this difficulty. The first is to join with other interested parties to develop the required programs on a joint basis. On the other hand if one is located near a higher educational

EXAMPLE BUILDING FRAME PROBLEM

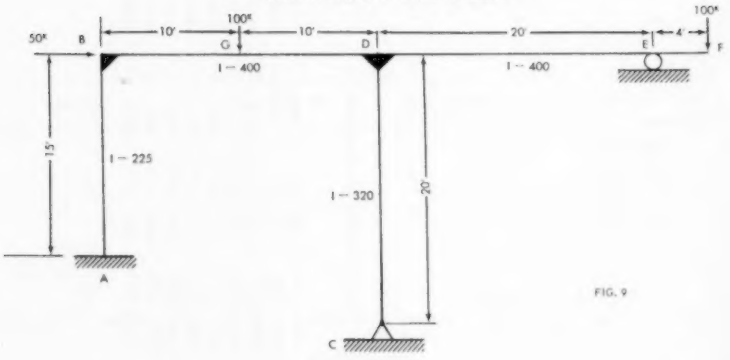

FIG. 9

STIFFNESS MATRIX COORDINATES

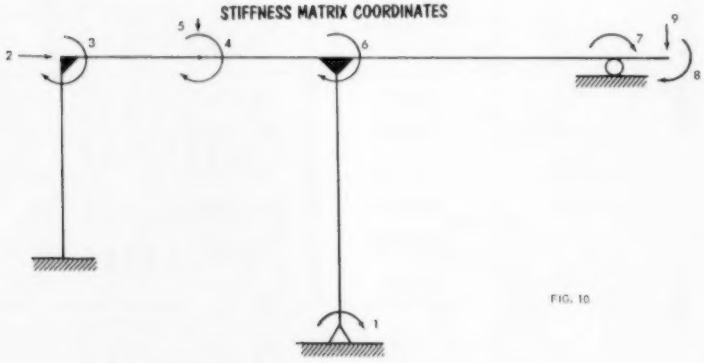

FIG. 10

CALCULATED MATRIX COEFFICIENTS

1	2	3	4	5	6	7	8	9
$.16 \times 10^9$	$-.1 \times 10^7$	0	0	0	$.8 \times 10^8$	0	0	0
$-.1 \times 10^7$	$.22 \times 10^5$	$-.125 \times 10^7$	0	0	$-.1 \times 10^7$	0	0	0
0	$-.125 \times 10^7$	$.55 \times 10^8$	$.2 \times 10^8$	$-.5 \times 10^7$	0	0	0	0
0	0	$.2 \times 10^8$	$.8 \times 10^8$	0	$.2 \times 10^8$	0	0	0
0	0	$-.5 \times 10^7$	0	$.16 \times 10^6$	$.5 \times 10^7$	0	0	0
$.8 \times 10^8$	$-.1 \times 10^7$	0	$.2 \times 10^8$	$.5 \times 10^7$	$.76 \times 10^9$	$.1 \times 10^9$	0	0
0	0	0	0	0	$.1 \times 10^9$	$.12 \times 10^{10}$	$.5 \times 10^9$	$-.3125 \times 10^8$
0	0	0	0	0	0	$.5 \times 10^9$	$.1 \times 10^{10}$	$-.3125 \times 10^8$
0	0	0	0	0	0	$-.3125 \times 10^8$	$-.3125 \times 10^8$	$.1302 \times 10^7$

(a) Stiffness Matrix

1	2	3	4	5	6	7	8	9
$.1005 \times 10^{-7}$	$.5312 \times 10^{-6}$	$.2172 \times 10^{-8}$	$-.3027 \times 10^{-9}$	$.9397 \times 10^{-7}$	$-.9608 \times 10^{-9}$	$.4804 \times 10^{-9}$	$.4804 \times 10^{-9}$	$.2306 \times 10^{-7}$
$.5312 \times 10^{-6}$	$.8725 \times 10^{-4}$	$.3035 \times 10^{-6}$	$-.8294 \times 10^{-7}$	$.8259 \times 10^{-5}$	$.2824 \times 10^{-7}$	$-.1412 \times 10^{-7}$	$-.1412 \times 10^{-7}$	$-.6776 \times 10^{-6}$
$.2172 \times 10^{-8}$	$.3035 \times 10^{-6}$	$.4098 \times 10^{-6}$	$.8873 \times 10^{-9}$	$.1394 \times 10^{-6}$	$-.5490 \times 10^{-9}$	$.2745 \times 10^{-9}$	$.2745 \times 10^{-9}$	$.1318 \times 10^{-7}$
$-.3027 \times 10^{-9}$	$-.8294 \times 10^{-7}$	$-.8873 \times 10^{-9}$	$.1580 \times 10^{-8}$	$-.1368 \times 10^{-7}$	$-.4314 \times 10^{-9}$	$.2157 \times 10^{-9}$	$.2157 \times 10^{-9}$	$.1035 \times 10^{-7}$
$.9397 \times 10^{-7}$	$.8259 \times 10^{-5}$	$.1394 \times 10^{-6}$	$-.1368 \times 10^{-7}$	$.1272 \times 10^{-4}$	$-.8471 \times 10^{-7}$	$.4235 \times 10^{-7}$	$.4235 \times 10^{-7}$	$.2033 \times 10^{-5}$
$-.9608 \times 10^{-9}$	$.2824 \times 10^{-7}$	$-.5490 \times 10^{-9}$	$-.4314 \times 10^{-9}$	$-.8471 \times 10^{-7}$	$.2275 \times 10^{-8}$	$-.1137 \times 10^{-8}$	$-.1137 \times 10^{-8}$	$-.5459 \times 10^{-7}$
$.4804 \times 10^{-9}$	$-.1412 \times 10^{-7}$	$.2745 \times 10^{-9}$	$.2157 \times 10^{-9}$	$.4235 \times 10^{-7}$	$-.1137 \times 10^{-8}$	$.5569 \times 10^{-8}$	$.5569 \times 10^{-8}$	$.2673 \times 10^{-6}$
$.4804 \times 10^{-9}$	$-.1412 \times 10^{-7}$	$.2745 \times 10^{-9}$	$.2157 \times 10^{-9}$	$.4235 \times 10^{-7}$	$-.1137 \times 10^{-8}$	$.5569 \times 10^{-8}$	$.9569 \times 10^{-8}$	$.3633 \times 10^{-6}$
$.2306 \times 10^{-7}$	$-.6776 \times 10^{-6}$	$.1318 \times 10^{-7}$	$.1035 \times 10^{-7}$	$.2033 \times 10^{-5}$	$-.5459 \times 10^{-7}$	$.2673 \times 10^{-6}$	$.3633 \times 10^{-6}$	$.1590 \times 10^{-4}$

(b) Flexibility Matrix

FIG. 11

CALCULATED RESULTS

Coordinate	Deflection	Coordinate	Deflection
1	.0383 rad.	6	—.0125 rad.
2	5.120 in.	7	.0303 rad.
3	.0304 rad.	8	.0399 rad.
4	—.00448 rad.	9	1.760 in.
5	1.889 in.		

(a.) DEFLECTIONS

Member	Moment (l.e.) In.~Lb.	Shear Lb.	Moment (r.e.) In.~Lb.
AB	$.4118 \times 10^7$	—33,074	$-.1835 \times 10^7$
BG	$-.1835 \times 10^7$	—27,603	$-.5148 \times 10^7$
GD	$-.5148 \times 10^7$	72,397	$.3540 \times 10^7$
DE	$-.5224 \times 10^6$	22,176	$.4800 \times 10^7$
EF	$.4800 \times 10^7$	—100,000	0
CD	0	—16,126	$-.4062 \times 10^7$

(b.) STRESSES

FIG. 12

center with adequate computing facilities, the required coding may be economically obtained through monetary support of a graduate thesis topic. Finally, the required program may be developed by modification of an existing program obtained through the IBM SHARE program.

In conclusion, structural analysis problems of all types may be solved on high speed computers using the stiffness matrix technique. This procedure appears particularly adaptable to the use of high speed digital computers. The application of the technique to the solution of Civil Engineering problems presents no greater difficulty than those already surmounted for the analysis of aircraft structures.

BIBLIOGRAPHY

1. G. Kron, Tensorial Analysis and Equivalent Circuits of Elastic Structures, Journ. Franklin Inst., Vol. 238, No. 6 (1944).

2. H. U. Schuerch, Vibration Mode Analysis For Delta Wing Structure, Convair, San Diego, Memo DG-G-100, 12-18-51.

3. S. Levy, Structural Analysis and Influence Coefficients For Delta Wings, Journal of Aeronautical Sciences, Vol. 20, No. 7, pp. 449, July 1953.

4. G. Best and M. P. Keating, A Stiffness Matrix Method of Delta Wing Stress Analysis, Convair, Ft. Worth, SRG-16, 9-8-53.

5. D. Williams, Recent Developments In The Structural Approach To Aeroelastic Problems, Journal of the Royal Aeronautical Society, June 1954.

6. Bisplinghoff, Ashley and Halfmann, Aeroelasticity, Addison-Wesley Publishing Company, Inc., Cambridge 42, Mass., 1955.

7. Wilbur, J. B. and Norris, C. H., Elementary Structural Analysis, McGraw - Hill Book Company, Inc., New York, 1948.

Paper 1815 October, 1958 ST 6

Journal of the
STRUCTURAL DIVISION
Proceedings of the American Society of Civil Engineers

NUMERICAL SOLUTIONS FOR INTERCONNECTED BRIDGE GIRDERS

Henry Malter,[1] A. M. ASCE
(Proc. Paper 1815)

SYNOPSIS

Two numerical methods for the solution of the problem of the interconnected bridge girder are considered for the particular case involving infinite torsional rigidity of the main longitudinal members. Formulas are developed for both deflection and moment for a two girder and four girder structure, and results from both cases are compared with those obtained by using rigorous formulas. Tables are included to compare solutions for various values of relative stiffness. The possibility of replacing the entire cross framing by a single center diaphragm for analysis purposes is clearly indicated.

INTRODUCTION

The interest shown by the engineering profession in the problem of the interconnected bridge girder is evident by the increasing frequency of articles devoted to the subject. This interest is engendered both by the theoretical aspects of the problem, as well as by the practicality of the results that may be employed in the expanding highway program both in the United States as well as throughout the world. Various theoretical solutions to the general problem have been proposed in recent years. These include moment distribution,(1) anisotropic plates,(2) and a method employing a Fourier Series loading.(3) In addition, many experimental and test results have been recorded and appear in the literature. A comprehensive survey of the various aspects of the problem has been included in an article by Professors Siess and Veletsos,(4) whereas a complete bibliography of recent articles appears in a discussion article by Professor Makowski.(5)

The general problem consists of a series of main longitudinal girders (simply supported or continuous) interconnected by either a slab, or a series

Note: Discussion open until March 1, 1959. To extend the closing date one month, a written request must be filed with the Executive Secretary, ASCE. Paper 1815 is part of the copyrighted Journal of the Structural Engineering Division, Proceedings of the American Society of Civil Engineers, Vol. 84, No. ST 6, October, 1958.

1. Prof., Hd. Dept. of Civ. Eng., Robert Coll., Istanbul, Turkey.

of diaphragms or both. A load placed upon any one of the girders will result in deflections of the adjacent beams of the structure as well as of the loaded one. Part of the load is thus transmitted through the diaphragms or slab to the other beams.

The two limiting conditions for the general solution of this problem are a) negligible torsional rigidity of the longitudinal beams, and b) infinite torsional rigidity of the longitudinal beams. The first case would include the usual I-Beam type of bridge with concrete deck slab, and is by far the more important of the two from a practical point of view at the present time. The second type would be encountered in a bridge made up of heavy concrete girders that are able to resist rotation.

This article will concern itself with but a limited aspect of the problem, namely, numerical methods for the solution of case (b), that of infinite torsional rigidity. The question of the applicability of any particular solution to a specific problem is more a matter of interpretation of the behavior of the structure under consideration, and becomes rather indefinite. Any practical conclusions must be governed to a great extent by experimental results and observations on full scale bridges, and no effort to consider the above will be undertaken in this article.

A solution for the particular problem being considered has been obtained by Pippard[6] and by Hetenyi,[7] both employing similar methods, and basing their derivations on a rigorous solution of the differential equations pertaining to the particular problem. Pippard has tabulated the solutions for 2, 3 and 4 girder structures, and the results to be obtained by the approximate methods will be compared with those obtained from a substitution in the Pippard formulas.

Although the numerical methods to be employed will emphasize only one particular problem, that of a concentrated load at the center of one of the longitudinals, it should be realized that this is being done merely for ease of comparison with the results obtained by the more rigorous method of Pippard. Also, this is usually the most critical case, and is therefore of greater importance. The method to be employed is just as applicable to distributed loadings or to concentrated loads placed not at the center. The ease of numerical solutions for particular cases will be obvious, although general formulas may also be derived, as will be done for several cases.

The various aspects of the problem can be understood by considering a two-girder bridge in which the connecting members are either a series of diaphragms or a concrete deck slab. The stiffness of the main members will be designated as E I, and the stiffness of the cross members per unit length of the structure as E I_c. This latter term may be obtained by assuming any cross member as being distributed uniformly over the cross member spacing, and adding to this the stiffness of the slab per unit length. (All terms will be defined where first encountered, and repeated in the Notation at the end of the article.) A load applied to any one girder will result in deflections along the length of the structure that will be different for each beam.

To enable ease of comparison between the various methods employed, only symmetrical structures will be considered. However, after grasping the technique employed, it will be obvious that no restrictions are placed on the type of problem that may be handled. Unsymmetrical structures, as well as beams of varying moment of inertia can be handled in the manner to be outlined for the symmetrical system. It should be remembered that the case of infinite torsional rigidity of the main girders is the case being considered.

Rigorous Method

The general problem could be solved directly. However, for cases involving symmetry, as is here assumed ($E I_1 = E I_2$), it is often preferable to utilize the familiar symmetrical and anti-symmetrical load systems, and to combine the results obtained. Thus if two anti-symmetrical loads, each of 1/2 P, are applied at the centers of beams 1 and 2 (Fig. 1), the resulting total deflection of 2y between the two beams will be observed, where y is the deflection of each beam from its initial position. This total deflection of 2y will produce in the cross beam a shear of

$$w = \frac{12\,EI_c}{l^3} \cdot \frac{2y}{}$$

where w is the shear per unit length of the structure, and l is the spacing of the main members. This shear now appears as a distributed load on the main girders, and is acting upwards on girder 1 and downwards on girder 2. Inasmuch as this distributed load is a function of deflection, it may be recognized as an elastic foundation reaction, and the equation for its solution will be

$$\frac{d^4y}{dx^4} = -\left[\frac{12EI_c}{l^3EI}\right] 2y = -2ky$$

where k is substituted for the term in the parenthesis, and the spring constant r may be defined by $r = 2kEI$. A solution to this problem may be easily obtained by recognizing it as one of the special cases considered by Hetenyi—that of a finite beam both simply supported and resting on an elastic foundation, and with a concentrated load at the center.

A consideration of the symmetrical case (Fig. 2) will indicate that both beams will deflect an equal amount, producing no diaphragm action. The deflections will be no different from that of a simply supported beam with a concentrated load at the center. If the assumed loads are in this case also 1/2 P, combining the two solutions will result in cancellation of the load on beam 2, whereas a total load of P will be found to occupy beam 1.

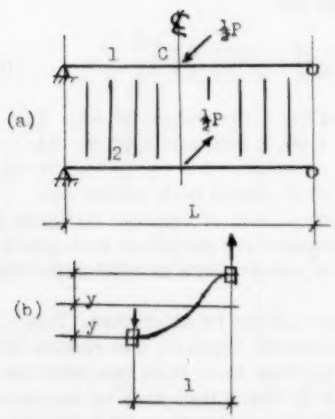

Fig. 1

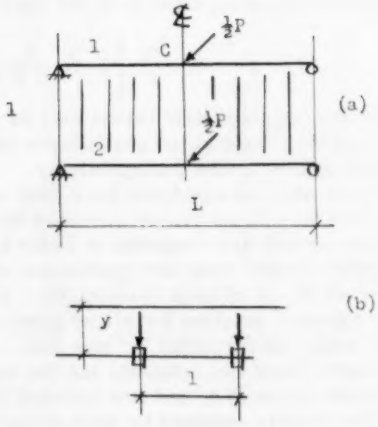

Fig. 2

If one were concerned only with center deflections, or center moments, then advantage could be taken of the special case solutions offered by Hentenyi. For the anti-symmetrical case with the loads of 1/2 P, the center deflections will be

$$\frac{C_1}{C_2} = \pm \frac{P\lambda}{4r}\left(\frac{\sinh \lambda L - \sin \lambda L}{\cosh \lambda L + \cos \lambda L}\right) \qquad \text{where} \qquad \lambda = \sqrt[4]{\frac{r}{4E\,I}}$$

using the plus sign for the downward deflection of beam 1, and the minus sign for the upward deflection of beam 2.

For the symmetrical case, with loads of 1/2 P, the deflections of both beams will be the same, each one being equal to $PL^3 / 96\ EI$.

Combining the two cases will produce a total center deflection of

$$\frac{C_1}{C_2} = \frac{P\,L^3}{48\ EI}\left[\frac{1}{2} \pm \frac{48\ EI}{L^3} \cdot \frac{\lambda}{4r}\left(\frac{\sinh \lambda L - \sin \lambda L}{\cosh \lambda L + \cos \lambda L}\right)\right]$$

where the plus sign is to be used for beam 1, now loaded with a concentrated load of P, and the minus sign is to be used for the unloaded beam 2. Since $k = 2\lambda^4$, this can be simplified to a final form of

$$\frac{C_1}{C_2} = \frac{P\,L^3}{48\ EI}\left[\frac{1}{2} \pm \frac{3}{\lambda^3 L^3}\left(\frac{\sinh \lambda L - \sin \lambda L}{\cosh \lambda L + \cos \lambda L}\right)\right] \qquad (1)$$

It will be recognized that the expression derived above is similar to the one obtained by Pippard, however with the trigonometric terms omitted. The influence of these latter terms will at all times be small when λL is large, and their omission will result in small errors, as is evident from the fact that the value of the terms in the parenthesis is 1.08, 1.05, 1.01 for λL values of 3, 4, and 5 respectively.

To obtain center moments, advantage is again taken of the special problems solutions offered by Hetenyi, but this time using the formula for center moment. In a manner similar to that outlined above for deflections, one will obtain the following final form for center moments

$$\frac{M_1}{M_2} = \frac{PL}{4}\left[\frac{1}{2} \pm \frac{1}{2\lambda L}\left(\frac{\sinh \lambda L + \sin \lambda L}{\cosh \lambda L + \cos \lambda L}\right)\right] \qquad (2)$$

Again the trigonometric terms may be ignored for large values of λL. The value of the terms in the parenthesis is 1.12, 1.00, 0.982, and 1.00 for λL values of 3, 4, 5, and 6 respectively.

These derived equations have been employed to obtain both center deflections as well as center moments for various values of relative stiffness k, and the results are recorded in Table I for comparative purposes with other methods. In all cases the results are shown as percentages of total deflection $PL^3 / 48\ EI$, or of total moment $PL / 4$.

A rigorous solution for a four girder bridge will not be attempted. However, using the formulas for this case as provided by Pippard, the results for both deflections and moments for the various girders have been tabulated for different values of k, and are included in Table II where they may be compared with the results obtained by each of the approximate methods to be outlined.

Center Diaphragm Method

The center diaphragm method (so called for want of a better name), presupposes that the entire cross diaphragm stiffness (whether continuous in the form of a slab, or consisting of distinct cross beams), may be replaced by three concentrated diaphragms, one at the center, and one each at the ends. The center diaphragm will have a stiffness of hEI_c, and the end diaphragms a stiffness of $1/2\ hEI_c$, where as before, EI_c is the cross stiffness per unit length of the structure, and h is the subdivision spacing, in this case 1/2 L. It should be evident that the ends of the beams do not deflect, and consequently the end diaphragms are of no factor in the analysis, and will hereafter be omitted.

Two-Girder Structure

For the case of anti-symmetrical loading, with loads of 1/2 P, the conditions will be as seen in Fig. 3.

The shear in the cross girder at the center will be

$$F = \frac{12\ EI_c}{l^3} \cdot 2Ch$$

where C represents the deflection of the structure from its original position at point C. This shear will now appear as concentrated loads as shown in Fig. 3c, and the center deflection of beam 1 will be

$$C = \frac{PL^3}{96\ EI} - \left[\frac{12\ EI_c}{l^3} \cdot \frac{1}{EI}\right] \frac{2Ch\ l^3}{48}$$

whereas the deflection of beam 2 will be only the second term and using the plus sign. Substituting k for the term in the bracket, and 1/2 L for h, and finally for simplicity using the term ϕ for $kL^4/96$ there will be obtained

$$C = \frac{PL^3}{96EI}\left(\frac{1}{1+2\phi}\right)$$

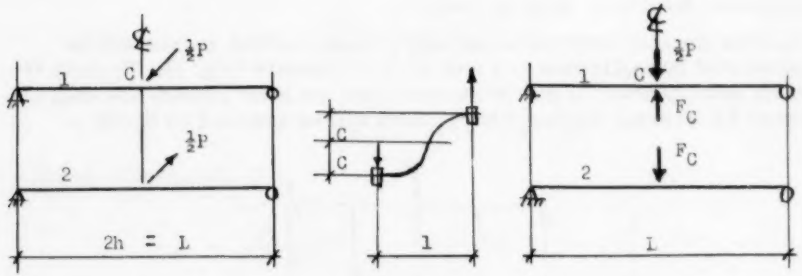

(a) (b) (c)

Fig. 3

For the symmetrical case the deflection of each beam will be $PL^3 / 96\ EI$, and in combining the two cases the final deflections will become

$$\frac{C_1}{C_2} = \frac{PL^3}{48\ EI}\left[\frac{1}{2} \pm \frac{1}{2}\left(\frac{1}{1 + 2\phi}\right)\right] \qquad (3)$$

To obtain center moments by this approximate method, it was observed that for both concentrated center loads and for triangular loadings, the deflections at the quarter points of simply supported beams is approximately 70 per cent of the center deflection. For a diaphragm spacing of h = 1/4 L the shear in the center diaphragm will now be

$$F_c = \frac{12\ EI_c}{l^3}\ \frac{L}{4}\ (C_1 - C_2)$$

for a beam loaded with a load P on beam 1. Substituting the value for $(C_1 - C_2)$ found above, the shear will become

$$F_c = \frac{P\phi}{2}\left(\frac{1}{1 + 2\phi}\right)$$

The concentrations due to the diaphragms at the quarter points will be 70 per cent of the above, and the conditions prevailing will be as shown in Fig. 4. For this loading the center moments will be

$$M_C = \frac{L}{4}\left(-F_{\frac{1}{4}} - F_{\frac{1}{2}} + P\right)$$

and the final center moments will be

$$\frac{M_1}{M_2} = \frac{PL}{4}\left[\frac{1}{2} \pm \frac{1}{2} \mp \frac{1.70\ \phi}{2}\left(\frac{1}{1 + 2\phi}\right)\right] \qquad (4)$$

Results for both deflections and moments are tabulated in Table I.

Four-Girder Structure: Load on Beam 1

To show the effectiveness of this approximate method, its use will be demonstrated by application to a four-girder structure (Fig. 5). To make the problem more general, it will be assumed that the inner girders are each of stiffness EI, whereas the two outer girders will be assumed as having a

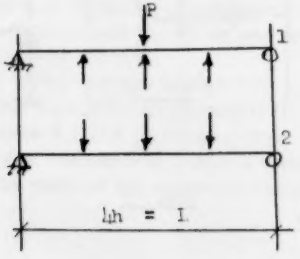

Fig. 4

stiffness of E nI. The unit stiffness of the cross members will be as before EI_c, and the value of the relative stiffness will be defined as the ratio $12\ EI_c / l^3\ E\ nI$, thus identifying it with the outer girder. The symbol k will again be used for relative stiffness. (This definition is the same as that employed in the two-girder case for which n = 1.) For this example two solutions will be required, the first with a load P on girder 1, and a second general solution with a load P on girder 2.

The method to be employed is similar to that used for the two-girder structure, however, that for each of the two cases, symmetrical and anti-symmetrical, two sets of simultaneous equations will be required to find the two unknown deflections C and E. For the symmetrical loads the situation is as shown in Fig. 5b, and the deflections at C and E will be

$$C = \frac{PL^3}{96\ E\ n\ I} - \frac{12\ EI_c}{l^3}\ \frac{L}{2}\ (C - E)\ \frac{L^3}{48\ E\ nI}$$

$$E = \frac{12\ EI_c}{l^3}\ \frac{L}{2}\ (C - E)\ \frac{L^3}{48\ EI}$$

Using the same substitutions as before for k and ϕ, and solving, will give for the symmetrical case

$$C = \frac{PL^3}{96\ E\ nI}\left[\frac{1 + n\ \phi}{1 + \phi + n\ \phi}\right]$$

$$E = \frac{PL^3}{96\ E\ nI}\left[\frac{n\ \phi}{X}\right]$$

where X has been substituted for the term $(1 + \phi + n\ \phi)$ appearing in the denominator.

For the anti-symmetrical case the beam positions will be as seen in Fig. 5c. The loading condition for beam 1 is the same as that for the symmetrical case, and its equation will be the same as that found above. For beam 2 however, the conditions will be different. The resulting equations will be (after substitutions)

$$C = \frac{PL^3}{96\ E\ nI} - \phi\ (C - E)$$

$$E = n\ \phi\ (C - E) - n\ \phi\ (2E)$$

A solution of these will give

$$C = \frac{PL^3}{96\ E\ nI}\left[\frac{1 + 3n\ \phi}{(1 + \phi)(1 + 3n\ \phi) - n\ \phi^2}\right]$$

$$E = \frac{PL^3}{96\ E\ nI}\left[\frac{n\ \phi}{Y}\right]$$

where Y has been substituted for the term $(1 + \phi)(1 + 3n\phi) = n\phi^2$.

Combining both cases will result in the solution for deflections caused by a load P on beam 1.

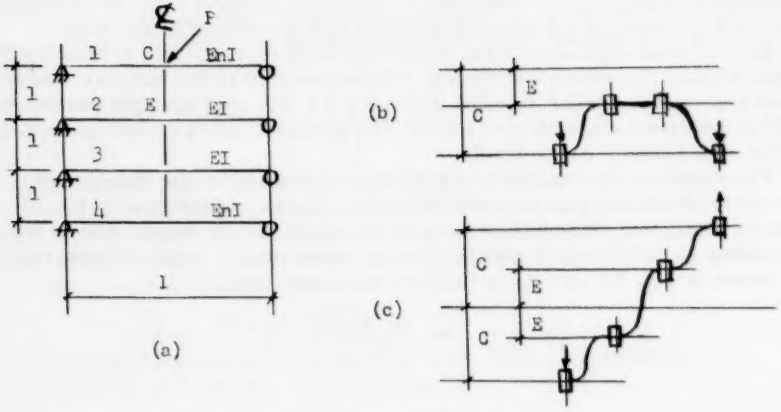

Fig. 5

These deflections will be

$$\frac{C^1}{C_4} = \frac{PL^3}{96\,E\,nI}\left[\frac{1+n\phi}{X} \pm \frac{1+3n\phi}{Y}\right] \tag{5}$$

$$\frac{E^2}{E_3} = \frac{PL^3}{96\,E\,nI}\left[\frac{n\phi}{X} \pm \frac{n\phi}{Y}\right] \tag{6}$$

To obtain moments by this method, it will again be assumed that the quarter point deflections are 70 per cent of the center deflections. The shear in the diaphragms, now assumed as existing both at the quarter points as well as at the center, will be a direct result of the difference in deflection of adjacent beams. These differences are

$$(C^1 - E^2) = \frac{PL^3}{96\,E\,nI}\left[\frac{1}{X} + \frac{1+2n\phi}{Y}\right]$$

$$(E^2 - E_3) = \frac{PL^3}{96\,E\,nI}\left[\frac{2n\phi}{Y}\right]$$

$$(E_3 - C_4) = \frac{PL^3}{96\,E\,nI}\left[\frac{-1}{X} + \frac{1+2n\phi}{Y}\right]$$

The concentrated loads produced at any point will be

$$F(\ ) = \frac{P\phi}{4}\left[\quad\right]$$

where the terms in the bracket are as seen immediately above.

For this type of loading, the final form of the equations for center moment will be

$$\frac{M^1}{M_4} = \frac{PL}{4}\left[\frac{1}{2} \pm \frac{1}{2} - \frac{1.70\,\phi}{4}\left(\frac{1}{X} \pm \frac{1+2n\phi}{Y}\right)\right] \quad (7)$$

$$\frac{M^2}{M_3} = \frac{PL}{4}\left[\frac{1.70\,\phi}{4}\left(\frac{1}{X} \pm \frac{1}{Y}\right)\right] \quad (8)$$

Results from the use of these equations as well as those for deflections have been tabulated in Table II where they can be compared with the results of the other methods.

Four-Girder Structure: Load on Beam 2

For beam 2 loaded, a similar method could be employed resulting in the following equations:

$$\frac{C^1}{C_4} = \frac{PL^3}{96EI}\left[\frac{\phi}{X} \pm \frac{\phi}{Y}\right] \quad (9)$$

$$\frac{E^2}{E_3} = \frac{PL^3}{96\,EI}\left[\frac{1+\phi}{X} \pm \frac{1+\phi}{Y}\right] \quad (10)$$

$$\frac{M^1}{M_4} = \frac{PL}{4}\left[\frac{1.70\,n\,\phi}{4}\left(\frac{1}{X} \pm \frac{1}{Y}\right)\right] \quad (11)$$

$$\frac{M^2}{M_3} = \frac{PL}{4}\left[\frac{1}{2} \pm \frac{1}{2} - \frac{1.70\,n\,\phi}{4}\left(\frac{1}{X} \pm \frac{1+2\,(1+\phi)}{Y}\right)\right] \quad (12)$$

Finite Difference Method

In all elementary textbooks on Resistance of Materials there appears the following equation for the solution of beam deflection problems;

$$\frac{d^4 y}{d x^4} = - \frac{w}{E I}$$

As in many problems involving differential equations, it has been found that difference operators may be substituted for the differential operators. Using the "molecule notation for central difference operators",(8) the fourth difference operator will be

$$\frac{\Delta^4}{\Delta x^4} = \frac{1}{h^4}\,(1,\ -4,\ +6,\ -4,\ 1)$$

It is assumed that one is familiar with the general procedure of finite difference operation, and only its application to the present problem will be emphasized.

A beam resting on an elastic foundation and subjected to vertical forces, will be deflected in some manner, and will result in foundation pressures that will vary along the length of the beam. This foundation pressure that is a continuous function, may be replaced by a set of concentrations at the various subdivision points of the beam. The concentrations may be represented in several ways. First, one may assume a "stepped" variation (Fig. 6a), resulting in subgrade reactions of rhB, rhC, etc., where r is the subgrade modulus,

h is the length of the subdivision, and the letters B, C, D etc. are the deflections of the beam at the points designated. Using a "straight line" variation (Fig. 6b) would result in a more accurate form of concentration (B + 4C + D)rh/6, but would require more labor. The parabolic formula suggested by Professor Newmark for his numerical integration process,(9) could be employed to give concentrations of the form (A + 10B + C)rh/12. The simplest method to employ is the "stepped" method, and it is the one that will be used.

Correction Factor

Before considering any bridge structure, a set of correction factors should be obtained for later use. These can be found through the solution by the finite difference method of a simply supported beam divided into 4 subdivisions, and with a load P at the center (Fig. 7). To obtain the unknown deflections at B and C one fictitious point will be required in the first equation. The following two simultaneous equations will be set up

$$-B - 4A + 6B - 4C + B = 0$$

$$-8B + 6C = \frac{Ph^3}{EI}$$

where P/h has been substituted for w at point C. Since the deflection at point A is zero, a solution of these equations can be easily obtained, and will produce the following deflections

$$B = \frac{PL^3}{64\ EI} \qquad C = \frac{3\ PL^3}{128\ EI}$$

These values are about 11 per cent too large, an error that is inherent in the use of the four division spacing. The correct values, as can be verified from any handbook should be

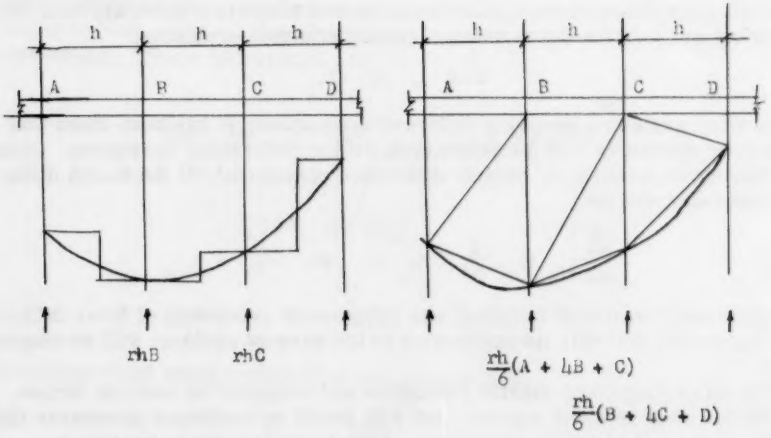

(a) Stepped (b) Straight Line

Fig. 6

$$B = \frac{11}{16}\,\frac{PL^3}{48\,EI} \qquad C = \frac{PL^3}{48\,EI}$$

In the solutions to be derived below, similar errors will occur, and they can be corrected for by substituting as follows

$$\frac{11}{16}\,\frac{1}{48} \text{ for } \frac{1}{64} \qquad \text{and} \qquad \frac{1}{48} \text{ for } \frac{3}{128}$$

Two-Girder Structure

In the two-girder structure (Fig. 8), it is assumed that the entire cross framing is concentrated in the evenly spaced diaphragms at the quarter points and at the center. When the structure is loaded with a set of anti-symmetric loads, the shear in the diaphragms, and the concentrations at the division points will be

$$F_B = \frac{12\,EI_c}{l^3}\,(2h\,B) = 2kh\,B\,EI$$

$$F_C = = 2kh\,C\,EI$$

The above structure has two unknown deflections, B and C, and consequently, two simultaneous equations will be required. These will be

$$-B - 4A + 6B - 4C + B = -2kh^4\,B$$

$$-8B + 6C = -2kh^4\,C + \frac{Ph^3}{EI}$$

replacing $kh^4 = kL^4/256$ by R, and recognizing that the deflection at A is zero, these equations become

$$6B - 4C = -2R\,B$$

$$-8B + 6C = -2R\,C + \frac{Ph^3}{EI}$$

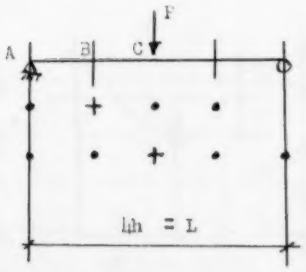

Fig. 7

A solution of these two equations will result in the deflections

$$B = \frac{PL^3}{64EI}\left[\frac{1}{2}\left(\frac{1}{(3+R)^2 - 8}\right)\right]$$

$$C = \frac{3PL^3}{128EI}\left[\frac{1}{6}\left(\frac{3+R}{Z}\right)\right]$$

where Z has been substituted for the term $(3 + R)^2 - 8$ appearing in the denominator. It is obvious that the terms 1/64, and 3/128 are in error and should be replaced by the correct values as outlined above.

For the symmetrical case, loads of 1/2 P placed at the center of each girder will result in deflections of

$$B = \frac{11}{16}\frac{PL^3}{96\ EI} \qquad \text{and} \qquad C = \frac{PL^3}{96\ EI}$$

The combined values will be

$$\frac{B^1}{B_2} = \frac{11}{16}\frac{PL^3}{48\ EI}\left[\frac{1}{2} \pm \frac{1}{2}\left(\frac{1}{Z}\right)\right] \qquad (13)$$

$$\frac{C^1}{C_2} = \frac{PL^3}{48\ EI}\left[\frac{1}{2} \pm \frac{1}{6}\left(\frac{3+R}{Z}\right)\right]$$

Having found the deflections, these values may be translated into loads at the quarter points and at the center. For the anti-symmetrical case these loads will simplify to

$$F_B = P\,R\left[\frac{11}{12}\left(\frac{1}{Z}\right)\right]$$

$$F_C = P\,R\left[\frac{4}{9}\left(\frac{3+R}{Z}\right)\right]$$

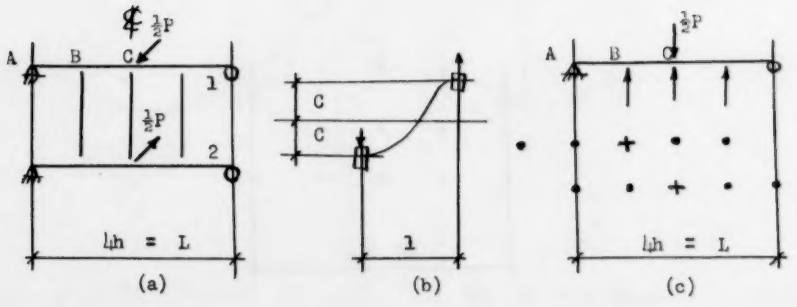

Fig. 8

and the combined value will be

$$F_B + F_C = P R \left[\frac{2.25 + 0.444 R}{Z} \right]$$

For the symmetrical case the center moments are PL/8, and combining both cases will result in the final form of the equation for moment

$$\frac{M_1}{M_2} = \frac{PL}{4} \left[\frac{1}{2} + \frac{1}{2} - R \left(\frac{2.25 + 0.444 R}{Z} \right) \right] \qquad (14)$$

The results for both center deflections, and for center moments for various values of relative stiffness k are recorded in Table I, where the close agreement with the other methods is evident.

Four-Girder Structure: Load on Beam 1

A solution of the four girder problem by the finite difference method does not lend itself easily to the setting up of simple formulas. However, individual cases of particular relative stiffness can be easily solved through the solution of four simultaneous equations each for the symmetrical and the anti-symmetrical case.

The structure to be considered (Fig. 9) will, as before, have EI as the stiffness of the inner girders, and E nI as the stiffness of the outer girders. Diaphragms will be assumed at the quarter points as well as at the center, and the four unknown deflections are B, C, D and E. For symmetrical loading the equations required will be

$$6B - 4C = -R (B - D)$$

$$-8B + 6C = -R (C - E) + \frac{Ph^3}{2E\,nI}$$

$$6D - 4E = nR (B - D)$$

$$-8D + 6E = nR (C - E)$$

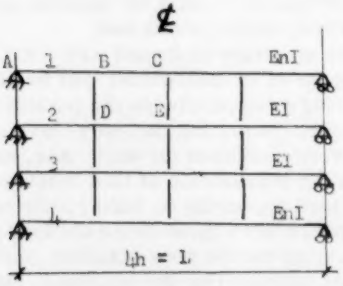

Fig. 9

For the anti-symmetrical case the four equations will be

$$6B - 4C = -R(B - D)$$

$$-8B + 6C = -R(C - E) + \frac{Ph^3}{2E\,nI}$$

$$6D - 4E = nR(B - D) - nR(2D)$$

$$-8D + 6E = nR(C - E) - nR(2E)$$

Solutions of the above equations will give the deflections, and once the latter have been found, the moments are easily arrived at. Solutions of the above for both deflection and moment have been tabulated for various values of k in Table II, and may be compared with the results of the other methods.

Tables

To indicate the accuracy that can be obtained by the approximate methods, Tables I and II have been prepared to show comparative results for both moments and deflections. Table I shows results for two-girder structures of length 600 inches and 1000 inches. For the two-girder structure both longitudinals have the same stiffness.

Table II has been prepared to show the distribution of moment and deflection on a four-girder structure with a load on beam 1 only. The ratio of outer to inner girder stiffness is 1/2. The moments appearing on each beam are shown as percentages of the maximum value PL/4. For deflections the values shown are percentages of $PL^3/48$ E nI for the outer girders, and of $PL^3/48$ EI for the inner girders. It should be noted that in Table II the use of the Pippard formulas for k values as low as 0.10×10^{-8} is not recommended. For this low value $\lambda L = 2.64$ and a correction factor is required.

To indicate the general trend in results obtainable, Tables III and IV have been prepared, using the Pippard formulas, although it should be evident that either of the approximate methods might have been used. Both Tables III and IV apply to four-girder structures, both 600 and 1000 inches in length, and having n values of both 1/2 and 1. For each structure two sets of results have been obtained, first with the load placed on beam 1, and then with the load placed on beam 2.

Table III has been prepared to show the moment percentage appearing on each beam for the various cases considered.

If each girder of the structure is loaded with a maximum load at the center, then the value of the moment in each girder will be 100 per cent of PL/4. However, normal spacing often precludes the possibility of loading all four girders at the same time. Assuming that only three of the girders are fully loaded, the moments were combined for each case, and the total moments are shown in Table IV. In the preparation of this chart for the case of n = 1/2 it was assumed that the load appearing on each girder was the maximum design load, and the inner girders were given twice the load of the outer girder. Two sets of combined maximum values were obtained, one for beam 1, and a second set for beam 2. It is of interest that the maximum obtainable moment is between 80 and 90 per cent of that on a fully loaded structure, or of the assumption that each beam carries its own load.

CENTER MOMENTS

k	L = 600 inches			L = 1000 inches		
10^{-3}	Pippard	Diaph. Meth.	Fin. Diff.	Pippard	Diaph. Meth.	Fin. Diff.
1.40	59.1	58.6	59.4	55.5	57.6	56.4
1.10	59.7	58.8	59.9	55.8	57.6	56.6
.80	60.5	59.4	60.8	56.3	57.6	56.7
.50	61.8	60.4	62.2	57.1	58.0	57.2
.20	65.5	64.2	66.5	58.9	58.5	59.1
.10	70.2	68.9	70.9	60.5	59.7	61.2
(center moments as percent of PI/4)						

CENTER DEFLECTIONS

1.40	51.8	51.3	51.8	50.3	50.2	50.3
1.10	52.2	51.6	52.1	50.4	50.2	50.3
.80	52.8	52.2	52.8	50.6	50.3	50.5
.50	53.9	53.5	54.1	50.8	50.5	50.8
.20	58.4	57.8	58.2	51.7	51.2	51.7
.10	64.2	63.5	63.6	52.8	52.3	52.8
(center deflections as percent of $PL^3/48EI$)						

TABLE I : Comparative Results for Two-Girder Structure

CENTER MOMENTS

k	Pippard				Diaph. Meth.				Finite Diff.			
10^{-8}	M_1	M_2	M_3	M_4	M_1	M_2	M_3	M_4	M_1	M_2	M_3	M_4
1.40	34.8	29.3	24.3	11.6	33.2	29.4	25.4	12.0	35.0	29.2	25.4	10.4
1.10	35.9	29.1	23.7	11.3	34.2	29.5	24.6	11.8	37.0	29.6	23.0	10.4
.80	37.6	28.7	22.9	10.8	36.1	29.7	23.5	10.7	39.0	29.6	21.6	9.7
.50	40.1	28.1	21.7	10.1	39.4	30.1	21.1	9.4	43.0	28.7	19.6	8.8
.20	46.2	26.8	18.6	8.4	49.0	30.4	15.2	5.4	52.5	28.0	14.5	4.9
.10	51.6	25.7	15.9	6.8	59.2	28.3	9.7	2.8	62.0	26.2	9.4	2.2

(center moment given as percent of $PL/4$)

CENTER DEFLECTIONS

	C_1	E_2	E_3	C_4	C_1	E_2	E_3	C_4	C_1	E_2	E_3	C_4
1.40	22.2	34.0	29.6	14.2	21.4	34.5	29.9	14.2	22.4	34.2	29.2	14.0
1.10	23.3	34.1	28.9	13.7	22.6	34.7	28.9	13.6	23.6	34.3	28.5	13.4
.80	25.1	34.3	27.7	12.9	24.6	35.1	27.7	12.6	25.4	34.5	27.3	12.6
.50	28.6	34.9	25.3	11.2	28.4	35.6	25.0	10.8	29.3	35.2	25.0	11.0
.20	40.5	36.3	17.3	5.9	40.0	35.6	17.8	6.5	40.2	34.9	17.9	6.8
.10	56.5	38.4	6.6	-	52.0	33.2	11.4	3.2	51.3	32.4	12.2	4.2

(center deflections given as percent of $PL^3/48\ E\ nI$ for beams 1, 4)
(" $PL^3/48\ E\ I$ for beams 2, 3)

Load on Beam 1 L = 600 inches n = $\frac{1}{2}$

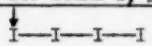

TABLE II : Comparative Results for Four-Girder Structure

	600 inches				1000 inches			
k 10^{-8}	P M_1	M_2	M_3	M_4	P M_1	M_2	M_3	M_4
1.40	41.3	22.0	18.8	17.8	34.8	23.2	21.3	20.7
1.10	42.3	21.8	18.5	17.3	35.4	23.1	21.1	20.4
.80	43.8	21.6	18.0	16.7	36.3	22.9	20.8	20.0
.50	46.1	21.1	17.1	15.8	37.6	22.7	20.2	19.4
.20	51.5	20.1	15.1	13.2	41.0	22.0	19.0	17.9
	M_1	P M_2	M_3	M_4	M_1	P M_2	M_3	M_4
1.40	22.0	38.3	20.8	18.8	23.2	33.0	22.5	21.3
1.10	21.8	39.0	20.6	18.5	23.1	33.4	22.4	21.1
.80	21.6	40.1	20.4	18.0	22.9	34.0	22.2	20.8
.50	21.1	42.2	19.7	17.1	22.7	35.3	21.8	20.2
.20	20.1	46.4	18.4	15.1	22.0	37.9	21.0	19.0

a) $I_1/I_2 = 1$

	P M_1	M_2	M_3	M_4	P M_1	M_2	M_3	M_4
1.40	34.8	29.3	24.3	11.6	27.5	30.9	28.0	13.6
1.10	35.9	29.1	23.7	11.3	28.2	30.8	27.6	13.4
.80	37.6	28.7	22.9	10.8	29.1	30.5	27.1	13.2
.50	40.1	28.1	21.7	10.1	30.7	30.2	26.3	12.7
.20	46.2	26.8	18.6	8.4	34.3	29.4	24.6	11.7
	M_1	P M_2	M_3	M_4	M_1	P M_2	M_3	M_4
1.40	14.7	47.0	26.2	12.1	15.4	41.5	29.1	14.0
1.10	14.6	47.8	25.8	11.8	15.4	42.0	28.8	13.8
.80	14.3	49.0	25.2	11.5	15.2	42.8	28.4	13.6
.50	14.1	50.9	24.1	10.8	15.1	43.9	27.8	13.2
.20	13.4	55.6	21.8	9.3	14.7	46.6	26.4	12.3

b) $I_1/I_2 = \frac{1}{2}$

Moments shown as percent of $PL/4$; load placed on either beam 1 or beam 2 as indicated

TABLE III : Four Beam Structure - Percentage Moment Distribution

	P P P I—I—I—I *		P P P I—I—I—I *		P 2P 2P ½P P P I—I—I—I—I—I *			
k	Beam 1		Beam 2		Beam 1		Beam 2	
10^{-8}	600 inches	1000	600	1000	600	1000	600	1000
1.40	82.1	79.3	81.1	78.7	88.3	86.3	87.9	86.1
1.10	82.6	79.6	81.4	78.9	88.7	86.6	88.2	86.2
.80	83.0	80.0	82.1	79.1	89.1	86.9	88.6	86.5
.50	84.3	80.5	83.0	79.8	89.9	87.3	89.1	86.8
.20	86.7	82.0	84.9	80.9	91.6	88.3	90.8	87.7
	$\frac{E I_1}{E I_2} = 1$				$\frac{E I_1}{E I_2} = \frac{1}{2}$			

Moments shown as percent of $PL/4$ for beam indicated with loads on beams 1, 2, and 3 of structure.

TABLE IV : Four Beam Structure - Moments for Combined Loads

The value of the relative stiffness factor k in each table is in units of 10^{-8} inches 4.

The Pippard formulas employed for the various structures considered are rather lengthy and will not be reproduced here. They may be found on pages 107 and 108 of reference 6.

REFERENCES

1. Newmark, N. M., "A Distribution Procedure for the Analysis of Slabs Continuous over Flexible Beams", Bulletin No. 304, Univ. of Illinois Eng. Expt. Stn., 1938.
2. Ewell, W. W., Okubo S. and Abrams, J. I., "Deflections in Gridworks and Slabs", Trans. ASCE, Vol. 117, 1952.
3. Hendry, A. W. and Jaeger, L. G., "The Load Distribution in Highway Bridge Decks", Proceedings ASCE, Vol. 82, 1956.
4. Siess, C. P. and Veletsos, A. S., "Distribution of Loads to Girders in Slab and Girder Bridges", Highway Research Board Report 14-B, 1953.
5. Makowski, Z. S., "Distribution of Loads on Bridge Decks", discussion article, Proceedings ASCE, Vol. 84, 1958.
6. Pippard, A. J. S., "Studies in Elastic Structures", Edward Arnold and Co., London, 1952, pp. 96-110.

7. Hetenyi, M., "Beams on Elastic Foundations", The University of Michigan Press, Ann Arbor, Michigan, 1946.

8. Salvadori, M. G., and Baron, M. L., "Numerical Methods in Engineering", Prentice Hall Inc., 1952, p. 69.

9. Newmark, N. M., "Numerical Procedure for Computing Deflections, Moments and Buckling Loads", Transactions, ASCE, Vol. 114, pp. 40-52.

Notation

L	- span of structure
h	- length of subdivision
l	- distance between main girders
M	- center moment of beam designated
P	- concentrated load applied at center of span
r	- subgrade modulus 2kEI
EI_1	- stiffness of girder 1; EI_2 = stiffness of girder 2
n	- ratio of EI_1/EI_2 in four girder structure
EI_c	- stiffness of cross framing per unit length of structure
B, C, D, E	- deflection of structure from original position at point indicated
k	$= 12\ EI_c / 1^3 E\ nI$
ϕ	$= kL^4 / 96$
R	$= kL^4/256$
X	$= (1 + \phi + n\phi)$
Y	$= (1 + \phi)(1 + 3\ n\phi) - n\phi^2$
Z	$= (3 + R)^2 - 8$
λ	$= \sqrt[4]{\frac{r}{4EI}}$

Paper 1816 October, 1958 ST 6

Journal of the
STRUCTURAL DIVISION
Proceedings of the American Society of Civil Engineers

GENERALIZATION OF THE SUCCESSIVE APPROXIMATIONS METHOD

Panagiotis D. Moliotis,[1] M. ASCE
(Proc. Paper 1816)

SYNOPSIS

The present study concerns the analysis of rigid frames, whose joints are not just points but small undeformed areas, by the method of successive approximations.

INTRODUCTION

The stresses in the members of a framework are usually calculated with the assumption that the connections between members are points to which they meet and are connected together by rigid or pinned joints.

In reality however joints are small areas to which the various members of a framework are connected.

Fig. (1a) shows a typical rigid joint k, where k is not in reality a point but the shaded area aa' - bb'. We can consider this area as suffering no diformation because the moments of inertia in the directions 1-1 and 2-2 are very large compared with those of the sections of members 1-1 and 2-2. In point of fact, in the case of reinforced concrete structures, after calculating the bending moments of the various members meeting at joint k, we work out the bending moments at the sections of the faces aa', bb', ab, a'b' and from these values we determine the required dimensions of the sections and reinforcement of the members.

Thus we accept that the area of joint k suffers no deformation.

In Fig. 1b the joint k is the wall of reservoir. In this case, due to the dimensions of the wall, joint k can safely be considered as an area suffering no deformation.

Note: Discussion open until March 1, 1959. To extend the closing date one month, a written request must be filed with the Executive Secretary, ASCE. Paper 1816 is part of the copyrighted Journal of the Structural Division, Proceedings of the American Society of Civil Engineers, Vol. 84, ST 6, October, 1958.

1. Dr. Civ. Eng. Asst., National Technical Univ., Athens, Greece.

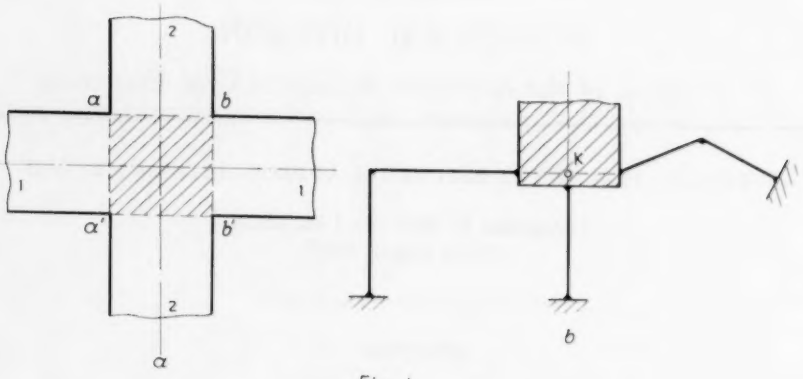

Fig. 1

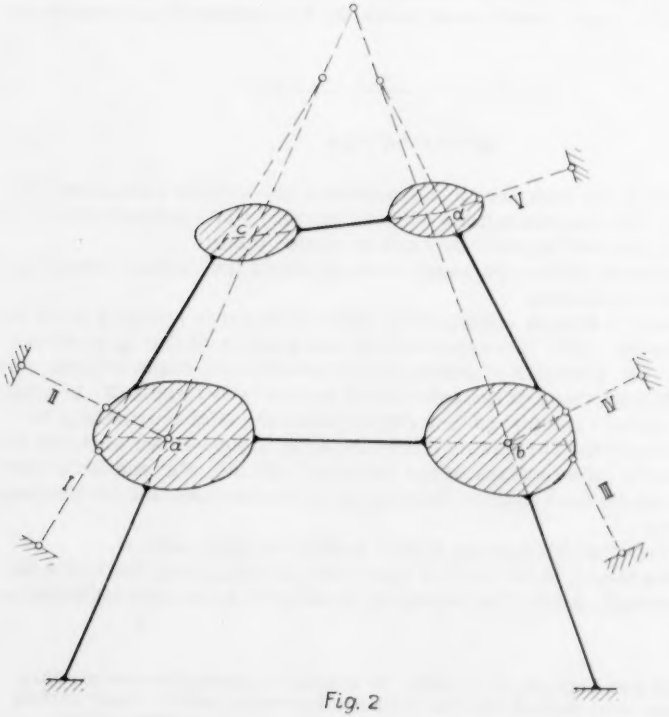

Fig. 2

We can now proceed with the stress analysis of rigid frames with straight members by the successive approximation method making the assumption that joints are small areas suffering no deformation i.e. absolutely rigid bodies.

Elastic Movement of Frame

As it is known, the elastic deflection of a rigid frame under load is characterized by the rotation and displacement of its joints. By knowing these and the external forces acting on the frame we can proceed with its stress analysis. Also deflections due to direct and shear stresses are very small compared with those due to bending and can be neglected. Neglecting therefore deflections due to direct and shear stresses the displacements of the various joints are not independent of each other and by making use of the "virtual displacement" we can express the displacement of all joints as functions of the displacement of a certain number of them.

If a rigid frame is converted into a pin-jointed frame by replacing rigid joints by pinned ones the resulting formation will as a rule be capable of suffering geometrical displacement. We can make this resulting formation a just-stiff frame by the addition of a certain number of pin jointed bars (roller restraints) Fig. 2. The number of bars required for this purpose gives us the degree of the elastic freedom of the original rigid frame.

Sign Convention(2)

Bending moments at sections by the joints are considered positive when clockwise.

Shearing forces are considered positive when the shearing couple tends to turn an infinite portion of the beam clockwise.

Normal forces are considered positive when they produce tension to the members.

Stress Analysis of Rigid Frames by the Method of Successive Approximations

Stress analysis of rigid frames of the classical case (joints-points) is carried out either in two (1) or one stages (2). Below are given the new factors for both cases.

Stress Analysis in Two Stages. 1st Stage

Here also we assume that joints are not deflected and that the bending moments shear and normal forces acting on the joints are those of a member built-in at both ends. We determine below the new distribution and carry-over factors when the joints are not allowed to deflect.

Reactions on Joints When Fixed

Assume all joints fixed (rotation not allowed). In this case all members are built-in at either end and exert to the joints bending moment, shearing and normal forces $\bar{M}_{\alpha i}$, $\bar{Q}_{\alpha i}$, $\bar{N}_{\alpha i}$

Due to these systems of forces the joint will rotate around the instantaneous center of rotation by an angle δ_α (Fig. 3)

By replacing these systems of forces $\bar{M}_{\alpha i}$, $\bar{Q}_{\alpha i}$, $\bar{N}_{\alpha i}$ by the equivalent ones we shall have

$$\bar{M}'_{ai} = \bar{M}_{ai} + \bar{Q}_{ai}\, d_{ai} \qquad \bar{Q}_{ai} \qquad \bar{N}_{ai} \tag{1}$$

It is obvious that joint a will suffer the same elastic rotation δ_a by either of the above two systems of forces.

Therefore is this case the bending moment which acts on joint a is:

$$\bar{M}'_a = \Sigma \bar{M}'_{ai} = \Sigma \bar{M}_{ai} + \Sigma Q_{ai}\, d_{ai} + M_a \tag{2}$$

where Ma represents any existing external couple on the joint.

The fixing moment of joint a is equal and opposite to $\bar{M}'_a$ acting on joint a as calculated by Eq. (2).

The forces on the joints by which we calculate the fixing forces $F_i^\circ \ldots$ are:

$$\bar{P}_a = \Sigma_i \bar{Q}_{xi} + \Sigma_i N_{xi} + P_a \tag{3}$$

where Pa: any existing external force on joint a.

In Eq. (3) the summation is geometrical.

The shearing forces $\bar{Q}_{ai}$ and $\bar{Q}_{bi}$ are calculated by considering B.M$_s$, $\bar{M}_{ai}$, $\bar{M}_{bi}$ and external load of span l_i and also B.M$_s$, $\bar{M}'_{ai}$, $\bar{M}'_{bi}$ and same external load of span l'_i. In other words the shearing forces of the built-in span l_i are taken as being the same as those of an imaginary built-in span l'_i with the same external load, and end fixing moments $\bar{M}'_{ai}$ and $\bar{M}'_{bi}$ (Fig. 3).

Distribution Factors

Joint a will, under the action of the B.M, Ma, suffer a rotation say δ_a around the instantaneous centre of rotation a. The section α_i of any member i will turn through and angle δ_a due to the rotation of joint a and will therefore be displaced at right angles to its axis by a distance $\delta_a \times d_{ai}$ (Fig. 4). The section b_i will suffer no rotation or displacement because joint b remains fixed.

Bending moments are given by the well known equations:

$$\begin{aligned} M_{ai} &= \left(\alpha_{ai} + u_{ai}\, \frac{d_{ai}}{l_i}\right) \delta_a \\ M_{bi} &= \left(\mu_i \alpha_{ai} + u_{bi}\, \frac{d_{ai}}{l_i}\right) \delta_a \end{aligned} \tag{4}$$

where: α_{ai} is the bending moment which should be applied on section α_i to obtain rotation of it equal to unity i.e. the factor of stiffness to rotation of member i. μ_i is the carry-over factor of member i for the rotation of the section only and: u_{ai}, u_{bi} are the B.Ms at the sections a_i and b_i of member i for a ration $\frac{\delta_{ai}}{l_i} = 1$ i.e. "factor of stiffness to displacement" of member i.(2)

Shearing forces are given by the equations:

$$Q_{ai} = Q_{bi} = \left[\alpha_{ai}\,(1+\mu_i) + (u_{ai} + u_{bi})\, \frac{d_{ai}}{l_i}\right] \frac{\delta_a}{l_i} \tag{5}$$

Joint a is in equilibrium under B.Ms, M_{ai}, M_a and shearing forces Q_{ai}. B.M. M'_{ai} is given by the equation:

$$M'_{ai} = M_{ai} + Q_{ai}\, d_{ai} \tag{6}$$

If in Eq. (6) we replace the values for Mai and Qai from Eqs. (4) and (5) we shall obtain

$$M'_{ai} = b_{ai}\, \delta_a \tag{7}$$

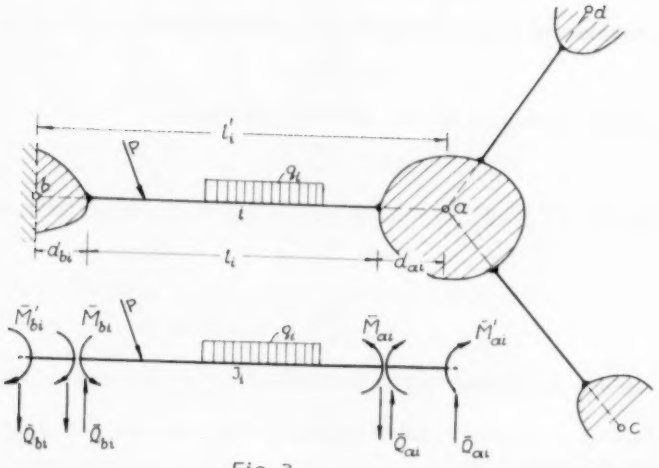
d
l'i
P
qi
b
i
a
dbi
li
dai
M'bi
Mbi
P
qi
Mai
M'ai
Jj
Qbi
Qbi
Qai
Qai
c

Fig. 3

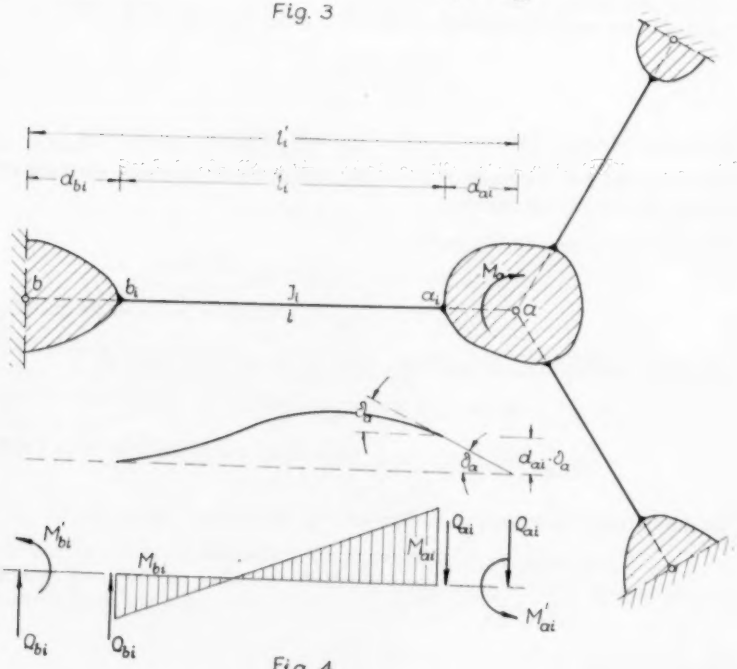
l'i
dbi
li
dai
b
bi
Ji
i
ai
Mo
a
ϑa
ϑa
dai·ϑa
M'bi
Mbi
Mai
Qai
Qai
M'ai
Qbi
Qbi

Fig. 4

where:

$$b_{ai}=\alpha_{ai}\left[1+(1+\mu_i)\frac{d_{ai}}{l_i}\right]+u_{ai}\frac{d_{ai}}{l_i}\left(1+\frac{d_{ai}}{l_i}\right)+u_{bi}\left(\frac{d_{ai}}{l_i}\right)^2 \tag{8}$$

The equilibrium of joint a is expressed by the equation:

$$M_a+\Sigma M'_{ai}=0 \tag{9}$$

and by replacing the values for M'_{ai} from (7) we obtain:

$$\vartheta_a=(-M_a)\frac{1}{\Sigma b_{ai}} \tag{10}$$

From (7) and (10) we have:

$$M'_{ai}=(-M)K_{ai} \tag{11}$$

where:

$$K_{ai}=\frac{b_{ai}}{\Sigma b_{ai}} \tag{12}$$

The factor K_{ai} is the new "factor of distribution" for the case of rigid frames examined.

The factor b_{ai} is the new index of stiffness of the member and Σb_{ai} the new index of stiffness of joint a.

If in Eq. (9) we replace the value for M'_{ai} from (11) we have:

$$\Sigma K_{ai}=+1 \tag{12'}$$

Special Cases—Straight Members with Constant Moments of Inertia

The factors bai for the case of straight members of constant moment of inertia have the following values.

(a) Member built-in at both ends.

$$\alpha_{ai}=\frac{4EJ_i}{l_i},\quad \mu_i=+\frac{1}{2},\quad u_{ai}=u_{bi}=\frac{6EJ_i}{l_i}$$

$$b_{ai}=\frac{4EJ_i}{l_i}\left[1+3\frac{d_{ai}}{l_i}+3\left(\frac{d_{ai}}{l_i}\right)^2\right] \tag{13}$$

(b) Member built-in at one end—Pin joint at section b_i (Fig. 5)

$$\alpha_{ai}=\frac{3EJ_i}{l_i}\qquad \mu_i=0\qquad u_{ai}=\frac{3EJ_i}{l_i}\qquad u_{bi}=0$$

$$b_{ai}=\frac{3EJ_i}{l_i}\left[1+2\frac{d_{ai}}{l_i}+\left(\frac{d_{ai}}{l_i}\right)^2\right] \tag{14}$$

(c) Member built-in at one end—Pin joint at section α_i (Fig. 5)

$$\alpha_{ai}=0\quad \mu_i=0\quad u_{ai}=0\quad u_{bi}=\frac{3EJ_i}{l_i}$$

$$b_{ai}=\frac{3EJ_i}{l_i}\left(\frac{d_{ai}}{l_i}\right)^2 \tag{15}$$

Carry-Over Factors

We express bending moment M'_{bi} in terms of the calculated bending moment M'_{ai}

$$M'_{bi}=M_{bi}+Q_{bi}\,d_{bi} \tag{16}$$

and by replacing the values for M_{bi} and Q_{bi} from (4) and (5) we obtain

$$M'_{bi}=\left(\mu_i \alpha_{ai}+u_{bi}\frac{a'_{ai}}{l_i}\right)\vartheta_a+\left[\alpha_{ai}(1+\mu_i)+(u_{ai}+u_{bi})\frac{a'_{ai}}{l_i}\right]\frac{a_{bi}}{l_i}\vartheta_a \tag{17}$$

and replacing the value for the angle ϑ_a and working out we obtain:

$$M'_{bi}=\mu_{ab}M'_{ai} \tag{18}$$

where

$$\mu_{ab}=\frac{\alpha_{ai}\left[\mu_i+(1+\mu_i)\frac{a_{bi}}{l_i}\right]+u_{ai}\frac{a'_{ai}}{l_i}\cdot\frac{a_{bi}}{l_i}+u_{bi}\left(1+\frac{a_{bi}}{l_i}\right)\frac{a'_{ai}}{l_i}}{b_{ai}} \tag{19}$$

which gives us the required carry-over factor of member i from joint a to joint b.

Special Cases—Straight Members with Constant Moments of Inertia

(a) Member built-in at both ends

$$\mu_{ab}=\frac{1}{2}\frac{1+3\frac{a'_{ai}+a_{bi}}{l_i}+6\frac{a'_{ai}a_{bi}}{l_i^2}}{1+3\frac{a'_{ai}}{l_i}+3\left(\frac{a'_{ai}}{l_i}\right)^2} \tag{20}$$

(b) Member built-in at one end. Pin joint at section b_i

$$\mu_{ab}=\frac{\frac{a_{bi}}{l_i}\left(1+\frac{a'_{ai}}{l_i}\right)}{1+2\frac{a'_{ai}}{l_i}+\left(\frac{a'_{ai}}{l_i}\right)^2} \tag{21}$$

(c) Member built-in at one end. Pin joints at section α_i

$$\mu_{ab}=\frac{1+\frac{a_{bi}}{l_i}}{\frac{a'_{ai}}{l_i}} \tag{22}$$

Calculating of Bending Moments M'_{ai}

The bending moments M'_{ai} of the rigid frame are calculated by successive approximation as done in the classical case.

For the calculation of bending moments M_{ai} we work out at first the shearing forces Q_{ai}

These are obtained from equation:

$$Q_{ai}=Q^o_{ai}+\frac{M_{ai}+M_{bi}}{l_i} \tag{23}$$

where Q^o_{ai} is the shearing force for the freely supported span l_i

Having obtained the value of shearing force Q_{ai} bending moments M_{ai} are calculated from the equation:

$$M_{ai}=M'_{ai}-Q_{ai}a_{ai} \tag{24}$$

In the above equation B.M. M_{ai} and S.F. Q_{ai} are entered with their appropriate signs.

2nd Stage

Having calculated the bending moments M'_{ai} of the 1st stage, we work out the shearing and normal forces Q_{ai}, N_{ai} . With these values and any other existing external forces on the joints we calculate the fixing forces F of the 1st stage. The stress condition of the 2nd stage is the stress condition of the rigid frame acted upon by the forces on the joints Q_{ai}, N_{ai} and P_a or by an equivalent loading by forces Z equal and opposite to the fixing forces F of the 1st stage.

We call "group of condisplaced joints" and "group of condisplaced members" all the joints or members of the frame which will be displaced together should one only roller restraint be removed.(2)

We number each roller restraint by I, II, III . . . . .

The solution of the 2nd stage in the classical case of frame is obtained, as it is known, by calculating the "partial stress condition" of the frame of a simple elastic freedom and obtaining a system of linear equations of the same number as the degree of elastic freedom of the frame by the help of which we obtain what are called the "convertion factors". The required "stress condition" of the 2nd stage is obtained by the addition of the partial stress conditions of simple elastic, freedom having multiplied them by the respective "convertion factors".(1)

On calculating the above "partial stress conditions" by the method of successive approximation, the fixing moments are worked out with the supposition that the joints of the frame can be displaced without rotating. The relative displacements of the joints are obtained by the help of the virtual displacement diagrams.(2)

Virtual Displacement Diagrams

As it is known from solid mechanics, any solid moving in a plane can have generally the possibility of two displacements and one rotation in the plane of the frame.

The movements of the joints depend therefore on the number of members which connect the joint with the ground or other rigidly fixed neighbouring joints (Fig. 5a, b).

Thus, joints a and b of Fig. 5a, by the addition of the member I have the possibility of rotation only.

We call joints of double elastic freedom those which have the possibility of displacement and rotation. Joints a and b of Fig. 5a and joint a of Fig. 5b are of "double elastic freedom".

We call joints of "single elastic freedom" those joints which can only rotate around an instantaneous centre 0.

In the rigid frame of Fig. 6, joints b and c are of a "single elastic freedom and joint a of "double elastic freedom". By the addition of member I pinned at both ends, a can suffer only rotation whereas and c can suffer neither rotation nor displacement.

For any movement δ_{c1} we can, by making use of the diagrams of virtual displacement, calculate the movement of any point of the joints of the frame.

Fixing Moments of 2nd Stage

In the classical case of rigid frames, i.e. when joints are taken as points, in order to calculate the fixing moments of the 2nd stage, we suppose that

joints do not rotate and by using the diagrams of virtual displacement we work out the relative displacement between two adjacent joints in the direction perpendicular to the member joining the joints under consideration.

By making use of these relative displacements of the ends of the members, we calculate the fixing moments at all sections by the joints of the rigid frame.

In the case considered and for the 2nd stage, we suppose that joints of "double elastic freedom" suffer no rotation during displacement, and joints of "single elastic freedom" rotate around the instantaneous center or rotation of the joint.

Thus, when member I is removed (Fig. 6), joint a is displaced without rotation, and joints b and c rotate around their instantaneous centres of rotation o_b and o_c .

Below are calculated the fixing moments of a member connecting joints of "single elastic freedom". The equations given are general. Special cases of joints of double elastic freedom and also of one joint of single elastic freedom and one of double elastic freedom are also considered.

(a) Joints of Single elastic freedom.

In Fig. 7 we have joints a and b of single elastic freedom connected together by member i and moments M_{ai} and M_{bi} at sections a_i and b_i are required as well as the moments at α° and β° distances a'_{ai} and a'_{bi} from the sections a_i and b_i and for a displacement δ_i of the point where the "imaginary" pin jointed member of joint b.

Using the diagram of virtual displacement and in connection with the displacement placement δ_i we calculate the rotations ϑ_b , ϑ_a and ϑ_i of joints b, a and member i respectively, by using the equations:

$$\vartheta_b = \rho_b \delta_i \qquad \vartheta_a = \rho_a \delta_i \qquad \vartheta_i = \rho_i \delta_i \tag{25}$$

where:

$$\rho_b = \pm \frac{1}{e_{bo}} \qquad \rho_a = \pm \frac{1}{e_{bo}} \cdot \frac{e_{bi}}{e'_{bi}} \cdot \frac{e'_{ai}}{e_{ai}} \qquad \rho_i = \pm \frac{1}{e_{bo}} \cdot \frac{e_{bi}}{e'_{bi}} \tag{26}$$

In Eqs. (26) constants are either positive or negative depending on whether the rotation ϑ around the instantaneous centres o_a , o_b, o_i are clockwise or counter-clockwise.

Displacements δ_{bi} , δ_i , δ_{ai} and $\delta_r = \delta_{ar}$ (Fig. 9) are found from the equations:

$$\delta_{bi} = c_{bi} \delta_i \qquad \delta_i = c_i \delta_i \qquad \delta_{ai} = c_{ai} \delta_i \qquad \delta_r = \delta_{ar} = c_{ar} \delta_i \tag{27}$$

where

$$c_{bi} = \pm \rho_b e_{bi} \qquad c_i = \pm \rho_i l_i \qquad c_{ai} = \pm \rho_a e_{ai} \qquad c_r = \pm \rho_a e_{ar} \tag{28}$$

Special Cases

(a) Members 0, 1 . . . which are connected to joint b are parallel.

In this case the constants ρ and c take the values:

$$\rho_b = 0 \qquad \rho_a = \pm \frac{1}{e'_{bi}} \cdot \frac{e'_{ai}}{e_{ai}} \qquad \rho_i = \pm \frac{1}{e'_{bi}} \tag{26'}$$

$$c_{bi} = \pm 1 \qquad c_i = \pm \rho_i l_i \qquad c_{ai} = \pm \rho_a e_{ai} \qquad c_r = \pm \rho_a e_{ar} \tag{28'}$$

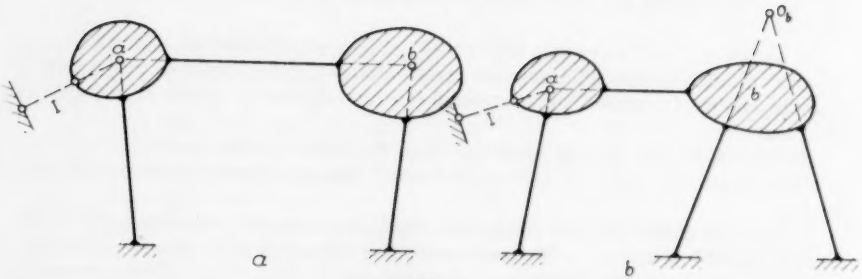

Fig. 5

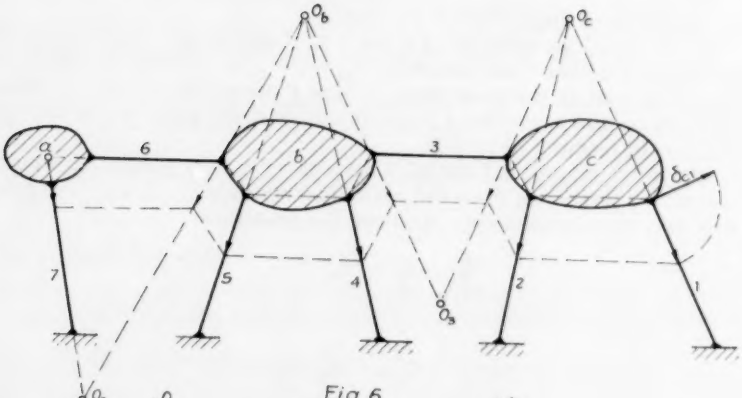

Fig. 6

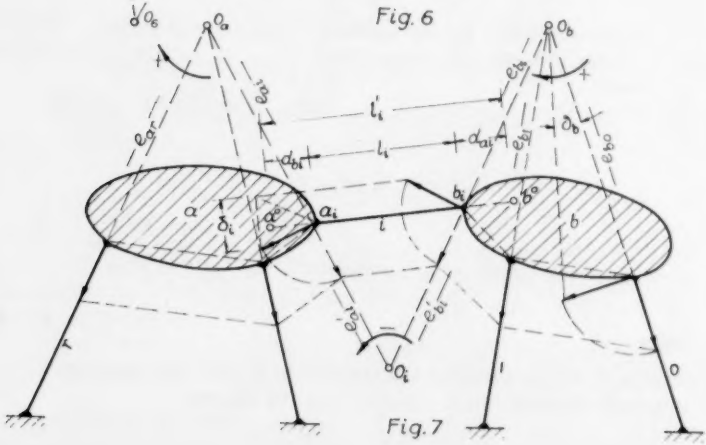

Fig. 7

b) The members connected to the joints a and b when taken as a total are parallel

$$\rho_b = 0 \qquad \rho_i = 0 \qquad \rho_a = 0 \tag{26''}$$

$$c_{bi} = \pm 1 \qquad c_i = 0 \qquad c_{ai} = \pm 1 \qquad c_F = \pm 1 \tag{28''}$$

Calculations of Moments M_{ai}, M_{bi}

Sections a_i and b_i (Fig. 7), due to the rotation of the joints a and b by ϑ_a and ϑ_b will rotate themselves, in accordance with the rules of solid mechanics, by the same angles ϑ_a and ϑ_b and in the same direction.

The equations with the help of which we calculate the moments M_{ai} and M_{bi} are:

$$\begin{aligned} M_{ai} &= -(\alpha_{ai}\vartheta_a + \mu_i \alpha_{bi}\vartheta_b) + u_{ai}\frac{\delta_i}{l_i} \\ M_{bi} &= -(\mu_i \alpha_{ai}\vartheta_a + \alpha_{bi}\vartheta_b) + u_{bi}\frac{\delta_i}{l_i} \end{aligned} \tag{29}$$

In the above Eq. (29), the moments due to the rotations by ϑ_a and ϑ_b are entered with negative signs because a clockwise rotation of the sections by ϑ_a and ϑ_b causes negative moments to the sections a_i and b_i .

Substituting the values for ϑ_a, ϑ_b and δ_i from (25) and (27) in (29) we obtain:

$$M_{ai} = u^o_{ai}\frac{\delta_i}{l_i} \qquad M_{bi} = u^o_{bi}\frac{\delta_i}{l_i} \tag{30}$$

where

$$\begin{aligned} u^o_{ai} &= u_{ai}\left[-\left(\frac{\alpha_{ai}}{u_{ai}}\rho_a + \mu_i\frac{\alpha_{bi}}{u_{ai}}\rho_b\right)l_i + c_i\right] \\ u^o_{bi} &= u_{bi}\left[-\left(\mu_i\frac{\alpha_{ai}}{u_{bi}}\rho_a + \frac{\alpha_{bi}}{u_{bi}}\rho_b\right)l_i + c_i\right] \end{aligned} \tag{31}$$

The shearing forces are given by the equation:

$$Q_i = Q_{ai} = Q_{bi} = \frac{u^o_{ai} + u^o_{bi}}{l_i}\cdot\frac{\delta_i}{l_i} \tag{32}$$

For straight members with constant moment of inertia, Eqs. (31) take the form:

1) Member built-in at both ends.

$$\begin{aligned} u_{ai} &= u_{bi} = \frac{6EJ_i}{l_i} \quad \alpha_{ai} = \alpha_{bi} = \frac{4EJ_i}{l_i} \quad \mu_i = +\frac{1}{2} \\ u^o_{ai} &= \left[-(2\rho_a + \rho_b)\frac{l_i}{3} + c_i\right]\frac{6EJ_i}{l_i} \\ u^o_{bi} &= \left[-(\rho_a + 2\rho_b)\frac{l_i}{3} + c_i\right]\frac{6EJ_i}{l_i} \end{aligned} \tag{33}$$

2) Member built-in at one end—Pinned at section

$$\begin{aligned} u_{ai} &= \frac{3EJ_i}{l_i} \quad u_{bi} = 0 \quad \alpha_{ai} = \frac{3EJ_i}{l_i} \quad \alpha_{bi} = 0 \quad \mu_i = 0 \\ u^o_{ai} &= (-\rho_a l_i + c_i)\frac{3EJ_i}{l_i} \\ u^o_{bi} &= 0 \end{aligned} \tag{34}$$

3) Member built-in at one end—Pinned at section

$$u^{\circ}_{ai}=0$$
$$u^{\circ}_{bi}=(-\rho_b l_i+c_i)\frac{3EJ_i}{l_i} \tag{35}$$

Calculation of Moments M'_{ai} and M'_{bi}

The moments M'_{ai} and M'_{bi} are given by the equations:

$$M'_{ai}=M_{ai}+Q_{ai}\,d_{ai}$$
$$M'_{bi}=M_{bi}+Q_{bi}\,d_{bi} \tag{36}$$

If in the above Eqs. (36) we substitute the values for M_{ai}, M_{bi} from Eqs. (30) and Q_{ai}, Q_{bi} from Eqs. (32), we obtain:

$$M'_{ai}=\bar{u}_{ai}\frac{\delta_i}{l_i}$$
$$M'_{bi}=\bar{u}_{bi}\frac{\delta_i}{l_i} \tag{37}$$

where:

$$\bar{u}_{ai}=u^{\circ}_{ai}\left(1+\frac{d_{ai}}{l_i}\right)+u^{\circ}_{bi}\frac{d_{ai}}{l_i}$$
$$\bar{u}_{bi}=u^{\circ}_{ai}\frac{d_{bi}}{l_i}+u^{\circ}_{bi}\left(1+\frac{d_{bi}}{l_i}\right) \tag{38}$$

Comparing Eqs. (30) and (37) we draw the conclusion that Eqs. (37) are the general form of those of Eq. (30) because when $d_{ai} = d_{bi} = 0$, by substituting these values in Eq. (37) we obtain Eq. (30), i.e. the moments M_{ai}, M_{bi} at sections a_i and b_i.

In accordance with the above, the moments M_{ai} and M_{bi} are calculated using Eqs. (37) where, for $d_{ai} = d_{bi} = 0$, we have

$$\bar{u}_{ai}=u^{\circ}_{ai} \qquad \bar{u}_{bi}=u^{\circ}_{bi} \tag{39}$$

Joints of "Double Elastic Freedom"

Joints a and b of Fig. 8 are of "double elastic freedom" and are connected together by the member i which has an instantaneous centre of rotation o_i.

The diagram of virtual displacement has been drawn for a given displacement δ_b.

Angle ϑ_i can be expressed in terms of δ_b (for infinitely small displacements) by the equation:

$$\vartheta_i=\frac{\delta_b}{e^{\circ}_{bi}} \tag{40}$$

From Fig. 8 we obtain the equations:

$$\delta_a=c_a\delta_b\,, \quad \delta_i=c_i\delta_b\,, \quad n_i=\frac{h_i}{e_{bi}} \tag{41}$$

where:

$$c_a=\frac{e^{\circ}_{ai}}{e^{\circ}_{bi}} \qquad c_i=\frac{e'_i}{e^{\circ}_{bi}} \tag{42}$$

Joints a and b when displaced suffer no rotation. By making this supposition, sections a_i and b_i will take the positions a'_i, b'_i (Fig. 8). The relative displacement of sections a_i, b_i normal to the direction of the member is that calculated δ_i.

The difference of the constant c_i for joints of a single and double elastic freedom results from the fact that in the first case we take the span l_i and in the second the span l_i'.

The moments M'_{ai}, M'_{bi}, M_{ai} and M_{bi} are calculated by making use of the general Eqs. (37) and (30) in which the factors $\bar{u}_{ai}$, $\bar{u}_{bi}$, u^o_{ai}, u^o_{bi} take the values:

For $\rho_a = \rho_b = 0$ we have (Eqs. (33 and 38))

$$u^o_{ai} = c_i u_{ai} \qquad u^o_{bi} = c_i u_{bi}$$

$$\bar{u}_{ai} = \left[u_{ai}\left(1+\frac{\alpha_{ai}}{l_i}\right) + u_{bi}\frac{\alpha'_{ai}}{l_i}\right] c_i \tag{43}$$

$$\bar{u}_{bi} = \left[u_{ai}\frac{\alpha'_{bi}}{l_i} + \left(1+\frac{\alpha'_{bi}}{l_i}\right) u_{bi}\right] c_i \tag{44}$$

In the case of straight members of constant moment of inertia, Eq. (43) and (44) take the forms:

1) Member built-in at both ends

$$u^o_{ai} = u^o_{bi} = \frac{6EJ_i}{l_i} c_i \tag{45}$$

$$\bar{u}_{ai} = \frac{6EJ_i}{l_i}\left(1+2\frac{\alpha_{ai}}{l_i}\right) c_i \tag{46}$$

$$\bar{u}_{bi} = \frac{6EJ_i}{l_i}\left(1+2\frac{\alpha'_{bi}}{l_i}\right) c_i$$

2) Member built-in at one end—Pinned at b_i

$$u^o_{ai} = \frac{3EJ_i}{l_i} c_i \qquad u^o_{bi} = 0 \tag{45'}$$

$$\bar{u}_{ai} = \frac{3EJ_i}{l_i}\left(1+\frac{\alpha'_{ai}}{l_i}\right) c_i \tag{46'}$$

$$\bar{u}_{bi} = \frac{3EJ_i}{l_i}\frac{\alpha'_{bi}}{l_i} c_i$$

Joint A of Double Elastic Freedom—Joint B of Single Elastic Freedom

In this case (Fig. 9) we have:

$$\delta_b = \rho_b \delta_i \qquad \delta_a = 0 \qquad \delta_i = \rho_i \delta_i \tag{47}$$

where

$$\rho_b = \pm\frac{1}{e_{bo}} \qquad \rho_i = \pm\frac{1}{e_{bo}}\cdot\frac{e_{bi}}{e_{bi}} \tag{48}$$

The displacements are given by the equations:

$$\left.\begin{aligned} \delta_{bi} &= c_{bi}\delta_i \qquad \delta_i = c_i \delta_i \\ \delta_a &= c_a \delta_i \qquad \delta_r - \delta_{ar} = c_{ar}\delta_i \end{aligned}\right\} \tag{49}$$

where:

$$\left.\begin{aligned} c_{bi} &= \pm\rho_b e_{bi} \qquad c_i = \pm\rho_i l_i' \\ c_a &= \pm e^o_{ai}\rho_i \qquad c_r = c_{ra} = \pm e_{ar}\rho_i \end{aligned}\right\} \tag{50}$$

The Moments M_{ai}, M_{bi} and M'_{ai} are calculated by using the general Eqs. (30) and (37) where the factors u^o_{ai}, u^o_{bi} and $\bar{u}_{ai}$ take the values: for $\rho_a = 0$ we have: (Eqs. (31) and (38))

$$\left.\begin{aligned} u^o_{ai} &= u_{ai}\left(-\mu_i\frac{\alpha_{bi}}{u_{ai}}\rho_b\, l_i + c_i\right) \\ u^o_{bi} &= u_{bi}\left(-\frac{\alpha_{bi}}{u_{bi}}\rho_b\, l_i + c_i\right) \end{aligned}\right\} \tag{51}$$

$$\left.\begin{aligned} \bar{u}_{ai} &= u^o_{ai}\left(1+\frac{\alpha_{ai}}{l_i}\right) + u^o_{bi}\frac{\alpha'_{ai}}{l_i} \\ \bar{u}_{bi} &= u^o_{bi} \end{aligned}\right\} \tag{52}$$

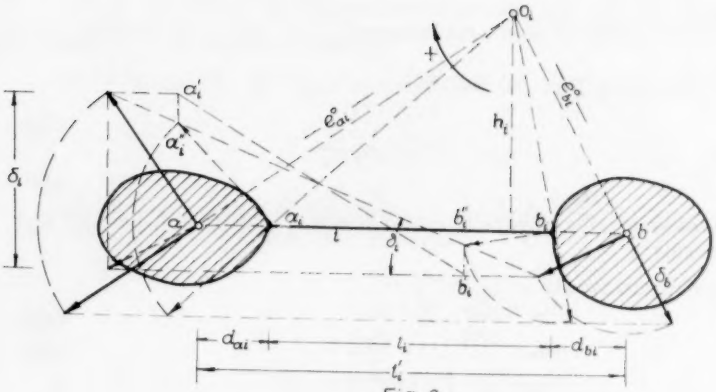

Fig. 8

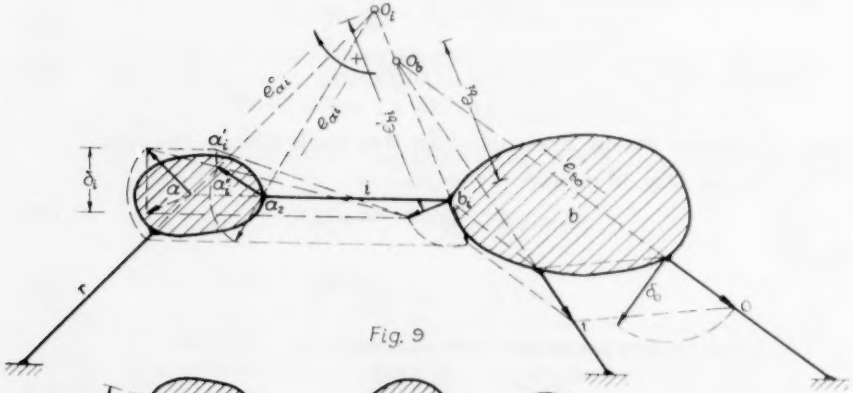

Fig. 9

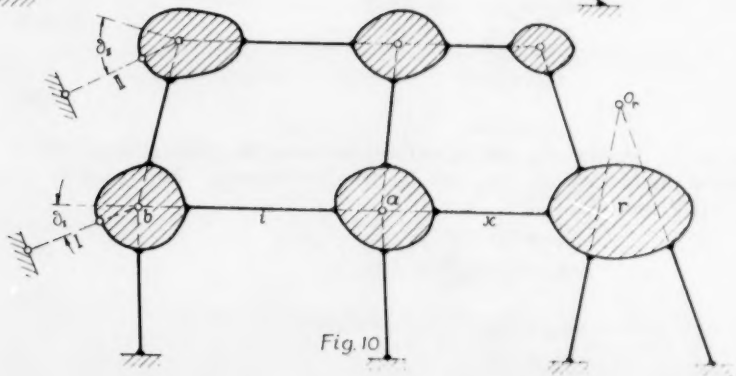

Fig. 10

For straight members with constant moment of inertia we have:

1) Member built-in at both ends:

$$\left.\begin{aligned} u^{o}_{ai} &= \frac{6EJ_i}{l_i}\left(-\rho_b \frac{l_i}{3} + c_i\right) \\ u^{o}_{bi} &= \frac{6EJ_i}{l_i}\left(-2\rho_b \frac{l_i}{3} + c_i\right) \end{aligned}\right\} \tag{53}$$

2) Member built-in at one end—Pinned at b_i

$$\left.\begin{aligned} u^{o}_{ai} &= u_{ai}\, c_i = \frac{3EJ_i}{l_i}\, c_i \\ u^{o}_{bi} &= 0 \end{aligned}\right\} \tag{53'}$$

3) Member built-in at one end—Pinned at a_i

$$\left.\begin{aligned} u^{o}_{ai} &= 0 \\ u^{o}_{bi} &= \frac{3EJ_i}{l_i}\left(-\rho_b l_i + c_i\right) \end{aligned}\right\} \tag{54}$$

Fixing Forces of 2nd Stage

The fixing forces of the second stage are calculated in a more simple way by the principle of virtual work.

We denote the diagrams of virtual displacement obtained by the removal of each of the imaginary pin jointed members (roller restraints) I, II, ... by the general symbols (Π^{I}) (Π^{II}) . . . . . respectively.

Also by δ_i^{I} , δ_i^{II} . . . . . c_i^{I} , c_i^{II}. . . . , we denote displacements δ and constants c of the respective member, for the removal of I, II . . .

The displacements δ_i^{I} , δ_i^{II} . . . and the constants c_i^{I} , c_i^{II} . . . are calculated with the help of the virtual displacement diagrams (Π^{I}), (Π^{II}), in conjunction with the geometry of the figure and the respective displacements δ_1 , δ_2 . . .

Also we denote by δ_a^{I} δ_a^{II} , . . . ρ_a^{I} ρ_a^{II} . . . . the rotations δ and the constants ρ of the joints of single elastic freedom.

If we now detach the members of the frame by taking sections close to the joints and apply to the joints forces Q^{I}_{ai} N^{I}_{ai} F_i^{I} F_i^{II} . . . and the moments M^{I}_{ai} for joints of single elastic freedom or M^{I}_{ai} for joints of double elastic freedom, each joint will be in equilibrium under these system of forces.

The equilibrium of the joints (taken as a whole) can be expressed by the principle of virtual work.

If we apply the principle of virtual work, e.g. for the stress condition which has resulted by the removal of the imaginary member I and (virtual) deformation the geometrical one which is taken from the diagram of virtual displacement (Π^{I}), we shall have:(2)

$$F_i^{I}\delta_i + \Sigma_\alpha \delta_\alpha \Sigma_\kappa M^{I}_{a\kappa} - \Sigma_i Q_i^{I}\delta_i^{I} = 0 \tag{55}$$

where: $Q_i^{I} = Q^{I}_{ai} = Q^{I}_{bi}$

Σ_α: summation extending to all joints of single elastic freedom.

Σ_κ : summation extending to all members of the group of condisplaced members I.

The sign of the third additive in (55) is minus because positive shearing force and positive displacement δ_i^{I} result in negative work.

The work done by the forces $F_{\beta}^{\prime}$, $F_{\beta}^{\prime}$, is equal to zero because the displacements of the points of application of II, III . . on the joints are normal to the directions of the imaginary pinned members I, II . . .

The forces $N_i^{\prime}$ do not appear in Eq. (55) because the work done by them, being equal and opposite, cancels each other.

Also the moments $M_{\alpha i}^{\prime}$ at the joints of double elastic freedom taken at each joint, give work equal to zero.

If in Eq. (54) we substitute the values for ϑ_{α} and $\delta_i^{\prime}$ as a function of δ_i , we obtain

$$F_i^{\prime} = \Sigma_i c_i^{\prime} Q_i^{\prime} - \Sigma_{\alpha} \varrho_{\alpha}^{\prime} \Sigma_{\kappa} M_{\alpha\kappa}^{\prime} \qquad (56)$$

Using Eq. (55) we calculate the fixing forces of the 2nd stage.

Stress Analysis of Rigid Frames by the Method of Successive Approximations in One Stage(2)

In the case of stress analysis of rigid frames by the method of successive approximations in one stage only, after the calculation of the fixed end moments and reactions, for joints suffering neither displacement nor rotation, we free to rotation successively the joints of double elastic freedom. Using the distribution and carry-over factors, the moments are calculated. By the help of the restraining factors(2) which will be calculated below, we work out the fixing forces F_{γ}^{α} . . . . . , F_{β}^{α} . . . . . , which are developed at the imaginary pin-jointed members due to allowing the joints to rotate.

After the successive freeing to rotation of the joints of the frame and the calculation of the fixing forces, we remove successively the imaginary pinned members applying at their points of connection equal and opposite forces to the calculated fixing forces. In this case we consider that joints of double elastic freedom are displaced without rotation and joints of single elastic freedom rotate around the instantaneous centre of rotation of the joint. With the help of the distribution factors due to displacement and shear carry-over which we shall work out below, we calculate the moments at the joints of the rigid frame and the fixing forces at the imaginary pinned members. The above work is repeated successively and thus we obtain the stress analysis of the rigid frame by successive approximations in one stage.(2)

Restraining Factors

In the stress analysis of (Fig. 10) all joints of double elastic freedom suffer no rotation except joint a on which acts the moment Ma.

To generalize the equation, we denote moments with the general symbol $(M_{\alpha i}^{\alpha})^{\prime}$ where:

$(M_{\alpha i}^{\alpha})^{\prime} = M_{\alpha i}^{\alpha}$ for joints of single elastic freedom

$(M_{\alpha i}^{\alpha})^{\prime} = M_{\alpha i}^{\alpha\prime}$ for joints of double elastic freedom

Lengths of members l_i are also denoted by the general symbol $(l_i)^{\prime}$ where:

$(l_i)^{\prime} = l_i$ for member joining joints of single elastic freedom

$(l_i)^{\prime} = l_i + \alpha_{\alpha i} + \alpha_{bi}$ for joints of double elastic freedom

$(l_i)^{\prime} = l_i + \alpha_{\alpha i}^{\prime}$ for joint a of double elastic freedom and joint b of single elastic freedom.

Moments $(M^{\alpha}_{\alpha i})'$ and $(M^{\alpha}_{bi})'$ are calculated from the equation (Fig. 16)

$$\left.\begin{aligned}(M^{\alpha}_{\alpha i})' &= (-M_{\alpha})\,\kappa_{\alpha i}\\ (M^{\alpha}_{bi})' &= (-M_{\alpha})\,\kappa_{\alpha i}\,\mu_{ab}\end{aligned}\right\} \tag{57}$$

The shearing force is given by equation:

$$Q^{\alpha}_{\alpha i} = Q^{\alpha}_{bi} = Q^{\alpha}_{i} = (-M_{\alpha})\,\frac{\kappa_{\alpha i}\,(1+\mu_{ab})}{(l_i)'} \tag{58}$$

The calculation of the fixing force $F_I{}^{a}$ is given below. The remaining F^{α}_{II} F^{α}_{III} . . . . , are calculated in a similar way as F^{α}_{i} .

If we express the equilibrium of the forces on the joints $M^{\alpha}_{\alpha i}$ Q^{α}_{i} N^{α}_{i} and $F^{a}{}_{I}$, $F^{a}{}_{II}$ . . . (taken as a whole) by the principle of virtual work, taking as virtual deformation the (Π'), we shall have the equation (Fig. 10)

$$F^{\alpha}_{i}\,\delta_i \cos\vartheta_i - \Sigma_i\, Q^{t}_{i}\,\delta^{t}_{i} + \Sigma_r\, M^{\alpha}_{rx}\,\vartheta^{t}_{r} = 0 \tag{59}$$

The moment M^{α}_{rx} , as a function of the factor of distribution due to rotation $K_{\alpha r}$ and the carry-over factor $\mu_{\alpha r}$, is given by the equation:

$$M^{\alpha}_{rx} = (-M_{\alpha})\,\mu_{\alpha r}\,\kappa_{\alpha x} \tag{60}$$

If now in Eq. (59) we replace δ^{t}_{i} and ϑ^{t}_{i} as functions of δ_i and substitute the values for Q^{α}_{i} and M^{α}_{rx} from Eqs. (58) and (60) we shall have:

$$F^{\alpha}_{i} = (-M_{\alpha})\,\epsilon_{\alpha i} \tag{61}$$

where

$$\epsilon_{\alpha i} = \frac{1}{\cos\vartheta_i}\left[\Sigma_i\,\frac{\kappa_{\alpha i}(1+\mu_{ab})\,c^{t}_{i}}{l_i} - \Sigma_r\,\rho^{t}_{r}\,\Sigma_x\,\mu_{\alpha x}\,\kappa_{\alpha x}\right] \tag{62}$$

The summation extends to the joints r of single elastic freedom next to the joint under consideration (Fig. 10)

For $\vartheta_i = 0$ we have:

$$\epsilon_{\alpha i} = \Sigma_i\,\frac{\kappa_{\alpha i}\,(1+\mu_{ab})\,c^{t}_{i}}{l_i} - \Sigma_r\,\rho^{t}_{r}\,\Sigma_x\,\mu_{\alpha x}\,\kappa_{\alpha x} \tag{62'}$$

By the Eqs. (62) or (62') we obtain the restraining factors of the joints of double elastic freedom of the rigid frame.

The dimensions of the "restraining factor" are 1/length.

Distribution Factors Due to Displacement

After the removal of the imaginary pinned member, e.g. I, we apply on the joint at the point of connections, force equal to $-F_i$, i.e. equal and opposite to the calculated fixing force at position I.

$$F_i = F^{\circ}_{i} + F^{\alpha}_{i} + F^{b}_{i} + \ldots . \tag{63}$$

where:

F°_{i} is the fixing force at position I for the case of perfectly rigid joints (neither rotation nor displacement allowed) of the frame.

Due to the force $-F_I$, the joints of the rigid frame will be displaced. We suppose that during this displacement, joints of double elastic freedom will not rotate and these of single elastic freedom will rotate around the instantaneous centre of rotation.

Due to the displacement of the joints of the rigid frame, forces Q_i^t , N_i^t and moments $(M_{ai}^t)'$ will develop at the sections next to the joints.

The moments $(M_{ai}^t)'$ and $(M_{bi}^t)'$, are given by the general Eqs. (37)

$$\left.\begin{aligned}(M_{ai}^t)' &= \bar{u}_{ai}^t \frac{\delta_i}{l_i} \\ (M_{bi}^t)' &= \bar{u}_{bi}^t \frac{\delta_i}{l_i}\end{aligned}\right\} \tag{64}$$

The shear forces are given by the general equation:

$$Q_i^t - Q_{ai}^t = Q_{bi}^t = \frac{\bar{u}_{ai}^t + \bar{u}_{bi}^t}{(l_i)'} \frac{\delta_i}{l_i} \tag{65}$$

If we express the equilibrium of the forces acting on the joint of the rigid frame by the "principle of virtual work" taking as virtual deformation the elastic one given by the diagram of virtual displacement (Π^t), we shall have the equation:

$$(-F_i)\,\delta_i \cos\vartheta_i - \Sigma_i\, Q_i^t\, \delta_i^t + \Sigma_r\, \vartheta_r^t \Sigma_x\, (M_{rx}^t)' = 0 \tag{66}$$

where Σ_i summation extending to all member i of group I.

Σ_r summation extending to all joints r of single elastic freedom of group I.

If in Eq. (66) we replace the values for Q^I_r, and $(M^I_{rk})'$ from Eq. (64) and (65) and express δ_i^t and ϑ_r^t as functions of the displacement δ^t we shall obtain:

$$\delta_i = (-F_i) \frac{\cos\vartheta_i}{\Sigma_i \frac{\bar{u}_{ai}^t + \bar{u}_{bi}^t}{(l_i)'} \frac{c_i^t}{l_i} \Sigma_r\, \varrho_r^t \Sigma_x \frac{\bar{u}_{rx}^t}{l_x}} \tag{67}$$

Combining (64) and (67) we have:

$$(M_{ai}^t)' = (-F_i)\, \bar{q}_{ai}^t \tag{68}$$

where:

$$\bar{q}_{ai}^t = \frac{\frac{\bar{u}_{ai}^t}{l_i}}{\Sigma_i \frac{\bar{u}_{ai}^t + \bar{u}_{bi}^t}{(l_i)'} \frac{c_i^t}{l_i} - \Sigma_r \varrho_r^t \Sigma_x \frac{\bar{u}_{rx}^t}{l_x}} \tag{69}$$

In the case of angle $\vartheta_i = 0$ Eq. (69) becomes:

$$q_{ai} = \frac{\frac{\bar{u}_{ai}^t}{l_i}}{\Sigma_i \frac{\bar{u}_{ai}^t + \bar{u}_{bi}^t}{(l_i)'} \frac{c_i^t}{l_i} - \Sigma_r \varrho_r^t \Sigma_x \frac{\bar{u}_{rx}^t}{l_x}} \tag{69'}$$

Eqs. (69) and (69') give us the distribution factors due to displacement.

Check

The shearing forces as function of the moments $(M_{ai}^t)'$ are given by the equations:

$$Q_i^t = (-F_i) \frac{\bar{q}_{ai}^t + \bar{q}_{bi}^t}{(l_i)'}$$

If we apply the principle of virtual works for the calculated, shearing forces, normal forces and moments of group I, due to $-F_I$ and virtual deformation" the geometrical one given by the diagram of virtual displacement (Π^t), we obtain:

$$(-F_i)\,\delta_i \cos\delta_i - \Sigma_i\,(-F_i)\,\frac{\bar{q}'_{ai}+\bar{q}'_{bi}}{(l_i)'}\,\delta'_i + \Sigma_r\,\delta'_r\,\Sigma_\kappa\,\bar{q}'_{r\kappa}\,(-F_i) = 0$$

If now in the above equation we place the values for δ'_i and δ'_r in terms of the displacement δ_i and the constants c'_i and ρ'_r, we have the equation:

$$\Sigma_i\,\frac{\bar{q}'_{ai}+\bar{q}'_{bi}}{(l_i)'}\,c'_i - \Sigma_r\,\rho'_r\,\Sigma_\kappa\,\bar{q}'_{r\kappa} = \cos\delta_i$$

For angle $\delta_i = 0$ the above relation becomes:

$$\Sigma_i\,\frac{\bar{q}'_{ai}+\bar{q}'_{bi}}{(l_i)'}\,c'_i - \Sigma_r\,\rho'_r\,\Sigma_\kappa\,\bar{q}'_{r\kappa} = 1 \qquad (69^n)$$

Remarks

The factors $\bar{u}'_{ai}$ take the following forms depending on whether the joint is of single or double elastic freedom.

1) For joints of single elastic freedom:

$$(M'_{ai})' = M'_{ai} \qquad \bar{u}'_{ai} = u^\circ_{ai} \qquad \text{(equation 31)}$$

2) For joints of double elastic freedom: $(M'_{ai})' = M'^{\,\prime}_{ai}$

$$\bar{u}_{ai} = u^\circ_{ai}\,\left(1+\frac{\alpha'_{ai}}{l_i}\right) + u^\circ_{bi}\,\frac{\alpha'_{ai}}{l_i}$$

$$\bar{u}_{bi} = u^\circ_{ai}\,\frac{\alpha'_{bi}}{l_i} + u^\circ_{bi}\,\left(1+\frac{\alpha'_{bi}}{l_i}\right) \qquad \text{(equation 38)}$$

Shear Carry-Over Factors

In the rigid frame, besides the pinned member I, exist also II, III, . . . Due to the removal of I and application to the joint where I is connected of force $-F_I$, fixing forces F^I_{II}, F^I_{III}, . . are developed on the remaining members II, III, . . . of which we require the value in terms of $-F_I$.

We give below the calculation of the fixing force F^I_{II}.

If we express the equilibrium of the forces acting on the joint, by the principle of virtual works, taking as virtual deformation that given by the diagram of virtual displacement (Π^{II}) we shall have the equation:

$$F'_{II}\cos\delta^{II}_{II}\,\delta_{II} - \Sigma_i\,Q'_i\,\delta^{II}_i + \Sigma_r\,\delta^{II}_r\,\Sigma_\kappa\,(M'_{r\kappa})' \qquad (70)$$

If in Eq. (70) we express the displacements δ^{II}_i, δ^{II}_r in terms of the constants c^{II}_i, ρ^{II}_r and displacement δ_{II}, and solve it with regards F^I_{II}, we obtain:

$$F'_{II} = \frac{\Sigma_i\,Q'_i\,c^{II}_i - \Sigma_r\,\rho^{II}_r\,\Sigma_\kappa\,(M'_{r\kappa})'}{\cos\delta^{II}_{II}} \qquad (71)$$

The shearing forces Q'_i and moments $(M'_{r\kappa})'$ are given by the equations:

$$Q'_i = \frac{\bar{q}'_{ai}+\bar{q}'_{bi}}{l_i}\,(-F_i) \qquad (72)$$

$$(M'_{r\kappa})' = (-F_i)\,\bar{q}'_{r\kappa} \qquad (73)$$

If in Eq. (71) we replace the values for Q^I_i and $(M'_{r\kappa})'$, from (72) and (73), we obtain:

$$F'_{II} = (-F_i)\,m^I_{II} \qquad (74)$$

where:

$$m_x' = \frac{1}{\cos \delta_x} \left[\Sigma_i \left(\bar{q}_{ai}' + \bar{q}_{bi}' \right) \frac{C_i''}{(l_i)'} - \Sigma_r \rho_r'' \Sigma_\kappa \bar{q}_{r\kappa}' \right] \tag{75}$$

For the case of angle $\delta_x = 0$ Eq. (75) becomes:

$$m_x' = \Sigma_i \left(\bar{q}_{ai}' + \bar{q}_{bi}' \right) \frac{C_i''}{(l_i)'} - \Sigma_r \rho_r'' \Sigma_\kappa \bar{q}_{r\kappa}' \tag{75'}$$

where:

Σ_κ summation extending to members κ connected to joint r of single elastic freedom.

Layout of the Work of Successive Approximation

The layout of the work of successive approximations is given again here in a table form (example 4th) as in the case where joints are taken as points.(2)

The final total moments are obtained by adding up all values, in the squares, of the bending moments at the sections by the joints of the members of the rigid frame.

CONCLUSION

The present study constitutes the general form of the method of successive approximation for rigid frames whose joints are not points or infinitely small areas, an assumption which is made in all up to day classical methods of stress analysis of rigid frames, but areas of limited dimensions, which at the analysis of the rigid frame, are taken as solid areas suffering no deformation.

We can say that the equations given, both for the analysis in one stage or two stages, constitute the generalized form of the method of successive approximation. The equations known up to day for the analysis of rigid frames can be considered as a special case of the generalized ones.

Besides the theoretical interest of the study, in certain cases either due to the interposition of partition or due to large dimensions of sections of certain members of the rigid frame, it is possible to have types of rigid frames for which the joints cannot be considered as being either points or infinitely small areas. The stress analysis of such types of frames by the method suggestion is in our opinion, simple and rapid.

In order to make more clear the application of this method, we give below four examples.

1st Example (Fig. 11)

Moments $M_{\alpha i}$

$$\bar{M}_{a1} = -\bar{M}_{b1} = \frac{2000 \times 5.5^2}{12} = 5050 \text{ kgm} \qquad \bar{M}_{b2} = -\bar{M}_{c2} = \frac{2000 \times 6.5^2}{12} = 7080 \text{ kgm}$$

$$\bar{M}_{c3} = -\bar{M}_{x3} = \frac{2000 \times 5^2}{12} = 4160 \text{ kgm}$$

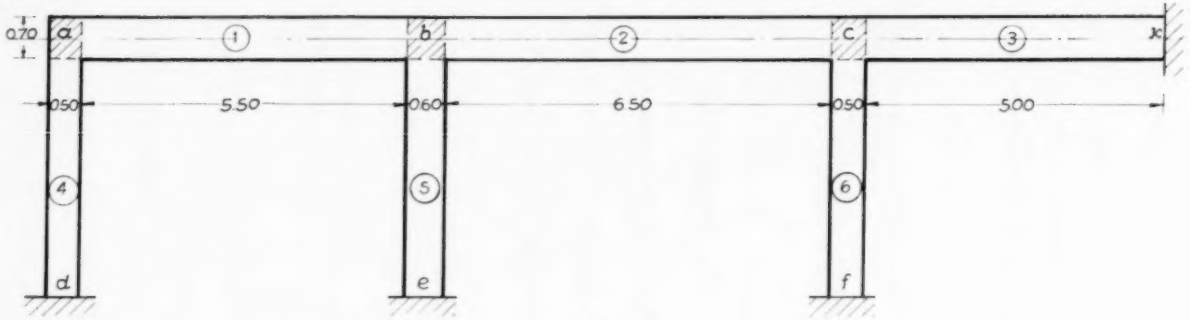
0.70
a
b
c
x
1
2
3
0.50
5.50
0.60
6.50
0.50
5.00
4
5
6
d
e
f

Fig. 11

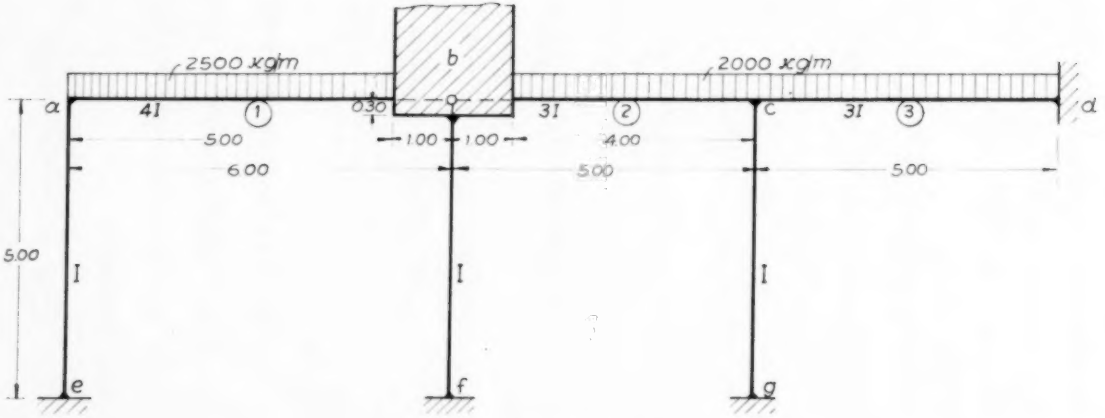
2500 kg/m
2000 kg/m
b
a
4I
1
0.30
3I
2
c
3I
3
d
5.00
1.00
1.00
4.00
6.00
5.00
5.00
5.00
I
I
I
e
f
g

Fig. 12

Shearing Forces

$$Q^{o}_{a1} = -Q^{o}_{b1} = \frac{2000 \times 5.5}{2} = 5500 \text{ kg} \qquad Q^{o}_{b2} = -Q^{o}_{c2} = \frac{2000 \times 6.5}{2} = 6500 \text{ kg}$$

$$\bar{Q}_{a1} = -\bar{Q}_{b1} = \bar{Q}^{o}_{a1} = -Q^{o}_{b1} \qquad \bar{Q}_{b2} = -\bar{Q}_{c2} = Q^{o}_{b2} = -Q^{o}_{c2}$$

$$Q^{o}_{c3} = \frac{2000 \times 5}{2} = 5000 \text{ kg} \qquad \bar{Q}_{c3} = Q^{o}_{c3}$$

Fixed-End Moments

$$\bar{M}'_{a1} = 5050 + 5500 \times 0.25 = 6425 \text{ kgm} \qquad \bar{M}'_{b1} = -5050 - 0.30 \times 5500 = -6700 \text{ kgm}$$

$$\bar{M}'_{b2} = +7080 + 0.30 \times 6500 = +9030 \text{ kgm} \qquad \bar{M}'_{c2} = -7080 - 0.25 \times 6500 = -8700 \text{ kgm}$$

$$\bar{M}'_{c3} = +4160 + 0.25 \times 5000 = +5410$$

Distribution Factors

$$I_1 = I_2 = I_3 = 2.75 I_4 \qquad I_5 = 1.6 I_4 \qquad I_6 = I_4$$

$$d_{a1} = 0.25 \qquad d_{a4} = 0.35 \qquad d_{b1} = 0.30 \qquad d_{b2} = 0.30 \qquad d_{b5} = 0.35 \qquad d_{c2} = 0.25$$

$$d_{c3} = 0.25 \qquad d_{c6} = 0.35$$

$$\frac{d_{a1}}{l_1} = \frac{0.25}{5.5} = 0.045 \qquad \frac{d_{a4}}{l_4} = \frac{0.35}{400} = 0.087 \qquad \frac{d_{b1}}{l_1} = \frac{0.30}{5.5} = 0.054 \qquad \frac{d_{b2}}{l_2} = \frac{0.30}{6.5} = 0.046$$

$$\frac{d_{b5}}{l_5} = \frac{0.35}{400} = 0.087 \qquad \frac{d_{c2}}{l_2} = \frac{0.25}{6.5} = 0.038 \qquad \frac{d_{c3}}{l_3} = \frac{0.25}{500} = 0.05 \qquad \frac{d_{c6}}{l_6} = \frac{0.35}{400} = 0.087$$

Working out for b_{ai} we neglect the quantity $\left(\frac{d_{ai}}{l_i}\right)^2$ as being very small:

Joint a:

$$b_{a1} = \frac{4E \times 2.75 \times I}{5.50}(1 + 3 \times 0.045) = 2.27 EI \qquad x_{a1} = \frac{2.27}{3.531} = 0.643$$

$$b_{a4} = \frac{4E \times I}{400}(1 + 3 \times 0.087) = \frac{1.261 EI}{3.531 EI} \qquad x_{a4} = \frac{1.261}{3.531} = \frac{0.357}{1.000}$$

Joint b:

$$b_{b1} = \frac{4E \times 2.75 I}{5.50}(1 + 3 \times 0.054) = 2.33 EI \qquad x_{b1} = \frac{2.33}{6.27} = 0.372$$

$$b_{b2} = \frac{4E \times 2.75 I}{6.5}(1 + 3 \times 0.046) = 1.92 EI \qquad x_{b2} = \frac{1.92}{6.27} = 0.306$$

$$b_{b5} = \frac{4E \times 1.6 I}{400}(1 + 3 \times 0.087) = \frac{2.02 EI}{6.27 EI} \qquad x_{b5} = \frac{2.02}{6.27} = \frac{0.322}{1.000}$$

Joint c:

$$b_{c2} = \frac{4E \times 2.75 I}{6.5}(1 + 3 \times 0.038) = 1.89 EI \qquad x_{c2} = \frac{1.89}{5.68} = 0.332$$

$$b_{c3} = \frac{4E \times 2.75 I}{500}(1 + 3 \times 0.05) = 2.53 EI \qquad x_{c3} = \frac{2.53}{5.68} = 0.446$$

$$b_{c6} = \frac{4E \times I}{4}(1 + 3 \times 0.087) = \frac{1.26 EI}{5.68 EI} \qquad x_{c6} = \frac{1.26}{5.68} = \frac{0.222}{1.000}$$

Carry-Over Factors:

$$\mu_{ab} = \frac{1}{2} \cdot \frac{1 + \frac{0.25 + 0.30}{5.5} \times 3 + 6 \times \frac{0.25 \times 0.30}{5.5^2}}{1.135} = 0.580$$

$$\mu_{ad} = \frac{1}{2} \cdot \frac{1 + 3 \times \frac{0.35}{4}}{1.261} \cong 0.500$$

$$\mu_{ba}=\frac{1}{2}\,\frac{1+3\,\frac{0.25+0.30}{5.5}+6\,\frac{0.25\times0.30}{5.5^2}}{1.162}=0.565$$

$$\mu_{bc}=\frac{1}{2}\,\frac{1+3\,\frac{0.30\times0.25}{6.5}+6\times\frac{0.25\times0.30}{6.5^2}}{1.138}=0.558$$

$$\mu_{be}=\frac{1}{2}\,\frac{1+3\,\frac{0.35}{4}}{1.261}\cong0.500$$

$$\mu_{cb}=\frac{1}{2}\,\frac{1+3\,\frac{0.30+0.25}{6.5}+6\,\frac{0.25\times0.30}{6.5^2}}{1.114}=0.568$$

$$\mu_{cx}=\frac{1}{2}\,\frac{1+\frac{0.25}{5}\times3}{1.15}\cong0.500 \qquad \mu_{cf}=\frac{1}{2}\,\frac{1+3\,\frac{0.35}{4}}{1.261}\cong0.500$$

The successive approximations and the values of M'_{ai} are given in Table I
Shearing forces

$$Q_{a1}=5500+\frac{2254-9277}{5.95}=4320 \qquad Q_{b1}=5500+\frac{2254-9277}{5.95}=-6680$$

$$Q_{b2}=6500+\frac{9468-7674}{7.05}=6754 \qquad Q_{c2}=-6500+\frac{9468-7674}{7.05}=-6246$$

$$Q_{c3}=5000+\frac{6921-3405}{5.25}=5670 \qquad Q_{a4}=\frac{-2254-1128}{4.35}=-795$$

$$Q_{b5}=\frac{-191-95}{4.35}=-47 \qquad Q_{c6}=\frac{753+376}{4.35}=+266$$

Total moments:

$$M_{a1}=2254-4320\times0.25=+1174 \qquad M_{b1}=-9277+6680\times0.30=-6277\ kgm$$

$$M_{b2}=9468-6754\times0.25=7783\ kgm \qquad M_{c2}=-7674+6246\times0.25=-6144\ kgm$$

$$M_{c3}=+6921-5670\times0.25=5501\ kgm$$

2nd Example (Fig. 12)

Distribution Factors:
Joint a:

$$b_{a1}=\frac{4E\times4I}{5.50}=2.91EI \qquad K_{a1}=\frac{2.91}{3.71}=0.785$$

$$b_{a4}=\frac{4EI}{5.00}=\frac{0.80EI}{3.71\,EI} \qquad K_{a4}=\frac{0.80}{3.71}=\frac{0.215}{1.000}$$

Joint b:

$$b_{a1}=\frac{4E\times4I}{5.5}\left[1+3\,\frac{1}{5.5}+3\left(\frac{1}{5.5}\right)^2\right]=4.78EI \qquad K_{b1}=\frac{4.78}{11.60}=0.412$$

$$b_{b2}=\frac{4E\times3I}{4.00}\left[1+3\,\frac{1}{4}+3\left(\frac{1}{4}\right)^2\right]=5.81EI \qquad K_{b2}=\frac{5.81}{11.60}=0.501$$

$$b_{b5}=\frac{4EI}{4.70}\left(1+3\,\frac{0.30}{4.70}\right)=\frac{1.01EI}{11.60EI} \qquad K_{b5}=\frac{1.01}{11.60}=\frac{0.087}{1.000}$$

Joint c:

$$b_{c2}=\frac{4E\times 31}{400}=3EI \qquad \varkappa_{c2}=\frac{300}{620}=0.485$$

$$b_{c3}=\frac{4E\times 31}{500}=240EI \qquad \varkappa_{c3}=\frac{240}{6.20}=0.386$$

$$b_{c6}=\frac{4EI}{500}=\frac{080EI}{620EI} \qquad \varkappa_{c6}=\frac{0.80}{6.20}=\frac{0.129}{1000}$$

Moments $\bar{M}_{ai}$

$$\bar{M}_{a1}=-\bar{M}_{b1}=\frac{2500\times 5.5^2}{12}=6300\ kg \qquad \bar{M}_{b2}=-\bar{M}_{c2}=\frac{2000\times 4^2}{12}=2660\ kg$$

$$\bar{M}_{c3}=-\bar{M}_{d3}=\frac{2000\times 5^2}{12}=4160\ kg$$

Shearing forces:

$$\bar{Q}_{b1}=Q^{o}_{b1}=-\frac{2500\times 5.5}{2}=-6880\ kg$$

$$\bar{Q}_{b2}=Q^{o}_{b2}=+\frac{2000\times 4.0}{2}=+4000\ kg$$

Fixed-end moments:

$$\bar{M}'_{a1}=+6300\ kg \qquad \bar{M}'_{b1}=-6300-6880\times 1.0=-13180\ kg$$

$$\bar{M}'_{b2}=+2660+4000\times 1=6660 \qquad \bar{M}'_{c2}=-2660\ kg$$

$$\bar{M}'_{c3}=-\bar{M}'_{d3}=4160\ kg$$

Carry-over factors:

$$\mu_{ab}=\frac{1}{2}\left(1+3\frac{1}{5.5}\right)=0.773 \qquad \mu_{ae}=0.500$$

$$\mu_{ba}=\frac{1}{2}\frac{\left(1+3\frac{1}{5.5}\right)}{1.644}=0.470 \qquad \mu_{bf}=\frac{1}{2}\frac{\left(1+3\frac{0.30}{4.70}\right)}{1.191}\cong 0.500$$

$$\mu_{bc}=\frac{1}{2}\frac{\left(1+3\frac{1}{400}\right)}{1.938}=0.452 \qquad \mu_{cg}=0.500$$

$$\mu_{cb}=\frac{1}{2}\left(1+\frac{3}{4}\right)=0.875 \qquad \mu_{ed}=0.500$$

For moments M'_{a1} see Table II:
Shearing forces:

$$Q_{b1}=-6880+\frac{1925-12895}{6.50}=-8570\ kg$$

$$Q_{b2}=+4000+\frac{11680-1761}{5.00}=5980\ kg$$

Total moments:

$$M_{a1}=1925 \qquad M_{b1}=-12895+8570\times 1.0=-4115\ kg$$

$$M_{b2}=+11690-5980\times 1.0=-5700\ kg \qquad M_{c2}=-1761\ kg$$

$$M_{c3}=+2366\ kg \qquad M_{d3}=-5057\ kg$$

Table I

	d	α		b			c			e	f	k
	4	4	1	1	5	2	2	6	3	5	6	3
K_{ai}	—	0.357	0.643	0.372	0.322	0.306	0.332	0.222	0.446	—	—	—
μ_{ab}		αd	ab	ba	be	bc	cb	cf	ck			
		0.500	0.580	0.565	0.500	0.558	0.568	0.500	0.500			
			+6425	-6700		+9030	-8700		+5410			-4160
	-1148	-2295	-4130	-2400								
			+15	+26	+23	+21	+12			+12		
						+620	+1090	+728	+1460		+364	+730
			-130	-230	-200	-190	-106			-100		
	+20	+41	+74	+43								
				-16	-14	-13	-7			-7		
							+37	+25	+51		+12	+25
M_{ai}	-1128	-2254	+2254	-9277	-191	+9468	-7674	+753	+6921	-95	+376	-3405

Table II

	e	α		b			c			d	f	g
	4	4	1	1	5	2	2	6	3	3	5	6
K	—	0.215	0.785	0.412	0.087	0.501	0.485	0.129	0.386	—	—	—
μ_{ab}	—	αe	ab	ba	bf	bc	cb	cg	cd	—	—	—
		0.500	0.773	0.470	0.500	0.452	0.875	0.500	0.500			
			+6300	-13180		+6660	-2660		+4160	-4160		
	-675	-1350	-4950	-3830								
			+2000	+4260	+900	+5190	+2350				+450	
	-215	-430	-1570	-1210		-1640	-1870	-500	-1480	-740		-250
			+550	+1170	+250	+1430	+645				+125	
	-59	-118	-432	-334		-274	-313	-83	-249	-125		-42
			+127	+250	+53	+305	+138				+27	
	-28	-27	-100	-77		-59	-67	-18	-53	-26		-9
				+56	+12	+68	+31				+5	
							-15	-4	-12	-6		-2
M_{ki}	-977	-1925	+1925	-12895	+1215	+11680	-1761	-605	+2366	-5057	+607	-303

Example No. 3 (Fig. 13)

$$l_o = \sqrt{4^2+2^2} = 4.47\ m \qquad l_2 = l_3 = \sqrt{8^2+2^2} = 8.22\ m$$

1st Stage
Active moments

$$\bar{M}_{a2} = \bar{M}_{b2} = \frac{2\times 8^2}{12} = 10.65\ tm \qquad \bar{M}_{b3} = -\bar{M}_{c3} = +10.65\ tm$$

$$\bar{M}_{c5} = -\bar{M}_{d5} = \frac{2\times 6^2}{12} = 6\ tm$$

Distribution factors
Joint b:

$$\varkappa_{b2} = 0.500 \qquad \varkappa_{b3} = 0.500$$

Joint c:

$$\alpha_{c3} = \frac{4E\times 5I_o}{8.22} = 2.44\,EI_o \qquad \varkappa_{c3} = \frac{2.44}{5.44} = 0.448$$

$$\alpha_{c4} = \frac{4E\times I_o}{4.00} = 1.00\,EI_o \qquad \varkappa_{c4} = \frac{1.00}{5.44} = 0.184$$

$$\alpha_{c5} = \frac{4E\times 3I_o}{6} = \frac{2.00EI_o}{5.44EI_o} \qquad \varkappa_{c5} = \frac{2.00}{5.44} = 0.368$$

Carry-over factors: $\mu = \pm\frac{1}{2}$
The moments of the 1st stage are given in Table III
Restraining forces of 1st stage: (Fig. 16)

$$V_\alpha = 16 + \frac{10.375 - 8.714}{16} = 16.104\ t$$

Moments relative to b: $2H + 10.375 - 11.199 - 16.104\times 8 + 16\times 4 = 0$

$$H = 32.82\ t$$

Moments relative to 0a:

$$8.94\,F_1 = 32.82\times 8 + 10.375 \qquad \vec{F}_1 = 30.56\ t$$

$$\overleftarrow{F}_2 = -32.91 + \frac{0.908+0.454}{4} = -32.47\ t$$

2nd stage:
Virtual displacement diagrams.

a) For removal of imaginary roller restraint I: (Fig. 14)

$$\delta'_\alpha = -\frac{1}{8.94}\cdot\delta_1 = -0.112\,\delta_1 \qquad \rho'_\alpha = -0.112 \qquad \delta'_{a1} = \delta'_1 = \frac{8.00}{8.94}\cdot\delta_1 = 0.895\,\delta_1$$

$$c'_1 = 0.895 \qquad \rho'_2 = -\frac{1}{8.94}\cdot\frac{8.00}{4.00} = -0.224 \qquad c'_2 = -0.224\times 8.22 = -1.84$$

$$\delta'_2 = -1.84\,\delta_1 \qquad c'_3 = +1.84 \qquad \delta'_3 = +1.84\,\delta_1$$

$$c'_4 = c'_5 = c'_6 = c'_7 = c'_8 = 0$$

Calculation of u°_{ai} and u°_{bi}

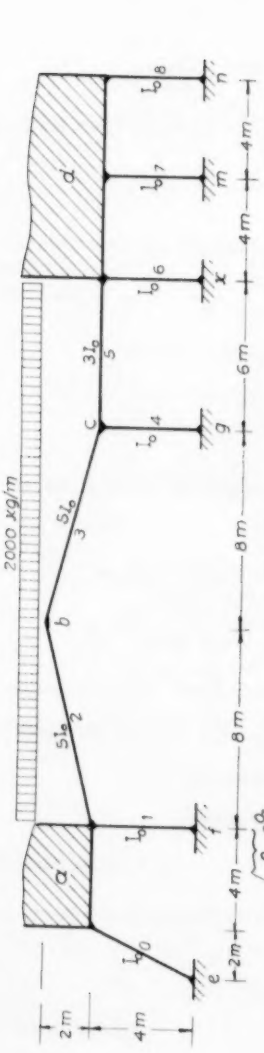

Fig. 13

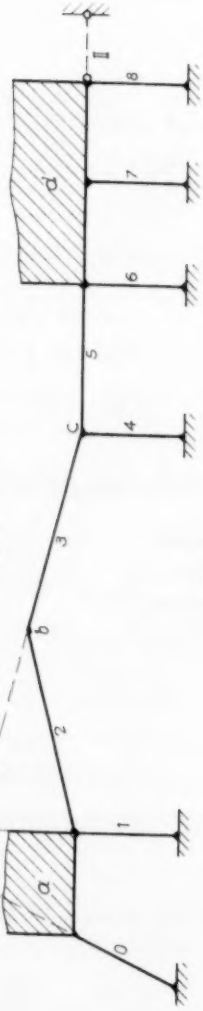

Fig 14

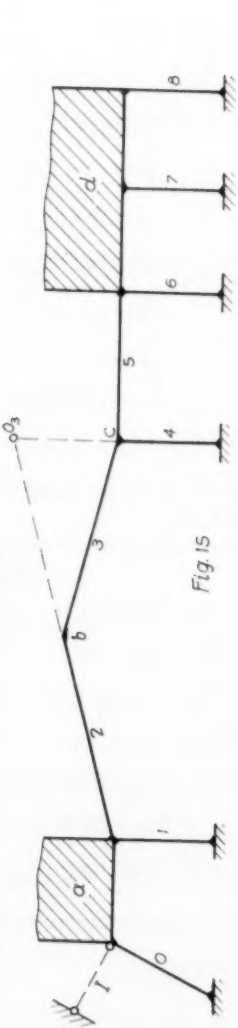

Fig 15

General formulas:

$$u^{o}_{ai} = \left[-(2\rho_a + \rho_b)\frac{l_i}{3} + c_i \right] \frac{6EI_i}{l_i}$$

$$u^{o}_{bi} = \left[-(\rho_a + 2\rho_b)\frac{l_i}{3} + c_i \right] \frac{6EI_i}{l_i}$$

$6EI_o = 100\ tm$

$u^{o}_{ao} = (2 \times 0.112 \times \frac{4.47}{3} + 1)\frac{6EI_o}{4.47} = 29.8\ tm$ $u^{o}_{eo} = (0.112 \times \frac{4.47}{3} + 1)\frac{6EI_o}{4.47} = 26.10\ tm$

$u^{o}_{a1} = (2 \times 0.112 \times \frac{4.00}{3} + 0.895)\frac{6EI_o}{4} = 29.8\ tm$ $u^{o}_{f1} = (0.112 \times \frac{4}{3} + 0.895)\frac{6EI_o}{4} = 26.10\ tm$

$u^{o}_{a2} = (2 \times 0.112 \times \frac{8.22}{3} - 1.84)\frac{6E \times 5I_o}{8.22} = -74.6\ tm$

$u^{o}_{b2} = (0.112 \times \frac{8.22}{3} - 1.84)\frac{6E \times 5I_o}{8.22} = -93.4\ tm$

$u^{o}_{b3} = u^{o}_{c3} = 1.84\ \frac{6E5I_o}{8.22} = 112.0\ tm$

$\bar{M}^{I}_{ao} = 29.8\frac{1}{4.47} = 666\ tm$ $\bar{M}^{I}_{eo} = 26.1\frac{1}{4.47} = 5.83\ tm$

$\bar{M}^{I}_{a1} = 29.8\frac{1}{4} = 7.45\ tm$ $\bar{M}^{I}_{f1} = 26.1\frac{1}{4} = 6.53\ tm$

$\bar{M}^{I}_{a2} = -74.6\frac{1}{8.22} = -9.07\ tm$ $\bar{M}^{I}_{b3} = -\frac{93.4}{8.22} = -11.35\ tm$

$\bar{M}^{I}_{b3} = \bar{M}^{I}_{c3} = +\frac{112}{8.22} = +13.60\ tm$

The moments for removal of the imaginary roller restraint I are given in Table IV.

Restraining forces—Shear forces

$M^{I}_{ao} = +6660\ xgm$ $M^{I}_{eo} = +5830\ xgm$ $M^{I}_{ai} = 7450\ xgm$

$M^{I}_{f1} = +6530\ xgm$ $M^{I}_{a2} = -8859\ xgm$ $M^{I}_{b2} = -10928\ xgm$

$M^{I}_{b3} = +10928\ xgm$ $M^{I}_{c3} = +7616\ xgm$ $M^{I}_{c4} = -2539\ xgm$ $M^{I}_{g4} = -1268\ xgm$

$M^{I}_{c5} = -5077\ xg$ $M^{I}_{d5} = -2536\ xgm$ $M^{I}_{d6} = M^{I}_{x6} = M^{I}_{d7} = M^{I}_{m7} = M^{I}_{d8} = M^{I}_{n8} = 0$

$Q^{I}_{o} = \frac{6660+5830}{4.47} = 2800\ xg$ $Q^{I}_{1} = \frac{7450+6530}{4.00} = 3490\ xg$

$Q^{I}_{2} = \frac{-8859-10928}{8.22} = -2400\ xg$ $Q^{I}_{3} = \frac{7616+10928}{8.22} = 2260\ xg$

$Q^{I}_{4} = \frac{-2539-1269}{4} = -950\ xg$

$F^{I}_{i} = 2800 + 0.895 \times 3490 + 2400 \times 1.84 + 2260 \times 1.84 + 0.112\ (6660 + 7450 - 8859)$

$F^{I}_{i} = 15.19\ t$

$F^{I}_{ii} = -2400 \times 2.065 - 2260 \times 2.055 - 0.950 \times 1 = -10.53\ t$

For removal of imaginary roller restraint II (Fig. 15)

$$\delta_4^{II}=\delta_6^{II}=\delta_7^{II}=\delta_8^{II}=1 \qquad C_4^{II}=C_6^{II}=C_7^{II}=C_8^{II}=+1 \qquad \delta_\alpha^{II}=0$$

$$e_{c3}=4.00\,m \qquad e_{b3}=16.44\,m \qquad \varphi_\alpha^{II}=0$$

$$\delta_3=-\frac{8.22}{4.00}\,\delta_4=-2.055\,\delta_4 \qquad C_3^{II}=-2.055 \qquad \delta_\alpha^{II}=0$$

$$\varphi_\alpha^{II}=0 \qquad C_2^{II}=+2.055 \qquad C_0^{II}=C_1^{II}=C_5^{II}=0$$

$$6EI_0=100\,t$$

$$\bar{M}_{c4}^{II}=\bar{M}_{g4}^{II}=\bar{M}_{d6}^{II}=\bar{M}_{d7}^{II}=\bar{M}_{m7}^{II}=\bar{M}_{d8}^{II}=\bar{M}_{n8}^{II}=\frac{6EI_0}{4}\,\frac{1}{4}=6.250\ kgm$$

$$\bar{M}_{a2}^{II}=\bar{M}_{b2}^{II}=\frac{6E\times 5I_0}{8.22}\,\frac{2.055}{8.22}=15.200\ kgm$$

$$\bar{M}_{b3}^{II}=\bar{M}_{c3}^{II}=-15.200\ kgm$$

The moments for the removal of the imaginary pinned member II are given in Table V

Moments:

$$M_{a0}^{II}=M_{e0}^{II}=M_{a1}^{II}=M_{f1}^{II}=0 \qquad M_{a2}^{II}=+14.672 \qquad M_{b2}^{II}=+14.144\ kgm$$

$$M_{b3}^{II}=-14.144 \qquad M_{c3}^{II}=-11.491 \qquad M_{c4}^{II}=+7.997 \qquad M_{g4}^{II}=+7.124\ kgm$$

$$M_{c5}^{II}=3.494 \qquad M_{d5}^{II}=1.747\ kgm$$

$$M_{d6}^{II}=M_{x6}^{II}=M_{d7}^{II}=M_{m7}^{II}=M_{d8}^{II}=M_{n8}^{II}=6.250\ kgm$$

Shear forces

$$Q_2^{II}=\frac{14.672+14.144}{8.22}=3.510\ kg \qquad Q_3^{II}=\frac{-14.144-11.491}{8.22}=-3.120\ kg$$

$$Q_4^{II}=\frac{7.997+7.124}{4}=3.780\ kg \qquad Q_5^{II}=\frac{3.494+1.749}{6}=.873\ kg$$

$$Q_6^{II}=Q_7^{II}=Q_8^{II}=\frac{6.250+6.250}{4}=3.125\ kg$$

Restraining forces:

$$F_1^{II}=-1.84\times 3.510-1.84\times 3.20+0.112\times 14.672=-10.54\,t$$

$$F_2^{II}=3.510\times 2.055+3.120\times 2.055+3.780+3\times 3.125=26.84\,t$$

Convertion factors:

$$+15.19\,x_1-10.54\,x_2+30.56=0$$

$$-10.53\,x_1+26.84\,x_2-32.47=0$$

$$x_1=-1.62 \qquad x_2=0.570$$

Total moments:

$$M_{a0}=-6.660\times 1.62=-10.780\ kgm \qquad M_{e0}=-5.830\times 1.62=-9.450\ kgm$$

$$M_{a1}=-7.450\times 1.62=-12.050\ kgm \qquad M_{f1}=-6.530\times 1.62=-10.580\ kgm$$

$$M_{a2}=+8.859\times 1.62+14.672\times 0.57+10.375=+33.085\ kgm$$

$$M_{b2}=+10.928\times 1.62+14.144\times 0.57-11.199=+14.561\ kgm$$

Table III

	α	b		c			d	g
	2	2	3	3	4	5	5	4
K_{ai}	—	0.500	0.500	0.448	0.184	0.368	—	—
	+10650	-10650	+10650	-10650		+6000	-6000	
			+1040	+2080	+860	+1710	+855	+430
	-260	-520	-520	-260				
			+58	+116	+48	+96	+48	+24
	-15	-29	-29					
M_{ai}	+10375	-11199	+11199	-8714	+908	+7806	-5097	+454

Table IV

	α	b		c			d	g
	2	2	3	3	4	5	5	4
K_{ai}	—	0.500	0.500	0.448	0.184	0.368	—	—
	-9070	-11350	+13600	+13600				
			-3050	-6100	-2500	-5000	-2500	-1250
	+200	+400	+400	+200				
			-45	-90	-37	-73	-36	-19
	+11	+22	+23	+12				
				-6	-2	-4		
M_{ai}	-8859	-10928	+10928	+7616	-2539	-5077	-2536	-1269

Table V

	α	b		c			d	g
	2	2	3	3	4	5	5	4
K_{ai}	—	0.500	0.500	0.448	0.184	0.368	—	—
	+15200	+15200	-15200	-15200	+6250			+6250
			+2000	+4000	+1650	+3300	+1650	+825
	-500	-1000	-1000	-500				
			+112	+224	+92	+184	+92	+46
	-28	-56	-56	-28				
				+13	+5	+10	+5	+3
M_{ai}	+14672	+14144	-14144	-11491	+7997	+3494	+1747	+7124

$$M_{b3} = -10928 \times 162 - 14144 \times 0.57 + 11199 = -14561 \text{ kgm}$$

$$M_{c3} = -7616 \times 162 - 11491 \times 0.57 - 8714 = -27574 \text{ kgm}$$

$$M_{c4} = +2539 \times 162 + 7997 \times 0.57 + 908 = +9578 \text{ kgm}$$

$$M_{g4} = 1268 \times 162 + 7124 \times 0.57 + 454 = +6564 \text{ kgm}$$

$$M_{c5} = 5077 \times 162 + 3494 \times 0.57 + 7806 = +18006 \text{ kgm}$$

$$M_{d5} = 2536 \times 162 + 1747 \times 0.57 - 5097 = +7 \text{ kgm}$$

$$M_{d6} = M_{x6} = M_{d7} = M_{m7} = M_{d8} = M_{n8} = 6250 \times 0.57 = 3560 \text{ kgm}$$

Example No. 4

The rigid frame of example 3 is worked out again by the one stage method.

Constants of diagrams of virtual displacement:
Group I:

$$C_0^I = +1 \quad C_1^I = 0.895 \quad C_2^I = -1.84 \quad C_3^I = +1.84 \quad \rho_\alpha^I = -0.112 \quad \rho_\alpha^I = 0$$

$$C_5^I = 0 \quad C_4^I = C_6^I = C_7^I = C_8^I = 0$$

Group II:

$$C_0^{II} = 0 \quad C_1^{II} = 0 \quad C_2^{II} = -2.055 \quad C_3^{II} = -2.055 \quad \rho_\alpha^{II} = 0 \quad \rho_\alpha^{II} = 0$$

$$C_5^{II} = 0 \quad C_4^{II} = C_6^{II} = C_7^{II} = C_8^{II} = +1$$

Distribution factors due to rotation:
Joint b:

$$\varkappa_{b2} = 0.500$$

$$\varkappa_{b3} = 0.500$$

Joint c:

$$\varkappa_{c3} = 0.448$$

$$\varkappa_{c4} = 0.184$$

$$\varkappa_{c5} = 0.368$$

Carry-over factors: $\mu = +\frac{1}{2}$
Restraining factors:

For the case of the rigid frame considered we have for all members:

$$(M_{\alpha i})' = M_{\alpha i} \qquad (l_i)' = l_i$$

General formula:

$$\sigma_{\alpha i} = \sum_i \frac{3}{2} \varkappa_{\alpha i} \frac{C_i^I}{l_i} - \sum_r \rho_r^I \sum \frac{\varkappa_{\alpha r}}{2}$$

Group I:

$$\sigma_{b1} = -\frac{184}{822} \cdot \frac{3}{2} \times 0.500 + \frac{184}{822} \cdot \frac{3}{2} \cdot 0.500 - (-0.112) \cdot \frac{0.500}{2} = +0.028$$

$$\sigma_{c1} = -\frac{184}{822} \times \frac{3}{2} \times 0.448 = +0.150$$

Group II:

$$\sigma_{b2} = +\frac{2055}{822} \times 0.500 \times \frac{3}{2} - \frac{2055}{822} \times 0.500 \times \frac{3}{2} = 0$$

$$\sigma_{c3} = -\frac{2055}{822} \times 0.448 \times \frac{3}{2} + \frac{1}{4} \times 0.184 \cdot \frac{3}{2} = -0.099$$

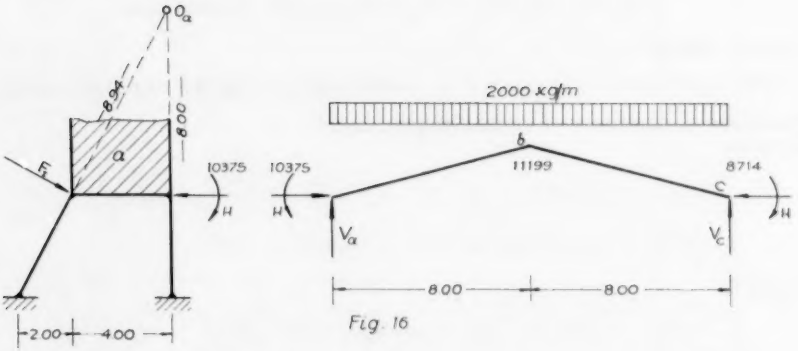
O_a
8.94
8.00
a
E_a
10375
H
2.00
4.00
2000 kg/m
b
11199
10375
8714
c
H
V_a
V_c
8.00
8.00

Fig. 16

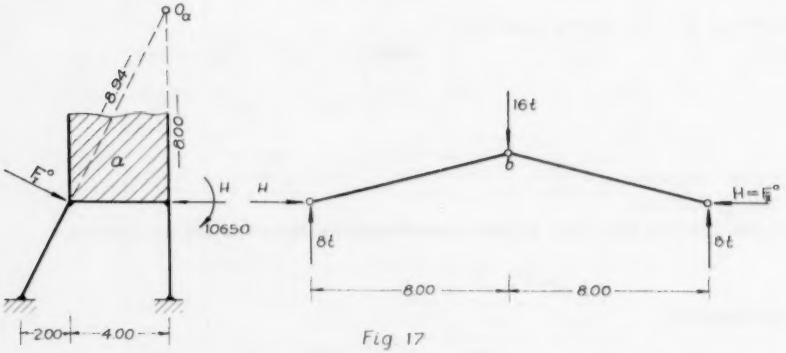
O_a
8.94
8.00
a
$E_a°$
H
10650
2.00
4.00
16t
b
H
H=$E_a°$
8t
8t
8.00
8.00

Fig. 17

Distribution factors due to displacement:

Group I:

Calculated $\bar{u}^{I}_{ai}$: In the case examined we have: $\bar{u}^{I}_{ai} = u^{I}_{ai}$

$$u^{oI}_{ao} = \left(2 \times 0.112 \times \frac{4.47}{3} + 6\right)\frac{6EI_o}{4.47} = 1.790\,EI_o$$

$$u^{oI}_{eo} = \left(0.112 \times \frac{4.47}{3} + 1\right)\frac{6EI_o}{4.47} = 1.565\,EI_o$$

$$u^{oI}_{a1} = \left(2 \times 0.112 \times \frac{4.00}{3} + 0.895\right)\frac{6EI_o}{4.00} = 1.790\,EI_o$$

$$u^{oI}_{f1} = \left(0.112 \times \frac{4.00}{3} + 0.895\right)\frac{6EI_o}{4.00} = 1.565\,EI_o$$

$$u^{oI}_{a2} = \left(2 \times 0.112 \times \frac{8.22}{3} - 1.84\right)\frac{6E5I_o}{8.22} = -4.48\,EI_o$$

$$u^{oI}_{b2} = \left(0.112 \times \frac{8.22}{3} - 1.84\right)\frac{6E5I_o}{8.22} = -5.60\,EI_o$$

$$u^{oI}_{b3} = 1.84 \times \frac{6E \times 5I_o}{8.22} = 6.72\,EI_o = u^{oI}_{c3}$$

$$\frac{u^{oI}_{ao} + u^{oI}_{eo}}{l_o} \cdot \frac{C^{I}_{o}}{l_o} = \frac{1.790 + 1.565}{4.47} \cdot \frac{1}{4.47}\,EI_o = +0.168\,EI_o$$

$$\frac{u^{oI}_{a1} + u^{oI}_{f1}}{l_1} \cdot \frac{C^{I}_{1}}{l_1} = \frac{1.790 + 1.565}{4.00} \cdot \frac{0.895}{4.00}\,EI_o = +0.187\,EI_o$$

$$\frac{u^{oI}_{a2} + u^{oI}_{b2}}{l_2} \cdot \frac{C^{I}_{2}}{l_2} = \frac{4.48 + 5.60}{8.22} \cdot \frac{1.84}{8.22}\,EI_o = +0.275\,EI_o$$

$$\frac{u^{oI}_{b3} + u^{oI}_{c3}}{l_3} \cdot \frac{C^{I}_{3}}{l_3} = \frac{6.72 + 6.72}{8.22} \cdot \frac{1.84}{8.22}\,EI_o = \frac{+0.367\,EI_o}{0.997\,EI_o}$$

$$\sum_r \rho^{I}_r \sum \frac{u^{oI}_{rx}}{l_x} = -0.112\left(\frac{1.79\,EI_o}{4.47} + \frac{1.79\,EI_o}{4} - \frac{4.48\,EI_o}{8.22}\right) = -0.031\,EI_o$$

$$\sum_i \frac{u^{oI}_{ai} + u^{oI}_{bi}}{l_i} \cdot \frac{C^{I}_{i}}{l_i} - \sum_r \rho^{I}_r \sum \frac{u^{oI}_{rx}}{l_x} = (+0.997 + 0.031)\,EI_o = +1.028\,EI_o$$

$$\bar{q}^{I}_{ao} = \frac{1.79/4.47}{1.028} = +0.390 \qquad \bar{q}^{I}_{eo} = \frac{1.565/4.47}{1.028} = +0.341 \qquad \bar{q}^{I}_{a1} = \frac{1.79/4.00}{1.028} = +0.436$$

$$\bar{q}^{I}_{f1} = \frac{1.565/4.00}{1.028} = +0.382 \qquad \bar{q}^{I}_{a2} = \frac{4.48/8.22}{1.028} = -0.531 \qquad \bar{q}^{I}_{b2} = \frac{5.60/8.22}{1.028} = -0.664$$

$$\bar{q}^{I}_{b3} = \bar{q}^{I}_{c3} = \frac{6.72/8.22}{1.028} = 0.795 \qquad \bar{q}^{I}_{c4} = \bar{q}^{I}_{f4} = \bar{q}^{I}_{c6} = \bar{q}^{I}_{d5} = \bar{q}^{I}_{d6} = \bar{q}^{I}_{x6} = \bar{q}^{I}_{d7} = \bar{q}^{I}_{m7} = \bar{q}^{I}_{d8} = \bar{q}^{I}_{m8} = 0$$

Check:

$$\frac{0.390 + 0.341}{4} \times 1 + \frac{0.436 + 0.382}{4} \times 0.895 + \frac{0.531 + 0.664}{8.22} \times 1.84 + \frac{0.795 + 0.795}{8.22} \times 1.84$$

$$-(-0.112)(0.390 + 0.436 - 0.531) = +1.004$$

Group II:

$$u^{oII}_{ao} = u^{oII}_{eo} = 0 \qquad u^{oII}_{a1} = u^{oII}_{f1} = 0 \qquad u^{oII}_{a2} = u^{oII}_{b2} = \frac{6E \times 5I_o}{8.22} \times 2.055 = 7.50\,EI_o$$

$$u^{oII}_{b3} = u^{oII}_{c3} = \frac{6E \times 5I_o}{8.22}(-2.055) = -7.50\,EI_o \qquad u^{oII}_{c5} = u^{oII}_{a5} = 0$$

$$u^{oII}_{c4} = u^{oII}_{g4} = \frac{6EI_o}{4} \times 1.0 = 1.50\,EI_o$$

$$u^{oII}_{d6} = u^{oII}_{x6} = u^{oII}_{d7} = u^{oII}_{m7} = u^{oII}_{d8} = u^{oII}_{n8} = 1.50\,EI_o$$

$$\frac{u^{oII}_{a2} + u^{oII}_{b2}}{l_2} \cdot \frac{C^{II}_{2}}{l_2} = \frac{2 \times 7.50\,EI_o}{8.22} \cdot \frac{2.055}{8.22} = 0.458\,EI_o$$

$$\frac{U_{b3}^{0I}+U_{c3}^{0I}}{l_3}\cdot\frac{C_3^{I}}{l_3}=\frac{2\times750EI_o}{822}\times\frac{(-2055)}{822}=0458\,EI_o$$

$$\frac{U_{c4}^{0I}+U_{g4}^{0I}}{l_4}\cdot\frac{C_4^{I}}{l_4}=\frac{2\times150EI_o}{400}\times\frac{1}{400}=0.1875\,EI_o$$

$$\Sigma_i\frac{U_{ai}^{0I}+U_{bi}^{0I}}{l_i}\cdot\frac{C_i}{l_i}=-\Sigma_r\rho_r^{I}\Sigma_x\frac{U_{rx}^{0I}}{l_x}=(2\times0.458+4\times0.1875)\,EI_o=1666\,EI_o$$

$$\bar{q}_{a0}^{I}=\bar{q}_{e0}^{I}=\bar{q}_{a1}^{I}=\bar{q}_{f1}^{I}=0$$

$$\bar{q}_{a2}^{I}=\bar{q}_{b2}^{I}=\frac{750/822}{1666}=0548 \qquad \bar{q}_{b3}^{I}=\bar{q}_{c3}^{I}=-0548$$

$$\bar{q}_{c4}^{I}=\bar{q}_{g4}^{I}=\frac{150/400}{1666}=0225 \qquad \bar{q}_{d6}^{I}=\bar{q}_{x6}^{I}=\bar{q}_{d7}^{I}=\bar{q}_{m7}^{I}=\bar{q}_{d8}^{I}=\bar{q}_{n8}^{I}=0225$$

Check:

$$4\times\frac{0548}{822}\times2055+8\times\frac{0225}{400}\times1=0998$$

Shear carry-over factors:
General formula:

$$m_I^{I}=\Sigma_i\left(\bar{q}_{xi}^{I}+\bar{q}_{bi}^{I}\right)\frac{C_i^{I}}{l_i}-\Sigma_r\rho_r^{I}\Sigma_x\bar{q}_{rx}^{I}$$

$$m_I^{I}=(-0531-0664)\frac{2055}{822}-\frac{2\times0795}{822}\times2055=-0697$$

$$m_I^{II}=-\frac{2\times184\times0548}{822}-\frac{0548\times184\times2}{822}-(-0112)\times0548=-0430$$

Fixing forces: (Fig. 17)

$$\bar{M}_{a2}=-\bar{M}_{b2}=-10650\ kgm \qquad \bar{M}_{b3}=-\bar{M}_{c3}=10650\ kgm \qquad \bar{M}_{c5}=-\bar{M}_{d5}=6000\ kgm$$

$$2H=8\times8 \qquad H=32\ t \qquad F_I^{o}=\frac{32\times8+1065}{894}=2980\ t$$

$$F_I^{o}=-3200\ t$$

The successive approximations and the arrangement of the operations is tabulated in the Table VI.

REFERENCES

1. Hardy Cross and Newlin Morgan, "Continuous Frames of Reinforced Concrete", New York, 1949.
2. P. Moliotis, "A General Method of Analysis of Rigid Frames", Proceedings ASCE No. 811 and Transactions Vol. 122.

Table VI

	e	f	ox			b		c			d				g	k	m	n	F_1	F_2
	0	1	0	1	2	2	3	3	4	5	5	6	7	8	4	6	7	8	m_1^1	m_2^1
K_{ai}	—	—	—	—	—	0.500	0.500	0.448	0.184	0.368	—	—	—	—	—	—	—			-0.697
δ_{ai}				—		+0.028		+0.150					—		—	—	—		m_1^2	m_2^2
δ_{aii}				—		+0.000		-0.090					—		—	—	—		-0.430	—
Q'_{ai}	+0.341	+0.382	+0.390	+0.436	-0.531	-0.664	+0.795	+0.795	—	—	—	—	—	—	—	—	—			
Q''_{ai}	—	—	—	—	+0.548	+0.548	-0.548	-0.548	+0.225	—	—	0.225	0.225	0.225	0.225	0.225	0.225	0.225		
					+10650	-10650	+10650	-10650		+6000	-6000								+29800	-32000
							+1040	+2080	+860	+1710	+855								+698	-418
					-260	-520	-520	-8570	+860	+7710					+430				-29	—
						-11170	+11170	260											+30469	+21200
	-10400	-11620	-11870	-13300	+16180	+20200	-24200	-24200											-4830	-11218
					+6160	+6160	-6160	-6160	+2530			+2530	+2530	+2530	+2530	+2530	+2530	+2530		
					+1000	+2000	+2000	+1000											+108	—
						+28360	-28360	+12120	+4990	+9980	+4990				+2495				+4060	-2440
							+6060	-17500	+7520	+9980										
	+242	+272	+278	+310	-378	-472	+566	+566											-712	-498
					+1610	+1610	-1610	-1610	+662			+662	+662	+662	+662	+662	+662	+662	-1260	-2938
					-1538	-3077	-3077	-1538											-172	—
						-1939	+1939	+860	+352	+708	+354				+176				+288	-173
							+430	-1722	+1014	+708										
	+390	+437	+447	+500	-608	-760	+910	+910											-1144	-800
					+534	+534	-534	-534	+219			+219	+219	+219	+219	+219	+219	+219	-418	-973
					-145	-290	-290	-145											-16	—
						-516	+516	-202	-83	-165	-82				-41				-68	+40
							-101	+29	+136	-165										
	+171	+191	+195	+218	-266	-342	+398	+398											-502	-360
					+170	+170	-170	-170	+70			+70	+70	+70	+70	+70	+70	+70	-132	-310
					+11	+22	+23	+11											+1	—
						-150	+150	-138	-57	-114	-72				-28				-46	+28
							-69	+101	+13	-114										
	+60	+68	+69	+77	-94	-117	+141	+141											-177	-123
					+52	+52	-52	-52	+22			+22	+22	+22	+22	+22	+22	+22		-95
						+23	+22	+11												
						-42	+42	-55	-22	-45										
								+45	+000	-45										
M_{ai}	-9537	-10652	-10881	-12195	+33078	+14543	-14543	-27617	+9543	+18074	+45	+3503	+3503	+3503	+6535	+3503	+3503	+3503		

Paper 1817 October, 1958 ST 6

Journal of the
STRUCTURAL DIVISION
Proceedings of the American Society of Civil Engineers

GOLDEN GATE BRIDGE VIBRATION STUDIES[a]

George S. Vincent,[1] M. ASCE
(Proc. Paper 1817)

SYNOPSIS

The records of bridge movement obtained over a period of years by means of instruments at ten locations on the main and side spans of the Golden Gate Bridge are analyzed. They are plotted against wind velocity and correlated with theoretical analyses of wave form and against model test indications of the response to winds of different velocities. It is shown that the oscillations are almost always in a symmetric mode with the amplitude inhibited by the sharply downward deflection of the prevailing west wind as it passes over a high hill before striking the north side span. It is shown that during one forty minute period the oscillation was in an asymmetric torsional mode, uninhibited, and reached amplitudes predicted from the model tests. A bottom lateral system has been installed. Tests indicate that it will prevent a reoccurrence of the objectionable torsional motion.

INTRODUCTION

The Inception of the Project

The failure of the Tacoma Narrows Bridge in 1940 led to a close scrutiny by engineers and scientists concerned with the problem of all evidence of wind-forced oscillation of suspension bridges. Oscillation sufficient to be of interest had been observed on the Golden Gate Bridge although even in the

Note: Discussion open until March 1, 1959. To extend the closing date one month, a written request must be filed with the Executive Secretary, ASCE. Paper 1817 is part of the copyrighted Journal of the Structural Division, Proceedings of the American Society of Civil Engineers, Vol. 84, No. ST 6, October, 1958.

a. A report on a cooperative research project conducted by the Golden Gate Bridge and Highway District and the Bureau of Public Roads, U. S. Dept. of Commerce. A contribution to the work of the Advisory Board on the Investigation of Suspension Bridges.

1. Bridge Engr., Division of Physical Research, Bureau of Public Roads, Washington, D. C.

severest storms in which a man could not stand erect the amplitude of oscillation had been insufficient to cause a computed stress of as much as 1,000 pounds per square inch in the chords of the stiffening truss, which is less than the stress due to temperature variation alone. Little concern was felt for the safety of the bridge, but the Advisory Board on the Investigation of Suspension Bridges expressed interest in a cooperative research project between the Golden Gate Bridge and Highway District and the Bureau of Public Roads. A cooperative undertaking for this purpose became effective May 15, 1943.

Under this agreement, instruments for measuring vertical movement of the bridge were developed and ten of them were installed upon the bridge. They were operated on a cooperative basis until June 30, 1950, at which time the cooperative agreement was terminated. All ten instruments have been operated continuously since that time at the expense of the Golden Gate Bridge and Highway District alone. The District has made available for the purpose of this report all data collected since the termination of the cooperative agreement.

Early Vibration Observations

The effect of earthquakes was taken into account in the design of the Golden Gate Bridge, and those responsible for its design and construction were alert during all phases of the work to the possible effects of vibration and resonance. Advantage was taken of the opportunity to measure any vibration which might occur at several stages of construction, using equipment and personnel provided by the United States Coast and Geodetic Survey.(1) Seismological instruments were set up on the piers, towers, cables and deck.

The piers showed a weak vibration at about the frequency of the waves, and this was attributed to wave impact. They also responded to the vibration of the towers.

Observations on the towers showed some variation in frequency from tower to tower, and at different times on the same tower, but with all of these there appeared rather broad bands of characteristic frequencies. In general, these frequencies responded to the changing mass and elastic properties as the towers were built up.

As the cables were completed and other elements of the superstructure were erected, their contributions to the mass and overall stiffness were reflected in altered frequencies. With the bridge completed, the instruments on the tower top showed a frequency of about 8.6 cpm (cycles per minute) for a movement parallel to the longitudinal axis of the bridge. This is near the frequency later observed for symmetric oscillation of the bridge which necessarily involves motion of the tower tops. Instruments on the cable and deck at mid-span showed a longitudinal oscillation of a few inches at frequencies of 5.46 to 7.5 cpm which range includes the frequency computed later for the first asymmetric vertical mode. It should be noted that longitudinal motion at mid-span indicates the first asymmetric mode.

The Coast and Geodetic Survey instruments showed also a lateral oscillation of small amplitude at mid-span at frequencies from 2.7 to 3.2 cpm. No such oscillation has subsequently been reported on the bridge. The instruments installed under the project herein reported respond only to the vertical component of motion.

Early Wind Excited Oscillation

The Golden Gate Bridge, in common with other suspension bridges, exhibited wind- or storm-excited oscillations during various stages of construction, from the cat-walk, used in cable construction, to the completed bridge. Only those occurring on the completed structure are considered in the present report.

Early observations were approximate and incomplete. In those recorded before the special instruments were installed the period of vibration was estimated or measured approximately by pocket watch. Several wave forms were noted and remembered in accordance with the impression of the observer. In some instances amplitudes were estimated by sighting on bridge elements. At other times, sightings were taken with a transit on rods attached to the bridge.

Mr. R. G. Cone, resident engineer during construction of the bridge, has recorded observations of two storms, one on February 9, 1938, some eight months after the bridge was opened to traffic, and the other on February 11, 1941 (see Appendix I).

The movements on February 9, 1938, evidently were a multi-noded vertical mode, with a phase difference which gave the effect of a running wave. No mention was made of evidence of a transverse or torsional oscillation. The high frequency observed, 20 to 30 cpm, corresponds to computations for the six-noded vertical oscillation (25.6 cpm)*. The computed loop length of the six-noded vertical motion averages 600 ft. (Cone estimated a motion of "as much as 2 ft. vertically in 300 ft. of bridge"). No other recorded observations describe movements having as high frequency or as short loops as these.

The movement during the first recorded period of the storm of February 11, 1941 suggests the second symmetric vertical mode having a computed period of 6.3 seconds (9.5 cpm) and a long end wave with the maximum amplitude near the quarter-point.** The change in frequency during the second recorded period to about 7.5 cpm (8 second period) with dominant motion still at the quarter-point suggests a shift to coupled torsional and vertical asymmetric oscillation such as occurred on December 1, 1951, described hereinafter, except that Mr. Cone mentioned no evidence of torsional motion.

Early Instrumental Observations

A. Anemometer. In January, 1942 a recording anemometer was installed on the bridge. A wind velocity transmitter (pressure cup type) and a wind direction transmitter were installed on a steel tower at mid-span, approximately 10 ft. west of the west cable and 5 ft. 3 in. above the top of the cable (14.5 ft. above the roadway). These were wired to a recorder placed inside the east leg of the south tower. Both velocity and direction were continuously recorded against time in ink on a paper roll, each roll covering a period of two weeks. The time scale was 1 in. equals 20 minutes.

B. Accelerometer. In March 1942, Professor Perry Byerly of the Department of Geology, University of California, was invited to visit the bridge and, on his recommendation, an instrument known as the Hall Recorder, loaned by the University to the Bridge District, was installed at the middle of the main span on the sidewalk. A photograph and description of this instrument have been previously published.(2) A brief description is in order since the instruments built later were patterned after it in some respects.

*See computed frequencies and wave forms, Fig. 6.

**See computed frequencies and wave forms, Fig. 6.

The Hall Recorder has two conical pendulums for measuring the two horizontal components of motion and a mass on a helical spring for measuring the velocity component. Each of the three has a weight of about twenty-five pounds. The spring suspension can be adjusted to give a considerable range of natural frequencies, permitting the selection of frequencies most favorable to the recording of the expected vibrations. The record is made by stylus on smoked paper on a drum which is revolved by clockwork in a spiral motion. A timing signal is also recorded on the drum at intervals.

This instrument was installed on the west sidewalk at the middle of the main span on March 18, 1942, and remained until replaced by the new instruments designed to record only the vertical motion.

Professor Byerly was employed by the Bridge District as a consultant to study and recommend the type of instrument to be used on the bridge. The design was developed by the late L. H. Nishkian, Consulting Engineer for the District, Professor Byerly and Mr. Otto W. Hahn, Consulting Mechanical and Electrical Engineer, and the first instrument was completed in Mr. Hahn's shop in December 1943, as the first major step under the cooperative agreement.

Development and Verification of Accelerometer

The Instrument

A diagram of the instrument is shown in Fig. 1 and Fig. 2 shows a partial view of its final form. The weight hung on the helical spring vibrates vertically with a natural period, T_o. When the instrument is mounted on a body, such as a suspension bridge, which oscillates vertically with a period, T_1, and a steady amplitude, y, the sprung weight will oscillate at the forced period, T_1, and will reach a steady state amplitude, a, measured with respect to the frame which supports the spring. The relation between a and y is expressed by the equation:(3)

$$a/y = \frac{1}{\sqrt{\left[1 - \left(\frac{T_1}{T_o}\right)^2\right]^2 + \frac{4 \log_{10}^2 \epsilon}{1.862 + \log_{10}^2 \epsilon} \left(\frac{T_1}{T_o}\right)^2}} \qquad (1)$$

In this equation ϵ is the damping ratio which is the ratio of the first to the second of any two successive single amplitudes in the same cycle after the sprung mass has been displaced and released to oscillate under the influence of no external force or acceleration other than gravity. If there were no damping ϵ would be 1.0.

When the spring weight moves a vertical distance, a, the horizontal arm attached to it will rotate about its pivoted end and the vertical arm, which carries the recording pen at its upper end and is rigidly attached at its lower end to the horizontal arm, will rotate through the same angle about the pivot. The movement of the pen, a_o, is related to the movement of the sprung weight, a, by the expression

$a_o/a = r_o/r$ in which

r_o = distance from the pivot to the pen

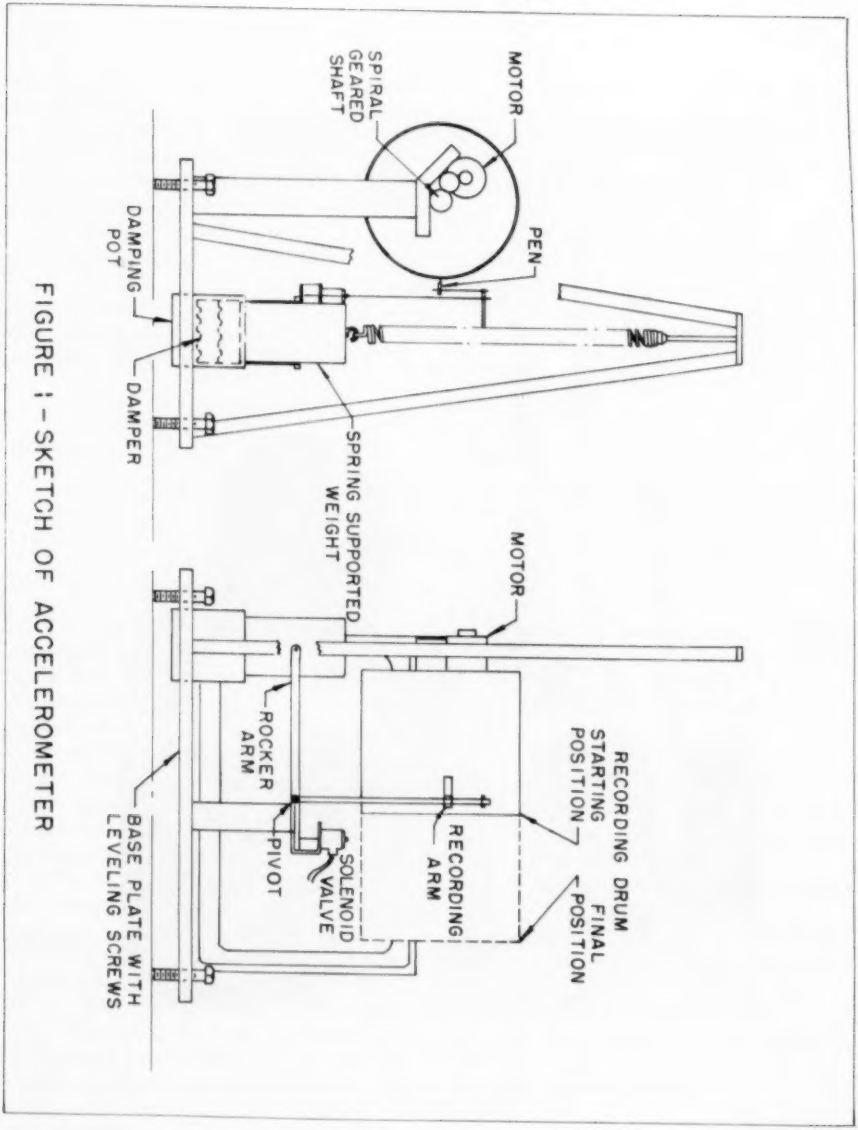

FIGURE 1 - SKETCH OF ACCELEROMETER

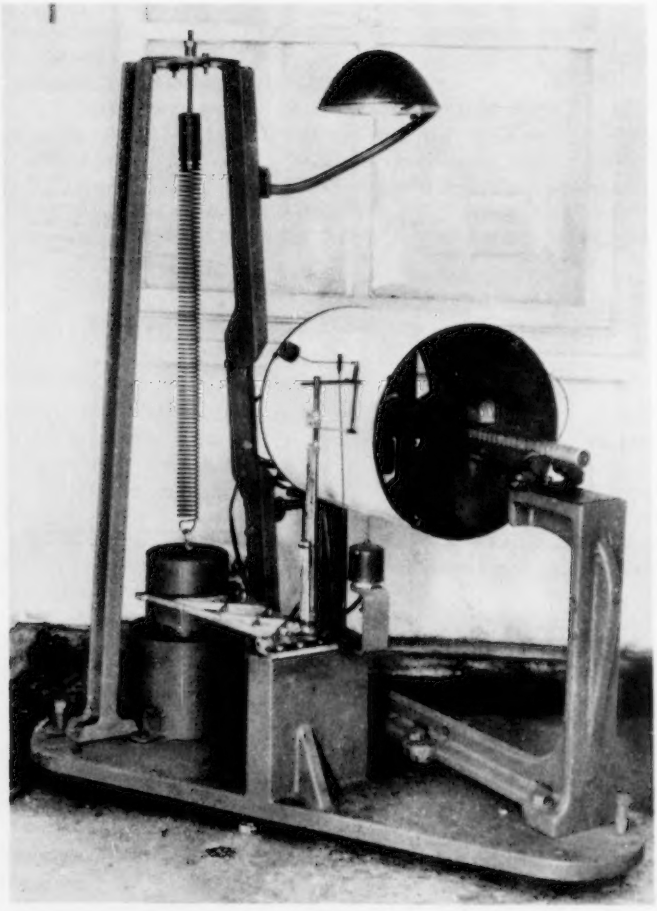

Figure 2 - Accelerometer.
Rocker arm and damper are pivoted to the spring-supported weight. Drive motor mounted on drum support is concealed by the drum. Relay for interrupting the recording is mounted on support partly under drum.

r = distance from the pivot to the center of sprung weight

Then the ratio of the recorded amplitude, a_o, to the amplitude of the oscillation of the supporting structure, y, is given by the expression:

$$a_o/y = a/y \quad (r_o/r) \tag{2}$$

and the value of a_o/y may be determined by multiplying the second term of Eq. (1) by r_o/r. The ratio, a_o/y, is referred to as the total magnification.

If T_o exceeds T_1, the displacement of the sprung mass is opposite in direction to the displacement of the spring support. If $T_o/T_1 = 2$ or more the instrument is a "vibrometer" or displacement-measuring device.(4) Such instruments are used to record earth tremors.

If, on the other hand, T_1 exceeds T_o, the sprung mass moves always in the direction of the movement of the spring support; i.e., a and y have the same sign. If T_1/T_o exceeds 2, the instrument acts satisfactorily as an "accelerometer" and the extension of the spring is nearly directly proportional to the acceleration acting on the instrument. Except for a phase lag caused by the damping the relation is nearly expressed by:

$$\text{acceleration} = \frac{a_t}{a_{st}} \quad g \tag{3}$$

in which:

a_t is the instantaneous displacement of the sprung weight from its rest position

a_{st} is the static extension of the spring due to the sprung weight, and

g is the acceleration of gravity.

For the low frequency oscillations of the Golden Gate Bridge with computed periods as great as 10.5 seconds (5.7 cycles per minute; see Fig. 6) the instrument with its period, T_o, of 1.07 seconds acts as an accelerometer. Fig. 3 is a graph showing the ratio, a_o/y plotted against the period, T_1, for different values of ϵ. The ratio, r_o/r of the instrument is 0.92.

Since the acceleration acting on a vibrating body increases as the square of the frequency, higher frequency vibrations are recorded at a much greater scale than are low frequency vibrations. To prevent exaggerated recording of transient high frequency vibrations, such as are produced by traffic, damping is introduced in accelerometers.

The drum upon which the record paper is wrapped is turned one revolution per hour by an electric clock motor through a train of gears. The axle is spirally grooved and supported on skewed knife edge rollers so that the drum advances longitudinally 0.4 in. per revolution. Twenty-six revolutions of the drum can be recorded on the 11 in. wide paper. The circumference of the drum is 37.43 in., giving a time scale on the record of 37.43/60 = 0.624 in. per minute. One of the gears of the driving train is mounted on a moveable bar which can be unpinned at one end to unmesh the gear and permit free rotation of the drum for adjustment or for damping measurements.

Calibration

The first model of the accelerometer was calibrated on a Scotch yoke at several frequencies in order to verify the applicability of Eq. (1) and Fig. 3. In the great majority of tests the actual and indicated amplitudes checked

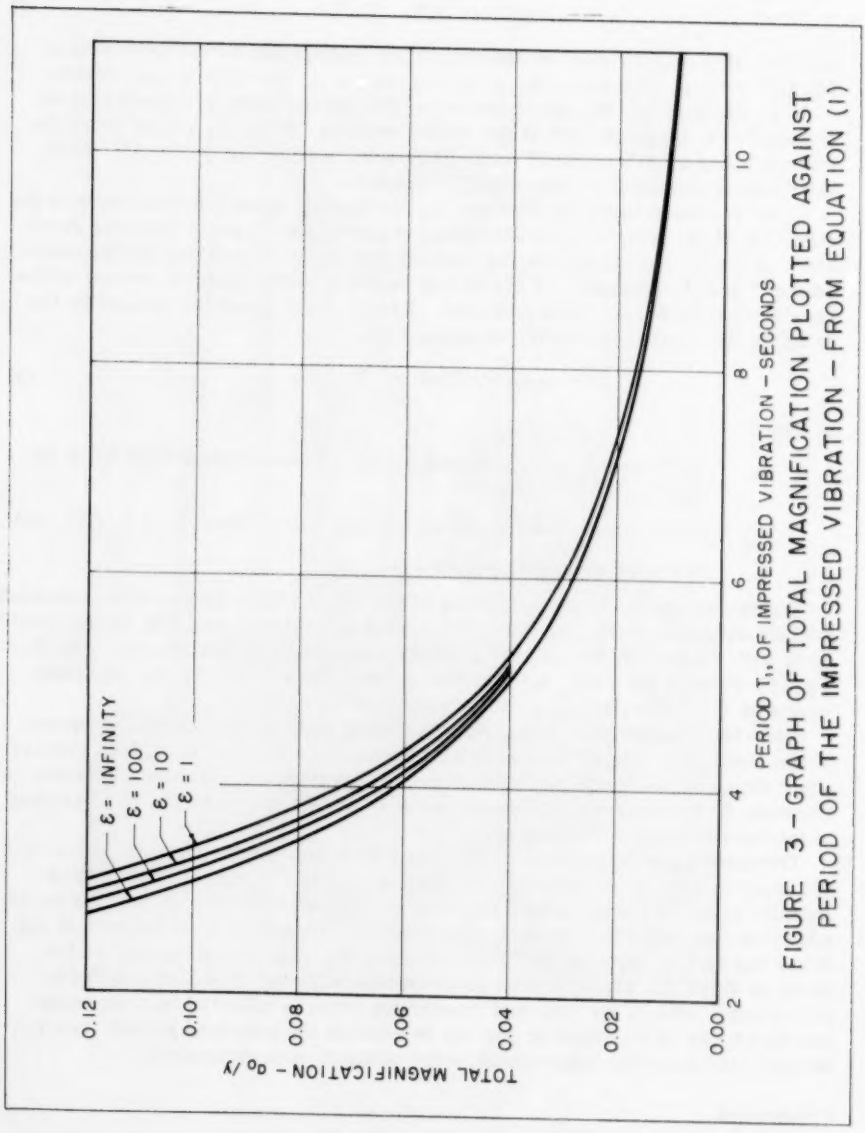

FIGURE 3 – GRAPH OF TOTAL MAGNIFICATION PLOTTED AGAINST PERIOD OF THE IMPRESSED VIBRATION – FROM EQUATION (1)

within less than one per cent. Discrepancies of about 3% were recorded in three cases. Those were all for short periods of 2.9, 3.5 and 4.8 seconds for which the prediction is more sensitive to ϵ as may be noted on Fig. 3.

Of course, if the motion is not simple harmonic the determination of the amplitude of the motion of the bridge may be uncertain. However, since the instrument responds to the applied acceleration, a fairly correct interpretation of the record is possible for motions in which a more complex oscillation can be represented by a combination of two or three harmonic motions (See Appendix II).

Damping Studies

It is, of course, essential that the damping ratio, ϵ, be known before Eqs. (1) and (2) or Fig. 3 can be used to determine the amplitude, y, of the oscillation of the test mount or the bridge from the measured amplitude, a_o, of the pen record. A simple test to determine ϵ was made frequently during the calibration runs and was made occasionally to check the damping of the instruments on the bridge. Fig. 4(a) illustrates the method.

First, the drum drive was thrown out of gear and the drum was rotated by hand so that the pen described the centerline, A. Then, with the drum stationary, the sprung weight was pressed down or lifted up till the pen was deflected about an inch to one side as shown by B, and released. Point C represents the amplitude reached by the pen one-half cycle after the release of the sprung weight. The damping ratio, $\epsilon = \frac{AB}{AC}$.

Eq. (1) was derived on the assumption that the damping is viscous (the damping force being proportional to the velocity of vibration) so that ϵ is constant for all amplitudes, i.e., any two successive amplitudes of opposite sign will have the same ratio as all other pairs of amplitudes. When the damping was materially increased in order to cope with extraneous vibration it became desirable also to know whether or not the damping was viscous. The test for this is illustrated by sketches (b), (c), and (d) of Fig. 4. After the drum was rotated to draw the centerline, a straight pencil line, D, was drawn from one side intersecting the centerline at an angle of about 45°. Then the drum was positioned so that with the weight depressed an inch or so the pen would be on the pencil line. Upon release of the weight the longest record shown on any of the three sketches would be drawn by the pen. Then each of the shorter records just touching the pencil line was similarly drawn. With viscous damping and constant ϵ, the end points of the recording indicating the amplitude of the first damped half cycle in each test must fall on the straight line, E, as shown by sketch (b).

If the damped amplitudes fell on a curved line as in sketch (c) it indicated that the damping effect was greater for large than for small amplitudes which would be true, for example, if the damping force varied as the square of the velocity of vibration. Records of this type were obtained when the damping was increased by means of discs which were nearly solid and nearly covered the cross sectional area of the damping-pot.

It was thought that viscous damping could be obtained by exploiting fluid friction by forcing the damping oil to pass through a maze of small channels. A simple device for testing this theory was provided by sandwiching one or two copper "chore balls" of fine copper turnings between two perforated metal discs. In some tests with these the copper turnings bulged beyond the disc

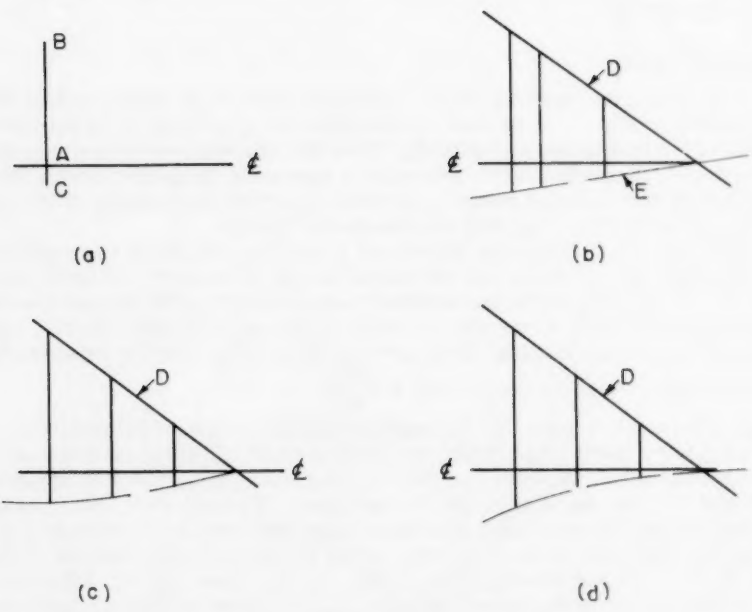

FIGURE 4 – SKETCHES ILLUSTRATING THE MEASUREMENT OF THE DAMPING RATIO.

and could be heard rubbing along the sides of the damping pot. In this condition the damping test record took somewhat the form of sketch (d) indicating the greater damping effect at lower amplitudes. This is recognized as characteristic of Coulomb friction damping.

Operation of Instruments

Installation

Following the verification tests the first available instrument was operated for a few months in 1944 on the San Francisco, Oakland Bay suspension bridge, on the bottom chord of the north truss at the middle of the 2310 ft. main span. No strong winds occurred during this period and the only significant vibrations recorded were caused by the passage of trains.

The instrument was then returned to the shop to facilitate preparations for making the additional accelerometers. Thirteen of these were made, nine for use on the Golden Gate Bridge, two for the San Francisco, Oakland Bay Bridge, and two for the Port of New York Authority. All were completed by the end of July 1945. Conduits and wiring circuits were installed on the Golden Gate Bridge and plywood houses to protect the instruments were placed at selected locations on the sidewalks. Nine instruments were installed in November and December, 1945. One instrument, No. 7, was kept at the shop and used for check tests which showed satisfactory performance. It was installed on the bridge March 1, 1946. The positions of the ten instruments are shown on Fig. 5. Number One was the first instrument made and differs in non-essential details from the others. A synchronizing clock was placed inside the east leg of the south tower. This was set to operate relays to lift the pens of all instruments for five seconds at five-minute intervals.

Operation and Development

Routine servicing of the instruments occupied one man's time for most of each forenoon. The accelerometer record sheets were changed daily and filed, and every two weeks the anemometer record roll was changed. The records were inspected regularly and memorandum notes were made of any sizeable amplitudes and the winds which caused them, but detailed analysis was deferred until many months of records were available.

The maintenance personnel of the Golden Gate Bridge and Highway District constantly studied the behavior of the instruments to detect deficiencies and devise improvements in many details. The windows of the houses were covered with plywood to exclude the direct sunlight which caused considerable variation in temperature, thus altering the damping. Reflector lamps were installed to maintain more uniform temperatures and prevent the absorption of atmospheric moisture which caused the paper on the drums to swell and wrinkle. Through steady experimentation the pens and their mountings were improved to correct defects which marred the earlier recordings.

The variability of the damping between instruments and, over a period of time, of the same instrument, was sometimes enough to affect the interpretation of the record. After some experimentation with various weights of motor oil, a silicone fluid was substituted in 1947. This gave damping that was quite constant but rather high, nearly critical. Values of ϵ of 100 to 1000 were used to interpret the record after this change in damping fluid.

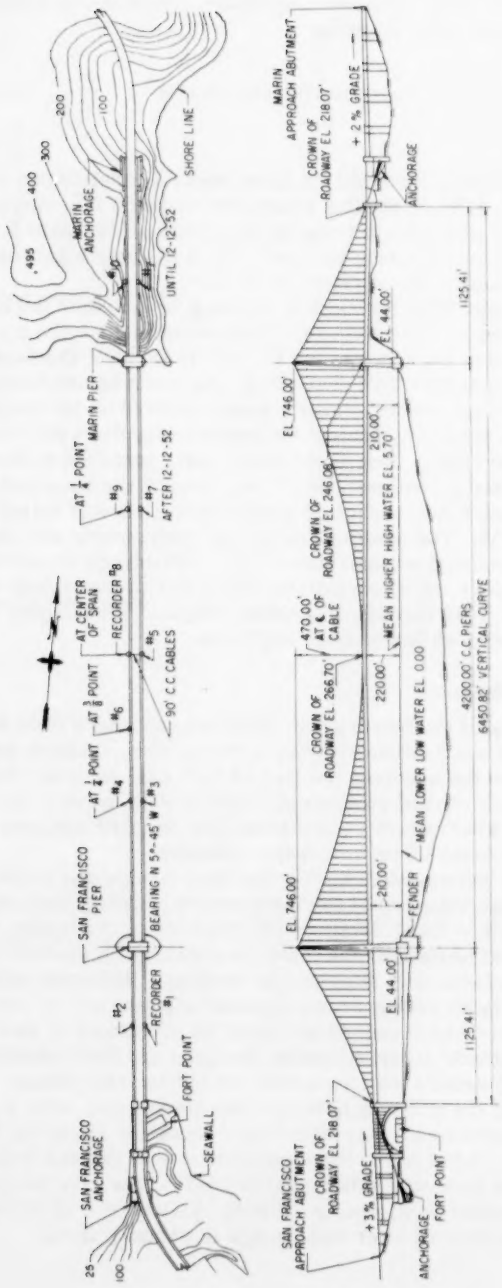

FIGURE 5 - GENERAL LAYOUT OF GOLDEN GATE BRIDGE
SHOWING POSITIONS OF ACCELEROMETERS.

In the fall of 1947 revised gear trains and stronger motors were installed to turn the drums and a spring action was provided in the meshing of gears to eliminate play and backlash and improve the uniformity of the record.

When the time scale of the record was selected, it was thought that it would only be necessary to determine the frequency over several cycles with sufficient accuracy to obtain T_1 in order to compute the amplitude and also to correlate the observations with theoretical calculations of the frequency of the modes of vibration of the bridge. The scale was adequate for these purposes and also for identifying pure vertical or torsional motion by noting which stations moved in phase or in opposite phase. However, subsequent experimental work[5] and theoretical analysis[6] revealed that a truss-stiffened suspension bridge such as the Golden Gate Bridge might be expected to oscillate in coupled vertical and torsional motion at an altered frequency and with a distinctive phase difference in the two motions. Evidence of such motion developed in the records, but the time scale was too small to permit the determination of phase differences.

In 1953 at the direction of Clifford E. Paine, Consulting Engineer for the Bridge District, a change was made whereby the throwing of a switch, mounted in the southeast tower leg, would treble the speed of rotation of all of the drums.

Observed Bridge Behavior

General Observations

Table I is a summary of major recorded bridge movements taken for the most part from the memorandum notes made from time to time by Mr. S. J. Dickson, Maintenance Superintendent, when he examined the records of wind and of bridge movement before filing them. General observations concerning the movements may be summarized as follows:

a) The oscillation usually had a frequency of about 8 cycles per minute although small oscillations of other frequencies were occasionally noted.
b) With the exception of the action on December 1, 1951, the predominant mode was symmetric, i.e., the wave form was essentially symmetrical about the center of the main span and, generally, the greatest amplitude was at the center.
c) The motion was principally vertical, but on all occasions there was also a transverse torsional motion, sometimes very marked. It should be noted that torsional oscillation of very small magnitude could be readily detected by sighting across the deck and noting the angular movement with reference to a distant sighting point. The instrument records also revealed the more pronounced torsional oscillations.
d) The amplitudes of vertical displacement were almost invariably greater along the leeward side than along the windward side of the bridge. This was noted also in laboratory tests of a section model of the bridge.[7]
e) Oscillation was likely to occur in any wind above 20 to 25 miles per hour and the amplitude increased with an increase in wind velocity.
f) On most occasions the amplitude increased sharply within a few cycles in response to a sudden increase in wind velocity and died down as quickly when the gust had passed.

TABLE I

SUMMARY OF MAJOR RECORDED OSCILLATIONS

Date	Maximum Double* Amplitude Inches	Velocity mph	Direction	Instrument Showing Prominent Movements**
1943				
1/21	15	70	S/S.W.	Midspan
12/9	15	74	N/N.W.	Midspan
1945				
10/30	12	75	South	Midspan
1946				
1/5	14	44	West	5 and 8
1947				
1/28	10	55	W/S.W.	5
11/1	14	40	S.W.	5and 8
1948				
2/22	17	50	West	3, 4, and 6
2/27	9	46	S/S.W.	5
3/2	14	40	West	5 and 8
3/19	16	30	West	3, 4, and 6
5/13	16	34	West	3, 4, and 6
5/17	27	46	W/S.W.	3, 4, 5, 6, and 8
10/29	17	35	West	3, 4, and 6
1949				
3/25-28	13-18	32	West	5, 6, and 8
4/13	14	30	West	5 and 8
5/17	19	34	S.W./W.	3, 4, 5, 6, and 8
10/5	21	38	W/N.W.	3, 4, 5, 6, and 8
1950				
6/6	45	45 to 56	West	3, 4, 5, 6, and 8
10/27	21	58 to 70	South	3, 4, 5, 6, and 8
11/16	14	60	S.W.	5 and 8
1951				
1/10	39	65	S/S.W.	3, 4, 5, 6, and 8
4/29	25	42	W/S.W.	5 and 8
4/30	22		S.W.	3, 4, 5, 6, and 8
10/24	33	70	S/S.W.	3, 4, 5, 6, and 8
12/1	132	69	West	all
1952				
6/10	17	38	West	3, 4, 5, 6, and 8

* The maximum amplitude usually occurred at Instrument No. 5 with a notable exception on December 1, 1951, when the maximum amplitude occurred at Instrument No. 3.

** See Figure 5 for instrument locations.

g) A wind of any velocity produced its maximum effect if it approached normal to the bridge axis. The amplitude for the same velocity was progressively less as the horizontal angle of approach deviated from 90°.

h) The maximum double amplitude was 45 inches except on December 1, 1951. In that storm the amplitude was three times as great and several special features of the motion were observed, as described later in this report. The only significant structural effect of this motion was damage to the bronze facing plates of the wind shoes which necessitated replacement of the plates.

The detailed study of the records was directed toward three major objectives:

a) To correlate the observed motions of the bridge with its computed natural modes of oscillation;
b) To determine the relation between the bridge motion and the velocity and direction of the wind which caused it;
c) To correlate the observed behavior of the bridge with the behavior of a 75-scale section model of it which was tested in the wind tunnel at the University of Washington on the initiative of the Washington Toll Bridge Authority.(7)

Some attention, also, was given to such evidence as could be obtained concerning the general character of the wind—its possible vertical angularity and degree of uniformity.

Wave Form and Frequency

In Fig. 6 are shown the wave forms and frequencies of several of the natural modes of motion of the Golden Gate Bridge computed by formulas developed in the cooperative research projects of the Washington Toll Bridge Authority, University of Washington and Bureau of Public Roads(8) and of the Oregon State Highway Department, American Institute of Steel Construction and Bureau of Public Roads.(6) The calculations took into account the vertical stiffness of the trusses, the extensibility of the cables and the torsional stiffness of the towers where these factors influenced the mode of motion. The torsional stiffness of the suspended structure without bottom laterals and the bending stiffness of the towers were found to be insufficient to influence the motion. In the study of the asymmetric oscillation which occurred on December 1, 1951, it was found necessary to develop an analysis taking into account the effect of the short hangers near the middle of the bridge. That analysis is described briefly in Appendix III.

Table II shows the modes of oscillation most frequently identified on the bridge together with their observed frequencies and their computed vertical and torsional frequencies. The observed frequency induced by wind action was consistently between the computed vertical and torsional frequencies which agrees with model tests and the theory of flutter (the wind-forced coupling of vertical and torsional oscillation).

Storm of December 1, 1951

a) Instrument Record. In the storm of December 1, 1951, the motion of the bridge differed in several respects from that usually observed. The wind direction was quite steady, changing gradually from southwest at 3 p.m. to west

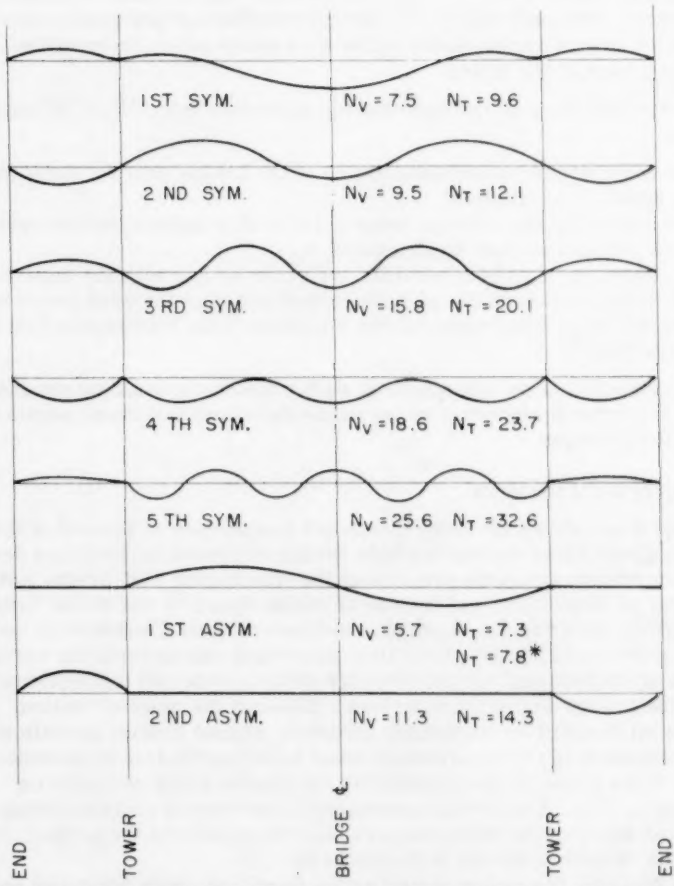

* WITH HANGER PULL EFFECT-FREQUENCIES IN CYCLES PER MINUTE
N_V IS FOR VERTICAL AND N_T FOR TORSIONAL OSCILLATION

FIGURE 6 - COMPUTED WAVE FORMS AND FREQUENCIES OF GOLDEN GATE BRIDGE WITHOUT BOTTOM LATERAL SYSTEM

at 9 p.m. During mid-afternoon, with the wind averaging nearly 50 mph, the usual symmetric oscillation built up to about 2 ft. double amplitude at mid-span, being a little greater at the east or leeward side than at the west. The motion was somewhat random; i.e., the peak amplitudes rose quickly but subsided in two or three cycles and often were not matched by comparable motion at the opposite side of the roadway. Occasional bursts of the first asymetric mode showed at the quarter-points. From 4:45 to 5:00 p.m. the wind died down from a 60 mph gust to an average of about 44 mph and then rose steadily to a 64 mph gust at 5:15. The bridge became relatively calm during this interval but as the more violent part of the storm, 5:15 to 6:20 p.m., began a change in the mode of oscillation took place. Between 5:20 and 5:30 the asymmetric mode became dominant, beginning as a rather spasmodic and random movement but changing quickly to a steadily increasing oscillation of quite constant frequency (about 8.4 cpm). At the south quarter-point where there were instruments on both sides the amplitude was greater on the east (leeward) side, as indicated by instrument No. 3 than on the west (windward) side, instrument No. 4. Also the two sides were usually out of phase from one-fourth to one-half cycle, indicating a coupling of vertical and torsional modes. Such comparisons cannot be made for the north quarter-points because there was no instrument on the east side.

By 5:40 the double amplitudes at the south quarter-points of the main span had reached nearly 80 inches on the east and about 45 inches on the west and a new movement developed. While the asymmetric oscillation continued to increase, a symmetric oscillation at 16.8 cpm (double the frequency of the dominant asymmetric mode) appeared with well defined amplitudes at the centers of the main and side spans. In this symmetric mode the side spans generally moved at opposite phase to the main span movement but much of the time the two side spans themselves were not in phase.*

In contrast to this unsteadiness in phase along the bridge and to the strong element of torsion in the dominant asymmetric motion, the symmetric oscillation was almost pure vertical motion. The reason for this became

*The small time scale of the records makes it impossible to be precise about phase observations. In a few instances during the more violent movements in this storm, the records for instruments Nos. 2 and 9 show obvious distortion possibly due to slack in the drum controls and some of the variation in apparent phase may be due to small slip of this kind. The statements in the text concerning phase relations are based upon enough readings to show clear trends in spite of individual imperfections.

TABLE II

Comparison of Computed and Observed Frequencies (cpm)

Mode	Computed Frequency Vertical	Computed Frequency Torsional	Observed Frequency
First Symmetric	7.5	9.6	8.0
First Asymmetric	5.7	7.3	6.5
Second Asymmetric	11.3	14.3	12 to 12.4

evident when the cause of the symmetric oscillation was recognized as discussed below.

Two characteristics of the first asymmetric mode give rise to a lifting motion at mid-span twice during each cycle of the oscillation. First, the so-called node at mid-span is not stationary but must rise slightly at each extreme of the oscillation because of the distortion of the cable from a symmetrical curve. It is this slight rise of the center of gravity of the bridge which stores the potential energy needed to maintain the oscillation. This slight distortion of the mode is shown in exaggerated form in sketch (a) of Fig. 7. For the Golden Gate Bridge a single amplitude of 5 ft. at the quarter point (equalled or exceeded from 5:50 to 6:10 p.m.) causes a computed mid-span rise of about 2 inches.

The second and greater factor tending to lift the mid-point is illustrated by sketch (b) of Fig. 7. In the first asymmetric mode the mid-point of the cable moves back and forth longitudinally, being shifted toward the depressed quarter-point. For the Golden Gate Bridge this longitudinal displacement from the normal position is about 17 inches for a single amplitude of 5 feet at the quarter-point and is proportional for other amplitudes. If the suspended deck structure remained stationary longitudinally, the hangers would be pulled out of plumb. At the short middle hangers this would lift the suspended structure 1 inch for a 5 foot quarter-point amplitude. If, however, the suspended structure should move in the opposite direction to the cable motion and to the maximum limit of the slot of the wind shoe at the tower, the lift at mid-span would be 4.5 inches. (That such relative longitudinal motion did occur will be demonstrated later.)

Since the vertical movement of the midpoint is upward at both extremes of the dominant asymmetric motion, it follows that the two sides of the roadway must rise together whether the asymmetric mode is vertical or torsional and the 16.8 cpm symmetric motion must be a vertical mode as observed.

These two factors cannot directly account for the single amplitudes of 8 to 12 inches at mid-span which accompanied single amplitudes of 6 ft. at the quarter-points. However, this lifting of the suspended structure near mid-span exerts periodic forces on the cable which could build up a symmetric vertical oscillation whose natural frequency happens to be about 17 cpm. Fig. 6 shows that the third and fourth symmetric vertical modes have frequencies near this value (15.8 and 18.6.) If the third symmetric mode had been excited (see Fig. 6) it should have shown its characteristic frequency and nearly maximum amplitude on the records for instruments Nos. 4 and 6 at the southwest quarter-point and three-eighths point, respectively, of the main span, whereas those records actually showed the dominant asymmetric mode frequency and their amplitudes were consistent with the wave form of that mode. On the other hand, the fourth symmetric mode as computed has its minimum amplitudes at the three-eighths points and its relatively small amplitude at the quarter point would be obscured by the large asymmetric motion. It would, therefore, be revealed only at the middle of the main and side spans where the double-frequency oscillation was actually measured (on instruments Nos. 1, 2, 5, 8, 7 and 10). This mode, with all parts of the bridge rising or falling simultaneously, involves relatively high cable stretch.(9) Periodic vertical pulls confined to the middle portion of the span might be expected to excite just such a mode. The records (typified by No. 2 of Fig. 8) suggest strongly that the actual movement may have been a combination of two vertical modes at frequencies of 8.4 and 16.8 cpm since larger and smaller amplitudes alternate

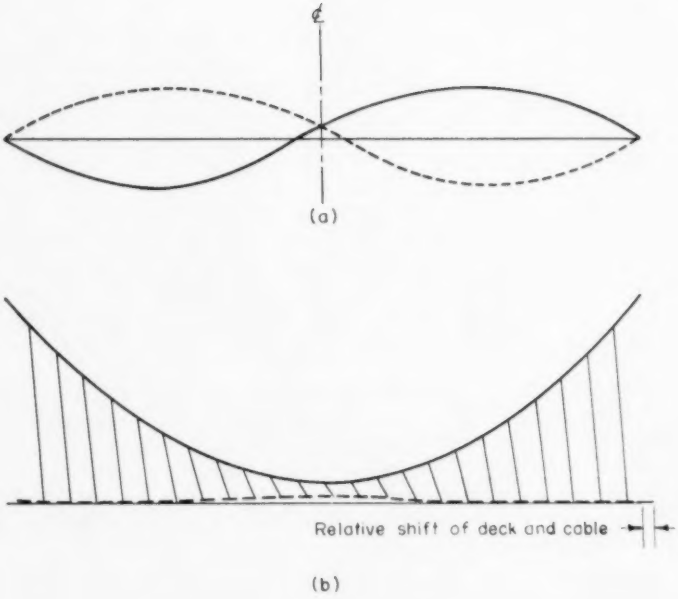

FIGURE 7 - SKETCHES ILLUSTRATING LIFTING AT MIDSPAN DUE TO FIRST ASYMMETRIC MODE.

and this supposition is well supported by the study shown in Appendix II and illustrated in Fig. A-1. The two modes involved might well have had the forms of the first and fourth symmetric. The phase of the side span oscillation differs in these two modes (see Fig. 6) so that the observed shifting of phase might be expected to occur.

Fig. 8 shows portions of the records for December 1, 1951 from two of the instruments. Each record has several parallel hourly traces. Thus, for instrument No. 3 the records shown from 5:52 p.m. to 6:02 p.m. overlap to some extent the parallel records for the corresponding 10-minute intervals beginning successively at 1:52, 2:52, etc. until 7:52 p.m.

The record for instrument No. 3 at the southeast quarter-point of the main span shows a uniform displacement of 0.98 in. along one side which was caused by the damper striking and resting momentarily upon the bottom of the damping pot during the downward displacement of the bridge. Due to the high damping of the instruments and the low frequency of the bridge in relation to that of the instrument, there was no rebound effect and the other half of the record, made while the bridge was above its normal position, was not affected and is therefore reliable. In view of the essential symmetry of the records, the downward displacements may be determined from the preceding and succeeding upward displacements.

The record for instrument No. 3 from 5:57 p.m. to 6:01 p.m. (interpolated between 5:52 and 6:02) shows an average amplitude for the upward displacement of 1.48 inches. Applying the magnification factor computed for the frequency of 8.4 cpm and critical damping indicates an average single amplitude of 6.2 feet. This average was equalled or exceeded sixteen times in this four-minute period, the maximum peak corresponding to a single amplitude of 7.1 feet.

Single amplitudes of 6.4 ft. and 4.0 ft. were recorded simultaneously several times at the southeast and southwest quarter-points, respectively. They were frequently at opposite phases so that the transverse slope was $(6.4 + 4.0)/84$* indicating a single amplitude in torsion of 7.5°.

Fig. 8 also shows a portion of the record for instrument No. 2 at the center of the south side span. This shows the symmetric mode at 16.8 cpm during the same period, 5:52 to 6:02 p.m.

b) Other Indications of Movement. Marks on the paint on the fingered roadway expansion joints between the main span and the towers showed that, at the curbs, the main span had reached positions 27 inches and 25 inches nearer to the north and south towers, respectively, than it occupied six days later on December 7, 1951 when measured in practical calm and at a temperature of about 40°, considerably lower than on the day of the storm. These measurements should be corrected for the effect of horizontal rotation due to lateral deflection which was not measured or estimated on December 1, 1951. In a similar storm on February 11, 1941, R. G. Cone reported the maximum lateral deflection as 5.6 ft. (See Appendix I). The end rotation caused by this much deflection would cause a longitudinal movement of about 2 inches at the curb line. Subtracting this from the measured displacement would leave 25 inches and 23 inches respectively.

It was evident from the damage to the wind shoes that the bearing blocks which transmit the lateral forces from the main span to bearings attached to

* The instruments were located on the sidewalks 3 ft. inside the trusses and 42 ft. from the centerline of the roadway.

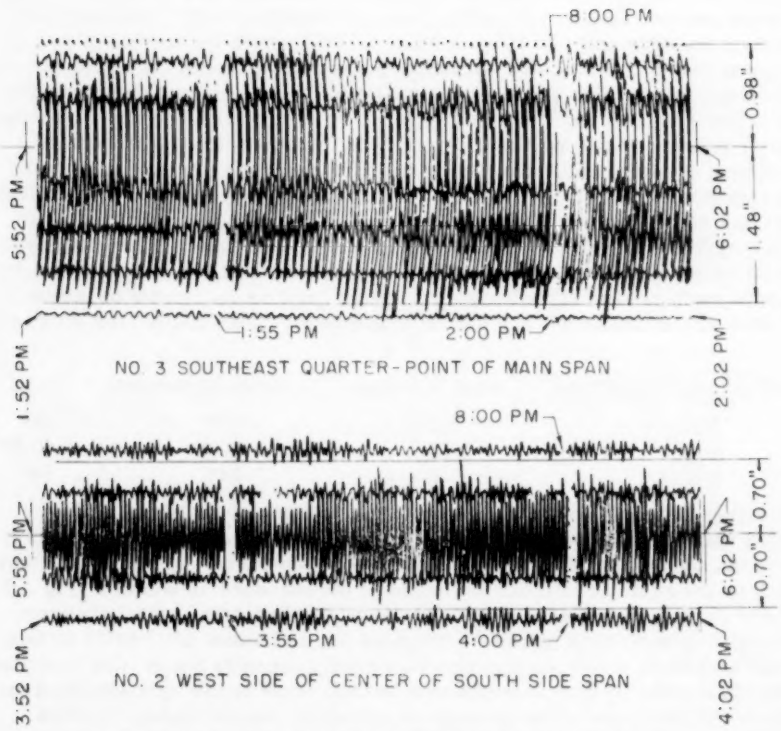

FIGURE 8 - OSCILLOGRAMS FOR STORM OF DECEMBER 1, 1951

the towers had moved longitudinally the full distance permitted by the design. The plans indicate clearance for movements from the normal position of 18 inches toward the tower and 21 inches toward the channel. Presumably these clearances are at 70°, assumed the normal temperature for the design.(10) At 40°, on the day of the inspection, the contraction of the suspended structure alone would increase the clearance toward the tower to about 23 inches. This agrees reasonably well with the marks on the roadway expansion joint noted above.

Fig. 9 shows dimensions in the vicinity of the hangers at mid-span. The hangers pressed against the edges of the steel platform with sufficient force to crimp the edge angles. Mere contact would account for movements of 27 inches in each direction, and the maximum movement must have been several inches more than this. Since the span oscillation was largely torsional, the two cables frequently moved in opposite directions and their pulls on the suspended structure were opposed. It must be presumed that the maximum movement of either cable relative to the deck occurred when its movement was opposite to that of the suspended structure. Its value would be the maximum end movement permitted by the slot plus the negligible change in half span length due to the curvature of the vibration wave plus the longitudinal displacement of the cable center. The first two factors probably account for about 20 inches. The approximate maximum relative movement of the cable and deck at the center of span for various quarter-point amplitudes would then be:

Quarter-point Amplitude	Deck Movement	Cable Movement	Total
5 ft.	20"	17"	37"
6 ft.	20"	20.5"	40.5"
7 ft.	20"	24"	44"

Further indication of relative longitudinal motion of cable and deck appeared where light standards Nos. 65 and 75 rubbed paint off the east cable. These standards are 375 ft. south and north, respectively, of midspan at which locations the cable is at about the height of the standard as shown in Fig. 10. Angular displacement, explained below, brought them into contact with the cable with enough force to rub off the paint for a distance of 44 to 45 inches, extending toward mid-span from points directly opposite the normal positions of the standards. If it is assumed that the full width of the light standard made contact with the cable at the position of maximum displacement, 5 inches should be deducted from the length of the mark to determine the maximum relative movement.

Fig. 11 illustrates how the mark on the cable near standard No. 65 could have been made. When the south half of the east cable moves down, the cable near mid-span moves south a distance which depends upon the quarter-point amplitudes as shown in the tabulation in the preceding paragraph. If the suspended structure also moved south the same distance contact would be made on the cable directly opposite the normal position of the standard at point "A" on Fig. 11 where one end of the mark on the paint was observed. When, on the other hand, the suspended structure moved in the opposite direction while the cable moved south, the contact point would be at the other end of the line at "B".

A relative rotation 5.9° was necessary in order to bring the light standard into contact with the cable as shown in Fig. 10. This rotation resulted from

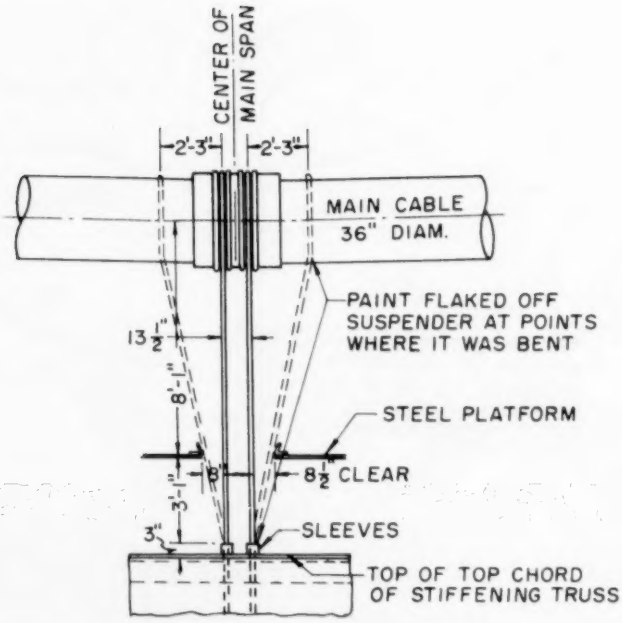

FIGURE 9 - SKETCH ILLUSTRATING RELATIVE MOVEMENT OF CABLE AND DECK AT MID - SPAN.

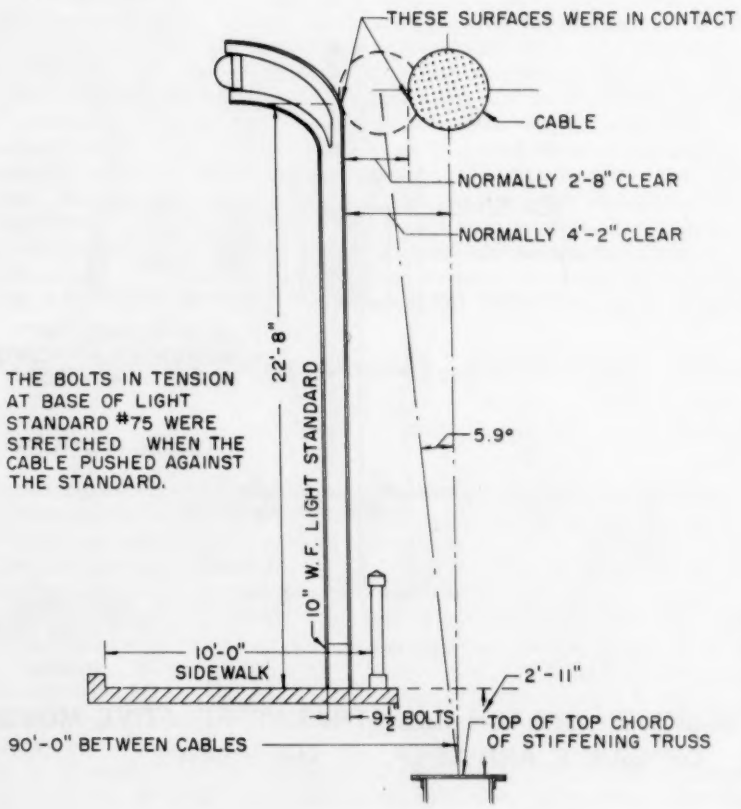

FIGURE 10—SKETCH SHOWING POSITION OF LIGHT STANDARDS 375 FT. FROM CENTER OF SPAN.

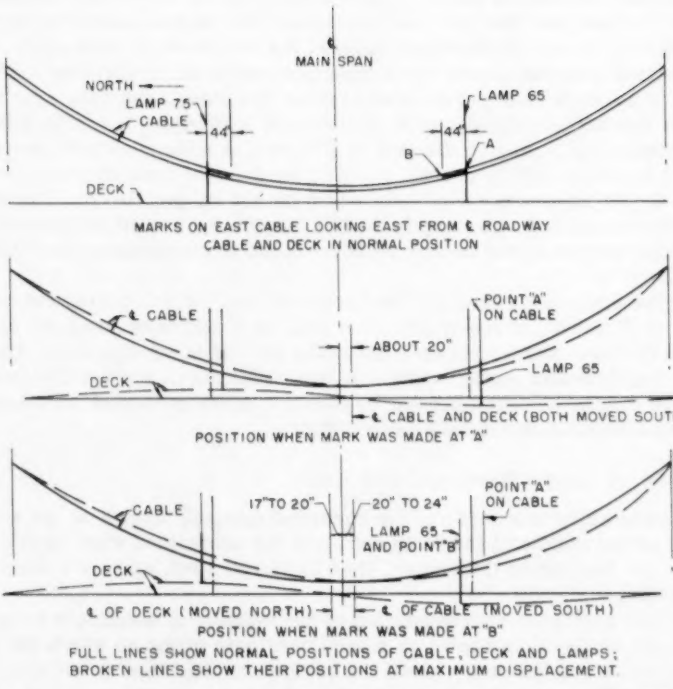

FIGURE 11 - SKETCHES ILLUSTRATING POSITIONS OF CABLE AND DECK WHEN LIGHT STANDARD #65 MADE CONTACT WITH CABLE.

the torsional oscillation and from the transverse slope of the hangers caused by the static pressure of the wind on the suspended structure as detailed below.

The wave form of the first asymmetric torsional mode is essentially a sine curve whose equation is $\theta = \theta_o \sin \pi x/2100$, with x measured from midspan and θ_o representing the amplitude at the quarter-point. At the light standard x = 375 ft. and $\theta = 0.532\theta_o$. For $\theta_o = 7.5^o$, a value often reached during the storm, θ would be 4.0^o.

The transverse wind pressure against the suspended structure is resisted by the cables and by the lateral truss. The division of the loading between them follows the general form of a probability curve, the truss sustaining 100% of the load per foot near the towers and the cables sustaining more than 100% (serving as an intermediate support for the truss) at mid-span. At some section near the center the cables just resist all of the wind load per foot. It is perhaps near the truth to assume that this is the case near these two light standards. The dynamic pressure of a 70 mph wind is 12.5 lb. per sq. ft. Assuming a drag coefficient of 2.8 for this wide structure gives a wind load of 2.8 x 12.5 = 35 lb. per sq. ft. With an exposed area of about 15 sq. ft. per lin. ft. the transverse wind load would be 525 lb. per lin. ft. The dead load of the suspended structure is 14,600 lb. per lin. ft. and the transverse slope of the hanger would be 525/14,600 = 0.036 corresponding to an angle of about 2^o.

Thus the static wind load and the torsional oscillation account for angular rotation of 2^o and 4^o, respectively, or a total of 6^o which is about the minimum required to make contact between the cable and the lamp standard. The additional displacement needed at light standard No. 75 to stretch the anchor bolts 5/16 in. can be accounted for by one of a dozen movements of greater amplitude than used in the above calculations.

Correlation of Bridge Movement with Wind

A detailed study was made of the recorded vertical motion on the west sidewalk at the middle of the main span and the associated wind velocity and direction for the period December, 1944 to March 1946, and for a number of later individual storms.

In Fig. 12 a graphic representation of the relation of amplitude to wind velocity and direction is shown on polar coordinate paper on which the points of the compass and the direction of the bridge axis had been previously indicated. An outline map of the vicinity of the bridge was also sketched in with the center of the bridge at the origin of coordinates.

The wind velocity was scaled outwardly from the center and plotted on the radius representing the direction of approach of the wind. At this point the observed amplitude was recorded. A marked correlation of amplitude with wind velocity and direction became apparent so that connecting points of equal amplitude resulted in consistent amplitude "contours" as shown in Fig. 12.

The contours show very forcefully the effect of wind direction. Moderate winds blowing at right angles to the bridge excite greater oscillation than do violent winds nearly parallel to the bridge. The contours cover little more than the quadrant between west and south; first, because the wind was usually from that quadrant, and secondly, because other winds had little effect on the bridge. During one storm (October 30, 1945) a south wind reached a gust velocity of 75 mph and ranged consistently around 50 mph; yet it produced a

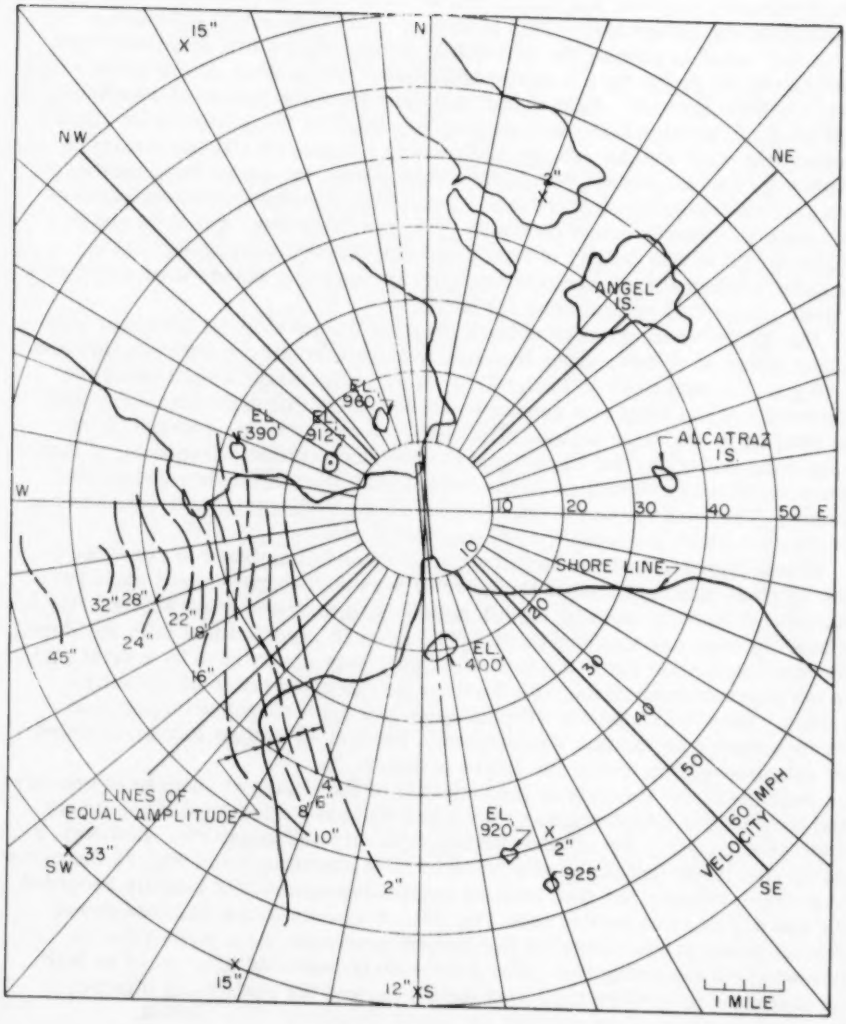

FIGURE 12 – DOUBLE AMPLITUDE OF FIRST SYMMETRIC MODE AT MID-SPAN, WEST SIDE, IN RELATION TO WIND VELOCITY AND DIRECTION, GOLDEN GATE BRIDGE.

double amplitude of only 12 inches.* A north-northeast and a south-southeast wind of 50 mph each produced only 2 inches of double amplitude. A 74 mph wind from north-northwest caused a double amplitude of 15 inches.

It should be noted that if only the normal component of the wind velocity were effective in producing oscillation of the bridge the contours would all be parallel to the bridge axis. This is almost true of the actual contours.

It was noted in plotting the points that occasionally a low amplitude from one storm would fall upon a higher amplitude from another storm of the same velocity and direction. Such variation arises from the degree of steadiness of the wind. In plotting this chart account was taken of the gustiness or steadiness of the wind and the velocity plotted was not necessarily the maximum peak velocity. In general, for fairly steady winds, the points were plotted at the gust velocities which were fairly frequent and uniform although much of the time the velocity might be 6 mph less than the peaks. For very gusty winds the point was usually plotted somewhat below the irregular and infrequent peak gusts. It would appear that an unusually steady wind might give higher values than indicated by the contours.

Fig. 13 shows to enlarged scale a graph of the envelope of the upper and lower limits of velocity taken from the anemometer record between 5:00 and 6:40 p.m. on December 1, 1951. Also shown is the single amplitude of the movement of the southeast quarter-point for the duration of the asymmetric oscillation in the same period. The curve shows a running average of the amplitude neglecting the higher peaks. The characteristic frequency of this mode could not be identified on the record until the amplitude reached 10 inches. This was due to the interference of the symmetric mode and random oscillation which preceded the asymmetric mode.

It may be noted that the amplitude built up and diminished in response to the increase and decrease of the velocity but the response lagged some two minutes or more at several significant changes in velocity and showed only a moderate response to sharp gusts. This is to be expected in a fully developed mode of oscillation since the increment of energy contributed by a brief gust is not great in comparison with the total energy of vibration of the entire bridge. This is in contrast with the quick and brief response on previous records where the motion was somewhat random and not so much controlled by synchronized motion of the entire structure.

Because of the time lag in the response of the bridge to changes in velocity and the reduced effectiveness of brief gusts the recorded amplitudes do not indicate accurately the relation between velocity and amplitude. However, a fairly consistent indication was found by first sketching from Fig. 13 the curve of average velocity and then plotting amplitudes against the velocity recorded 2.5 and 5.0 minutes earlier (see Fig. 14). A smooth curve was then drawn through these points indicating the highest amplitude for a given velocity, following the reasoning that these more nearly indicated what could be built up at that velocity while the lower values showed the restricting effect of a too brief duration of the velocity for which the points were plotted.

Fig. 15 shows response curves in which the amplitude of oscillation is plotted against the velocity of the wind which caused the oscillation. The coordinates shown are for the bridge itself. The curves from model tests have been adjusted to prototype coordinates by proper scale factors.

---

*During this storm there was only the one instrument on the bridge, at midspan. An asymmetric oscillation of greater amplitude could have occurred without detection.

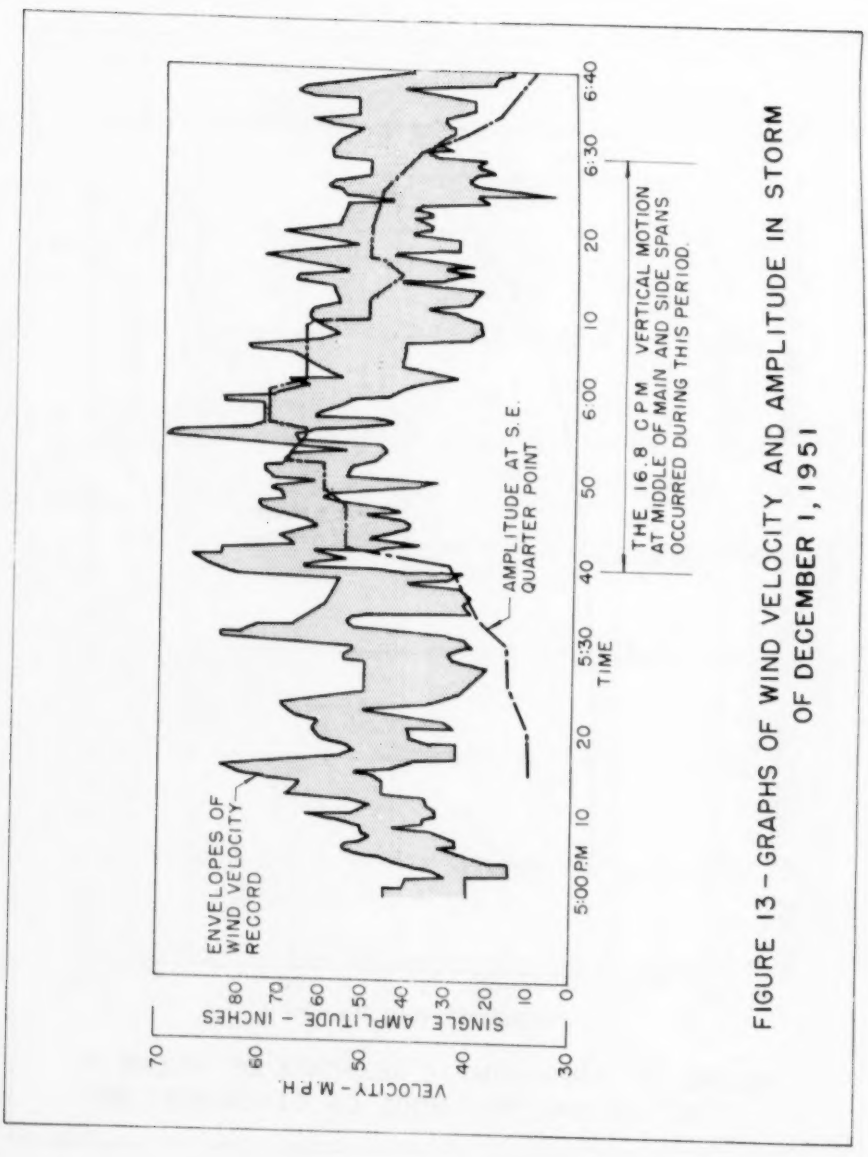

FIGURE 13 – GRAPHS OF WIND VELOCITY AND AMPLITUDE IN STORM OF DECEMBER 1, 1951

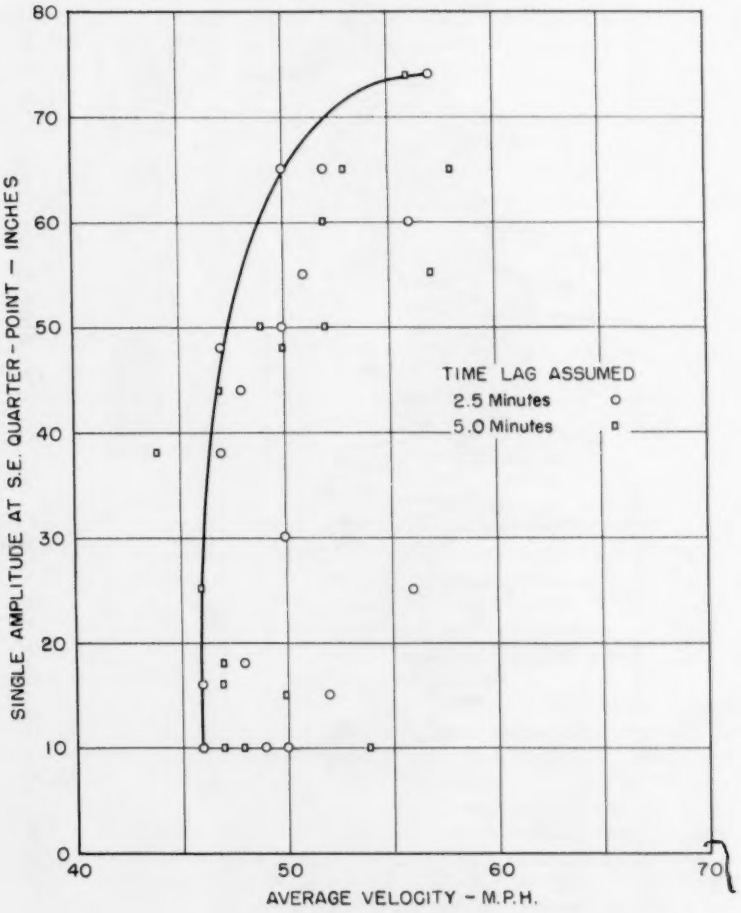

FIGURE 14 – APPROXIMATE RESPONSE OF BRIDGE IN FIRST ASYMMETRIC MODE ON DECEMBER 1, 1951.

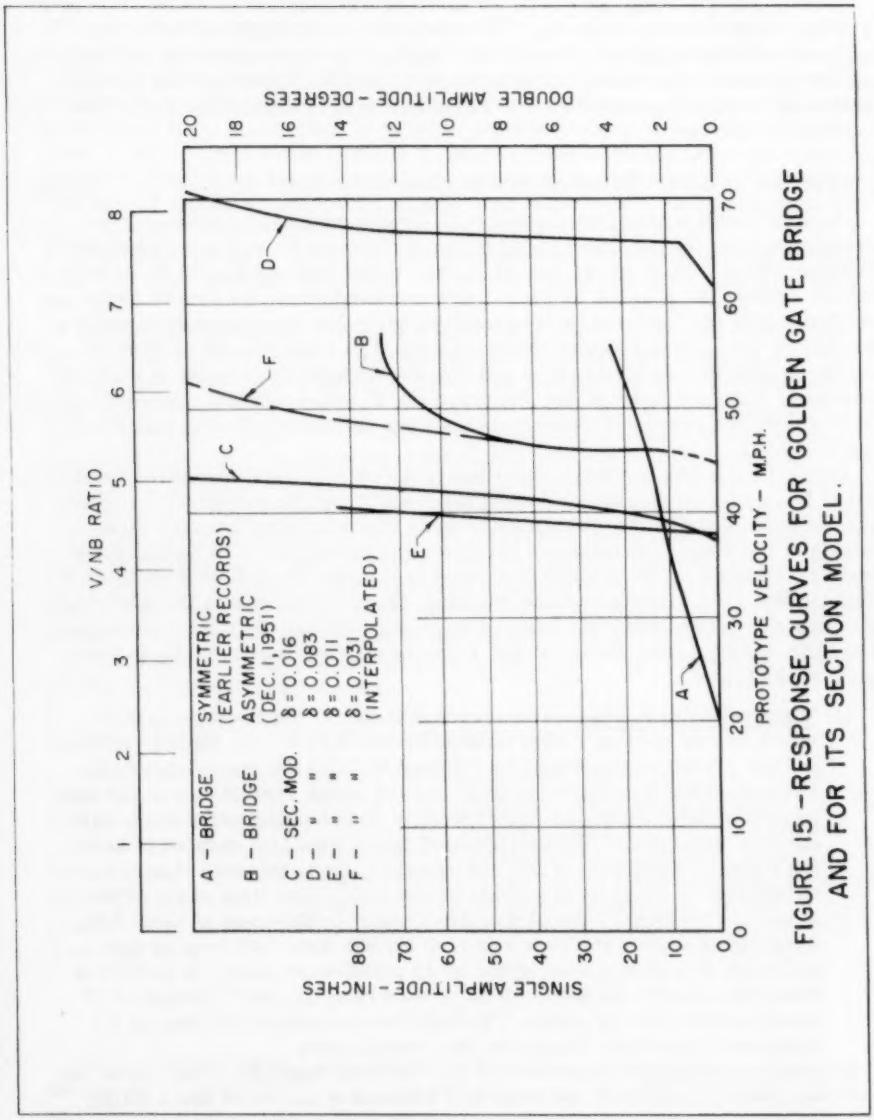

FIGURE 15 - RESPONSE CURVES FOR GOLDEN GATE BRIDGE AND FOR ITS SECTION MODEL.

Curve A was obtained by plotting amplitude against wind velocity as taken from Fig. 12 on a line extending westward from the origin at right angles to the axis of the bridge. It represents an average response curve of the bridge in the symmetric mode having a frequency of about 8 cpm.

Curve B is the response curve for the first asymmetric mode of December 1, 1951, taken directly from Fig. 14. The scale on the right indicates the torsional double amplitude involved in response curve B, assuming the vertical amplitudes of the southwest quarter-point at 0.6 of those plotted for the southeast (leeward) quarter-point. The actual ratio varied from about one-half to two-thirds.

Correlation of Bridge Behavior with Section Model Tests

Section model tests of the Golden Gate Bridge which were made in connection with the investigation of the Tacoma Narrows Bridge are described in Chapter VII of Part IV of the report on that bridge and in Chapter IV of Part V.(11) Curves, C, D and E of Fig. 15 are torsional response curves from section model tests plotted to the prototype scale for the asymmetric mode at 3 different structural damping levels. Curve C is from Fig. 85 of Part IV, for $\beta = 0^\circ$ (horizontal wind) and $\delta = 0.016$ (logarithmic decrement of model in still air). Curve D is from Fig. 82(c) for $\beta = 0^\circ$ and $\delta = 0.083$. Curve E is from a test, the results of which have not been published. In this test $\beta = 0^\circ$ and $\delta = 0.011$.

Curve F represents a reasonable interpolation of a section model response curve for a logarithmic decrement of about 0.031. If the structural damping of the Golden Gate Bridge in this mode were known a fairly accurate prediction of the maximum response curve for the prototype could be computed from model tests by the method described in Chapter IV of Part V of U. of W. Bulletin No. 116. Lacking data on damping, curve F represents the best available basis for correlating the laboratory indications and the field observations. The difference between curves B and F can be attributed principally to two factors as follows:

(1) Time required to build—The curves coincide at the lower amplitudes which can be built up rather quickly by the wind but the higher velocities did not continue long enough in the field to build the maximum amplitudes of which they were capable. A very rough idea of this factor may be gained from "Time-to-build" studies on the model setup from which curve C was taken.* These indicated that a wind just capable of building a double amplitude of 18°, for example, required more than a minute to build to 16° from an amplitude of about 10°. The time scale of the model is the square root of its linear scale, in this case $\sqrt{75}$ or 8.66. Applying this scale the time required for the same build-up on the prototype in a steady wind would be 10 minutes or more. It is evident from Fig. 13 that the fluctuations in wind velocity over a period of 10 minutes must greatly reduce its effectiveness toward building up the maximum amplitudes attainable by a steady wind.

(2) Dynamic damping—It is believed that the often opposing direction of the longitudinal motion of the cable and suspended structure had a strong dynamic damping effect on the dominant asymmetric oscillation, absorbing part of the energy which would otherwise have contributed to building

*See Fig. 88 of Part IV, U. of Washington Bulletin No. 116.

up higher amplitudes. A significant amount of energy was also dissipated at the wind shoe bearing plates. In addition, the influences of this longitudinal motion as it changed phase with respect to the asymmetric oscillation constantly altered the relative amplitude and phase of the vertical and torsional components of the coupled oscillation so that they could not maintain the optimum relation conducive to the most effective action of the wind. Furthermore, the symmetric vertical oscillation of the side spans and part of the main span at an observed frequency double that of the dominant asymmetric oscillation, caused primarily by the action of the shorthangers near the center of the main span, was incongruous with the slower coupled motion which the wind tended to impose and thus must have increased the aerodynamic damping. It will be noted from Fig. 13 that this symmetric oscillation prevailed from 5:40 to 6:30 including the period of high wind velocity when the motion might have been expected to reach greater amplitudes than did occur.

In addition to the two sharply defined factors above, the effectiveness of the wind was further weakened by any non-uniformity of the wind velocity along the span.

The thought naturally arises as to why the bridge oscillation in the more prevalent symmetric mode never approached the amplitude developed in the asymmetric mode on December 1, 1951, even though the wind velocity was often comparable to that storm. In 1945 the Washington Toll Bridge Authority's first section model test on this bridge indicated the possibility of much greater motion than had been recorded in the field. It was suspected that this might be a result of non-uniformity in the prevailing west wind which was deflected sharply downward after passing over the high hill just west of the north side span. A simple laboratory test demonstrated the soundness of this theory. The full model of the first design for the new Tacoma Narrows Bridge, with solid deck, was subjected to a wind condition which produced a vigorous oscillation. Then the vanes controlling the vertical inclination of the wind were adjusted over the greater portion of one side span to produce a sharp downward inclination. This had the effect of quickly reducing the oscillation to a small, somewhat random motion.

Correlation with Bleich Flutter Analysis

Dr. Friedrich Bleich applied the mathematical theory of flutter to suspension bridges[6] and extended it to take into account the modifying wind forces caused by the blunt edges.[12] He applied this to section model test data for the Golden Gate Bridge and predicted a critical velocity (at which flutter begins) of 9.2 fps at a frequency of 107 cpm for δ (structural damping) of 0.003. Converted to prototype scale for the first asymmetric mode the critical velocity would be 38 mph, corresponding quite closely to curve C and E of Fig. 15.

SUMMARY

The observations on the Golden Gate Bridge have served to demonstrate the essential reliability of the formulas derived to show the wave forms and frequencies of the various modes of motion of a suspension bridge and also to give considerable confidence in the methods that have been developed for predicting the behavior of suspension bridges in the wind by means of section model tests. This has proved true notwithstanding the presence of structural

factors not taken into account in the analysis and of non-uniformity and unsteadiness in the wind, factors whose influence can be judged qualitatively but not, as yet, on a quantitative basis.

The provision for increasing the time scale of the recordings should increase their usefulness in verifying theoretical analyses of motion. Closer correlation with test indications might be expected if additional anemometers were provided and if the vertical angle of the wind were measured to give a more comprehensive conception of the wind structure associated with the measured bridge response. However, the bottom lateral system which was completed in 1954 is expected to restrict materially the torsional motion of the bridge and may reduce all oscillation to random movements of no significance.*

REFERENCES

1. "Observed Vibrations of Bridges," by Dean S. Carder, Bulletin of the Seismological Society of America, Vol. XXVII, p. 267 (October 1937).
2. "Vibrations Due to Street Traffic," by Elmer E. Hall, Engineering News, Vol. 68, p. 198 (August 1, 1912).
3. "Seismology," by Perry Byerly, Prentice-Hall, New York (1942) Eq. 19.
4. "Mechanical Vibrations," by J. P. Den Hartog, McGraw-Hill (1940) second edition, p. 73. (Fourth edition (1956) p. 57).

*In January 1952, Clifford E. Paine, Consulting Engineer for the Golden Gate Bridge and Highway District, reported to the District's Board of Directors that in his opinion the addition of a bottom lateral system would be highly desirable and he recommended that two engineers be appointed to collaborate with him in an investigation to determine whether or not this should be done. Accordingly, Mr. Othmar H. Ammann and Mr. Charles E. Andrew were engaged by the District to constitute a Board of Engineers with Mr. Paine as chairman. Incidental to the Engineering Board's evaluation of probable benefits arising from the addition of a bottom lateral system it was decided to have conducted a series of section model tests in a wind tunnel. This was to supplement the analytical studies already made which clearly showed that the bracing system would be highly effective and desirable. It was felt that a comparison of section model tests of the bridge with and without bracing would show the effect of the bracing on the general behavior of the structure.

The primary purpose of the bottom lateral system was to prevent torsional oscillation of any objectionable magnitude. Mr. Paine has reported that since its installation winds have often exceeded 40 mph with gusts as high as 68 mph. No torsional oscillation has been recorded and the maximum double amplitude of vertical oscillation was of the order of 22 inches. The tabulation of individual storm records for this period is very consistent with the plot shown in Fig. 12 for the unobjectionable symmetric vertical movement in earlier storms. This movement, of course, is not affected by the bottom lateral system.

5. "Aerodynamic Stability of Suspension Bridges with Special Reference to the Tacoma Narrows Bridge," University of Washington, Bulletin 116, Parts I to V, incl., by F. B. Farquharson, F. C. Smith and G. S. Vincent.

6. "The Mathematical Theory of Vibration in Suspension Bridges," by Friedrich Bleich, C. B. McCullough, Richard Rosecrans and G. S. Vincent, Government Printing Office.

7. University of Washington Bulletin 116, Part IV, Chapter VII.

8. University of Washington Bulletin 116, Part II, "Mathematical Analyses", by F. C. Smith and G. S. Vincent.

9. See Section 15 of "Aerodynamic Stability of Suspension Bridges with Special Reference to the Tacoma Narrows Bridge; Part II, Mathematical Analyses", by Frederick C. Smith and George S. Vincent, University of Washington Engineering Experiment Station Bulletin No. 116, Part II.

10. Report of the Chief Engineer to the Board of Directors of the Golden Gate Bridge and Highway District, page 81. (Published by Golden Gate Bridge and Highway District, 1938.)

11. "Aerodynamic Stability of Suspension Bridges with Special Reference to the Tacoma Narrows Bridge, Part IV, Model Investigations which Influenced the Design of the New Tacoma Narrows Bridge", by F. B. Farquharson, and "Part V, Extended Studies: Logarithmic Decrement, Field Damping, Prototype Predictions, Four Other Bridges", by George S. Vincent. University of Washington Engineering Experiment Station, Bulletin No. 116, Parts IV and V.

12. "Dynamic Instability of Truss-Stiffened Suspension Bridges Under Wind Action", by Friedrich Bleich, ASCE Transactions, Vol. 114, (1949), p. 1177.

APPENDIX I

Observations of Bridge Oscillation

R. G. Cone

Storm of February 9, 1938 (Report of January 7, 1941 at San Francisco)

About 1:00 p.m. on the afternoon of February 9, 1938, a wind of unusually high velocity was blowing through the Golden Gate with the direction normal to the axis of the Bridge as nearly as could be determined. The force of the wind was so strong that it was impossible to stand erect on the sidewalk or on the roadway of the Bridge.

The writer drove to the San Francisco tower in a closed car and was able to open the door on the leeward side and get out on the roadway. By crouching and standing in the lee of the west leg of the San Francisco tower, it was possible to cross the roadway. Sighting along one of the offsets in the tower to the Marin shore, it could be seen that the center of the Bridge was deflected between eight and ten feet from its normal position and was holding this deflected position. It was also observed that the suspended structure of the Bridge was undulating vertically in a wavelike motion of considerable amplitude. The undulations were fairly rapid, in the neighborhood of 20 to 30

vibrations per minute. Because of their rapidity their amplitudes could only be estimated but it appeared that the stiffening truss was being distorted as much as two feet vertically in 300 feet of bridge. The wave motion appeared to be a running wave similar to that made by cracking a whip. The truss would be quiet for a second, and then in the distance one could see a running wave of several nodes approaching. The force of this wave was taken up in the movement of the expansion joint and the rocker arms at the top.

While this movement was going on one of the electricians, Mr. F. L. Pinkham, came by driving a truck. The writer motioned to Mr. Pinkham to stop and get out of the truck. He did so and attempted to climb over the curb slightly north of the tower but the force of the wind blew him back over the curb and down onto the roadway. He crawled over to where the writer was standing in the protection of the tower, and was asked to observe the movements and actions of the Bridge, as a witness to substantiate what had been seen since the oscillations and deflections of the Bridge were so pronounced that they would seem unbelievable. Mr. Pinkham stood for some time observing the Bridge.

The writer then decided to try and secure a record of some of the deflections on film and returned to the office for his camera. Returning with the camera a few minutes later, he noticed that the roadway had stopped oscillating but it was still deflected out of line. He then went to the top of the tower to get a record of the deflection in the camera but by that time the wind had diminished so that the deflection was not pronounced enough to show clearly in the picture.

Storm of February 11, 1941 (Report of March 14, 1941)

Direction of Wind:

From southwest at an angle of approximately 45 degrees with the axis of the Bridge.

Velocities at top of San Francisco Tower:

1:00 p.m.	48 mph
1:15 p.m.	60 mph
2:50 p.m.	62 mph
3:10 p.m.	60 mph
3:30 p.m.	60 mph

First Series Readings:

12:45 to 1:15 p.m. interrupted by heavy rain obscuring sights. Transit was set up in shelter of east leg of San Francisco tower on a line 50 inches east of the east edge of the top chord. 12:45 p.m. foresight on same point, Marin tower.

Deflections laterally:

12:45 p.m.	1.75 ft.
12:50 p.m.	2.30 ft.
1:00 p.m.	2.90 ft.
1:05 p.m.	4.90 ft.
1:15 p.m.	4.00 ft.

During this period vertical oscillations were observed simultaneously at three points along the span by sighting on the stadia hairs in the transit. The period of these oscillations varied from 5-1/2 seconds to 6-1/2 seconds for the full amplitude up and down. At the quarter point and at the third point (San Francisco) the magnitude of the oscillations was from 9 inches to 20 inches as determined from using a 5-inch casting on the chord for a measure.

Second Series Readings:

2:50 p.m. to 3:30 p.m.—wind southwest.

Time	Lateral Deflection	Velocity	Oscillation Quarter point	Center
2:50 p.m. -	5.6 ft	62 mph	2.0 ft	1.6 ft
3:10 p.m. -	4.6 ft	60 mph	1.8 ft	
3:15 p.m. -	2.9 ft	60 mph	1.8 ft	

The period of the oscillations were in the neighborhood of 8 seconds for the full up and down movement.

APPENDIX II

Analysis of Accelerometer Records of Secondary Symmetric Vertical Oscillation of December 1, 1951

Fig. A-1 illustrates the relation between the trace of the accelerometer chart and the actual motion when the latter is a combination of two simple harmonic motions, the frequency of one being twice that of the other.

Curve (c) showing the acceleration, Fig. A-1(b), to a reduced time scale, is similar to the charts for instruments 5, 8, 1 and 2 made during the asymmetric oscillation of the bridge on December 1, 1951 and illustrated by Chart No. 2 of Fig. 8. It was derived from a curve for the motion shown by the full line in Fig. A-1(a) which is composed of two simple harmonic motions one having a circular frequency, 2ω, and amplitude, A, and the other a lower frequency, ω, and a greater amplitude, B. It will be noted that the motion corresponding to acceleration curve (c) shows sharp amplitude peaks nearly equal to A + B at a frequency, ω, alternating with brief periods when there is scarcely any movement. This is quite different from the amplitudes which would be obtained by applying Eqs. (1) and (2) or the curve in Fig. 3 at the frequency, 16.8 cpm, to the alternating high and low amplitudes of the instrument charts. Motions have been seen on small suspension bridges and on models which exhibited the delayed motion and quick whip illustrated by Fig. A-1.

To analyze the charts by this method it is first necessary to determine the acceleration acting at the peak amplitudes. For this purpose Eq. (3) is sufficiently accurate. The actual displacement, a_t of the sprung mass of the instrument with respect to its support is obtained by dividing the single amplitude of the recording, a_o, by .92 which is the ratio of the pen movement to the mass movement by virtue of the mechanical linkage. The static deflection, i.e., the deflection of the sprung mass due to the acceleration of gravity is 11.2" as computed from the known mass and the spring constant. Introducing these values in Eq. (3) the acceleration, α is found to be

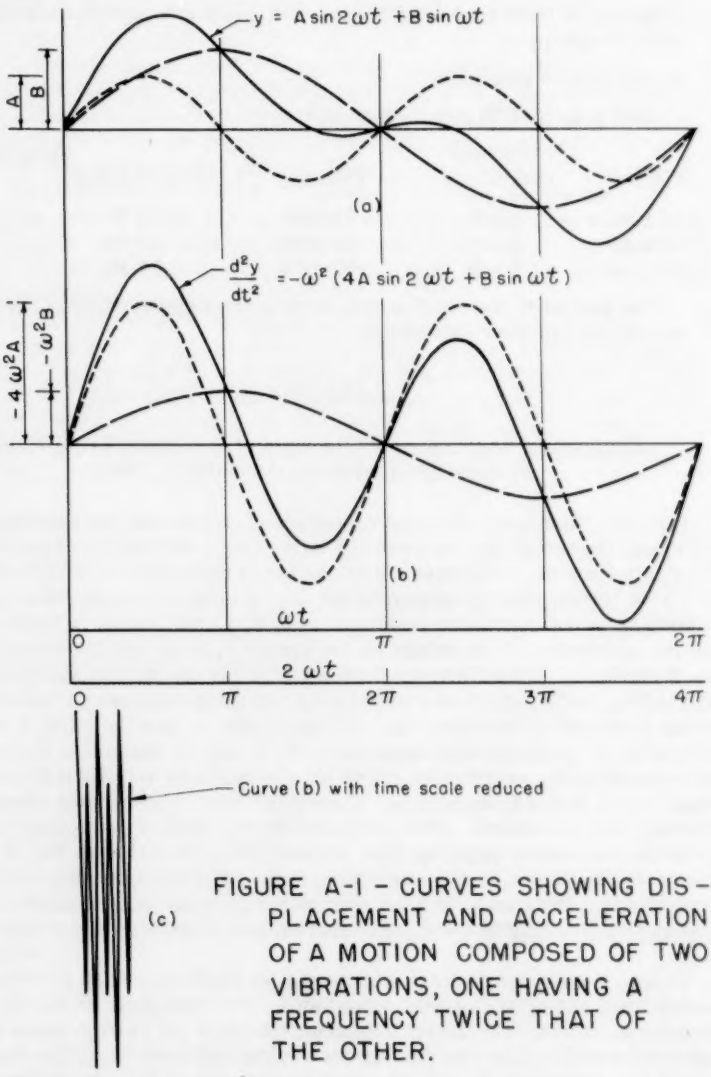

FIGURE A-I - CURVES SHOWING DISPLACEMENT AND ACCELERATION OF A MOTION COMPOSED OF TWO VIBRATIONS, ONE HAVING A FREQUENCY TWICE THAT OF THE OTHER.

$$\alpha = \frac{a_o}{0.92 \times 11.2} \times 32.2 = 3.12\, a_o \text{ ft/sec}^2 \qquad (a)$$

in which a_o is measured in inches. This acceleration may be substituted for $\frac{d^2y}{dt^2}$ (Fig. A-1(b) at the high peak and the low peak giving the two equations which can be solved for A and B, which determine the amplitude of the motion of the bridge, sketch (a). The equations depend upon the relative amplitudes, A and B, and must be solved by trial. In studying the motions of points 5, 8, 1, 2, 7 and 10 at about 6:08.4 during a period of relatively smooth oscillation it was found that the equations were roughly

$$\text{large peak, } \alpha = \omega^2(4A + .77B) \qquad (b)$$
$$\text{small peak, } \alpha = \omega^2(4A - 77B) \qquad (c)$$

in which ω is the circular frequency, $2\pi N$, which in this case is $\frac{8.4}{60} \times 2 = .88$. The circular frequency, 2ω, corresponding to the higher frequency, 16.8 cpm, is 1.76.

Values of α for the large and small peaks at 6:08.4 were computed for points 5, 8, 1, 2, 7 and 10 and these were substituted in Eqs. (b) and (c) to obtain the values of A and B, which were then used to determine the amplitudes of the vertical oscillations of the bridge at the points indicated. The results, shown in the tabulation below, are reasonably approximate indications of the magnitude of the symmetric oscillation at the time selected for comparison.

At approximately that time the single amplitudes outlining the dominant asymmetric mode were

Station 4, South 1/4-pt. main span west	54"
Station 6, South 3/8-pt. main span west	43"
Station 9, North 1/4-pt. main span west	57"

The measurements made are not actually simultaneous—the time scale is too small to permit such measurements—and it is not known which of the high or low peaks of the tabulation may have synchronized with the main sine wave outlined quite well by stations 4, 6, and 9. It is seen, however, that the maximum amplitudes at the center of the main span were about one-fifth of the maximum quarter-point amplitudes of the asymmetric mode.

Station	A (inches)	B (inches)	Approximate Amplitudes (inches) Large	Small
5 center main-east	6.5	7.5	12	2
8 " " west	5	8	11	0.5
1 " S. side-east	6	12	16	0
2 " " " west	5	10	13	0
7 " N. " east	3.5	7	9	0
10 " " " west	6	10	14	0

APPENDIX III

Frequency of Asymmetric Mode as Affected by Longitudinal Component of Hanger Pull

The hangers are long enough to permit relative longitudinal movement of the cable and deck in either direction but they oppose the relative motion by the longitudinal component of the hanger pull when inclined from the vertical. If the first asymmetric mode of oscillation is pure torsion with the cables moving in opposite directions and their longitudinal motions therefore opposed, the deck must either remain stationary with the hangers sloping in opposite directions to the two cables, or it must continuously change its motion with respect to the cables. If it swings with one of the cables, it will not oppose the motion of that cable but its opposition to the other will increase and this difference will result in the two sides oscillating at unequal frequencies so that their phase relation must change. Such action is indeed evident in the records for the storm of December 1, 1951, and considerable variation in frequency is found if only one or two cycles are measured. However, the frequency when averaged over 8 to 30 cycles is quite consistently found to be 8.4 cpm which suggests that the average effect was that of the deck remaining stationary so that the hangers opposed the longitudinal motion of both cables.

An approximate solution for the frequency of the first asymmetric mode was obtained by using Eq. (4.10) from Part II, University of Washington Engineering Experiment Station Bulletin No. 116[8] after substituting for h the computed value of the sum of all the hanger horizontal components for half of the main span. To compute these horizontal components it was necessary to obtain a formula for the longitudinal displacement, ζ_x, at each hanger location. The formula was derived from Eq. (b) on page 15 of Part II. It was solved for each hanger. Then the slope of each was computed as the displacement divided by the hanger length and the longitudinal component of the dead load pull in each hanger was computed. Summing these up for the half span, h was found in terms of η_o, the quarter-point amplitude, and substituted in Eq. (4.10) which was then solved for μ_2 from which the frequency was computed from the relationships given in Part II.

In Eq. (4.10) h is applied to the cable at midspan as a concentrated longitudinal load. This condition is approximated in the present analysis because the longitudinal component of the hanger load drops off rapidly as the hanger length increases and most of the horizontal force comes from a few hangers near midspan.

The computed frequency for the torsional mode was 7.75 cpm which is still 8% less than the observed frequency. Other elements of resistance not considered in this approximate analysis must account for the difference. One such neglected element is the torsional resistance of the tower, not ordinarily considered a factor in the asymmetric modes but brought into limited play in this case by the action of the longitudinal component of the hanger pull.

Paper 1818 October, 1958 ST 6

Journal of the
STRUCTURAL DIVISION
Proceedings of the American Society of Civil Engineers

CONCRETE BEAMS AND COLUMNS WITH BUNDLED REINFORCEMENT

N. W. Hanson[1] and Hans Reiffenstuhl[2]
(Proc. Paper 1818)

SYNOPSIS

Tests of pairs of large beams with conventionally spaced and with bundled longitudinal reinforcement are reported. The bundles of reinforcement used comprised groups of four No. 6, four No. 8 or three No. 9 touching bars. Pairs of beams were compared with respect to width of flexural cracks, steel stress distribution, deflection, and ultimate strength. No significant difference in behavior or ultimate strength was found for bundled as compared to spaced reinforcement.

Tied columns were tested by concentric loading to compare spaced and bundled longitudinal reinforcement consisting of twelve No. 6 or twelve No. 8 bars. Comparison with respect to ultimate strength indicated that bundling is a safe detailing procedure when adequate ties are provided, even for 6.6 per cent longitudinal reinforcement. Splicing of bundled reinforcement in columns was explored and found feasible.

INTRODUCTION

Bundled reinforcement in structural concrete refers to reinforcement placed in groups of touching bars. As compared to the minimum bar spacings commonly used in beams, for instance those given by the 1956 ACI Building Code Requirements for Reinforced Concrete, ACI 318-56 Section 505(a), bundling permits the necessary bars to be placed in much narrower sections. As a result, bundling permits construction of lighter, more graceful and more

Note: Discussion open until March 1, 1959. To extend the closing date one month, a written request must be filed with the Executive Secretary, ASCE. Paper 1818 is part of the copyrighted Journal of the Structural Division, Proceedings of the American Society of Civil Engineers, Vol. 84, No. ST 6, October, 1958.

1. Associate Development Engr., Research and Development Division, Portland Cement Association, Chicago, Ill.
2. Visiting Engr., Research and Development Division, Portland Cement Assn., Chicago, Ill.

economical beams of box, channel or T-section. In beams of normal width, the clear distance between bundles will be considerably greater than the distance between individual evenly spaced bars. Particularly when heavy negative moment reinforcement must be embedded in the top of beams, bundling greatly facilitates concrete placement and insertion of spud vibrators. In columns, bundled reinforcement permits a reduced concrete cross section, which may be an important advantage in the lower stories of tall buildings. Bundling also permits interior ties to be omitted, so that concrete placement is facilitated. Finally, bundled bars in beams and columns may be a satisfactory alternate solution for large sizes of specially rolled reinforcing bars which are occasionally used in very large structures.

Practical use of bundled reinforcement in beams has been pioneered by Mr. H. M. Hadley; the list of references at the end of this paper indicates that he has reported extensively regarding experience with bundling. Several structures with bundled reinforcement have been built,(2,4-7) and good service records have been reported.

Laboratory tests that have been reported(1,3) concern principally bundles of four 1/2-in. square bars in beams, and there may be some question regarding the performance of bundles of larger bar sizes. No tests of bundled reinforcement in columns have been reported. An experimental investigation was therefore carried out in the Research and Development Laboratories of the Portland Cement Association during 1955-57 to investigate the performance of large deformed bars placed in bundles as longitudinal beam and column reinforcement.

Test Beams

As compared to spaced bars, bundling may be questioned primarily with respect to the bond integrity of beams. The most serious conditions may then be expected for bars placed as negative reinforcement near the top of deep and short beams. Previous tests have clearly indicated that, due to adverse effects of settlement, the bond resistance of top bars is less than that of bottom bars; and a short beam span leads to high bond stress before the flexural ultimate strength is developed.(8) The test specimens for this investigation were therefore short, deep beams, with the tension steel at the top as cast.

In the beam designations, the first number shows the number of bars and the second number their size; the letter S indicates spaced bars and B indicates bundled bars; H indicates high-strength steel.

The five test beams with spaced reinforcement shown in Fig. 1, Beams 8-6S, 8-6SH, 8-8S, 8-8SH and 6-9S were designed by first determining the minimum beam width for a chosen group of bars. By ACI 318-56, 505(a), this width is governed by a minimum protective cover of 1-1/2 in. and, for 1-1/2 in. maximum size aggregate, a clear distance of 2 in. between parallel bars. The beam depth was chosen so that the ratio of reinforcement was 1.5 per cent. Finally, the distance from the face of a centrally located column stub to the beam support was chosen as twice the effective beam depth. The beams and all bars were extended 6 in. beyond the supports. The gross concrete dimensions of Beams 8-6S, 8-8S and 6-9S excluding the column stubs were 13x21x97 in., 14.5x33.5x146.5 in. and 11.5x38.8x163.8 in.

The beams with bundled reinforcement, Beams 8-6B, 8-8B and 6-9B were identical to the corresponding beams with spaced bars except for the bar

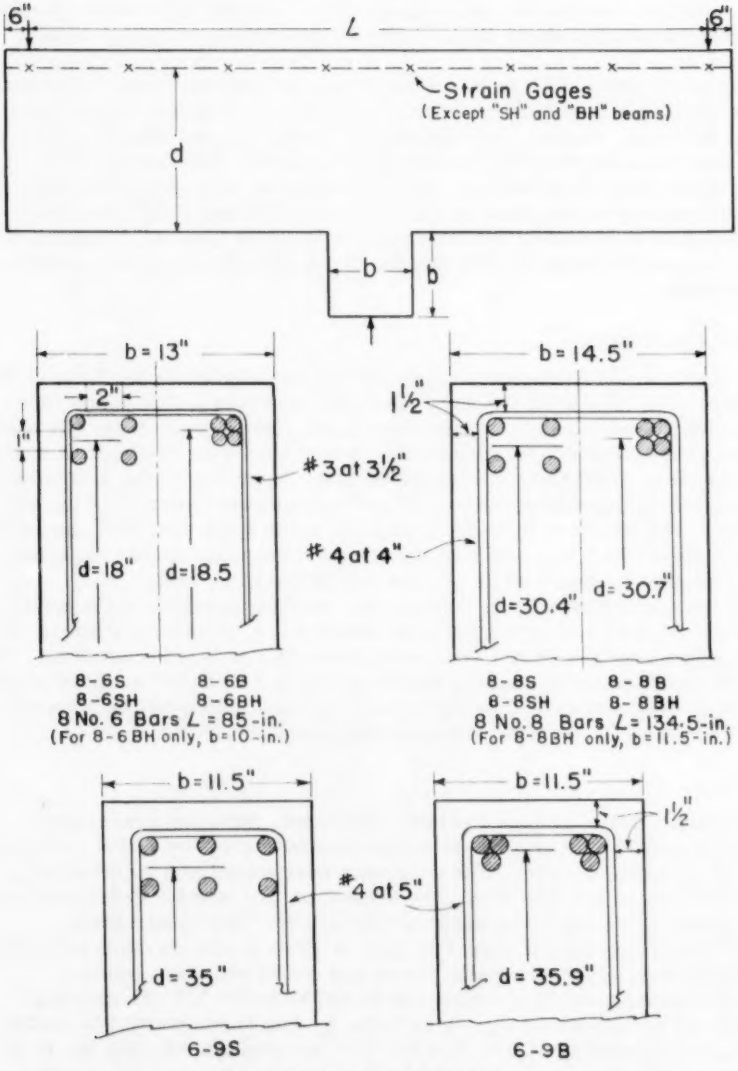

FIG. 1 - TEST BEAMS

arrangement. The effect of decreasing the beam width for bundled reinforcement was investigated through Beams 8-6BH and 8-8BH. For these two beams, and their companions with spaced reinforcement, high-strength reinforcement was used to delay flexural failure and develop very high bond stress.

The column stubs of all beams were reinforced with four bars of the same size as the longitudinal beam reinforcement, and these bars were extended through the beam. Vertical stirrup reinforcement was provided as shown in Fig. 1 to prevent diagonal tension and shear failures. The stirrups also served the function of preventing horizontal splitting that might otherwise have been caused by high bond stress. Beams 8-6SH and 8-6BH had two No. 6 bars placed as compression reinforcement to prevent flexural compression failure, Beams 8-8SH and 8-8BH had two No. 8 bars placed as compression reinforcement.

Properties of Bundles

The external perimeter for a bundle of four bars as shown for Beam 8-6B and 8-8B in Fig. 1 is $3\pi D$, that is, 25 per cent less than for the same bars spaced in the usual manner. On the other hand, a single very large bar with the same cross-section area as a bundle of four bars with diameter D would have a diameter of 2D and a perimeter of $2\pi D$. Accordingly, the bundle of four bars has an exposed perimeter 50 per cent greater than that of the single large bar. The bundle of three bars used for Beam 6-9B similarly has an exposed perimeter 16.7 per cent less than that for the same spaced bars, and 44 per cent greater than that of a larger bar of the same area.

These geometric properties indicate that bundling leads to only a moderate increase in bond stress as compared to spaced bars. Replacing a single very large bar by a bundle with the same area, leads to a reduced bond stress. It should be noted, however, that lug height by ASTM A-305-53T would be greater for a single very large bar than for a bundle of bars, and bond resistance for top bars is known to increase with increasing lug height.(8)

Materials

A laboratory blend of Type I cements was used. Sand and gravel aggregates were combined to gradations within the limits given by ASTM C-33-55T for 1-1/2 in. maximum size. The concretes were mixed in 6 cu ft batches, and had a slump of 2-1/2 to 3 in. The cement content was 4.0 to 4.2 bags per cu yd, and the w/c ratio by weight was 0.62 to 0.70. The compressive strengths reported with the beam test data in Table 1 are averages of twelve to sixteen 6x12 in. cylinders made, cured and tested with each beam.

All reinforcing steel used conformed to ASTM A-305-53T for deformations and had the yield points given in Table 1. Lug height was 0.048, 0.055, 0.067 in. and lug spacing was 0.35, 0.48, 0.50 in., respectively, for No. 6, 8, and 9 bars. The steel was purchased in such lengths that each bar yielded two beam lengths and a test coupon. By using one of these lengths in each beam of a pair, variation in steel properties between pairs was minimized. The No. 3 stirrups used in beams with eight No. 6 longitudinal bars had a yield point of 52,100 psi, the No. 4 stirrups used in the remaining beams 48,700 psi. All reinforcement for each beam was tied together without welding.

TABLE I - BEAM STRENGTH

Beam No.	Main Steel f_y psi	Cylinder Strength f'_c psi	Test Age in Days	Yield Load P_{yield} kips	Ultimate Load P_{test} kips	Flexure Calculated P_{calc} kips	$\frac{P_{test}}{P_{calc}}$	Calculated Bond Stress at Ult.Load psi	Mode** of Failure
8-6S	47,000	2935	15	137.5	150	142	1.05	252*	F
8-6B	47,000	3080	16	137.5	161	148	1.09	351*	F
8-8S	48,300	4375	26	280	314	281	1.12	235*	F
8-8B	48,300	4240	28	260	349	283	1.23	345*	F
6-9S	46,800	4480	14	240	308.5	255	1.21	238*	F
6-9B	46,800	4600	15	240	281	256	1.10	253*	F
8-6SH	84,200	4960	14	---	310	262	1.18	520	FB
8-6BH	84,200	3805	16	---	235	253	---	513	B
8-8SH	80,000	4870	14	---	450	462	---	337	B
8-8BH	80,000	3840	14	---	396	443	---	391	B

*These bond stresses were sustained with no indication of bond failure; the beams failed by yielding of the steel.

**F = flexural failure, B = bond failure, FB = flexural failure after bar slip at beam ends.

Casting

All beams were cast in plastic-coated plywood forms with the column stub down so that the longitudinal reinforcement was embedded near the top as it is near the columns in continuous beams. Concrete was placed by spud vibrators in the test beams and their companion 6x12 in. cylinders. It was found, of course, that bundling of the bars eased the placing operation substantially. After testing the beams it was found that mortar had penetrated into and filled the cavity between the bars of all bundles. The test beams and their companion cylinders were cured one week under moist burlap. The beams were then turned upside down and stored in the laboratory until they were tested at the ages given in Table 1.

Test Method

All beam specimens were tested as shown in Fig. 2, supported on a roller at one end and on a rocker at the other, with a 6-in. overhang at each end. The testing machine load was applied in increments to the column stub through a 2-in. steel plate. The total duration of each beam test was about two hours.

Deflection dial gages were mounted directly below the column edges and mid-way between these edges and the supports. The widths of all cracks were measured by a graduated microscope at the level of the centroid of the longitudinal reinforcement.

To minimize the bar surface area isolated from bond by water-proofing of electric strain gages, SR-4 Type A-12 gages were placed in the intermediate grade bars in milled slots 3/32 in. wide, 3/8 in. deep, and about 6 in. long. The high-strength bars could not be milled. A gage was cemented to the side of each slot, lead wires were attached, and the slot was filled to the bar surface with wax waterproofing. Tension tests indicated that gages so placed yielded measurements in close accord with mechanical strain measurements over the same reduced section. The stress at any bar load was 5 to 9 per cent higher in the slotted section than in the full bar section. Eight strain gages for each beam were located as shown in Fig. 1. Two gages were placed on each of four bars symmetrically about mid-span. The measured strain without correction was assumed to represent the average strain in all bars at the location of the gage. Therefore, measured strain is reported herein as stress obtained by multiplying the average strain in the two half spans by the modulus of elasticity for the full section of the various bar sizes as obtained in tension tests.

Beam Test Results

All beams with intermediate grade steel, Beams 8-6S through 6-9B in Table 1, failed by yielding of the longitudinal reinforcement followed by large deflections and final crushing of the concrete compression zone at the column face. As shown in Fig. 2, both flexural and diagonal cracks tended to extend upward toward the corner at the column stub so that it was hardly possible to differentiate between "flexural" and "diagonal" cracks. No indication of bond failure was found in any of these beams, and no visual difference in behavior was noted for beams with bundled as compared to spaced bars.

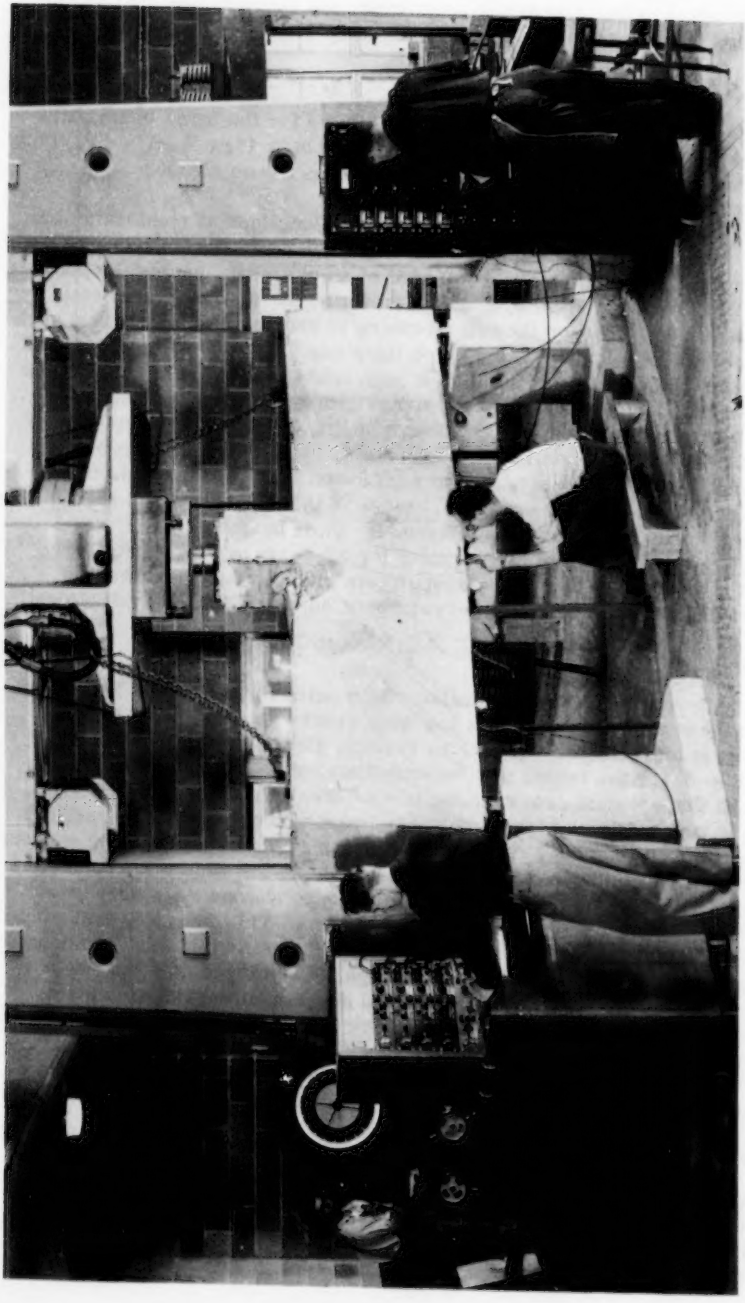

FIG. 2- TESTING ARRANGEMENT FOR BEAMS

Three beams with high strength reinforcement failed in bond as indicated by large amounts of bar slip at the beam ends; for Beam 8-6SH the tension steel yielded following bar slip at the beam ends.

Steel Stress and Deflection

Measured steel stress and deflection are shown for the three beam pairs with intermediate grade steel at various load levels in Figs. 3, 4, and 5. Both steel stress and deflection are given as an average of two measurements symmetrical about midspan for each beam.

Distribution of measured steel stress along a longitudinal reinforcing bar in a beam specimen may be expected to reflect bond distress. Preceding a final destruction of bond, an abnormal rise of steel stress should take place toward the beam ends. Figs. 3, 4, and 5 show that the distribution of steel stress was closely alike for the two members of each pair of test beams even at high steel stress. It may be noted, on the other hand, that the steel stress for all beams was practically uniform at high loads in the middle third of the span. This was certainly caused by a stress redistribution resulting from the deep-beam type of crack pattern shown in Fig. 2. It is also seen that the overhangs contributed to the bonding action because the steel stress of all beams is not zero over the supports at high loads. It is felt that this behavior is related to local stress disturbances in the support region where heavy reaction forces entered the abnormally short beams.

The deflection curves are also similar for all beam pairs. Accordingly, both steel stress and deflection measurements indicate that there was no significant difference in behavior between bundled and spaced reinforcement.

Crack Width

Crack patterns were closely similar within pairs for all tests. Bond distress may be expected to open up a few wide cracks near the beam ends rather than to increase the width of all cracks. Crack widths are therefore given in Fig. 6, for the beams with intermediate grade steel, as the average width of the three widest cracks in the beam. Steel stress is given in the figure as values calculated from applied moment at the column face section, taking the internal moment arm as 7/8 times the effective depth. It is seen that there is no systematic difference between the crack widths for bundled and for spaced reinforcement. Furthermore, no crack opened suddenly before yielding of the reinforcement was in progress. This indicates that even the high local bond stress which acts near cracks resulted in only the normal minor bond slip for bundled as well as for spaced reinforcement.

For the four beams with high strength reinforcement, a similar lack of systematic difference was observed between crack widths for bundled and spaced reinforcement. However, for Beams 8-6BH, 8-8SH, and 8-8BH, a few cracks near the beam ends became very wide shortly before final bond failure took place as the ultimate load was reached.

Flexural Strength, Beams with Intermediate Grade Steel

It is seen in Table 1 that some of the beams with intermediate grade steel carried loads considerably above their yield loads, which yield loads are listed as detected by strain and crack width measurements. The calculated flexural ultimate loads, P_{calc}, were obtained by the equation for ultimate

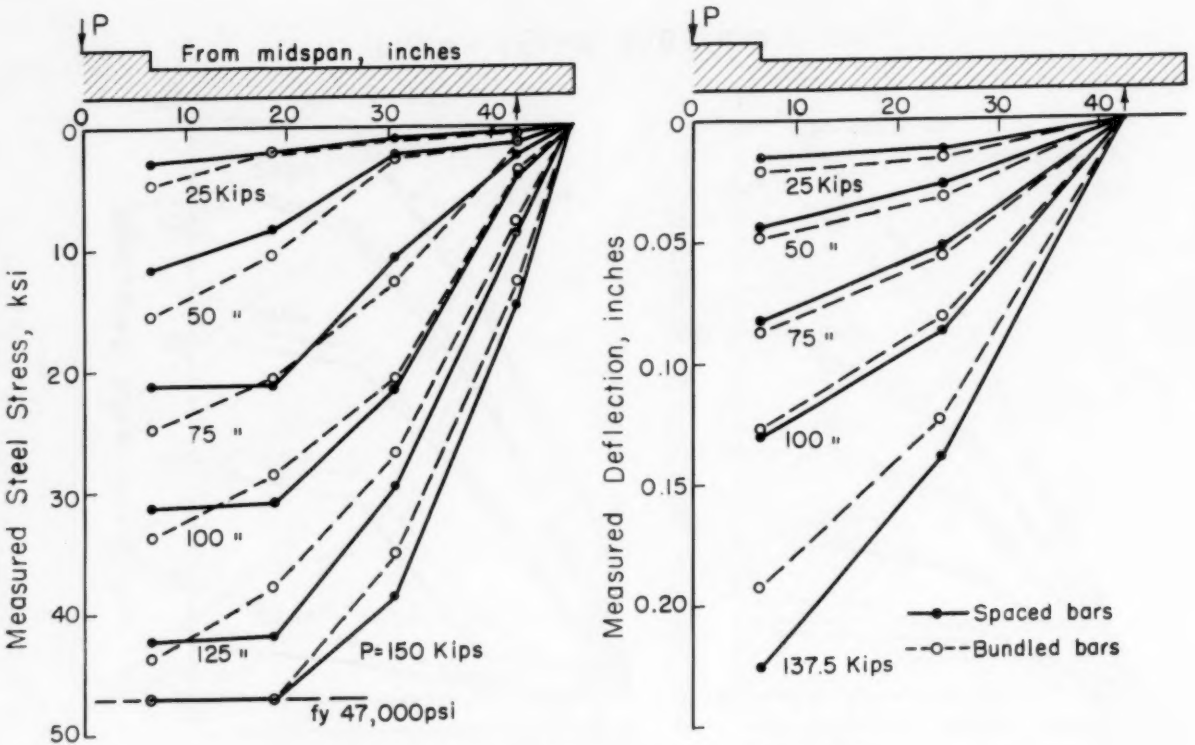

FIG. 3 - BEAMS 8-6S and 8-6B

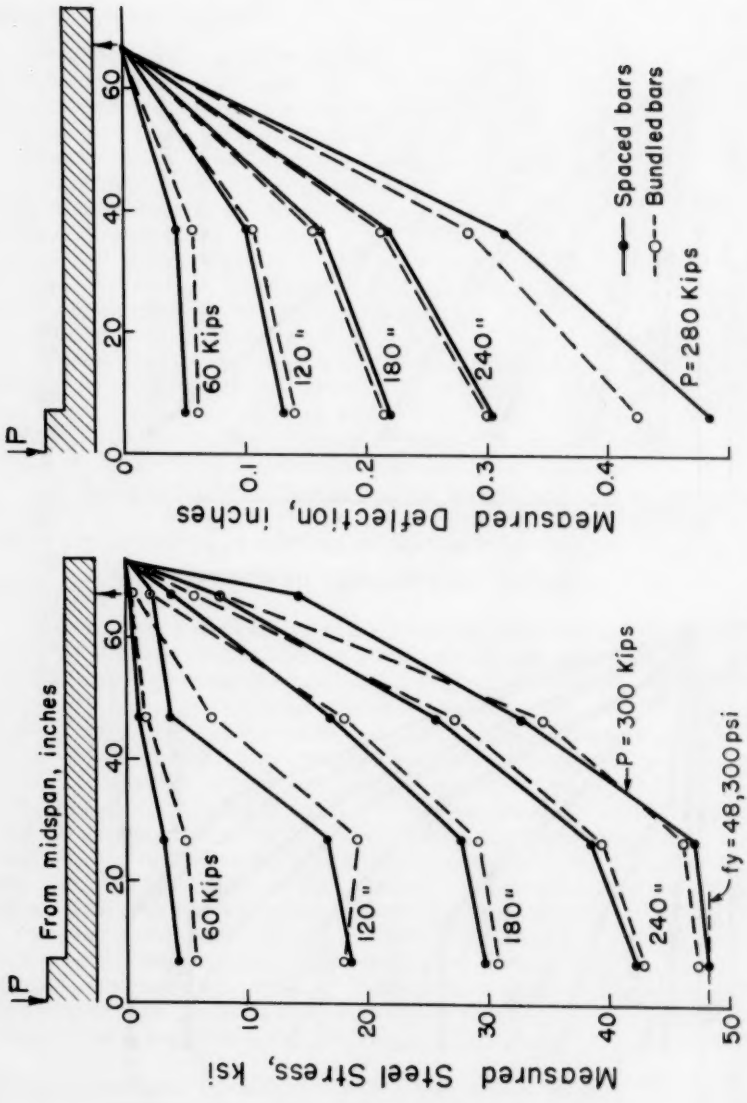

FIG. 4 - BEAMS 8-8S and 8-8B

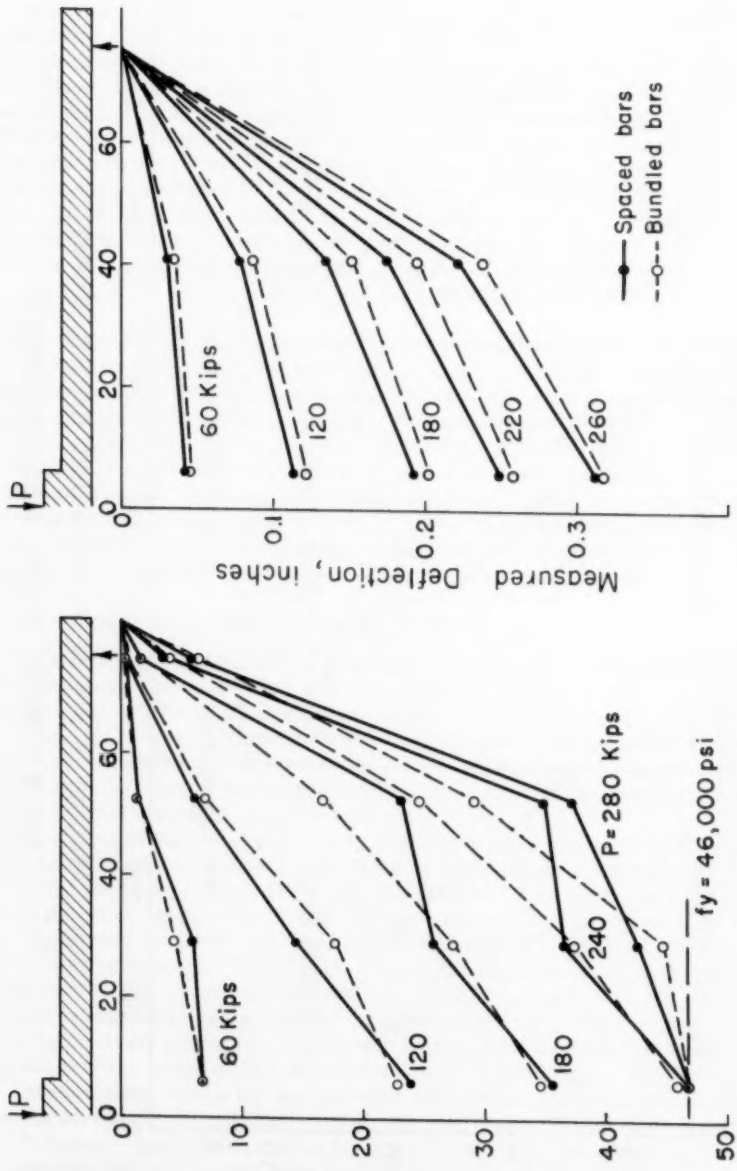

FIG. 5 - BEAMS 6-9S and 6-9B

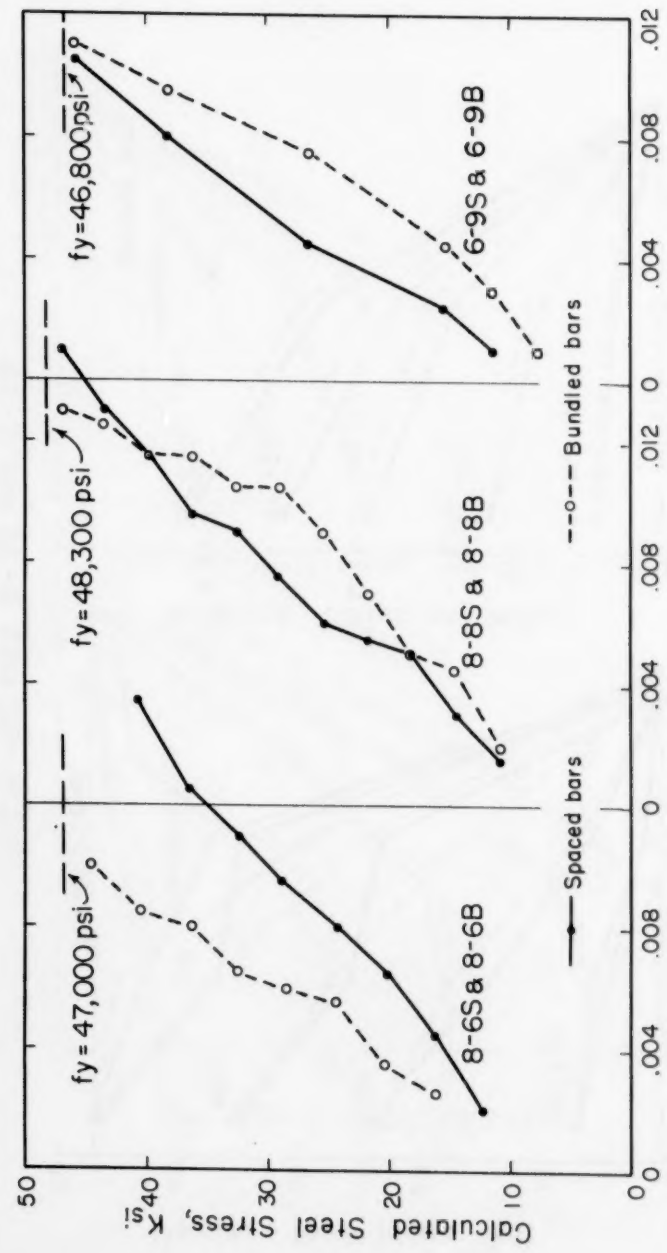

Average Width of Three Widest Cracks, inches

FIG. 6 - CRACK WIDTH MEASUREMENTS

internal moment $M_u = bd^2f'_c\ q(1-0.59q)$ given in ACI 318-56, A605(b), considering the external moment at the face of the column. The ratio of measured to calculated ultimate load exceeds one for all beams. The average ratio for the three beams with spaced bars is 1.13, and the average ratio for the beams with bundled bars is also 1.13. This indicates that there was no systematic difference in ultimate flexural strength developed by spaced and by bundled bars except that the beams with bundled bars were slightly stronger by virtue of the slight increase in effective beam depth.

The average ratio of 1.13 also confirms previous findings that the equation for ultimate moment, which was developed essentially by tests of small beams, is indeed applicable also to the large beams of this investigation. It is believed that the excess of measured ultimate loads over the calculated load resulted principally from strain hardening of the reinforcement. A biaxial state of stress at the column stub appeared to delay crushing of the compression zone so that large steel strains were developed locally at the major flexural cracks.

Bond stresses are given in Table 1 as calculated at ultimate load by dividing the shearing force by the external perimeter of the bars times 7d/8. These bond stresses, for the beams with intermediate grade steel, were sustained without any indication of bond failure. They are in no way to be regarded as ultimate bond stresses. To develop higher bond stresses with intermediate grade steel it would have been necessary to make special test beams with part of the tension zone removed, or to make the beams so short that they would act as walls rather than beams. Both of these cases were thought not to represent practical conditions under which bundled bars may be used. High-strength steel was therefore used to study ultimate load stress.

Bond Strength, Beams with High-Strength Steel

Table 1 shows that the beams with high-strength reinforcement failed at ultimate loads close to the flexural strengths calculated by ACI 318-56, A606(a). Beam 8-6SH failed in flexure after bond slip had been observed at the beam ends. The remaining three beams failed at loads below the computed flexural ultimate. Failure was in bond, as indicated by large amounts of bar slip observed by dial gages as a relative movement between bar ends and the concrete surface at the beam ends.

Bar slip is plotted as a function of calculated bond stress in Fig. 7. Bond stresses at ultimate strength, calculated by dividing shearing force by external bar perimeter times 7d/8, are also shown. It is seen that bond slip was in progress when Beam 8-6SH failed in flexure at a bond stress of 520 psi. By comparison with the slip records for Beams 8-8SH and 8-8BH in Fig. 7, both of which failed in bond, it must be expected that Beam 8-6SH would have failed in bond at a stress only slightly greater than 520 psi if flexural failure had been prevented by a yet higher steel yield point. Hence, the ultimate bond stress for spaced No. 6 bars must be expected to exceed only slightly the value of 513 psi observed for bundled bars. For No. 8 bars, the ultimate bond stress for spaced bars was 337 psi, which is slightly less than the stress of 391 psi observed for bundled bars. It should be noted in Fig. 7, however, that bond stress for a given slip value was always lower for bundled than for spaced bars.

It can be concluded that, when only external bar perimeter was used to calculate bond stress, there was no systematic difference in ultimate bond stress developed by spaced and bundled bars.

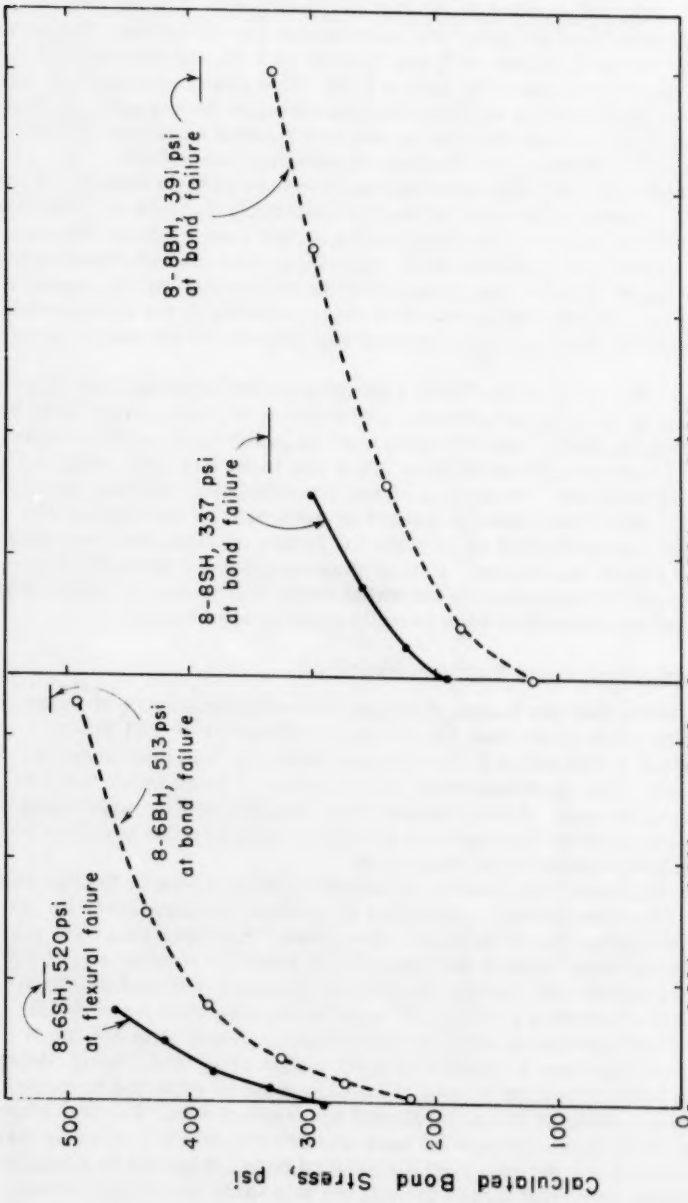

FIG. 7 - BAR SLIP MEASUREMENTS

Test Columns

The beam tests indicated that bundling of tension reinforcement is a satisfactory detailing procedure. A series of 10 tied columns was then designed to study bundled compression reinforcement. Concentric loading was chosen.

An outline of the test program is shown in Fig. 8. All columns were 12x12 in. with a height of 6 ft. Two amounts of longitudinal reinforcement were used, namely, 6.58 and 3.67 per cent made up by 12 No. 8 and 12 No. 6 bars, respectively. The 1/4 in. tie diameter used is the minimum permitted by ACI 318-56, 1104 (c). The corresponding maximum tie spacing of 48 tie diameters is 12 in., which is also the maximum spacing as governed by the 12-in. column size and by 16 times the diameter of the No. 6 bars.

Six columns with 12 No. 8 bars were tested. Column 12-8S contained bars spaced in the regular manner and surrounded by a square tie. The interior bars were held firmly by two interior rectangular ties. All ties were spaced 12 in. Column 12-8B-1 contained bars bundled at the corners. Interior ties were omitted, and the exterior tie spacing was maintained at 12 in. For Column 12-8B-2, the exterior tie spacing was decreased to 6 in. A splice was provided at mid-height of Column 12-8B-3 as shown in Fig. 8. The spliced bars were cut by a saw, and each bar was touching its longitudinal extension. The bars of Column 12-8B-4 were cut at the splice with a hydraulic bar cutter so that the bar ends were wedge-shaped. A clear spacing of 1/4 in. was provided between the two parts of each longitudinal bar. It should be noted that the splice lap is only 10 bar diameters as compared to the minimum amount of 20 diameters given by ACI 318-56, 1103(c). A similar group of six columns with 12 No. 6 bars was tested.

Materials

A laboratory blend of Type I cements was used. Sand and gravel aggregates were combined to gradations within the ASTM C-33-55T limits for 3/4-in. maximum size. The mix ratio, cement: sand: gravel, was 1:3.58:2.38 by weight, and the w/c ratio by weight was 0.64 to 0.68.

Two concrete batches were used for each column. In previous column tests[9] it has been found that failure generally takes place near the top of vertically cast columns. To explore this phenomenon, the bottom batch of some columns was made with a slightly higher w/c-ratio than the top batch. Compressive strengths representing averages of three to four 6x12 in. cylinders for each batch made and cured with the corresponding columns are given in Table 2.

All reinforcement was intermediate grade steel and was tied into cages without welding. The ties were 1/4-in. plain bars, the longitudinal reinforcement conformed to ASTM A-305-53T for deformations and had the yield points reported in Table 2. All reinforcing bars were cut by a saw to a length tolerance of 1/32-in., and 3/4-in. bearing plates were placed touching the bars at the top and bottom of the columns. The lower plate was placed in the form before casting, the upper plate was set in a thin layer of high-strength plaster after the concrete was cured. The heavy tie reinforcement shown in Fig. 8 prevented failure at the column ends by possible local non-uniform stress conditions.

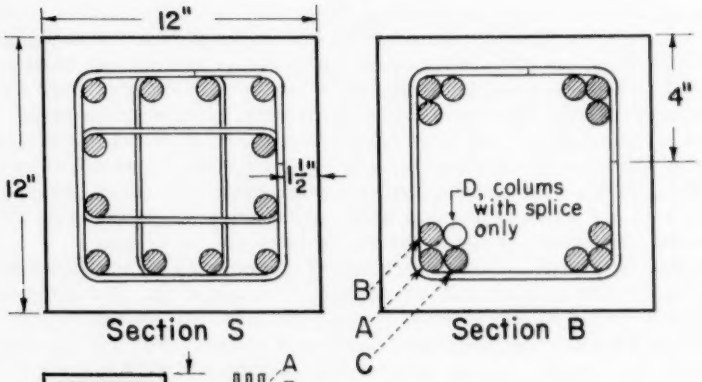

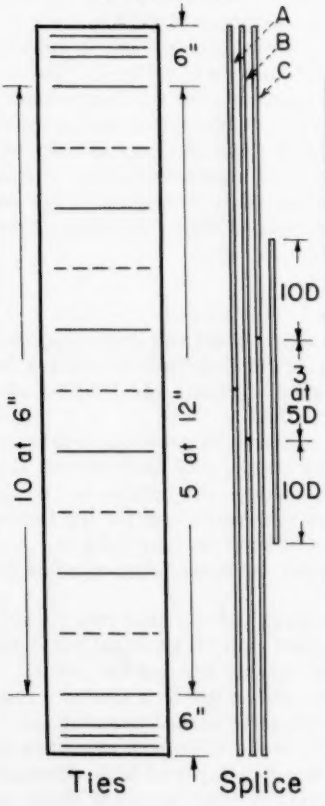

Column No.	Section	Tie Spacing inches	Longitudinal Reinforcement
12-8S	S	12	12 No. 8 BARS Continuous
12-8B-1	B	12	"
12-8B-2	B	6	"
12-8B-3	B	6	Spliced touching
12-8B-4	B	6	Spliced 1/4" clear
12-6S	S	12	12 No. 6 BARS Continuous
12-6B-1	B	12	"
12-6B-2	B	6	"
12-6B-3	B	6	Spliced touching
12-6B-4	B	6	Spliced 1/4" clear

FIG. 8 - TEST COLUMNS

TABLE II - COLUMN STRENGTH

Column No.	Main Steel f_y psi	Cylinder Strength f'_c, psi			Test Age in Days	Measured Ultimate Load P_{test} kips	Calculated Ultimate Load P_{calc} kips	$\frac{P_{test}}{P_{calc}}$	Location of Failure
		Top	Bottom	Average					
12-8S	49,610	3220	3290	3250	5	915	842	1.09	Top
12-8B-1	49,500	3290	3150	3220	8	783	836	0.94	Top
12-8B-2	49,800	3930	3680	3800	6	909	906	1.00	Top
12-8B-3	50,000	3550	3150	3350	6	889	856	1.04	Top
12-8B-4	48,470	3280	3360	3320	7	789	839	0.94	Mid-height
12-6S	48,510	3970	3470	3720	8	726	695	1.04	Top
12-6B-1	49,300	3840	3310	3570	7	702	681	1.03	Top
12-6B-2	48,800	4200	3820	4010	7	758	730	1.04	Top
12-6B-3	50,200	3270	2540	2900	4	702	607	1.16	Bottom
12-6B-4	48,250	2960	2860	2910	6	626	597	1.05	Mid-height

Casting

All columns were cast in a vertical position in plywood forms protected by an epoxy resin paint. Concrete was placed in columns and companion cylinders by spud vibrators, and it was noted that the absence of interior ties in the columns with bundled reinforcement eased the concrete placing operation substantially. By inspection after testing the columns, it was found that mortar had filled the cavity between the bars of all bundles. The test columns and their companion cylinders were cured four to five days under wet burlap. They were then stored in the Laboratory until they were tested at the ages given in Table 2.

Test Method

All columns were tested under concentric loading as shown in Fig. 9, with both ends fixed against rotation. Spherical bearings permitted rotation at both column ends until a load of 20 kips was applied, and the bearings were then blocked by steel wedges. Electric strain gages applied at mid-height of all four column faces were monitored by a continuous strain recorder. The spread between the four gage readings was less than 15 per cent even at ultimate strength, which indicates that a closely concentric loading was obtained for all columns. In addition to electric strain measurements, the total shortening over the entire column height was measured by a dial gage. A continuous loading speed of 160 kips per minute was maintained for all columns.

Column Test Results

The column test results were evaluated essentially in terms of the equation for ultimate strength of concentrically loaded tied columns established during the ACI Column Investigation in the 1930's, $P_o = 0.85\, f'_c\, (A_g - A_{st}) + A_{st}\, f_y$. This equation has been confirmed by several recent investigations(9) and is used in Section A608(b) of ACI 318-56. A comparison of measured and calculated ultimate loads is given in Table 2 together with concrete and steel properties.

The test data were also studied in terms of the relationship between applied load and total column shortening expressed as strain. The load-shortening curves for the columns with 12 No. 8 bars are given in Fig. 10.

Type of Failure

All columns failed by crushing of the concrete followed by buckling of the longitudinal reinforcement. Failure took place in the upper half of all columns except three. The typical nature of such a failure is shown in Fig. 9(a). The strength of the concrete placed in the lower half of some columns was reduced to explore the phenomenon of top failure, which has also been observed in numerous previous tests.(9) Though the cylinder strength of the bottom batch for Columns 12-8B-1, 12-8B-2, 12-8B-3, 12-6S, 12-6B-1 and 12-6B-2, was 4 to 14 per cent less than that of the top batch, failure took place in the upper half of the columns. For Column 12-6B-3, cylinder strength of the bottom batch was 22 per cent below that of the top batch, and in this case failure took place in the lower half of the column as shown in Fig. 9(c). Even so, the measured ultimate load exceeded by 24 per cent the

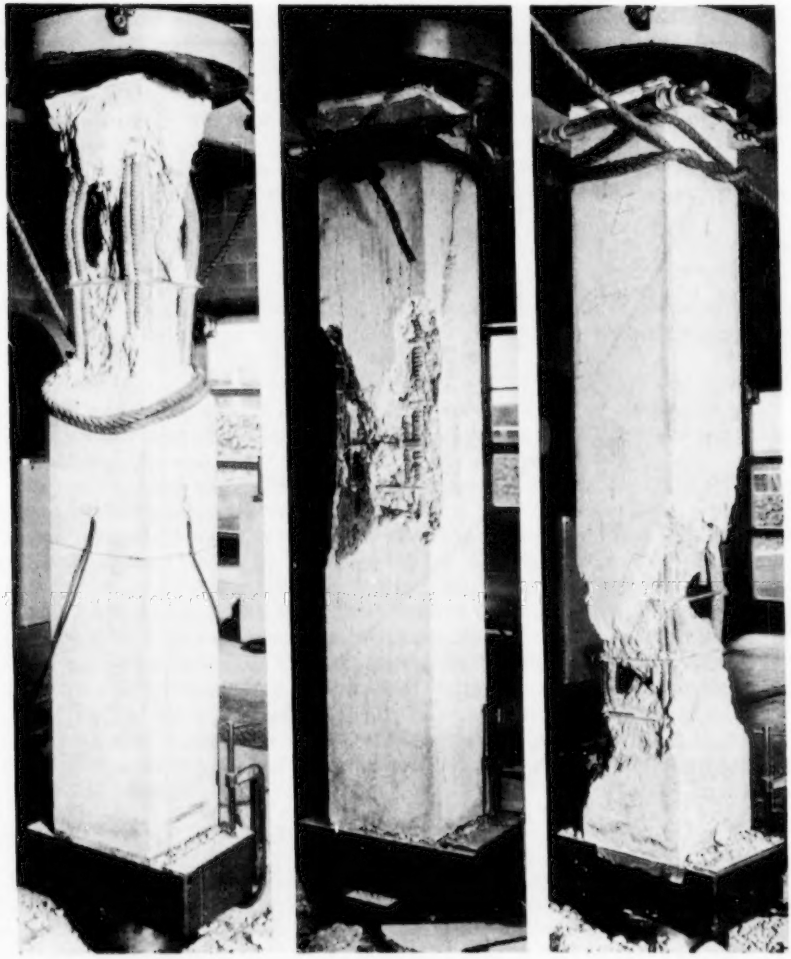

No. 12 - 8B - 1
(a)

No. 12 - 8B - 4
(b)

No. 12 - 6B - 3
(c)

FIG. 9 - TYPICAL COLUMN FAILURES

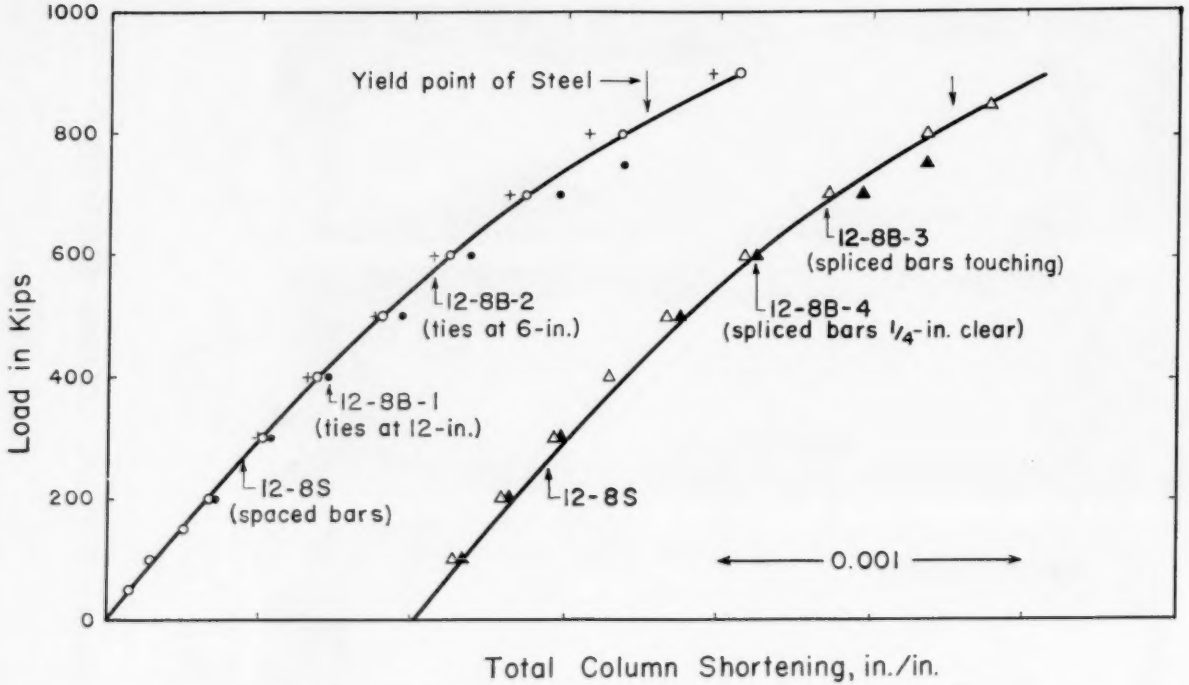

FIG. 10- LOAD-SHORTENING CURVES FOR COLUMNS, 12-8

value calculated on the basis of the cylinder strength for the bottom batch.

These findings confirm the previously reported observation that the column strength of the concrete placed in the lower half of columns is increased, probably by the improved compaction afforded when the upper half is cast. Similarly, the column strength of the concrete placed in the upper half may decrease somewhat by water gain from below. To evaluate effects of bundling, therefore, measured ultimate loads were compared to calculated values based on the average cylinder strength for the top and bottom batch of each column.

The two spliced columns 12-8B-4 and 12-6B-4, which had 1/4 in. clear between bars at the splice, failed in the splice region at mid-height as shown in Fig. 9(b).

Effect of Bundling

The ratios between measured and calculated ultimate load given in Table 2 exceed one for all except two columns. This confirms previous findings that led to the ACI Column Investigation equation.

The load ratios of Columns 12-6B-1 and 12-6B-2 were 1.03 and 1.04 as compared to a value of 1.04 for Column 12-6S that had conventionally spaced bars. For 3.67 per cent longitudinal reinforcement, therefore, no detrimental effect of bundling was found regardless of tie spacing.

For the columns with 6.58 per cent reinforcement, which exceeds the maximum value of 4 per cent given by ACI 318-56, 1104 (a), the 12-in. tie spacing of Column 12-8B-1 led to a load ratio of 0.94 as compared to 1.09 for Column 12-8S with spaced bars. By reducing the tie spacing to 6 in. for Column 12-8B-2, the load ratio increased to 1.00. Furthermore, Column 12-8B-3, which had a 6-in. tie spacing and failed above the splice, had a load ratio of 1.04. Even for 6.58 per cent reinforcement, therefore, no detrimental effect of bundling was found when the tie spacing for bundled bars was reduced to 6 in., that is, 24 tie diameters, or one-half of the least dimension of the column.

Bundling did not significantly affect the relationship between applied load and column shortening. This is shown for the columns with No. 8 bars in Fig. 10. The results for the columns with No. 6 bars indicated a similar lack of effect of bundling.

Splicing

Bundled reinforcement placed in the corners of a column section may be spliced in the same manner as single corner bars. The bars from below may be offset to a position inside the bars above the splice, and a proper amount of lap may then be provided. The bars may also be butted and welded.

In these tests, a splice particularly suitable for bundled bars was explored. As shown in Fig. 8, the splices of the three bundled corner bars were staggered a distance of five bar diameters, and a fourth splice bar 35 bar diameters long was added at each corner. For Columns 12-8B-3 the bars were cut by a saw, and each bar was touching its longitudinal extension. The contact was not perfect; after testing, a mortar layer 1/32 to 1/16 in. thick was found between the bars. Both of these columns failed outside the splice, and the measured ultimate loads exceeded the calculated values by 4 and 16 per cent, respectively.

To simulate less accurate manufacture of reinforcement, the bars of Columns 12-8B-4 and 12-6B-4 were cut at the splice by a hydraulic bar cutter

with 60-degree cutting edges. The bar ends were wedge-shaped by the cutting to an angle of about 90 degrees, and a clear distance of 1/4 in. was provided between the bars when the reinforcing cages were tied. Both columns failed at mid-height in the splice. However, in spite of the unfavorable conditions for a direct stress transfer between bars in the longitudinal direction, the No. 6 bar column developed an ultimate strength 5 per cent over the calculated value. The ultimate strength of the No. 8-bar column was only 6 per cent below the calculated value. As shown for the No. 8-bar columns in Fig. 10, the splice did not significantly change the relationship between load and column shortening.

It was planned in subsequent tests to strengthen the splice by longitudinal welds between the four bars at each splice. Even without welds, however, three out of four spliced columns developed an ultimate strength in excess of the calculated values, and it is obvious that the strength of splices with longitudinal welds would exceed that of the three bars outside the weld. Therefore, no columns with welded splices were made.

It is believed that the short lap used in the splices did not suffice to transfer stress by bond. The mortar between meeting bars was probably subjected to a triaxial state of stress so that a compressive strength far in excess of the cylinder strength could be developed. To assure that the longitudinal bars do not buckle in the splice, the reduced tie spacing used in the tests, 24 tie diameters or one-half the column dimension, may be necessary. If a splice of the type studied is used in eccentrically loaded columns so that tensile stress may be developed in the longitudinal bars, the mortar between bars cannot be expected to transfer stress and welds, or a longer lap, are obviously necessary.

CONCLUDING REMARKS

The test results reported confirm the previous findings of Mr. H. M. Hadley and others that the use of bundled reinforcement is a sound detailing procedure.

It can be expected that bundling of tension reinforcement in beams will not lead to detrimental consequences as compared to spaced bars, if: (1) there are not more than four touching bars in each bundle, (2) bond stress computed on the basis of external bar perimeter is limited to the values now permitted for spaced bars, (3) each bar in a bundle is a deformed bar and is individually well anchored, and (4) stirrup reinforcement is provided in regions of high bond stress.

Bundling of compression reinforcement in tied columns can also be used even for high ratios of longitudinal reinforcement, if the provisions of ACI 318-56 regarding other details are strictly complied with. For large amounts of longitudinal bundled reinforcement, it is advisable to reduce the maximum tie spacing to about one half of that given by the ACI Building Code.

Since bundling of reinforcement was found to be a safe detail in tests involving the extreme cases of bending alone and compression alone, bundling should also be a satisfactory detail for members subject to combined bending and axial load.

REFERENCES

1. Hadley, H. M.: "Precast Box Beams for High Strength," ENGINEERING NEWS-RECORD, Vol. 125, No. 25, Dec. 19, 1940, pp. 838-839.

2. Hadley, H. M;: "Unusual Concrete Roof of Hollow Girders and Precast Slabs," ACI JOURNAL, Feb. 1941, Proceedings Vol. 37, pp. 453-460.

3. Hadley, H. M.: "Tests of Beams Reinforced with 'Bundle Bars,' " CIVIL ENGINEERING, Vol. 11, No. 2, February 1941, pp. 90-93.

4. Boase, A. J.: "Brazil's Wonder Hotel and Casino," ENGINEERING NEWS-RECORD," Vol. 136, No. 2, January 10, 1946, pp. 112-116.

5. Anon.: "Bundle Reinforcing Saves Materials," ENGINEERING NEWS-RECORD, Vol. 140, No. 14, April 1, 1948, pp. 509-510.

6. Hadley, H. M.; "Bridge with 'Bundled' Reinforcement" Western Construction, Vol. 26, No. 6, June 1951, pp. 89-90.

7. Hadley, H. M.: "'Bundled' Reinforcement," ACI JOURNAL, October 1952, Proceedings Vol. 49, pp. 157-159.

8. Menzel, C. A. and Woods, W. M.: "An Investigation of Bond, Anchorage and Related Factors in Reinforced Concrete Beams," Portland Cement Association, Research Department, Bulletin 42, Nov. 1952, 114 pp.

9. Hognestad, E.: "A Study of Combined Bending and Axial Load in Reinforced Concrete Members," University of Illinois Engineering Experiment Station, Bulletin 399, 1951, 128 pp.

Paper 1819 October, 1958 ST 6

Journal of the
STRUCTURAL DIVISION
Proceedings of the American Society of Civil Engineers

MATRIC FORMULATION OF SLOPE-DEFLECTION EQUATIONS

Chu-Kia Wang,[1] M. ASCE
(Proc. Paper 1819)

SUMMARY

A simple and systematic way is outlined so that the slope-deflection equations may be put in matric form. With the use of the electronic computer, the method suggested here will expedite the exact analysis of many complex rigid frames under many loading conditions, including sidesway.

NOTATION

The important notations used in this paper are listed below.

X = a column matrix showing values of all joint rotations and all sidesway displacements

ϕ = a column matrix showing values of elastic rotations at ends of all members due to end moments

M = a column matrix showing values of moments acting on ends of all members, exclusive of fixed-end moments

P = a column matrix showing values of unbalanced moments at all joints and of all unbalanced sidesway forces

A = the statics matrix, expressing the joint (moment) conditions and the sidesway (shear) conditions in terms of the end moments

B = the geometry matrix, expressing the elastic rotations at ends of all members in terms of the joint rotations and sidesway displacements

S = the stiffness matrix, expressing the end moments in terms of the elastic end rotations

Note: Discussion open until March 1, 1959. To extend the closing date one month, a written request must be filed with the Executive Secretary, ASCE. Paper 1819 is part of the copyrighted Journal of the Structural Division, Proceedings of the American Society of Civil Engineers, Vol. 84, No. ST 6, October, 1958.

1. Prof. of Architectural Eng., Univ. of Illinois, Urbana, Ill.

$K = ASB = ASA^T$ = the spring matrix

INTRODUCTION

The slope-deflection method of analyzing statically indeterminate beams and rigid frames has been well established. It involves the solution of a system of simultaneous equations, equal in number to the unknown joint rotations and sidesway displacements. The moment-distribution method, in general, consists in solving the simultaneous equations in the slope-deflection method by successive approximations. Equilibrium of joints and balance of sidesway may be carried in alternate cycles in the same distribution or by combining results from separate distribution tables.

With the recent advance in electronic computation, a matric method is outlined here so that complex rigid frames, such as continuous gable frames or tall building frames, may be analyzed quickly for many different loading conditions including sidesway. The fundamentals of matrix algebra, and its application to the analysis of continuous beams, have been treated by Benscoter.[2] As electronic computing machines are becoming more widely available and used, they may be, in ordinary cases, asked only to produce the inverse of a square matrix, of which the number of rows or columns is equal to that of the unknown joint rotations and sidesway displacements.

Derivation

Consider a statically indeterminate beam or rigid frame. Let m be the total number of members, j the total number of unknown joint rotations, and s the total number of unknown sidesway displacements. Let P be a column matrix of (j + s) rows showing values of unbalanced moments at the joints and unbalanced sidesway forces, due to loads acting on the structure and settlements of supports. Let M be a column matrix of 2m rows showing values of moments acting on ends of all members, exclusive of fixed-end moments due to loads and settlements of supports. Define the statics matrix A of (j + s) rows and 2m columns as conditions expressing the balancing moments at the joints and balancing sidesway forces in terms of the end moments. Then, by definition,

$$\left\{P\right\}_{(j+s)x1} = \left[A\right]_{(j+s)x2m} \left\{M\right\}_{2mx1} \qquad (1)$$

Let X be a column matrix of (j + s) rows showing values of all joint rotations and all sidesway displacements. Let ϕ be a column matrix of 2m rows showing values of elastic rotations at the ends of all members, as caused by the end moments M, exclusive of fixed-end moments. Define the geometry matrix B of 2m rows and (j + s) columns as conditions expressing values of elastic end rotations ϕ in terms of values of joint rotations or sidesway displacements X. Then, by definition,

2. Stanley U. Benscoter: Matric Analysis of Continuous Beams, Tran. ASCE, V. 112, 1947, P. 1109.

$$\{\phi\}_{2mx1} = [B]_{2mx(j+s)} \{X\}_{(j+s)x1} \quad (2)$$

Consider a member jk, the j-end of which is connected to the ith joint. The end moment M_j, which acts clockwise on the member jk and counterclockwise on the ith joint, will balance an externally applied clockwise moment $P_i = M_j A_{ij} = M_j$ at joint i. Thus $A_{ij} = +1$. Geometrically, a clockwise rotation of X_i of joint i will cause a clockwise rotation of $\phi_j = X_i B_{ji} = X_i$ at end j of member jk. Thus $B_{ji} = +1$, and $A_{ij} = B_{ji}$.

Next consider the effect of the end moment M_j on sidesway. The free body for sidesway is usually a joint or a horizontal member and the force acting on this free body and resulting from M_j may be determined by considering member jk or a group of members like jkl, etc. as a free body. If, as an example, the positive direction of the externally applied force P_i on the ith free body for sidesway is horizontal to the right, the positive direction of the balancing force $M_j A_{ij}$ resulting from M_j should be to the left on the ith free body for sidesway, but is again to the right on the free body for member jk or the group of members like jkl, etc. As the member jk or the group of members like jkl, etc. is given a rigid-body motion of X_i horizontal to the right at the point where the force $M_j A_{ij}$ acts, the counterclockwise rotation at end j of member jk is defined to be $\phi_j = X_i B_{ji}$ (A counterclockwise rotation of the axis of a member will add to the clockwise elastic rotation). During this rigid-body motion, the positive work done by the force $M_j A_{ij}$ to the right in going through X_i to the right must be numerically equal to the negative work done by the clockwise moment M_j in going through the counterclockwise rotation $\phi_j = X_i B_{ji}$. Or,

$$(M_j A_{ij})(X_i) = (M_j)(X_i B_{ji})$$

from which

$$A_{ij} = B_{ji}$$

By virtue of both considerations discussed above, it is seen that

$$A = B^T \quad (3)$$

Consider a member AB with variable cross section, as shown in Fig. 1a, subjected to transverse loads P_1 and P_2, and with end B displaced to B' such that angle BAB' = R. The member shown in Fig. 1a is equivalent, both statically and geometrically, to the superposition of those shown in Fig. 1bcd.

In Fig. 2, define S_{AA} and S_{BB} as the stiffness factors at A and B, and C_{AB} and C_{BA} the carry-over factors from A to B and from B to A, respectively.[3] Then, referring to Fig. 1d,

$$\begin{aligned} M_{AB} &= S_{AA}\phi_A + S_{AB}\phi_B \\ M_{BA} &= S_{BB}\phi_B + S_{BA}\phi_A \end{aligned} \quad (4)$$

in which

$$S_{AB} = S_{BA} = C_{AB}S_{AA} = C_{BA}S_{BB} \tag{5}$$

Also, referring to Fig. 1c,

$$\begin{aligned} M'_{FAB} &= (S_{AA}+S_{AB})\ R \\ M'_{FBA} &= (S_{BB}+S_{BA})\ R \end{aligned} \tag{6}$$

For prismatic members,

$$\begin{aligned} S_{AA} &= S_{BB} = 4EI/L \\ S_{AB} &= S_{BA} = 2EI/L \end{aligned} \tag{7}$$

The stiffness matrix S is a square matrix of 2m rows and 2m columns in which the end moments M are expressed in terms of the elastic end rotations ϕ. Entries in the stiffness matrix are those as shown in Eqs. (4) and (5) for members with variable cross section and in Eq. (7) for prismatic members. Then, by definition,

$$\left\{M\right\}_{2mx1} = \left[S\right]_{2mx2m} \left\{\phi\right\}_{2mx1} \tag{8}$$

Substituting (2) and (3) into (8),

$$M = SA^{T}X \tag{9}$$

Substituting (9) into (1),

$$P = ASA^{T}X \tag{10}$$

Defining the spring matrix $K = ASA^{T}$,

$$P = KX \tag{11}$$

and

$$X = K^{-1}P \tag{12}$$

Procedure

The procedure for analyzing a statically indeterminate beam or rigid frame by the matric slope-deflection method may be summarized as follows.

1. Draw the P-X diagram. Number the unknown joint rotations (j) and the unknown sidesway displacements (s) consecutively from 1 to (j + s). Draw arrows (clockwise for joint rotations) on a diagram of the unloaded structure and label them P_1-X_1, P_2-X_2, etc.

3. For full treatment of the statements in this paragraph, see C. K. Wang, Statically Indeterminate Structures, McGraw-Hill Book Co., 1953, Arts. 44 and 54.

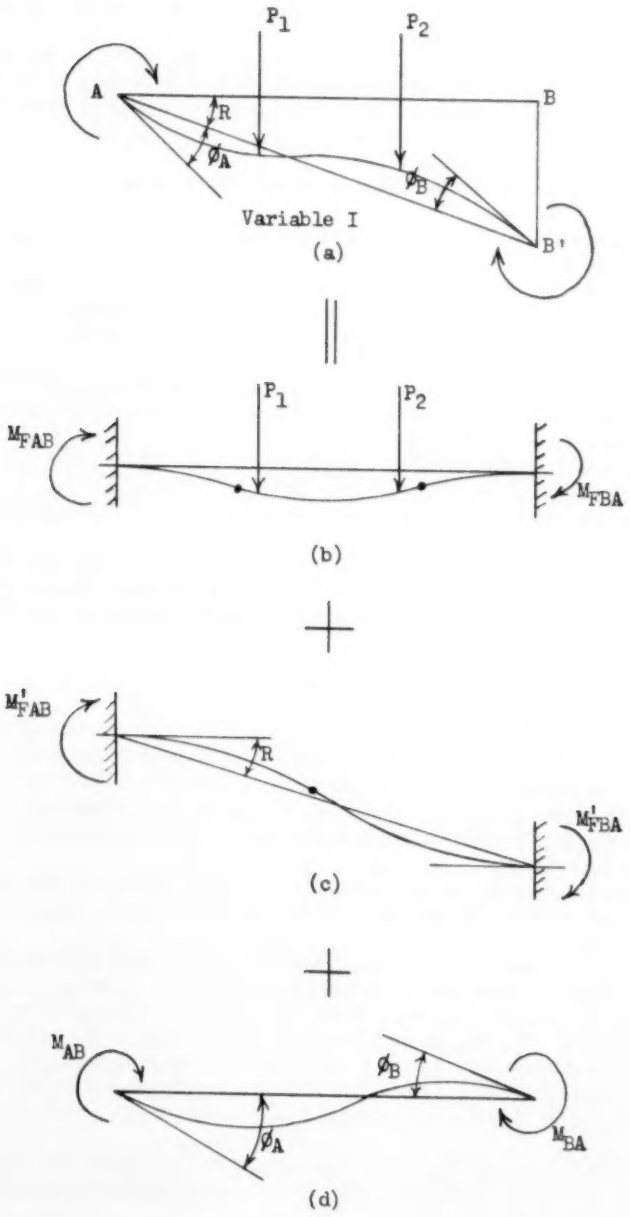
P1
P2
A
B
R
ØA
ØB
Variable I
B'
(a)
P1
P2
MFAB
MFBA
(b)
M'FAB
R
M'FBA
(c)
MAB
ØB
ØA
MBA
(d)

FIG. 1

2. Draw the M-ϕ diagram. Number the unknown end moments (exclusive of fixed-end moments due to loads or settlements) from 1 to 2m. Draw clockwise arrows to act on ends of members and label them M_1-ϕ_1, M_2-ϕ_2, etc.

3. Draw equilibrium diagrams of all joints and all sidesway conditions. Number these free-body diagrams from 1 to (j + s).

4. Construct the A matrix of (j + s) rows and 2m columns, expressing P in terms of M by observing the equilibrium of the free bodies drawn in step 3.

5. Construct the B matrix of 2m rows and (j + s) columns, expressing ϕ in terms of X by geometric considerations.

6. Check and see that $B = A^T$.

7. Construct the S matrix of 2m rows and 2m columns, expressing M in terms of ϕ.

8. Compute the SA^T matrix of 2m rows and (j + s) columns, expressing M in terms of X.

9. Compute the $K = ASA^T$ matrix of (j + s) rows and (j + s) columns, expressing P in terms of X. Note that the K matrix is symmetric.

10. Find the inverse of the K matrix. Use the Crout[4] method on a desk calculator or the electronic computer.

11. Compute all fixed-end moments and unbalanced sidesway forces, due to known loading systems and/or known settlements of supports. Construct the column matrix P of (j + S) rows.

12. Find the X matrix from $X = K^{-1}P$.

13. Find the M matrix from $M = SA^TX$.

14. Combine the fixed-end moments with the M values to obtain final end moments.

15. Draw the free-body diagram of each member and check the consistency of the two final end moments with the values of X pertinent to this member by the moment-area method as is ordinarily known to structural engineers.

Examples

Three representative examples are shown. The conventional slope-deflection and moment-distribution solutions of these examples are contained in Wang's Statically Indeterminate Structures, McGraw-Hill Book Co., 1953. Refer to Examples 55, 57, 71, and 73 in this textbook for Example 1, to Examples 62, 65, 78, and 81 for Example 2, and to Examples 66, 67, 82, and 83 for Example 3.

Example 1. Analyze the continuous beam shown in Fig. 3a due to the loads shown in Case 1, Fig. 3b, and due to a 1/2 in. settlement at support B shown in Case 2, Fig. 3c.

The complete solution is shown in Tables 1.1 through 1.9 inclusive and in Fig. 3d through h. Note that in this problem j = 3, s = 0, and m = 3.

Example 2. Analyze the rigid frame shown in Fig. 4a due to the loads shown in Case 1, Fig. 4b, and due to a rotational slip of 0.002 rad clockwise and a vertical settlement of 0.45 in. at joint D shown in Case 2, Fig. 4c.

The complete solution is shown in Tables 2.1 through 2.9 inclusive and in Fig. 4d through h. In this problem j = 2, s = 1, and m = 3. Note that the A

4. P. D. Crout, A Short Method for Evaluating Determinants and Soving Systems of Linear Equations with Real or Complex Coefficients, Tran. AIEE, V. 60, 1941, P. 1235

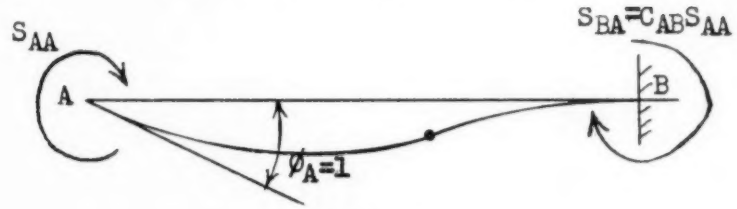

Variable I

(a)

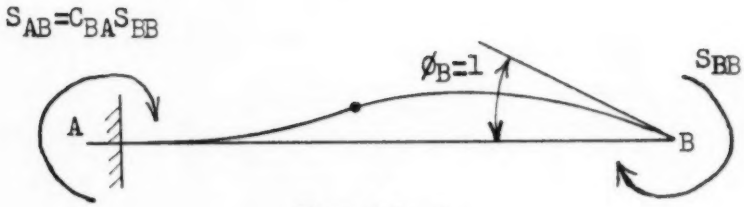

Variable I

(b)

FIG. 2

matrix actually expresses the two joint conditions and the one shear condition. The B matrix is determined entirely by geometric considerations; for instance, when member BC shifts a horizontal distance X_3 to the right, the ϕ values at ends 1 and 2 of member 1-2 will be decreased by $X_3/15$ and those at ends 5 and 6 of member 5-6 decreased by $X_3/10$. It is indeed interesting and desirable to check and see that $A = B^T$.

Example 3. Analyze the gable frame shown in Fig. 5a, due to the loads shown in Case 1, Fig. 5b, and in Case 2, Fig. 5c.

The complete solution is shown in Tables 3.1 through 3.9 inclusive and in Fig. 5d through j. In this problem j = 3, s = 2, and m = 4. Note that H and V in Fig. 5f are found by solving the two simultaneous equations $\Sigma M_B = 0$ (BC as a free body) and $\Sigma M_D = 0$ (CD as a free body). The Williot construction shown in Fig. 5g and h is made in order that the last two columns in the B matrix may be found entirely by geometric considerations. Note also that the unbalanced H forces on joints B and D are found from simultaneous free-body considerations of members BC and CD. In Case 1, H and V are found to be +24 and 0 (Fig. 5i), respectively; and they are +1.5 and +0.75 (Fig. 5j), respectively, in Case 2.

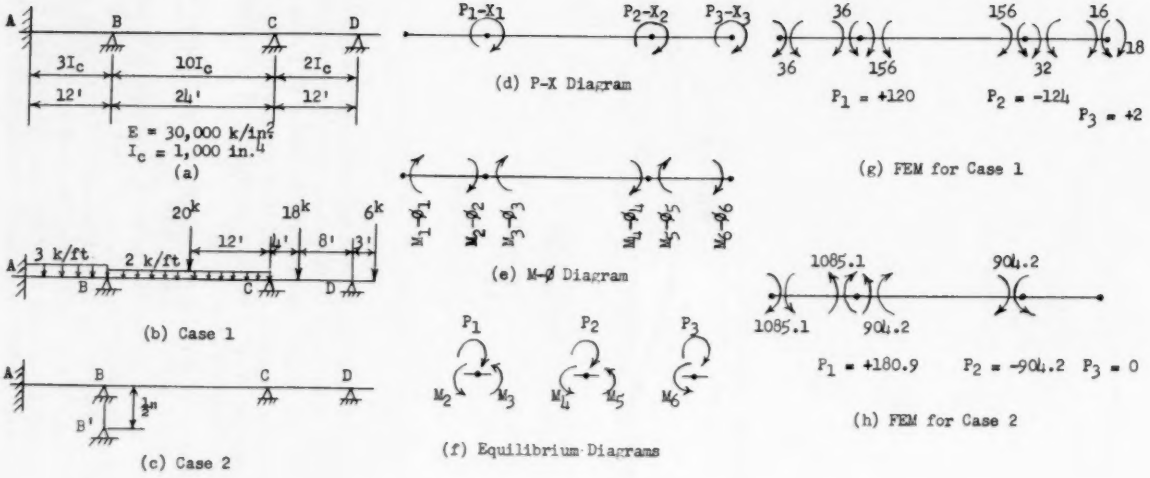
A
B
C
D
3Ic
10Ic
2Ic
12'
24'
12'
E = 30,000 k/in.²
Ic = 1,000 in.⁴
(a)
20k
18k
6k
3 k/ft
2 k/ft
12'
4'
8'
3'
(b) Case 1
½"
B'
(c) Case 2
P1-X1
P2-X2
P3-X3
(d) P-X Diagram
M1-φ1
M2-φ2
M3-φ3
M4-φ4
M5-φ5
M6-φ6
(e) M-φ Diagram
P1
P2
P3
M2
M3
M4
M5
M6
(f) Equilibrium Diagrams
36
156
16
18
32
P1 = +120
P2 = -124
P3 = +2
(g) FEM for Case 1
1085.1
904.2
P1 = +180.9
P2 = -904.2
P3 = 0
(h) FEM for Case 2

FIG. 3

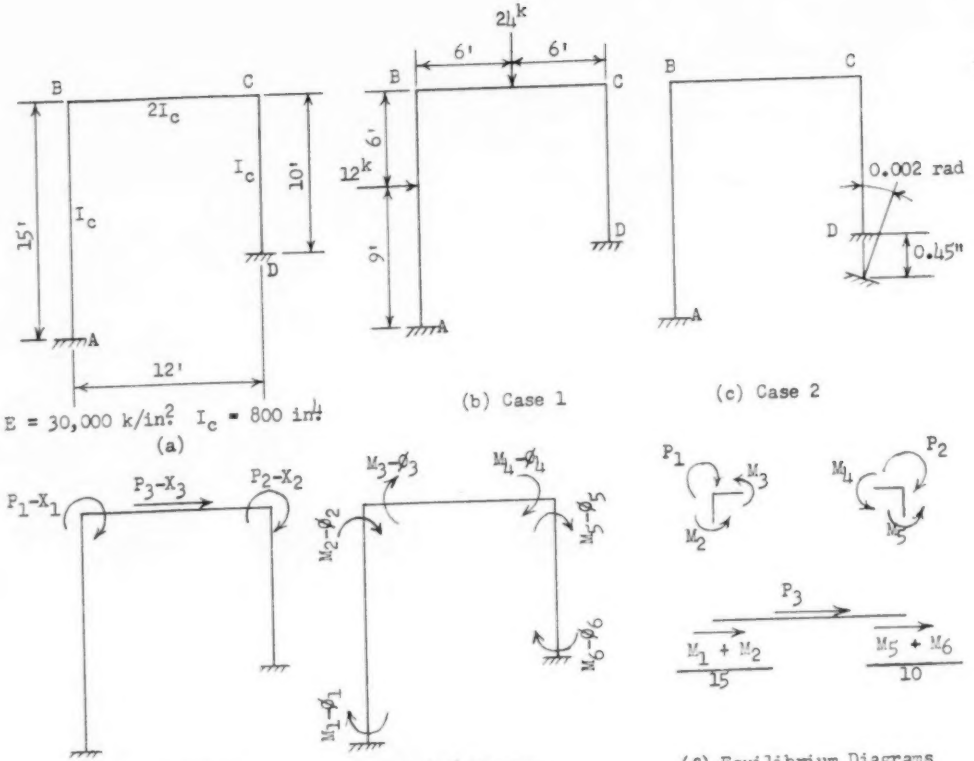

FIG. 4 (to be continued)

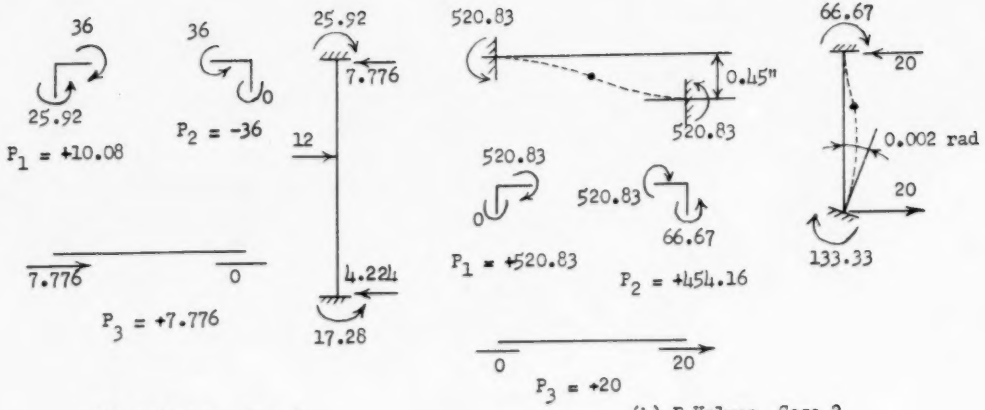

(g) P-Values, Case 1

(h) P-Values, Case 2

FIG. 4 (concluded)

FIG. 5 (to be continued)

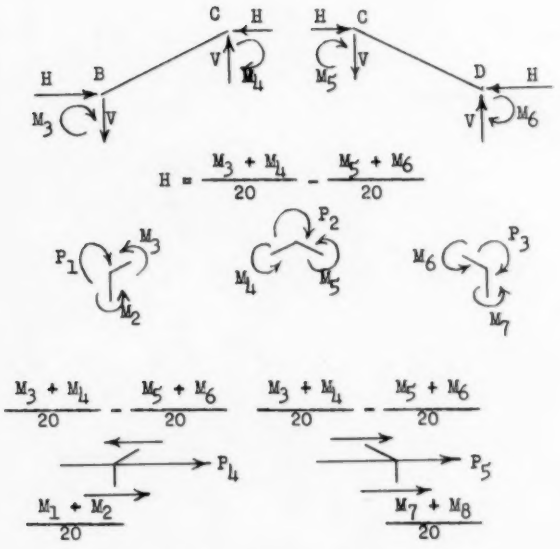

(f) Equilibrium Diagrams

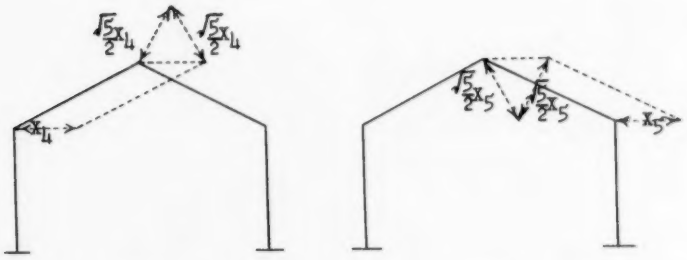

(g) (h)

FIG. 5 (to be continued)

(i) P-Values, Case 1

(j) P-Values, Case 2

FIG. 5 (concluded)

ACKNOWLEDGMENT

The contents in this paper are the results of the continuation of a study jointly undertaken during the summer of 1957 by the writer and P. H. Denke, Strength Analysis Methods Engineer, Douglas Aircraft Co., Inc., Santa Monica, California.

Table 1.1

A (P=AM)						
	M_1	M_2	M_3	M_4	M_5	M_6
P_1		+1	+1			
P_2				+1	+1	
P_3						+1

Table 1.2

B (Ø=BX)			
	X_1	X_2	X_3
$Ø_1$			
$Ø_2$	+1		
$Ø_3$	+1		
$Ø_4$		+1	
$Ø_5$		+1	
$Ø_6$			+1

Table 1.3

S (M=SØ) Multiplier = EI_c						
	$Ø_1$	$Ø_2$	$Ø_3$	$Ø_4$	$Ø_5$	$Ø_6$
M_1	+1	+1/2				
M_2	+1/2	+1				
M_3			+5/3	+5/6		
M_4			+5/6	+5/3		
M_5					+2/3	+1/3
M_6					+1/3	+2/3

Table 1.4

SA^T (M=SA^TX) Multiplier = EI_c			
	X_1	X_2	X_3
M_1	+1/2		
M_2	+1		
M_3	+5/3	+5/6	
M_4	+5/6	+5/3	
M_5		+2/3	+1/3
M_6		+1/3	+2/3

Table 1.5

K = ASA^T (P=KX) Multiplier = EI_c			
	X_1	X_2	X_3
P_1	+8/3	+5/6	
P_2	+5/6	+7/3	+1/3
P_3		+1/3	+2/3

Table 1.6

K^{-1} (X=K^{-1}P) Multiplier = $1/EI_c$			
	P_1	P_2	P_3
X_1	+0.4262	-0.1639	+0.0820
X_2	-0.1639	+0.5246	-0.2623
X_3	+0.0820	-0.2623	+1.6310

Table 1.7

P		
	Case 1	Case 2
P_1	+120	+180.9
P_2	-124	-904.2
P_3	+ 2	0

Table 1.8

X Multiplier = $1/EI_c$		
	Case 1	Case 2
X_1	+71.63	+225.3
X_2	-85.24	-503.9
X_3	+45.63	+252.0

Table 1.9

M		
	Case 1	Case 2
M_1	+35.82	+112.6
M_2	+71.63	+225.3
M_3	+48.35	- 44.4
M_4	-82.38	-652.0
M_5	-41.62	-252.0
M_6	+ 2.01	0

Table 2.1

A (P=AM)						
	M_1	M_2	M_3	M_4	M_5	M_6
P_1		+1	+1			
P_2				+1	+1	
P_3	-1/15	-1/15			-1/10	-1/10

Table 2.2

B (Ø=BX)			
	X_1	X_2	X_3
$Ø_1$			-1/15
$Ø_2$	+1		-1/15
$Ø_3$	+1		
$Ø_4$		+1	
$Ø_5$		+1	-1/10
$Ø_6$			-1/10

Table 2.3

S (M=SØ) Multiplier = EI_c						
	$Ø_1$	$Ø_2$	$Ø_3$	$Ø_4$	$Ø_5$	$Ø_6$
M_1	4/15	2/15				
M_2	2/15	4/15				
M_3			2/3	1/3		
M_4			1/3	2/3		
M_5					2/5	1/5
M_6					1/5	2/5

Table 2.4

SA^T (M=SA^TX) Multiplier = EI_c			
	X_1	X_2	X_3
M_1	+2/15		-2/75
M_2	+4/15		-2/75
M_3	+2/3	+1/3	
M_4	+1/3	+2/3	
M_5		+2/5	-3/50
M_6		+1/5	-3/50

Table 2.5

K = ASA^T (P=KX) Multiplier = EI_c			
	X_1	X_2	X_3
P_1	+14/15	+1/3	-2/75
P_2	+1/3	+16/15	-3/50
P_3	-2/75	-3/50	+7/450

Table 2.6

K^{-1} ($X=K^{-1}P$) Multiplier = $1/EI_c$			
	P_1	P_2	P_3
X_1	+1.21356	-0.33487	+ 0.78877
X_2	-0.33487	+1.28967	+ 4.4004
X_3	+0.78877	+4.4004	+82.611

Table 2.7

P		
	Case 1	Case 2
P_1	+10.08	+520.83
P_2	-36	+454.16
P_3	+ 7.776	+ 20

Table 2.8

X Multiplier = $1/EI_c$		
	Case 1	Case 2
X_1	+ 30.82	+ 495.76
X_2	- 15.58	+ 499.32
X_3	+491.9	+4061.5

Table 2.9

M		
	Case 1	Case 2
M_1	- 9.06	- 42.21
M_2	- 5.01	+ 23.89
M_3	+15.09	+496.95
M_4	- 0.25	+498.13
M_5	-35.75	- 43.96
M_6	-32.63	-143.83

Table 3.1

A (P=AM)								
	M_1	M_2	M_3	M_4	M_5	M_6	M_7	M_8
P_1		+1	+1					
P_2				+1	+1			
P_3						+1	+1	
P_4	-1/20	-1/20	+1/20	+1/20	-1/20	-1/20		
P_5			-1/20	-1/20	+1/20	+1/20	-1/20	-1/20

Table 3.2

B (ϕ=BX)

	X_1	X_2	X_3	X_4	X_5
ϕ_1				-1/20	
ϕ_2	+1			-1/20	
ϕ_3	+1			+1/20	-1/20
ϕ_4		+1		+1/20	-1/20
ϕ_5		+1		-1/20	+1/20
ϕ_6			+1	-1/20	+1/20
ϕ_7			+1		-1/20
ϕ_8					-1/20

Table 3.3

S (M=Sϕ)
Multiplier = EI_c

	ϕ_1	ϕ_2	ϕ_3	ϕ_4	ϕ_5	ϕ_6	ϕ_7	ϕ_8
M_1	0.20000	0.10000						
M_2	0.10000	0.20000						
M_3			0.35777	0.17888				
M_4			0.17888	0.35777				
M_5					0.35777	0.17888		
M_6					0.17888	0.35777		
M_7							0.20000	0.10000
M_8							0.10000	0.20000

Table 3.4

SA^T ($M=SA^TX$)
Multiplier = EI_c

	X_1	X_2	X_3	X_4	X_5
M_1	+0.10000			-0.015000	
M_2	+0.20000			-0.015000	
M_3	+0.35777	+0.17888		+0.026832	-0.026832
M_4	+0.17888	+0.35777		+0.026832	-0.026832
M_5		+0.35777	+0.17888	-0.026832	+0.026832
M_6		+0.17888	+0.35777	-0.026832	+0.026832
M_7			+0.20000		-0.015000
M_8			+0.10000		-0.015000

Table 3.5

$K = ASA^T$ $(P=KX)$ Multiplier = EI_c					
	X_1	X_2	X_3	X_4	X_5
P_1	+0.55777	+0.17888		+0.011832	-0.026832
P_2	+0.17888	+0.71554	+0.17888		
P_3		+0.17888	+0.55777	-0.026832	+0.011832
P_4	+0.011832		-0.026832	+0.0068664	-0.0053664
P_5	-0.026832		+0.011832	-0.0053664	+0.0068664

Table 3.6

K^{-1} $(X=K^{-1}P)$ Multiplier = $1/EI_c$					
	P_1	P_2	P_3	P_4	P_5
X_1	+ 2.7186	-0.78533	+ 0.42277	+ 12.080	+ 19.335
X_2	- 0.78533	+1.7902	- 0.78533	- 7.8535	- 7.8535
X_3	+ 0.42277	-0.78533	+ 2.7187	+ 19.336	+ 12.080
X_4	+12.080	-7.8535	+19.336	+542.76	+438.07
X_5	+19.335	-7.8535	+12.080	+438.07	+542.76

Table 3.7

P		
	Case 1	Case 2
P_1	+40	-15
P_2	0	- 5
P_3	-40	0
P_4	-24	+10.5
P_5	+24	+ 1.5

Table 3.8

X Multiplier = $1/EI_c$		
	Case 1	Case 2
X_1	+ 266.0	+ 119.0
X_2	0	- 91.4
X_3	- 266.0	+ 218.7
X_4	-2802.7	+6214.2
X_5	+2802.7	+5162.7

Table 3.9

M		
	Case 1	Case 2
M_1	+ 68.64	-81.31
M_2	+ 95.24	-69.41
M_3	- 55.24	+54.41
M_4	-102.82	+16.78
M_5	+102.82	-21.78
M_6	+ 55.24	+33.70
M_7	- 95.24	-33.70
M_8	- 68.64	-55.57

Paper 1820 October, 1958 ST 6

Journal of the
STRUCTURAL DIVISION
Proceedings of the American Society of Civil Engineers

EQUIVALENT SYSTEMS FOR THE DEFLECTION OF VARIABLE STIFFNESS MEMBERS

D. G. Fertis,[1] J.M. ASCE, and E. C. Zobel[2]
(Proc. Paper 1820)

SYNOPSIS

A general method is presented for calculating the deflection of members with variable stiffness to any desired degree of accuracy. The method is based on fundamental principles and concepts of engineering mechanics which are known to structural engineers. A member of variable stiffness, EI, loaded in some manner, may be replaced by selected members of uniform stiffnesses, which will have the identical deflection curve of the original member. The loading on these members are changed, but the boundary conditions and length are kept the same. The equivalent systems of uniform stiffness are derived and proved mathematically. To facilitate the mathematical computations, an accurate approximation is suggested by the authors which yields results to any desired degree of accuracy.

This method may be applied to any statically determinate or indeterminate problem which deals with members of variable stiffnesses.

INTRODUCTION

The problem of calculating the deflection of structures with members of variable stiffnesses and acted upon by static or dynamic loads is of great importance in the analysis and design of structures. In this paper, only static loads will be considered.

Several methods have been suggested in the past for the direct or indirect solution of the problems of deflections. Some of the best known are the double integration, the moment–area, the conjugate beam, the three-moment theorem, the Hardy Cross method of moment distribution, the slope deflection and the energy methods. These methods, when applied to members of variable

Note: Discussion open until March 1, 1959. To extend the closing date one month, a written request must be filed with the Executive Secretary, ASCE. Paper 1820 is part of the copyrighted Journal of the Structural Division, Proceedings of the American Society of Civil Engineers, Vol. 84, No. ST 6, October, 1958.

1. Asst. Prof. of Eng. Mechanics, Wayne State Univ., Detroit, Mich.
2. Asst. Prof. of Eng. Mechanics, Wayne State Univ., Detroit, Mich.

stiffness, EI, become very complicated and difficult to solve. However, it is possible to convert a member of variable stiffness to a member of uniform stiffness utilizing the theory of the equivalent systems. When this is accomplished, any of the above methods may be readily applied for the solution of the problem. In this manner the computational work and the complexity of the problem can be greatly simplified.

The purpose of this paper is to give first the mathematical derivation of the equivalent systems and then simplify its application to the engineering problems. The conjugate-beam method will be used in the mathematical proof of the theory retaining its original assumptions. In addition, it is assumed that the line joining the centroids of adjacent cross-sections of members of variable stiffness is straight and that all loads are applied in the plane of bending about a principal axis. If this line is curved, but the ratio of the section depth to the radius of curvature is small, straight beam theory will hold with good accuracy.

Numerical examples will be presented in the later pages to illustrate both the mathematical derivation of the equivalent systems and the technique which greatly simplifies the application of the method.

Derivation of the Equivalent Systems

Consider a simply-supported beam, MN, acted upon by distributed loads which yield the deflection curve shown in figure 1-a. The moment diagram divided by the stiffness, EI, is shown in figure 1-b. The area of the $\frac{M}{EI}$ diagram between the points M and N is designated by the letter A and the one between the point M and any section n, at distance, u, from the left support is designated by A_n. $\bar{x}$ represents the distance between the center of gravity of the $\frac{M}{EI}$ diagram and the right support N.

The "Second Area Moment Proposition" states that the total displacement δ_N of point N from the tangent MQ will be equal to the static moment of the $\frac{M}{EI}$ diagram between the points M and N taken about N. Referring to figure 1-a, note that:

$$\delta_N = A\bar{x} = \int_0^L \frac{M_x dx}{EI}(L-x)$$

and

$$\theta_M = \frac{A\bar{x}}{L} = \frac{\int_0^L \frac{M_x dx}{EI}(L-x)}{L}$$

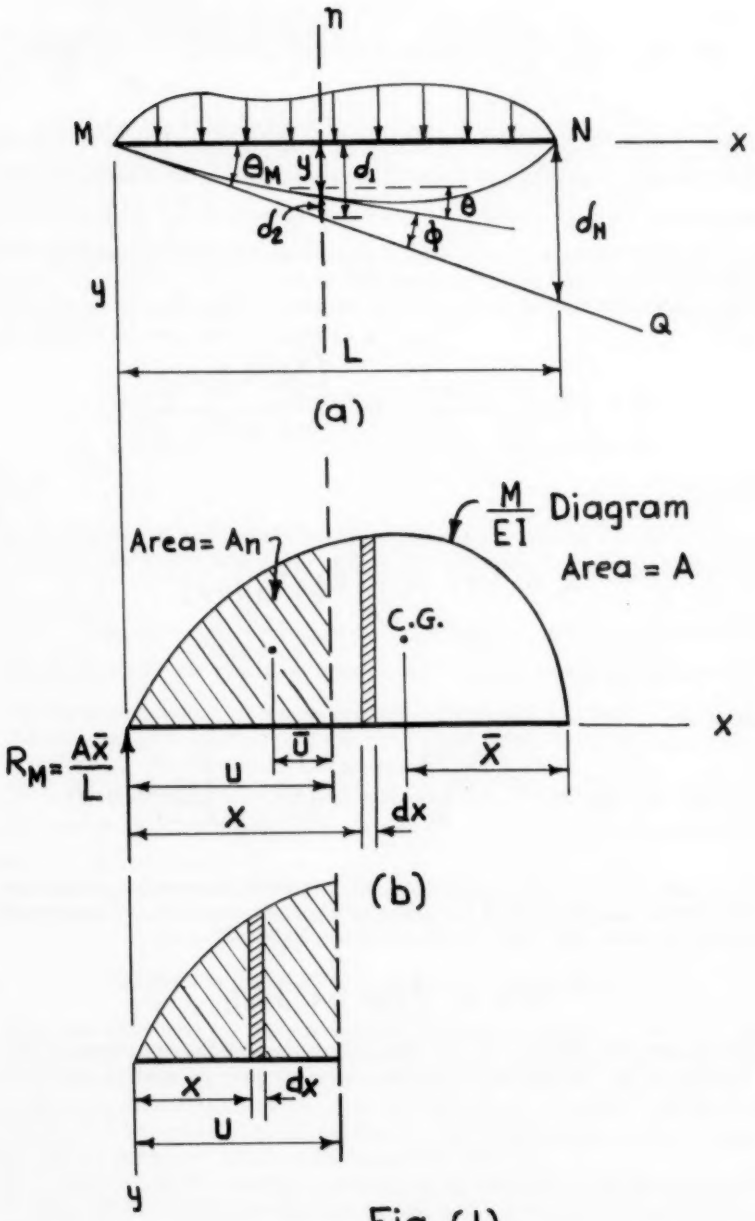
η
M
N
x
θ_M
y
d_1
d_2
θ
φ
d_H
Q
y
L
(a)
M/EI Diagram
Area = A
Area= An
C.G.
$R_M = \frac{A\bar{x}}{L}$
$\bar{u}$
$\bar{x}$
u
x
dx
(b)
x
dx
u
y

Fig. (1)

The actual slope, θ, at any section, η, is

$$\theta = \theta_M - \phi = \frac{A\bar{x}}{L} - A_n = \frac{\int_0^L \frac{M_x dx}{EI}(L-x)}{L} - \int_0^U \frac{M_x dx}{EI}$$

Considering the $\frac{M}{EI}$ diagram as the loading on a beam of span L with supports at M and N, a fictitious beam is derived which is referred to as the conjugate beam. The left reaction of this beam is equal to $\frac{A\bar{x}}{L}$ or θ_M and the slope, θ, at any section, n, is equal to the reaction minus the load A_n, which is the shear in the conjugate beam at that section.

The displacement y at n, figure 1-a, is equal to $\delta_1 - \delta_2$. But,

$$\delta_1 = (\theta_M)(U) = \frac{A\bar{x}}{L} U = \frac{\int_0^L \frac{M_x dx}{EI}(L-x)}{L}(U)$$

and

$$\delta_2 = A_n \bar{u} = \int_0^U \frac{M_x dx}{EI}(U-x)$$

Therefore, the displacement y at any section n may then be written as:

$$y = \delta_1 - \delta_2 = \frac{\int_0^L \frac{M_x dx}{EI}(L-x)}{L}(U) - \int_0^U \frac{M_x dx}{EI}(U-x) \qquad (1)$$

For a beam with variable stiffness, EI, the same expression for the deflection curve may be used if E_xI_x, the stiffness at any point, is expressed as a function of some reference stiffness value, E_1I_1. That is,

$$E_xI_x = f(a + bx^n) E_1I_1 \qquad (2)$$

Substituting Eq. (2) into Eq. (1), the expression for the deflection, y, at any section, n, for the variable stiffness member may be written as:

$$y_1 = \frac{\int_0^L \frac{M_x dx\,(L-x)}{f(a+bx^n)E_1I_1}}{L}(u) - \int_0^u \frac{M_x dx\,(u-x)}{f(a+bx^n)E_1I_1} \qquad (3)$$

$$= \frac{\frac{1}{E_1I_1}\int_0^L \frac{M_x dx\,(L-x)}{f(a+bx^n)}}{L}(u) - \frac{1}{E_1I_1}\int_0^u \frac{M_x dx\,(u-x)}{f(a+bx^n)}$$

If a beam of constant stiffness, E_1I_1 is selected so that the length and boundary conditions are identical to that of the original beam, but with loading which yields moment Me_x at any point x, the expression for the deflection at any section n, may then be written as:

$$y_2 = \frac{\frac{1}{E_1I_1}\int_0^L Me_x dx\,(L-x)}{L}(u) - \frac{1}{E_1I_1}\int_0^u Me_x dx\,(u-x) \qquad (4)$$

The deflection y_1, of the variable stiffness beam will be identical to y_2, the deflection of the equivalent beam of uniform stiffness E_1I_1 if:

$$Me_x = \frac{M_x}{f(a+bx^n)} \qquad \text{At any point x.}$$

The moment diagram of the equivalent system may be determined by dividing the moment of the actual beam at each point by the value of the function, $f(a + bx^n)$, of the stiffness at each corresponding point.

The loading on the equivalent beam of constant stiffness can be found utilizing the fundamental relations, $\frac{dM}{dx} = V$ and $\frac{dV}{dx} = w$, stated in all texts of mechanics of materials.

There is an infinite number of equivalent systems for any one variable stiffness beam, since the reference stiffness value selected was arbitrary.

Application of the Theory of the Equivalent Systems

When the equations for the moment and stiffness curves of a loaded member of variable cross-section are known, the exact equivalent systems may be obtained as prescribed in preceding pages. If the above curves cannot be expressed mathematically as a continuous function of x. approximations are necessary for the solution of the problem. The resulting accuracy in this case depends upon the nature of the approximation.

It is known from the theory of mechanics of materials that the moment of a member at any point is a function of the load. If the moment and stiffness function diagrams are accurately plotted, then the $\frac{M}{f(a + bx^n)}$, which is the

moment diagram of the equivalent beam of uniform stiffness, E_1I_1, may be accurately plotted. The shape may be closely approximated by straight lines of length Δs. The number of Δs increments for an excellent accuracy depends upon the shape of the $\frac{M}{f(a + bx^n)}$ curve. Usually three to five increments, judiciously selected, are sufficient.

The equivalent system will then be a constant stiffness member of length and boundary conditions the same as the original system, acted upon by three or four concentrated loads determined from the equivalent shear force diagram in the usual manner.

This method of determining an equivalent system has the advantage of being applicable to any member of variable stiffness, whether or not the variation of stiffness and moment can be expressed as a continuous function of x. It is advisable to approximate the $\frac{M}{f(a + bx^n)}$ diagram quite closely in the region corresponding to the least stiff portions of the original system of variable stiffness.

When the equivalent system has been obtained, any of the known methods in mechanics may be used to determine the deflection at required points. If the problem is statically indeterminate, the redundants are first determined utilizing the theory of the equivalent systems. A new equivalent system may then be obtained as explained in preceding pages, which will be used to determine the deflection at required points.

To demonstrate the application of the theory of the equivalent systems, a cantilever beam loaded as shown in figure 2-a will be considered. The stiffness function, $f(a + bx^n)$, and the moment diagram of the actual beam are plotted in figures 2-b and 2-c, respectively. The $\frac{M}{f(a + bx^n)}$ diagram, which is the moment diagram of the equivalently loaded beam, is shown in figure 3-a. The dashed line on this diagram represents the approximation of the $\frac{M}{f(a + bx^n)}$ curve. The equivalent shear force diagram is presented in figure 3-b. For example, the shear at point B is equal to the difference in moment between the points C and B divided by the length of Δx_2. The equivalent system of uniform stiffness, E_1I_1 acted upon by four concentrated loads, is shown in figure 3-c.

EXAMPLE 1:

A cantilever beam with rectangular cross-section of width B and depth d, given by the expression $d_x = \left(\frac{L+3x}{L}\right)^{\frac{1}{3}} d_1$ is loaded with a uniformly distributed load w lbs. per inch. The modulus of elasticity is constant and equal to E_1. The variation of the moment of inertia along the length of the beam is linear. Determine the exact equivalent system of uniform cross-section which will have a constant stiffness E_1I_1 and the length and boundary conditions of the original beam. Neglect the weight of the beam. For sketch, see figures 4-a and 4-b.

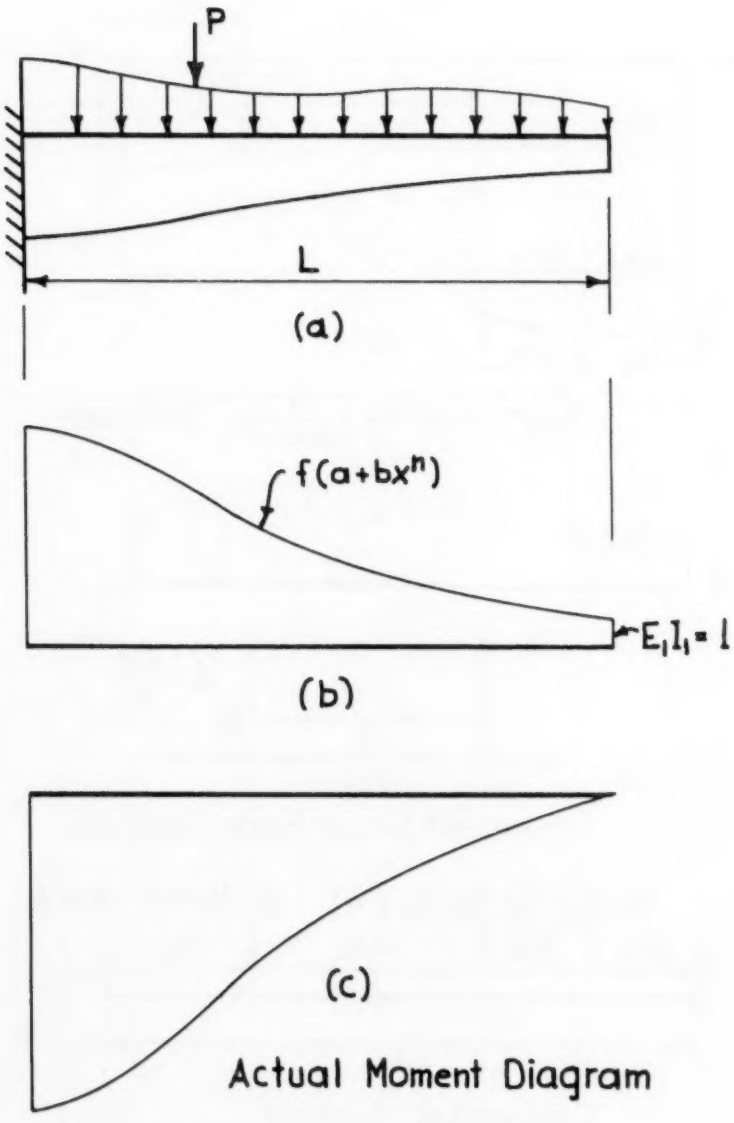

Fig. (2)

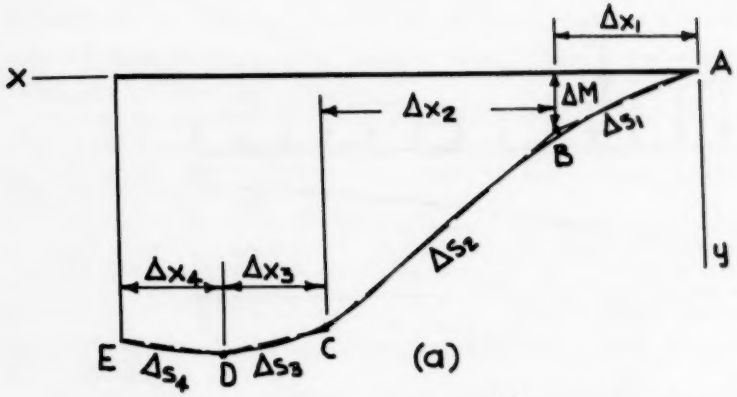

Approximated $\frac{M}{f(a+bx^n)}$ Diagram

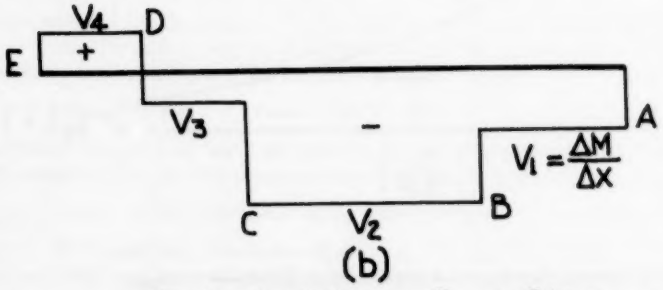

Equivalent Shear Force Diagram

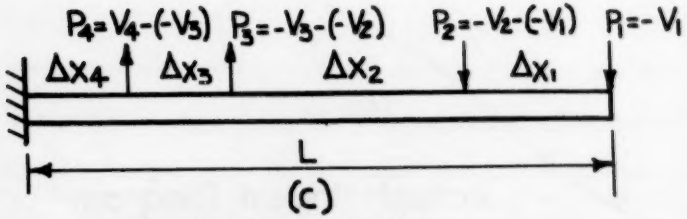

Equivalent System

Fig. (3)

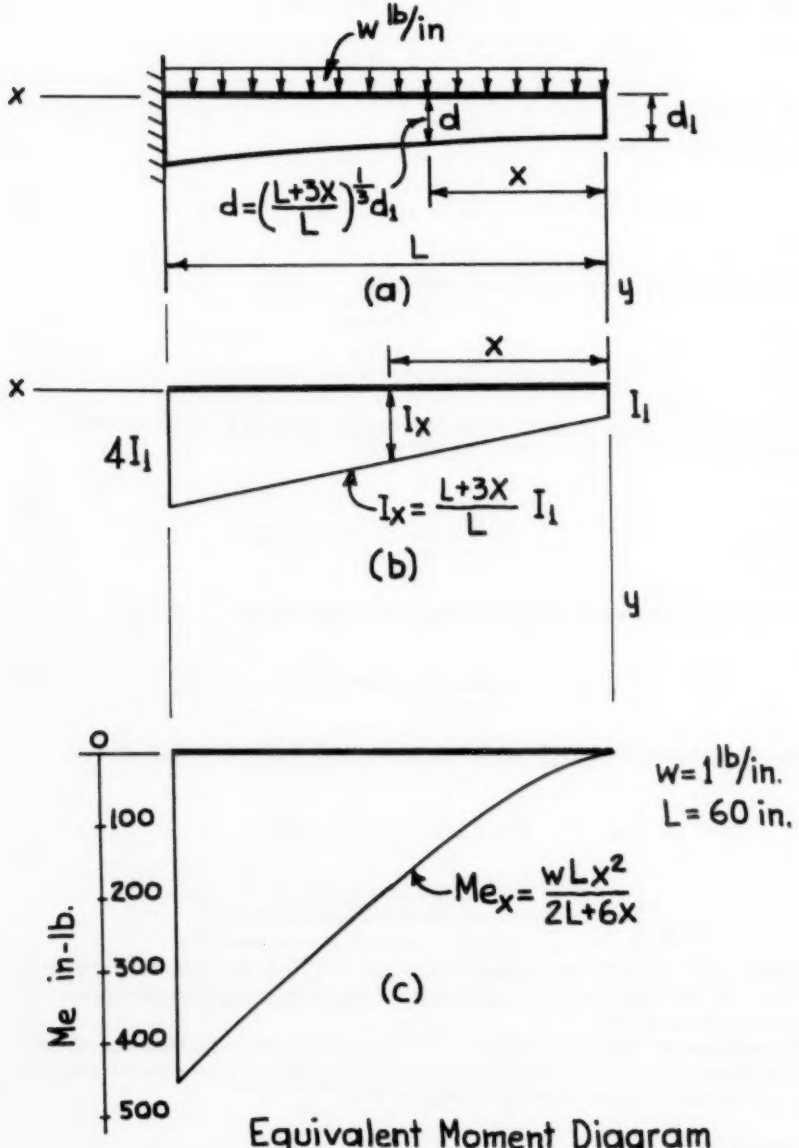

Equivalent Moment Diagram

Fig. (4)

Solution:

The moment of inertia at any point x of the beam is:

$$I_x = \frac{L + 3x}{L} I_1$$

from which the function

$$F(a + bx^n) = \frac{L + 3x}{L} \tag{5}$$

The moment of the beam at any point x is:

$$M_x = -\frac{wx^2}{2} \tag{6}$$

The moment, Me_x, at any point x of the equivalent system of uniform cross-section and constant stiffness E_1I_1 is:

$$M_{e_x} = \frac{Mx}{(a + bx^n)} = -\frac{wLx^2}{2L + 6x} \tag{7}$$

The shear force equation of the equivalent system is:

$$\frac{dMex}{dx} = \frac{(2L + 6x)(-2wLx) + (wLx^2)(6)}{(2L + 6x)^2} = V_{e_x} \tag{8}$$

The distributed load, w_{e_x}, at any point x of the equivalent system is:

$$\frac{dVex}{dx} = w_{e_x} = \frac{(2L + 6x)^2(-4wL^2 - 12wLx)}{(2L + 6x)^4} - \frac{[(2L + 6x)(-2wLx) + 6wLx^2][12(2L + 6x)]}{(2L + 6x)^4} \tag{9}$$

Equations 7, 8 and 9 are plotted in figures 4-c, 5-a and 5-b, respectively. The load, w, and the length, L, are taken as equal to one pound per inch and 60 inches, respectively.

The equivalent system of figure 5-b, of uniform cross-section and of constant stiffness E_1I_1 will produce the identical deflection curve as the original beam of variable stiffness shown in figure 4-a.

EXAMPLE 2:

In example 1, determine an accurate equivalent system of uniform cross-section and constant stiffness E_1I_1 by approximating the shape of the $\frac{M}{f(a + bx^n)}$ curve.

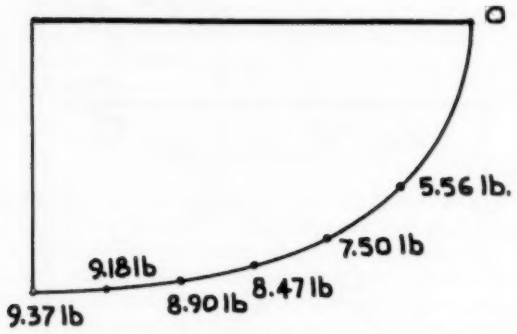

(a)

Equivalent Shear Force Diagram

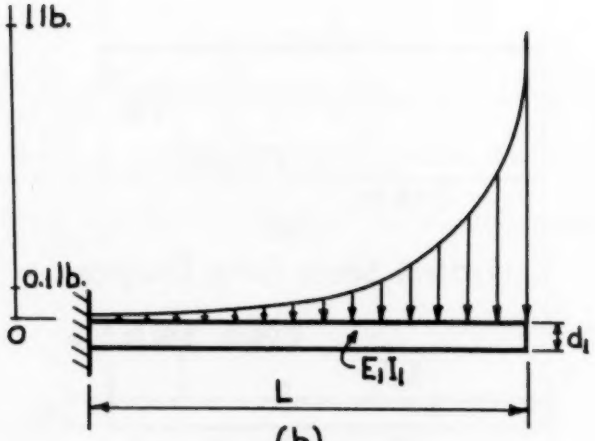

(b)

Equivalent System

Fig. (5)

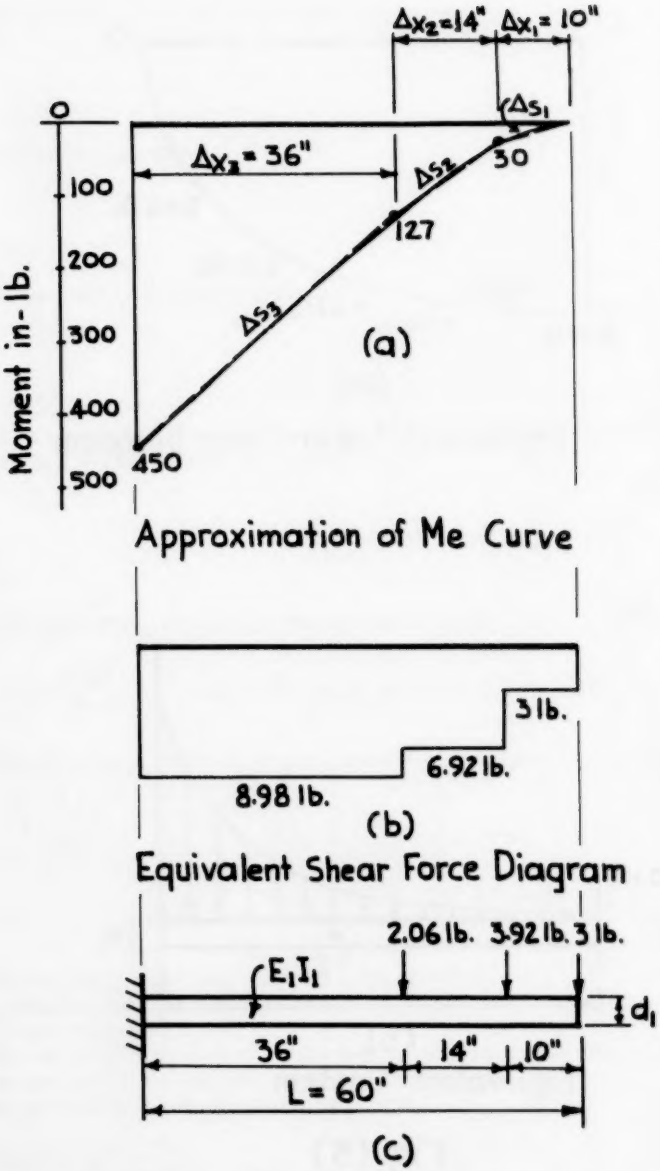
Δx2=14" Δx1= 10"
Δs1
0
Δx2 = 36"
Δs2
30
100
127
200
Δs3
300
(a)
400
450
500
Moment in-lb.
Approximation of Me Curve
3 lb.
6.92 lb.
8.98 lb.
(b)
Equivalent Shear Force Diagram
2.06 lb. 3.92 lb. 3 lb.
E1I1
d1
36"
14"
10"
L = 60"
(c)
Equivalent System

Fig. (6)

Solution:

The approximation of the M_e curve with three straight lines, Δs_1, Δs_2 and Δs_3 is shown in figure 6-a. The equivalent shear force diagram is plotted by dividing the variation of moment by the corresponding increments of length Δx_1, Δx_2 and Δx_3 and it is shown in figure 6-b. The equivalent system of uniform cross-section with constant stiffness, E_1I_1 is shown in figure 6-c.

CONCLUSIONS

From the foregoing, we may conclude that the theory of the equivalent systems, derived from the fundamental principles and concepts of mechanics, may be applied to structures with variable stiffness members. This method provides a relatively simple procedure for determining the deflections of complicated structures without requiring prepared tables, graphs or charts. A slide rule, a firm understanding of the principles of mechanics and the engineer in industry may readily apply this theory to the most complicated problems. The method is very general and it may be extended for the solution of staticaly indeterminate problems, such as continuous structures of variable stiffness, trusses, plates and shells without complicating the procedure. It may also be used for the determination of the natural frequencies of vibration of the above structures.

It should be emphasized that the approximation with straight lines of the M_e diagram, greatly reduces the complexity of the solution and yields results to any desired degree at accuracy.

BIBLIOGRAPHY

1. L. C. Maugh, Statically Indeterminate Structures, John Wiley and Sons, Inc., New York, 1951.
2. S. Timoshenko, Theory of Elastic Stability, McGraw-Hill Book Company, Inc., New York, 1936.
3. F. R. Shanley, Strength of Materials, McGraw-Hill Book Company, Inc., New York, 1957.

Paper 1821 October, 1958 ST 6

Journal of the
STRUCTURAL DIVISION
Proceedings of the American Society of Civil Engineers

AMPLIFICATION OF STRESS AND DISPLACEMENT IN GUYED TOWERS

Robert S. Rowe,[1] A.M. ASCE
(Proc. Paper 1821)

SUMMARY

This paper pertains to certain problems dealing with the amplification of stress and displacement in guyed towers when changes in geometry are included in the analysis. A simplified method for determining the slack stress in the guy and horizontal displacements due to wind load has also been developed and presented.

SYNOPSIS

A simplified method for the determination of the slack stress in the guys of a tower subjected to wind load has been presented. Equations for the determination of displacements at guy levels have been developed in terms of the wind load, initial guy tension, and slack stress.

A simplified method which is useful in solving problems pertaining to the buckling or amplification of stress and displacement in guyed towers has been developed. Only fundamental concepts are used; these are extended to include the displacement of the tower axis due to external loads and internal distortions. The increase, or amplification, of the computed stress and displacement or bending moment at the center of a loaded section of the tower (when the displacements of the axis are included in the analysis) is developed and presented in graphic form.

The amplification charts are useful in showing the entire range of structural action for members subjected to axial compression and transverse bending. These charts are divided into (A) the ordinary range, where the usual methods of structural mechanics apply with little error; (B) the flexible range, where the ordinary methods of analysis must be extended to include the

Note: Discussion open until March 1, 1959. To extend the closing date one month, a written request must be filed with the Executive Secretary, ASCE. Paper 1821 is part of the copyrighted Journal of the Structural Engineering Division, Proceedings of the American Society of Civil Engineers, Vol. 84, No. ST 6, October, 1958.

1. Prof. and Chmn., Dept. of Civ. Eng., Duke Univ., Durham N. C.

effects of displacement; and (C) the dangerous range, where the amplification of stress is so large that there is a possibility of structural collapse.

Charts of this type are valuable because they present graphically (a) the range of structural action for a given tower, (b) the magnitude of the amplification factor when displacements of the axis are included in the analysis, and (c) possible modifications that may be made to reduce the amplification.

INTRODUCTION

The guyed tower is a structural form which has become increasingly important because of the need for high television and radio towers. A typical guyed tower is shown in Figure 1. This tower is an example of a typical television tower, and has the following properties:

Tower:

Height = 1000 feet
Cross-section = 10' Triangular
Legs = 5" Round, T1-Steel
Girts and Diagonals = A7-Steel
Total Weight = 440,000 pounds

Guys:

	Bridge Strands For Single Guys Figure 1d	For Double Guys Figure 1e	
	Size	Size	Initial Tension per Guy
G3	1-3/8" Dia.	2 - 1" Dia.	22.8 kips
G2	1-9/16" Dia.	2 - 1-1/8" Dia.	28.7 kips
G1	1-5/8" Dia.	2 - 1-3/16" Dia.	31.7 kips

Considerable time is expended on the preliminary design and analysis of tall steel towers because of the lack of a simplified method for performing these operations. It is not permissible to use the ordinary methods of structural mechanics for flexible steel towers, because the displacements (which are normally neglected) may increase or amplify the stresses which, in turn continue to increase the displacements. It should be realized that any refinements which are introduced into an analysis are included for reasons of safety rather than economy.

In order to determine the stresses in a guyed tower, it is first necessary to assume a preliminary design. In general, the effect of variations can only be determined by analyzing several designs. Because of the great amount of time and labor required in this process, elaborate analysis is seldom practical. A device useful in determining the influence of displacements on the preliminary design is termed an "amplification chart," whereby the structural action (as well as the effects of varying the tower proportions) can be visualized easily. This amplification chart can be modified for conditions other than those originally specified. Thus, one chart can serve for the

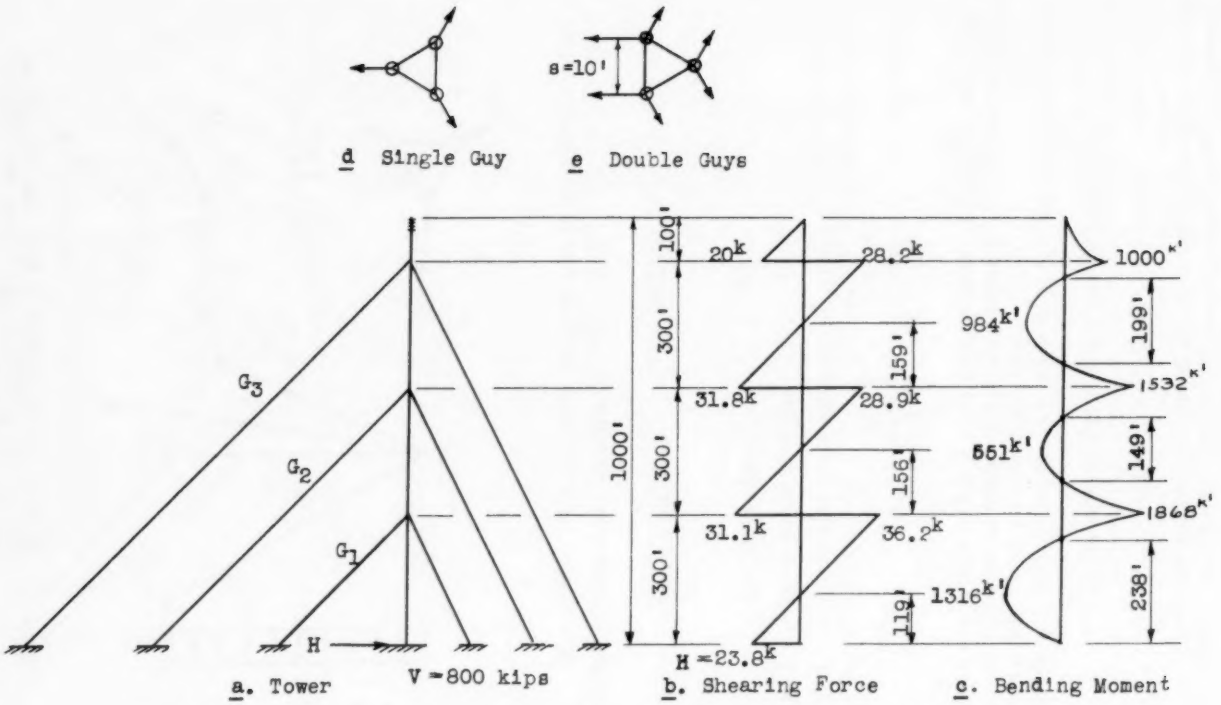

Figure 1. Sketch showing a Typical Guyed Tower, 1000 feet in Height, with a Shearing Force and Bending Moment Diagrams for a wind load of 200 pounds per foot of tower.

various tower types, proportions, materials, loading, and for various computed stresses. The amplification chart is developed from simple structural concepts. The results obtained by use of the chart are extended, by successive correction, to include the displacement of the tower axis. These results agree closely with the results arrived at by the formal methods of structural mechanics.

Horizontal Displacements Due to Wind

The horizontal displacements of a tower depend upon the wind direction, slack stress, and initial tension in the guys.

For the wind direction shown in Figure 2 (Wind I), the horizontal displacements of the tower axis at a guy level may be computed approximately by Equation 1.

$$\Delta H_I = \frac{(P_{LL} + P_S - P_i)}{\sin \alpha} \cdot \frac{L_g}{A_g E_g} \qquad (1)$$

where ΔH_I = Horizontal Displacement for Wind I

P_{LL} = Wind Force in a Guy

For single guys $P_{LL} = \frac{H}{\sin \alpha}$ (2)

For double guys $P_{LL} = \frac{H}{2 \sin \alpha}$ (3)

P_S = Slack force in a guy

P_i = Initial force in a guy

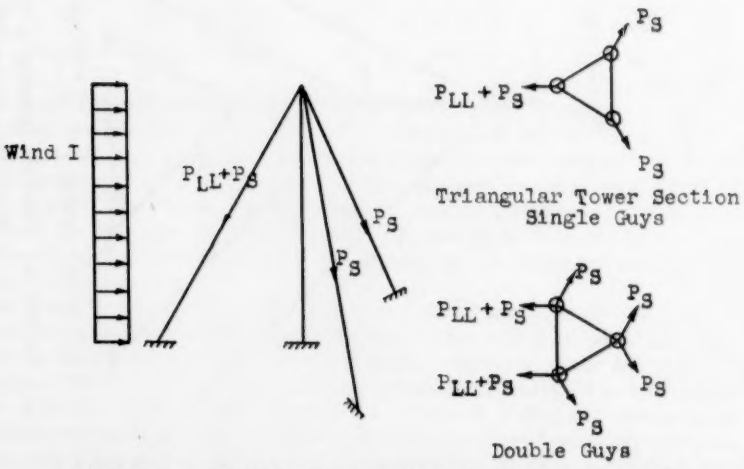

Figure 2. Sketch Showing Wind I and the Resulting Forces in a Triangular Tower for Single and Double Guys

H = Total horizontal wind reaction at guy junction

A_g = Area of an individual guy

Thus, before it is possible to determine horizontal displacements, it is necessary to determine the slack force P_S. The slack force depends upon the wind reaction, H, and the initial force, P_i, in the guy. The relation between the various forces may be obtained from statics.

Second order differences resulting from changes in guy geometry are negligible and for convenience are not included in the following development.

From $\Sigma V = 0$

Then $(P_{LL} + 3\ P_S - 3\ P_i)\ \cos \alpha = 0$

But $\cos \alpha \neq 0$

Therefore $(P_{LL} + 3\ P_S - 3\ P_i) = 0$

and for a selected factor of safety, F. S. = 2.5, the design load, P_W may be computed as follows:

$$P_W = P_{LL} + P_S = \frac{B.S.}{F.S.} = 0.4\ B.S. \tag{4}$$

where B.S. is the breaking strength of the cable.

The slack force would be

$$P_{S_I} = 1.5\ P_i - 0.2\ B.S. = P_i - 1/3\ P_{LL} \tag{5}$$

Similarly, for the wind direction (Wind II) shown in Figure 3, the horizontal displacement may be computed by Equation 6.

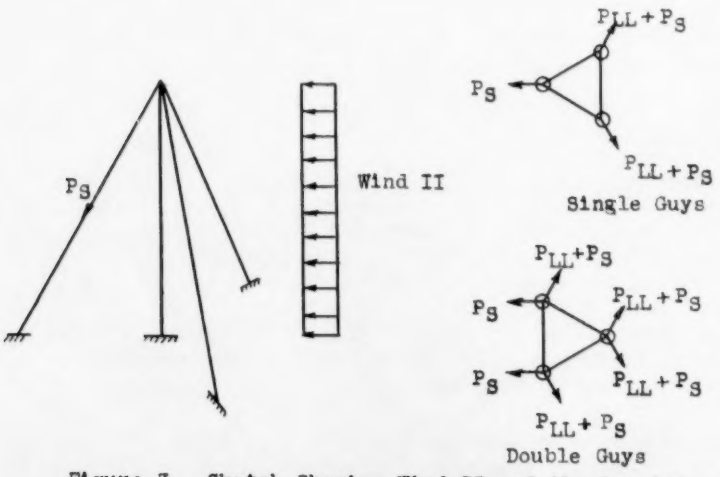

Figure 3. Sketch Showing Wind II and the Resulting Forces in a Triangular Tower For Single and Double Guys.

$$\Delta H_{II} = \frac{2 (P_{LL} + P_S - P_i)}{\sin \alpha} \frac{L_g}{A_g E_g} \quad (6)$$

The corresponding slack force for Wind II would be

$$P_{S_{II}} = 3 P_i - 0.8 \text{ B.S.} = P_i - 2/3 P_{LL} \quad (7)$$

Thus the slack stress for Wind I is not the same as for Wind II even though the wind load, P_{LL}, and the initial tensions, P_i, are equal in both cases.

For example, consider an arbitrarily chosen value for the Initial Tension

$$P_i = 0.2 \text{ B.S.}$$

Then the corresponding value of the slack force for Wind I would be

$$P_{S_I} = 0.1 \text{ B.S. and for Wind II, } P_{SII} = 0$$

The allowable value of the wind load would be

$$P_{LL} = 0.3 \text{ B.S.}$$

The corresponding magnitude of the horizontal displacement, ΔH, for both Wind I and Wind II, as computed by Equations 1 and 6, would be equal for this case as follows:

$$\Delta H = \frac{0.2 \text{ B.S.}}{\sin \alpha} \frac{L_g}{A_g E_g} = \frac{2}{3} \frac{P_{LL}}{\sin \alpha} \frac{L_g}{A_g E_g} \quad (8)$$

Upon substituting Equation 2, in 8, the horizontal displacement for single guys would be

$$\Delta H = \frac{2}{3} \frac{H}{\sin^2 \alpha} \frac{L_g}{A_g E_g} \quad (9)$$

And by substituting Equation 3 in Equation 8, the horizontal displacement for double guys would be

$$\Delta H = \frac{1}{3} \frac{H}{\sin^2 \alpha} \frac{L_g}{A_g E_g} \quad (10)$$

The displacements computed by Equations 9 and 10 are the same when the total cross sectional area for double guys is twice the area for single guys.

However, this is a limiting condition for Wind Direction II as the slack force would be equal to zero. It is thus recommended that the guys be designed so that the slack force is slightly greater than zero for both wind conditions.

The magnitude of the various guy forces as a function of the breaking strength (B.S.) of the guy for conditions, other than the example above, may be conveniently obtained from Figure 4.

The chart of Figure 4 is entered with a design value of P_i in terms of the breaking strength and then vertically up to the corresponding value of P_S and P_W for either Wind I or Wind II.

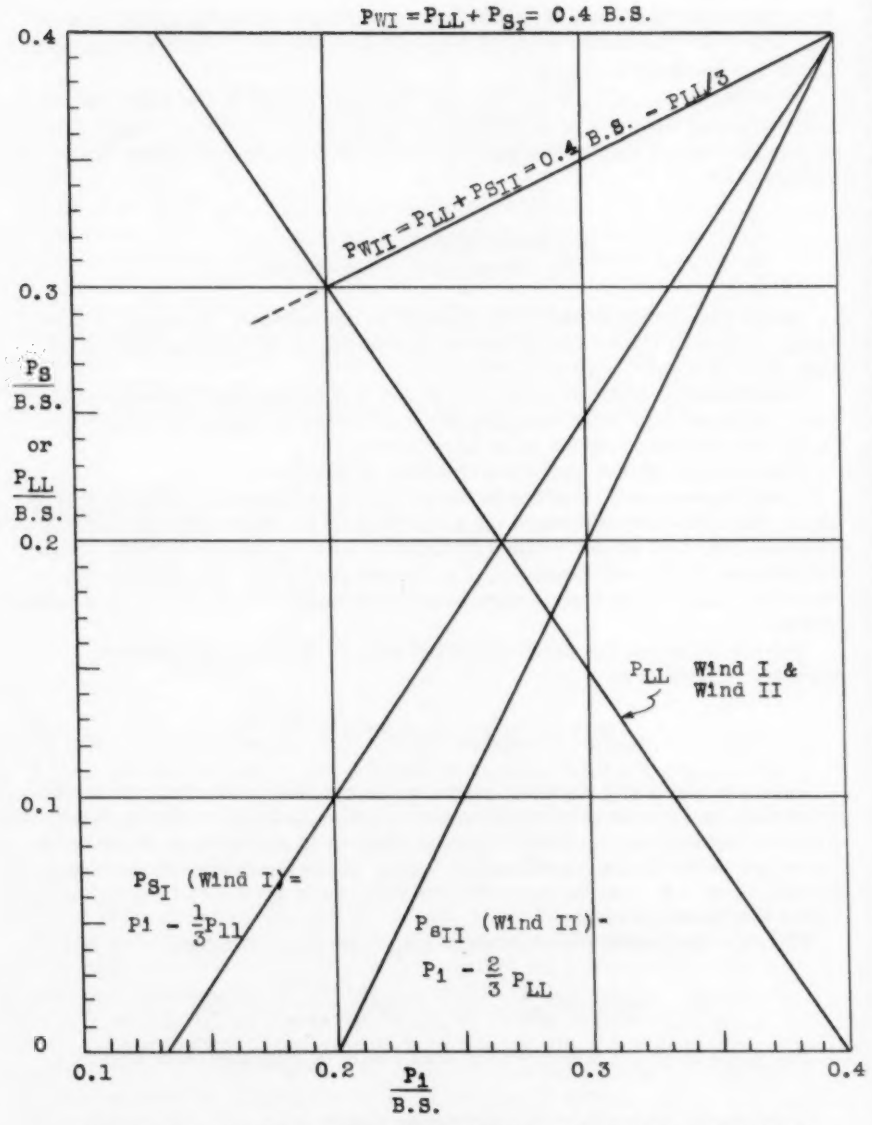

Figure 4. Chart Showing the Relationship between the Live-load Force, the Initial Tension and the Slack Stress in the Guys of a Guyed Tower. Secondary Effects not Included.

For a factor of safety of 2.5, Figure 4 shows that the larger working strength P_{wI} results from Wind I and the smaller Slack Stress ($P_{s_{II}}$) results from Wind II. The slack stress is zero for Wind II when the initial tension $P_i = 0.2$ B.S. The initial force (Pi) should probably be slightly greater than 0.2 of the breaking strength.

Knowing the value of P_{LL}, P_S, and P_i from Figure 4, the magnitude of the horizontal displacement corresponding to Wind I or Wind II may be determined for towers with single guys from Equation 9 and with double guys from Equation 10.

Horizontal Displacements Due to Guy Lengthening or Shortening

Guyed towers are sensitive to changes in guy tension. Extreme caution must be used to insure simultaneous lengthening or shortening of all guys that meet at a particular tower level.

Small changes in tension of a single guy will change the geometry of the tower axis and may cause buckling because the small horizontal displacements are amplified by the large axial forces.

Consider the typical guyed tower shown in Figure 1.

From fundamental relations between statics and geometry and the way in which they are related through the properties of the materials, the horizontal displacement may be determined from Equation 11, which is derived for guy lengthening or guy shortening, $\triangle_e$, at a given guy level: corrections due to changes in sag are of a secondary nature and negligible for properly designed towers.

For convenience, the cross-sectional area of the tower is assumed constant. Therefore:

$$\Delta H = \Delta_e \frac{2}{\sin \alpha} \left(1 + 3 \cos^3 \alpha \frac{A_g E_g}{A_T E_T}\right) \tag{11}$$

However, the above equation, based on the original geometry, is only approximate as changes in tower geometry must be included in the analysis. A convenient technique useful to include changes in geometry is to multiply computed values by the amplification factor. Thus the computed transverse displacement $\triangle H$ may be corrected for changes in geometry by multiplying by the amplification factor Φ .

The total horizontal displacement, $\triangle H_t$, may then be computed as follows:

$$\Delta H_t = \Delta e \frac{2}{\sin \alpha} \left(1 + 3 \cos^3 \alpha \frac{A_g E_g}{A_T E_T}\right) \Phi \tag{12}$$

The value of Φ for displacement may easily be obtained from Figure 5.

Amplification Chart

The amplification chart (Figure 5) shows in graphic form the increase or amplification, of displacements due to combined axial compression plus the transverse bending when the displacements of the axis are included in the analysis. This chart is based on a computed total stress, $f = f_a + f_b$, of

20 kips per sq. inch at the center of a tower section between points of inflection which supports a uniformly distributed wind load throughout the tower height. This selected wind loading is used even though it does not produce the maximum bending unit stress, but it is easy to analyze and very nearly correct. For a computed stress, $f = f_a + f_b$, (in kips per square inch) at the center of the tower section between points on inflection which is not equal to 20 kips per square inch, (that is, for the higher working stresses associated with the higher strength steels), the value of $1/r$ should be multiplied by $\sqrt{f/20}$.

Transverse loads on a guyed tower cause the elastic curve to move away from the tower axis. The displacements resulting from transverse bending are the moment arms for the dead load and the live load axial forces. Although the displacements are small, the additional bending moments may be large because the live-load plus the dead-load axial forces are large. In flexible members the bending stresses and displacements are increased, or amplified, by the additional bending moment resulting from the product of the large axial forces and the transverse bending displacements. The total horizontal displacement, ΔH_t, with changes in geometry included is:

$$\Delta H_t = \Delta H \, \Phi \tag{13}$$

and the amplified total combined stress is

$$f_t = f_a + f_b \cdot \Phi \tag{14}$$

where

$$\Phi = \frac{1}{1 - \frac{f_a}{n E}\left(\frac{L}{r}\right)^2} \tag{15}$$

where ΔH is the horizontal displacement neglecting changes in geometry and f_a is the axial stress and f_b represents the bending stress before amplification and resulting from the dead load plus the live load. The amplification factor is represented by Φ and may be obtained in Figure 5. In the equation for the amplification factor, n is a shape factor that depends upon the loading and properties of the member, and $\frac{L}{r}$ is the slenderness ratio. In Figures 5 and 6 the value of n is 1/10, and E is equal to 30,000,000 per square inch.

The amplification chart, Figure 5, shows the amplification factor for bending moment or displacement, Φ, plotted against the slenderness ratio L/r and the ratio of axial stress and bending stress f_a/f_b or f_b/f_a. By use of both f_a/f_b and f_b/f_a, extremes can be shown conveniently on one chart. In addition to demonstrating the magnitude of the amplification of bending moment or displacements when displacements are included in the analysis, this chart also shows arbitrary ranges of structural action.

For convenience, the amplification factor for total stress Φ' is obtained from Figure 6. The amplification of total stress is obtained from the following equations:

$$\Phi' = \frac{f_a + f_b \Phi}{f} \tag{16}$$

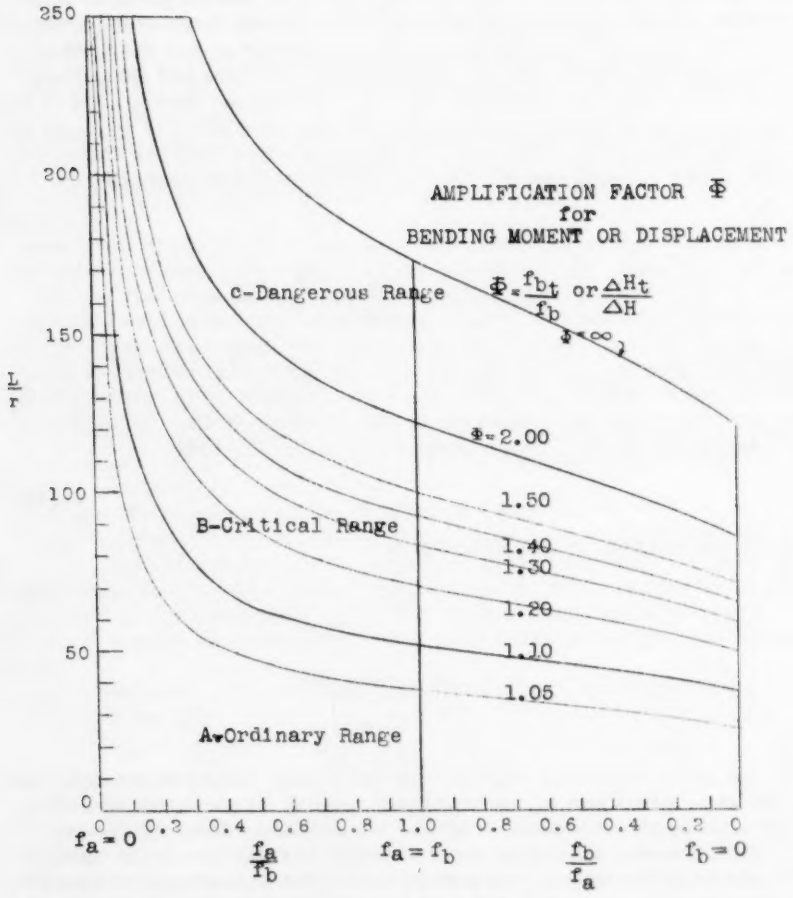

Figure 5. Amplification Chart Showing the Amplification Factor, Φ, for Bending Moment or Displacement as a Function of the Slenderness Ratio as ordinate and the ratio of the Axial and Bending Stress as Abscissus.

and

$$f_t = f\,\Phi\,, \tag{17}$$

Use of the Amplification Chart

The amplification chart can be used (a) to determine the magnitude of the amplification factor for bending moment or displacement and stress when displacements of the axis are included in the analysis, (b) to show the influence of modifications of design on the amplification of displacement, and (c) to describe, in a general manner, the structural behavior of guyed towers for

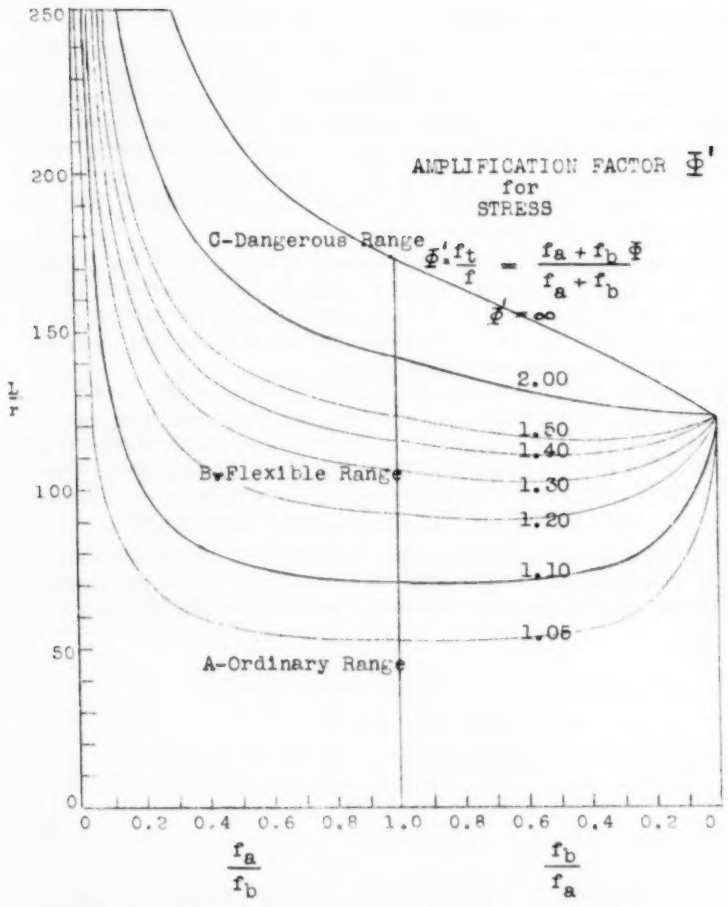

Figure 6. Amplification Chart for Total Stress as a Function of the Slenderness Ratio as Ordinate and the Ratio of Axial and Bending Stress as Abscissus

the entire range of structural action. A similar chart has been developed for arches.(1)

The ratios needed to determine the magnitude of the amplification factor at the center of any section between points of inflection of a guyed tower may be computed as follows:

1. The slenderness ratio L/r is computed and then modified for the computed stress which depends upon the type of steel. Figures 5 and 6 are based on a steel with a computed stress of 20 kips per square inch. Higher

computed stresses may be allowed for the higher strength steels. If the computed stress, $f = f_a + f_b$, is other than 20 kips per square inch, the modified slenderness ratio $(L/r)_{mod.}$ needed to enter the chart is determined by multiplying the slenderness ratio for the stress other than 20 kips per square inch by the square root of the quotient of the other stress divided by 20 kips per square inch. The lengths between points of inflection can be determined approximately by sketching the elastic curve for the loads on the tower. It is important to note that the (L/r) values pertain to the bending stress at the center of a loaded tower section between points of inflection. These values vary with the loading, guy tensioning, guy lengthening, type of steel, and the properties of the cross section.

2. The ratio of bending stress to axial stress, f_b/f_a, is computed. The slenderness ratio and the ratio of bending to axial stress are all that are needed to enter the amplification chart. Variations in guy location, depth of section, moment of inertia, and cross-sectional area are included when the ratio of axial and bending stress is determined.

The amplification chart is entered from the abscissa with the ratios of either f_a/f_b or f_b/f_a (whichever is the smaller) and thence vertically up to the value of (L/r) mod. The intersection represents the range of structural action and the magnitude of the amplification factor for bending moment or displacement, Figure 5, and for total stress, Figure 6, at the center of the section when displacements of the axis are included in the analysis.

Example 1. Amplification of stress due to Wind Load. Consider a steel tower of proportions similar to those shown in Figure 1. From the proportions of the tower and the loadings, the ratios needed to enter the chart are computed:

$$L = 238 \text{ feet}$$

$$r = I/A = 0.405\ (10) = 4.05 \text{ ft.}$$

$$L/r = 238/4.05 = 58.8$$

$$f = f_a + f_b \tag{18}$$

Therefore $$f = \frac{668{,}000}{60} + \frac{1{,}868{,}000\ (5.75)}{990} = 11{,}100 + 10{,}800 = 21{,}900 \text{ psi.}$$

Because the charts are based on a computed stress of 20 kips per square inch, it is necessary to modify the slenderness ratio for any other computed stress. The computed stress (from Equation 18) is 21.9 kips per square inch; (guy eccentricity not included) therefore, the modified slenderness ratio would be

$$\left(\frac{L}{r}\right)_{mod.} = \frac{L}{r}\sqrt{\frac{f}{20}} = 58.8\ (1.04) = 61.5$$

The ratio of the bending stress to the axial stress is then computed:

$$\frac{f_b}{f_a} = \frac{10.8}{11.1} = 0.97$$

The chart shown in Figure 5 is entered with the ratio of f_b/f_a equal to 0.97 - thence, vertically up to the value of 1/r equal to 61.5 The intersection shows the range of structural action and the approximate value of the amplification of the bending moment or displacement when changes in the dimensions of the arch axis are included. The amplification of the displacement midway between points of inflection interpolated from the chart, is approximately 1.16 and in the flexible range of structural action. Thus the actual stress is obtained from Equation 14 and is:

$$f_t = f_a + f_b \Phi = 11,100 + 10,800 \ (1.16) = 23,600 \text{ psi}$$

Similarly the total stress could also be obtained from Figure 6 where the amplification factor for total stress Φ', interpolation from the chart, is 1.07. Thus the total stress as computed by Equation 17 is

$$f_t = f \Phi' = 21,900 \ (1.07) = 23,500 \text{ psi.}$$

Example 2. Amplification of stress due to guy lengthening or guy shortening.

To illustrate the dangers of guy lengthening or shortening, suppose that after the tower has been erected it is discovered that the tension in the lower set of guys needs to be increased or decreased by 15% of the buy breaking strength.

For the typical tower shown in Figure 1, with a set of single guys 1-5/8 inch in diameter, at the first guy level, 15% of the breaking strength of 300,000 lbs. corresponds to a change in tension of 45,000 lbs. This change corresponds to the following guy lengthening or shortening (changes due to sag are of a secondary nature and negligible here):

$$\Delta e = \frac{P\,L}{A\,E} = \frac{45,000 \times 424 \times 12}{2.05 \times 30,000,000} = 3.73 \text{ in.}$$

The corresponding horizontal displacement of the tower at the first guy level is computed from Equation 11 as follows:

$$\Delta H = \Delta e \ \frac{2}{\sin \alpha} \left(1 + \cos^3 \alpha \ \frac{A_g\, E_g}{A_t\, E_t}\right) = 3.73 \times \frac{2}{0.707} \ (1 + 0.012) = 10.6 \text{ in.}$$

If only one guy is lengthened or shortened instead of all three guys which meet at the same level simultaneously, the axis of the tower will change in accordance with the geometry shown in Figure 7. Secondary effects are small and not included here.

The length between points of inflection has increased greatly from the original length of 238 feet (see Figure 1) to 430 feet (Figure 7) corresponding to a slenderness ratio of $\frac{L}{r} = 120$.

The critical buckling stress for a steel tower with the slenderness ratio of 120 may be computed from the following formula:

$$f_x = \frac{\pi^2 \ E}{(L/r)^2} = 20,600 \text{ psi.} \qquad (19)$$

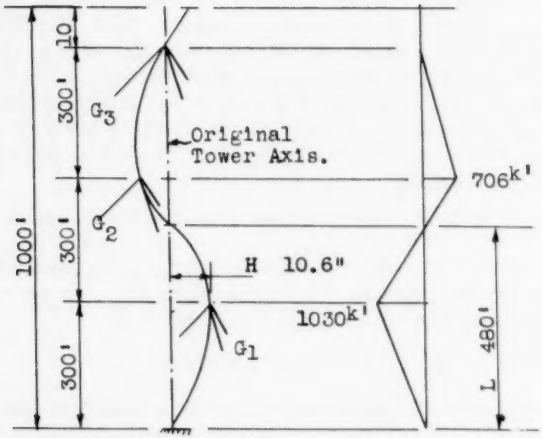

a. Displaced Tower Axis b. Bending Moment Diagram

Figure 7. Sketch Showing The Displaced Tower Axis due to Guy Lengthening of G_1

It is noted that the critical stress, fx, is an ultimate stress with no factor of safety included.

The portion of the bending moment due to a horizontal displacement may be obtained from the following formula:

$$M_b = c \cdot \frac{6 E I \Delta e}{L^2} = 1{,}030{,}000 \text{ lb, ft.}$$

Where c is a factor that depends upon the end fixity at the supports. For the problem under consideration c = 0.6.

Additional bending moments, M_a, result from the axial forces times the relative horizontal tower displacements. The axial force above the section under consideration is composed of the tower weight, P_d = 264,000 pounds, and initial guy tension, P_i = 218,000 pounds.

Thus

$$M_a = (P_d + P_i) \Delta e \qquad (20)$$

$$= (264{,}000 + 218{,}000)(10.6/12) = 425{,}000 \text{ lb. ft.}$$

The computed bending moment is the sum of the above moments due to tower displacement plus the moment resulting from the axial force times displacement and is:

$$M = M_b + M_a \qquad (21)$$

$$M = 1{,}030{,}000 + 425{,}000 = 1{,}455{,}000 \text{ lb. ft.}$$

The corresponding computed stress with changes in geometry due to loads not included, is obtained as follows:

$$f = f_a + f_b$$

$$f = \frac{480,000}{59} + \frac{1455,000}{990} \quad (5.75)$$

$$f = 8140 + 8450 = 16,590 \text{ psi.}$$

Thus the stress computed in the usual manner is not the total stress in the tower as changes in geometry must be included.

The actual total stress, amplification included, may be obtained by use of Equation 14 as follows:

From Figure 5, for $L/r = 120$ and $f_a/f_b = 0.96$, $\Phi = 1.7$

Thus $f_t = f_a + f_b \Phi$

and $f_t = 8140 + 8450\ (1.7) = 22,510$ psi

Similarly, the total stress compution by use of Figure 6 would be

$$f_t = f \Phi' = 16,590\ (1.36) = 22,560 \text{ psi.}$$

Thus the tower of this example will probably collapse since the computed total stress of 22,500 psi exceeds the critical stress of 20,600 psi.

The corresponding amplified horizontal displacement as computed by Equation 13 is

$$\Delta H_t = \Delta H \cdot \Phi = 10.6 \times 1.7 = 18.0 \text{ in.}$$

Possible remedies would include simultaneous lengthening or shortening of all the guys that meet at a given level and by increasing the number of guy levels from three to four or five.

Influence of Modifications on the Amplification of Stress

The amplification of stress in guyed towers subjected to combined axial compression and transverse bending is influenced by the slenderness ratio $1/r$, the type of steel or computed stress, and the ratio f_a/f_b. The amplification of stress can be reduced by decreasing the slenderness ratio. For a given length between inflection points, the amplification of stress decreases for increasing values of the radius of gyration.

A higher allowable computed stress is permitted for certain types of steel and for wind load. The relative amplification of stress is influenced by variations in the allowable or computed stress (Equation 15). An increase in the computed stress results in a disproportionate increase in amplification particularly for larger values of the slenderness ratio.

Use of the Amplification Chart to Describe Structural Action

The amplification chart may be useful in describing the range of the structural action of guyed towers. The chart has been divided into three arbitrary ranges: (a) the ordinary range, (b) the flexible range, and (c) the dangerous range.

The ordinary range shows that the analysis, by customary methods of structural mechanics, gives sufficiently accurate results. In the ordinary range, changes in the dimensions of the tower cross section and changes in the displacement of the tower axis have little influence on the amplification of stress; therefore, (to that degree) superposition of effects is applicable. In the ordinary range, for a given slenderness ratio of less than 70 and for values of f_a/f_b from 0.5 to 2.0, the amplification of stress remains sensible constant, irrespective of the loading and proportions of the tower. For decreasing values of f_a/f_b and f_b/f_a less than 0.5, the amplification of stress decreases for constant values of $1/r$. Figure 6 has been drawn for a total stress before amplification, of 20 kips per square inch. If the computed stress is greater than 20 kips per square inch, it is necessary to consider the corresponding disproportionate increase in the amplification. The amplification of displacements, Figure 5, for constant $\frac{L}{r}$ increases with increasing values of f_a/f_b. In the ordinary range, elastic buckling is highly improbable except for relatively small values of f_b/f_a - at which values the amplification of displacements is relatively large.

In the flexible range, the ordinary methods of structural mechanics must be modified and extended to include the effects of displacements. Superposition of effects is not applicable, and it is not permissible to separate live load and dead load. The amplification of stress in this range has been arbitrarily limited from 10% to 50%. The area of constant amplification of stress for a given $1/r$ - ratio is less pronounced in the flexible range. The amplification of stress increases for increasing values of f_a/f_b up to a certain value and then decreases. The amplification of displacements continues to increase for increasing values of f_a/f_b. Variations in loading and in properties of the tower have more influence on the amplification of stress in the flexible range than in the ordinary range. Amplification of stress is more pronounced for small changes in the slenderness ratio. Attention is given to variations in the computed stress because increases in the computed stress result in disproportionate increases in the amplification. Elastic buckling may be possible at the relatively larger values of $1/r$ and for values of f_a/f_b greater than unity.

In the dangerous range, the amplification of stress is greater than 50%. In this range the amplification of stress and displacement is so large that there is danger of elastic or plastic buckling. The line separating elastic and plastic buckling depends, to some extent, on the type of steel used. The higher allowable stresses associated with silicon, nickel, and T-1 steel, result in disproportionate increases in amplification.

For an assumed tower design, the amplification chart shows immediately if danger exists, and what modifications are indicated to avoid this danger without elaborate computations.

Amplification of Stress and Displacement

The bending moment obtained from the wind live load only is not the actual bending moment in the structure. For convenience, the moments resulting from guy eccentricity have not been included in this discussion. The bending moment resulting from the transverse loads is increased (or amplified) by additional bending caused by the axial forces. Usually a guyed tower is

designed so that the live load deflections are small. The bending moment due to the axial force is computed by multiplying the axial force by the distance from the elastic curve to the original tower axis.

If the displacements of the tower are neglected, the same bending moment will be determined for the wind load only as for the wind load plus axial forces. Thus, by the usual theory, it is permissible to separate the wind load from the guy tensioning and to add the partial effects to obtain the total effect.

In a guyed tower the displacements of the tower axis, although small, may form a large part of the dead-load plus the wind-load bending moment, as shown in Figure 8. If the displacements of the tower axis are included, larger bending moments will be determined for the wind-load plus the dead-load than for the wind-load only. The transverse displacements are moment arms for the combined wind-load plus the dead-load axial forces. When the displacements of the axis are included, it is not permissible to separate the live load from the dead load. Not only are the bending moments and the displacements increased or amplified by the live-load plus dead-load axial forces, but the sums of the partial effects of the live-load and the dead-load are not equal to the total effect. However, it is often convenient to permit an arbitrary allowable increase, to the results obtained by assuming that the structure does not deform, and still be safe.

The stages of additional bending continue and may be represented by a mathematical series which may or may not converge. If the bending continues to increase (non-convergent series), the structure will collapse. In Figure 8 there is shown a straight member subjected to both axial and transverse loads. The equation for the displacement at the center of the beam is:

$$\Delta = \frac{n M L^2}{E I} \qquad (22)$$

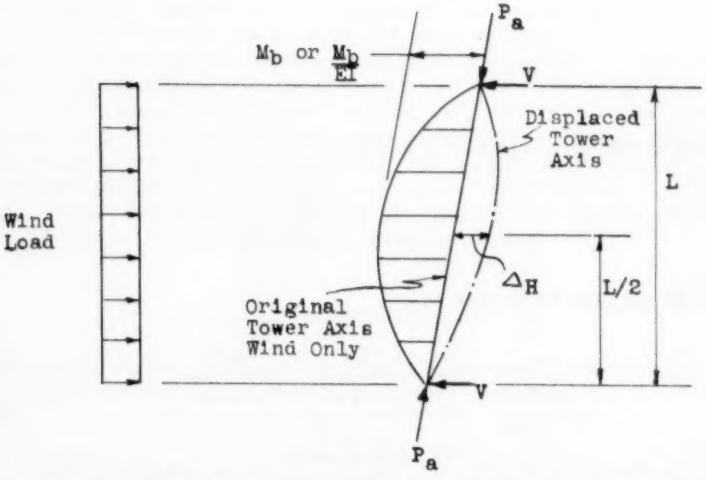

Figure 8. Sketch Showing Axial Forces and the Transverse Wind Load on a Tower Section Between Points of Inflection.

in which M is the ordinate of the bending moment diagram at the center of the beam; and $n = \frac{1}{9.6}$ for a simply supported beam with uniformly distributed wind live load. For a more complete development of the amplification factor than presented here see Reference (1).

The bending moment for the transverse loads is increased by additional bending caused by the axial forces. The shape factor for the transverse loads n_b is not the same as the shape factor for the axial loads n_a. For ordinary guyed towers, the error resulting from setting $n_a = n_b$ is small and in the order of 3%.

The additional bending moment (Figure 8) is

$$M_{ad} = P_a \Delta_b \tag{23}$$

which causes a further displacement

$$\Delta_{ad} = \frac{n_a P_a \Delta_b L^2}{E I} \tag{24}$$

and an increased bending moment

$$M'_{ad} = P_a \frac{n_a P_a \Delta_b L^2}{E I} \tag{25}$$

This process is continued, and the total bending moment can be represented by:

$$M = M_b + P_a \Delta_b + P_a \Delta_b n'_a \frac{P_a L^2}{E I} + P_a \Delta_b n''_a \frac{P_a L^2}{E I} + \ldots + \tag{26}$$

If

$$\frac{n_a P_a L^2}{E I} < 1 \tag{27}$$

and letting successive values of n equal n_a,

$$M = M_b + \frac{P_a \Delta_b}{1 - \frac{n_a P_a L^2}{E I}} \tag{28}$$

Equation 28 can also be written as

$$M = M_b \frac{1 - \frac{n_a P_a L^2}{E I} + \frac{n_b P_a L^2}{E I}}{1 - \frac{n_a P_a L^2}{E I}} \tag{29}$$

By setting n_a equal to n_b, an approximate expression for the amplification of displacements and bending moments is obtained.

$$M = \frac{M_b}{1 - \frac{n_a P_a L^2}{E I}} = M_b \Phi \qquad (30)$$

and $\Delta = \Delta_b \Phi$

Slight errors less than 3% are caused by neglecting successive changes in n_a.

The quantity $\frac{1}{1 - \frac{n_a P_a L^2}{E I}}$ is the amplification factor Φ.

The total stress for a straight member or tower section, subjected to both axial and transverse loads can be computed from

$$f_t = f_a + f_b \Phi \qquad (31)$$

The effects of temperature change, plastic flow, and movement of the tower base are not included in Equation 14.

This investigation and the amplification formula for a horizontal, straight member are applicable also to a curved member with supports on the same elevation.(1)

SUMMARY

Simplified equations for the determination of displacements of guy levels in a tower have been developed in terms of the wind load, initial guy tension and slack stress. Amplification charts for stress and displacement which have been found useful in the predesign of guyed towers have also been presented. These charts demonstrate graphically the increase or amplification of stress and displacement at the center of a section between points of inflection of a guyed tower when displacements of the axis are included in the analysis. In the development of the chart only familiar concepts were used.

The value of the chart is that it shows immediately when elaborate methods of analysis are necessary in the design of flexible towers. The chart also indicates what modifications may be made, sc that the ordinary methods of structural mechanics give adequate results.

ACKNOWLEDGMENT

The writer wishes to acknowledge his indebtedness to Mr. Hardy Cross, from whose teaching and inspiration this paper was possible.

BIBLIOGRAPHY

1. "Amplification of Stress in Flexible Steel Arches," by R. S. Rowe, Transactions, ASCE, Vol. 119, 1954, p. 910-26.

2. "Design of Multi-Level Guyed Towers: Wind Loading," by E. Cohen, and H. Perrin, Proceedings, ASCE, Sept. 1957, p. 1355-1 (with Bibliography).

3. "Design of Multi-Level Guyed Towers: Structural Analysis," by E. Cohen, and H. Perrin, Proceedings, ASCE, Sept. 1957, p. 1356-1 (with Bibliography).

4. "Numerical Procedure for Computing Deflection, Moments, and Buckling Loads," by N. M. Newmark, Transactions, ASCE, Vol. 108, 1943, p. 1168.

5. "The Relation of Structural Mechanics to Structural Engineering," by H. Cross, Proceedings, Fifth International Cong. of Applied Mechanics, 1939.

Paper 1827 October, 1958 ST 6

Journal of the

STRUCTURAL DIVISION

Proceedings of the American Society of Civil Engineers

CONTENTS

DISCUSSION
(Proc. Paper 1827)

Page

The Deas Island Tunnel, by Per Hall, Troels Brondum-Nielsen, and H. R. Kivisild. (Proc. Paper 1436, November, 1957. Prior discussion: 1656. Discussion closed)
by Per Hall, Troels Brondum-Nielsen, and H. R. Kivisild (closure) 1827-3

Analysis of Helical Beams Under Symmetrical Loading, by Alan M. C. Holmes. (Proc. Paper 1437, November, 1957. Prior Discussion: 1656. Discussion closed.)
by Alan M. C. Holmes (closure) 1827-7

A Method of Design of Reinforced Concrete Sections, by P. D. Moliotis. (Proc. Paper 1509, January, 1958. Prior Discussion: none. Discussion closed.)
by Juergen Plaehn 1827-11
Corrections. 1827-20

Analysis of Braced Frames, by K. H. Gerstle. (Proc. Paper 1560, March, 1958. Prior Discussions: 1656. Discussion closed.)
by I. M. Nelidov 1827-23

Numerical Solutions for Beams on Elastic Foundations, by Henry Malter, (Proc. Paper 1562, March, 1958, Prior Discussion: 1787. Discussion closed.)
by Victor R. Bergman 1827-29
by N. J. Ryker, Jr. 1827-29

Progress Report of the Committee on Deflection Limitations of Bridges of the Structural Division. (Proc. Paper 1633, May, 1958, Prior Discussion: 1787. Discussion closed.)
by A. Kabaila. 1827-35

Note: Paper 1827 is part of the copyrighted Journal of the Structural Division, Proceedings of the American Society of Civil Engineers, Vol. 84, ST 6, October, 1958.

THE DEAS ISLAND TUNNEL[a]

Closure by Per Hall, Troels Brondum-Nielsen, and H. R. Kivisild

PER HALL,[1] A.M. ASCE, TROELS BRONDUM-NIELSEN,[2] and H. R. KIVISILD[3].—The authors wish to thank Messrs. Rooney and Eremin for their comments on the paper.

As regards comparative costs of alternative bridge and tunnel structures, the writers wish to mention that the reasons for a tunnel structure being competitive are partly those mentioned by Mr. Rooney, viz. severe navigation clearance restrictions and poor ground conditions for bridge foundations, and partly the following: First the extremely flat, low lying terrain in the area, the rigid maximum grade specifications and the clearance requirements would necessitate much longer approaches for a bridge than for the tunnel. Secondly the price of heavy structural steel in British Columbia is considerably higher than elsewhere.

In regard to the ventilation system, the writers should like to comment that the system employed in the Deas Island Tunnel is designated as semi-transverse. Air is exhausted laterally into the ventilation duct, for the first half of the tube and introduced into the roadway for the second half of the tube, as is shown in Figure 1.

Basic ventilation is provided by four fans with a capacity of 1,000,000 cfm, which create the main circulation of air in the tunnel. A secondary circulation is created by the movement of traffic through the tunnel. The fans operate in a pre-set, time-controlled pattern with automatic alteration controlled by carbon monoxide detectors, visibility meters and fire detectors with a manual override for use during peak traffic periods and emergencies.

No spare fans are installed in the tunnel. When one fan is out of operation for any reason a damper at the midpoint of the ventilation duct can be opened so that the other fan can serve the full length of the tube.

As all the fans are reversible it is possible, in case of fire in the roadway tunnel, to combine suction and pressure in such a way that the air movement above the fire will be in the direction of the normal traffic flow. In this way smoke and heat will be moved away from any cars held up by the fire.

In regard to the question of automatic control, both ventilation and lighting are completely automatic, with provision for manual override. Lighting within the tunnel is controlled by the programming clock, with an overriding control by photo cells mounted at the tunnel entrances. Traffic signals are

---

a. Proc. Paper 1436, November, 1957, by Per Hall, Troels Brondum-Nielsen, and H. R. Kivisild

1. Exec. Vice-Pres., Foundation of Canada Eng. Corp., LTD., Montreal, Quebec, Canada.
2. Christiani and Nielsen.
3. Foundation of Canada Eng Corp., LTD., Montreal, Quebec, Canada.

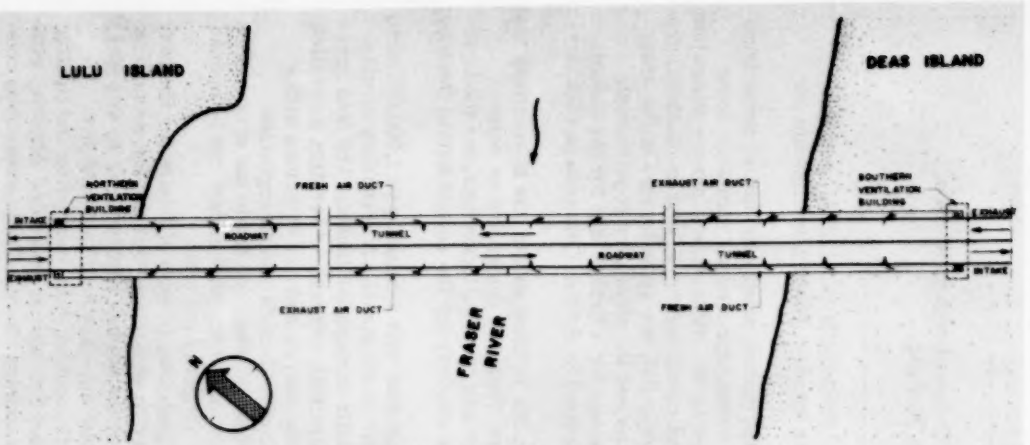

LAYOUT PLAN OF VENTILATION SYSTEM

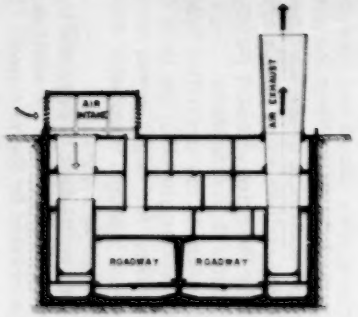

AIR FLOW IN VENTILATION BUILDINGS

operated manually from the control room, where the operator can detect emergency conditions visually over a closed circuit T.V. system. The traffic signals can also be operated manually from stations at the tunnel entrances. In cases of emergency, with excessive carbon monoxide content, red lights at the tunnel entrances are automatically activated by the carbon monoxide meters to stop traffic entering the tunnel.

Further control of operation and traffic under all conditions is provided by means of telephone and loudspeaker communication systems. These features complement the T.V. system to provide the operators with complete visual and vocal contact with motorists in case of emergency. During normal daytime operation and at night, all installations will operate automatically, each action being registered on chart recorders, while during peak hours the control will be manual. A small staff will be employed on the tunnel to take care of inspection, manual operation and maintenance.

Mr. Eremin's comments on structural rigidity and protective measures are interesting. In regard to the protective armour, the writers would like to add that the blanket consists of rock ranging in size from 1500 lb. on top of the tunnel to 500 lb. on the river bed. This rock is placed on reinforced concrete mattresses which act as a filter against the underlying sand and as a reinforcement for the rock blanket during periods of heavy scour action.

The settlements observed during placing of the tunnel elements were as follows:

Element No.	North End	South End
1	9.0 m.m.	11.5 m.m.
2	1.0	9.1
3	4.8	15.5
4	2.4	6.8
5	Not Available	
6	0.0	7.2

These figures include rebound of the temporary foundation blocks as well as the settlement of the elements themselves. The rebound is estimated to be about 1.0 m.m.

The reason for the higher values for South End movement is that in all cases the North End was the one connected to the previously placed element, the South End being more or less free. An average figure could be obtained by interpolation between the two figures shown.

Before sinking the first tunnel element the sinking procedure was changed so that Fig. 12.2(d) of the paper is not up-to-date. A sketch of the sinking rig finally used appears in Figure 2.

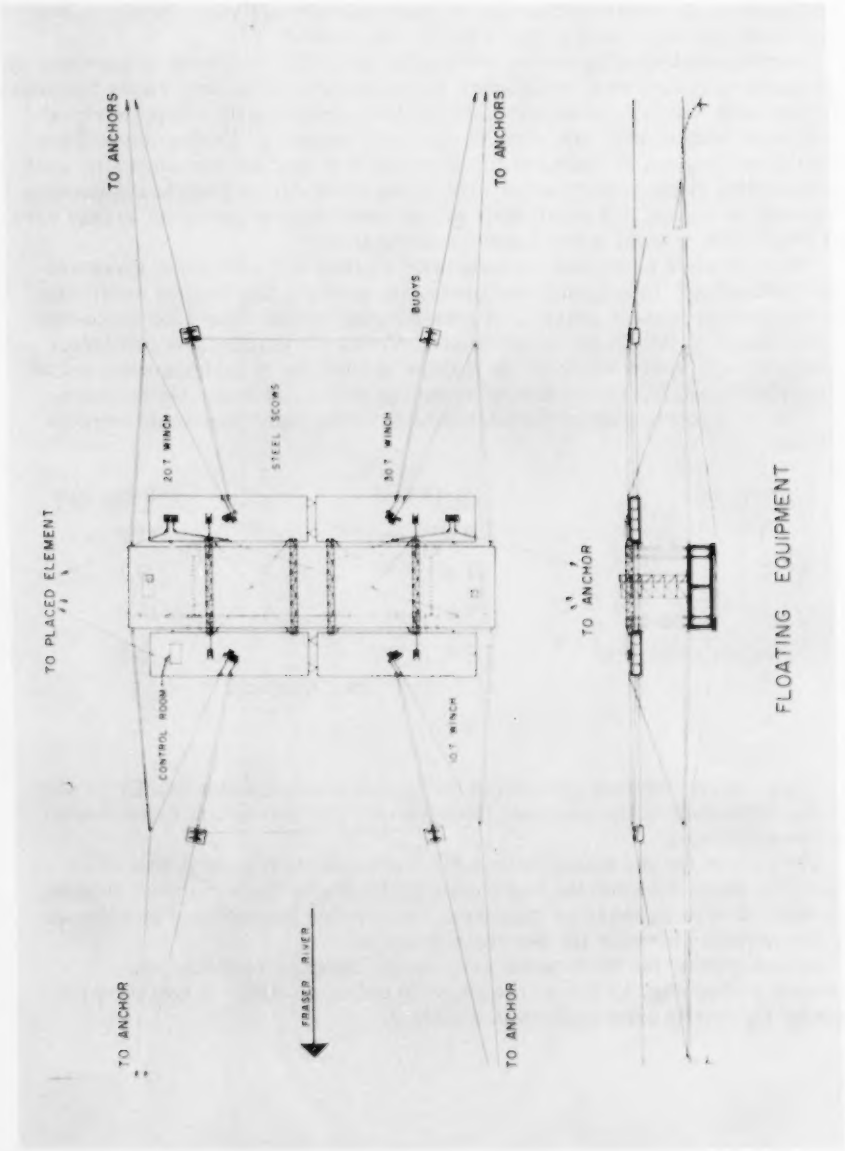
TO ANCHORS
TO ANCHORS
BUOYS
STEEL SCOWS
20 T WINCH
30 T WINCH
TO PLACED ELEMENT
CONTROL ROOM
10 T WINCH
FRASER RIVER
TO ANCHOR
TO ANCHOR
TO ANCHOR
FLOATING EQUIPMENT

ANALYSIS OF HELICAL BEAMS UNDER SYMMETRICAL LOADING[a]

Closure by Alan M. C. Holmes

ALAN M. C. HOLMES,[1] J.M. ASCE.—The writer thanks Mr. Hall for his discussion of the paper. Certainly the term "Modified Polar Moment of Inertia" leaves something to be desired, even if only brevity.

Numerous terms were considered and debated with fellow engineers, among them "Torsional Moment of Inertia" and "Torsion Factor." It was decided that the latter was not specific enough. The term gives no clue as to its units and could be used to apply to "μ" (in the original paper), or to the empirical constant used in the torque-shear stress relationship for rectangular cross-sections.

The writer is not aware of any established practice in this respect, and there was no intention of dictating what the term should be.

Thanks are due to Mr. Bergman also for discussing at such length the reasons why the solution presented is not "exact." A service has been rendered to the engineer in reminding him of the folly of thinking his answer "exact." However, it seems Mr. Bergman misinterpreted the statement, that moments calculated by the method presented in this paper can be mathematically "exact."

The words "can be" were intended to mean that there are certain cases where (under ideal conditions) the moments could be exact. A wire of small diameter bent into a helix of fairly large radius and securely clamped at both ends could be such a case. Surely the words "can be" do not mean "are always." Mr. Bergman repeatedly used the word "exact" in quotes to denote that it is a manner of speaking. Reference to the original text will show that the word "exact" is in quotes.

"A precise MATHEMATICAL solution" was the writer's method of differentiating between a method that takes no "mathematical shortcuts" and one which uses a rough mathematical approximation, so that even if the "input data" of the problem were reasonably accurate, the answer could never be. The approximation of a helix by a ring lying entirely in one plane is an inexact mathematical procedure. The intention was to present a mathematical tool, applicable to a fairly wide range of situations, and with limitations to be determined by the user. It seemed hardly necessary to point out that the "output data" could be no more accurate than the "input data."

The value of K is perhaps questionable, but pointing out that the stress is higher at the inner edge of a curved beam than the value calculated for the stress in a straight beam throws no light on the subject.

---

a. Proc. Paper 1437, November, 1957, by Alan M. C. Holmes.

1. Structural Designer, Skidmore, Owings & Merrill, Chicago, Ill.

For a curved beam such as the one Mr. Bergman describes (width = centerline radius, and presumably lying in one plane), it can be shown (Figure 17) that even though the stress is higher at the inner edge by 52%, the value of K ("the measure of resistance to rotation per unit length due to unit moment") remains essentially the same. For a helical beam where the curvature is more complex, this may still be an approximation, but it is conceivable that there is some value of K which it would be correct to use in the solution, and that this value could be obtained by mathematical or empirical methods. For the small deviations that may occur in the K of a helical beam of reasonable proportions, it is simpler to recognize that the answer is approximate and to make an allowance for it, or to determine the variation in maximum moments for the range over which K is likely to vary. It can be said from experience that the maximum calculated moments vary less (from this cause) than we know concrete to vary in its properties.

On the basis of this solution, and the model test which showed close agreement, the writer has designed eight circular stairs (see Figs. 18 and 19). These are now built and performing satisfactorily. The largest, which has an arc of 360°, an outer diameter of 24 ft, and slab width of 7 ft, was recently load-tested. Under a total load of 30 tons (uniformly distributed), the midpoint deflection was 0.092 in., which is in line with the theoretical value. Strain gages indicated that stresses were about those anticipated, although a precise comparison is neither possible nor justified because of extraneous factors.

COMPARISON OF MOMENTS OF INERTIA

STRAIGHT BEAM

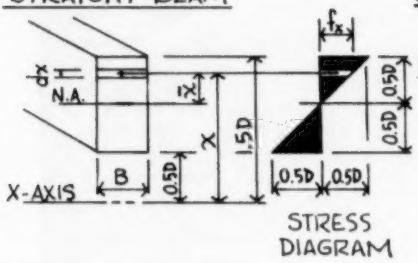

CURVED BEAM *

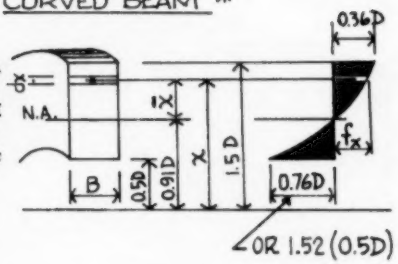

STRESS IS EXPRESSED AS A PROPORTION OF THE BEAM'S DEPTH SO THAT I, USUALLY WRITTEN $\int \bar{x}^2 dA$, CAN BE WRITTEN AS

$$I = \int \bar{x} f_x \, dA$$

$$\bar{x} = (1-x)D$$

$$f_x = (1-x)D$$

$$I_s = \int_{0.5}^{1.5} (1-x)^2 D^2 . dA$$

$$= BD^3 \int_{0.5}^{1.5} (1-x)^2 \, dx$$

$$= BD^3 \left[x - x^2 - \frac{x^3}{3} \right]_{0.5}^{1.5}$$

$$I_{\text{STRAIGHT BEAM}} = 0.083 \, BD^3 = \frac{1}{12} BD^3$$

STRESSES IN CURVED* BEAM ARE THOSE DERIVED IN THE USUAL MANNER.

$$\bar{x} = (0.91-x)D$$

$$f_x = 0.92 \frac{(0.91-x)}{x} D$$

$$I_c = \int_{0.5}^{1.5} \frac{0.92}{x} (0.91-x)^2 D^2 . dA$$

$$= 0.92 \, BD^3 \int_{0.5}^{1.5} (0.91-x)^2 \frac{dx}{x}$$

$$= 0.92 \, BD^3 \left[0.83 \ln x - 1.82x + \frac{x^2}{2} \right]_{0.5}^{1.5}$$

$$= 0.92 \, BD^3 (0.091)$$

$$I_{\text{CURVED BEAM}} = 0.084 \, BD^3 \cong \frac{1}{12} BD^3$$

* CURVATURE IN ONE PLANE ONLY

FIGURE 17

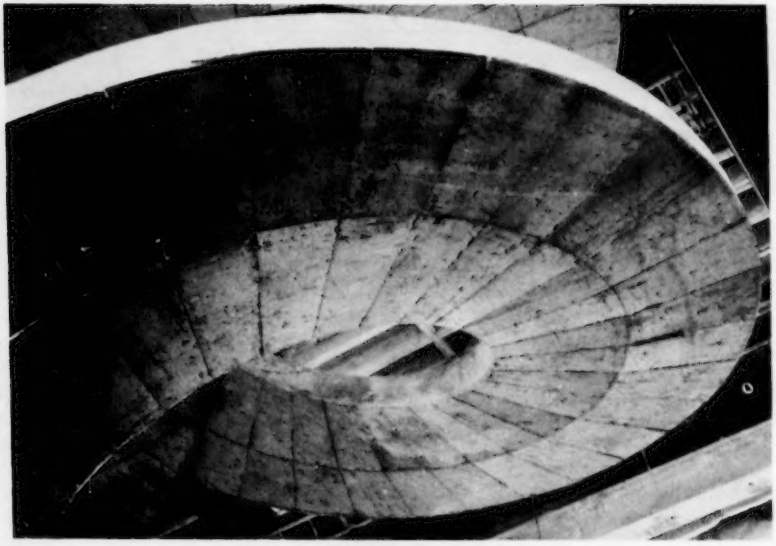

Fig. 18. Free-standing spiral stair at the Air Force Academy Viewed from below.
Arc: 360 degrees Outer diameter: 24 ft.
Height: 18 ft. 4 in. Inner diameter: 10 ft.

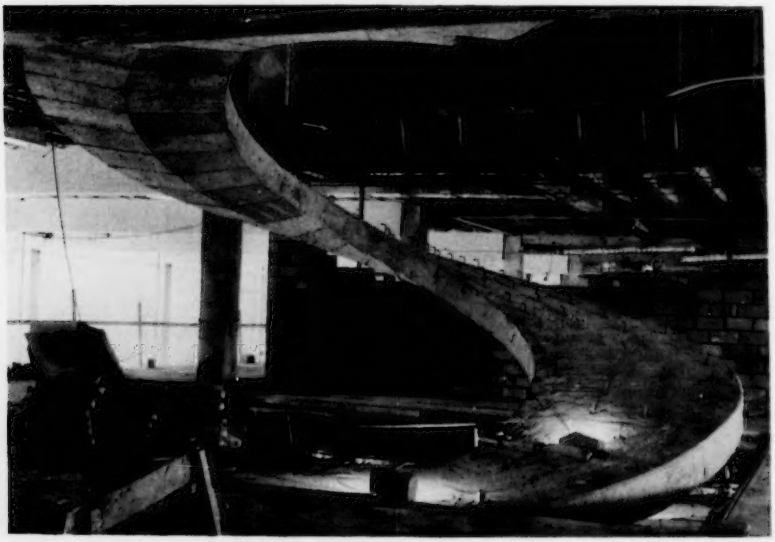

Fig. 19. Free-standing spiral stair at the Air Force Academy Viewed from side.
Arc: 290 degrees Outer diameter: 24 ft.
Height: 14 ft. Inner diameter: 10 ft.

A METHOD OF DESIGN OF REINFORCED CONCRETE SECTIONS[a]

Discussion by Juergen Plaehn

JUERGEN PLAEHN[1].—Mr. Moliotis presents a method for the design of any section of reinforced concrete. This method reduces the calculation of any section with a symmetrical axis to that of the rectangular section.

The writer believes that the derived design formulas are difficult to survey. The designing engineer runs the risk of seeing only the factors and formulas and not seeing the basic ideas on which his work is based. This results in misinterpretation and reading and writing errors with all of their consequences. Such difficulties can be avoided, if the design problem is solved step by step instead of using implicit design formulas. With the generally accepted assumptions for the design of reinforced concrete sections in mind each problem with one symmetrical axis can be solved quickly. One table set up for rectangular sections can be used for several purposes without having the user confronted with inconceivable coefficients. Table 1 of the "Reinforced Concrete Design Handbook" of the American Concrete Institute may be used as the only necessary table. A similar table which is more adaptable to slide rule computation is given below.

The assumptions are:

1. The Bernoulli Hypothesis that plane sections remain plane.
2. The Hooke Law that stresses are proportional to strains.
3. The Straight Line Law for both composite materials, derived from assumption 1 and 2.
4. The concrete section is cracked in the tensile area. The steel has to resist all tension forces.

Particularly assumption 2 (therefore also 3) is not in agreement with the behavior of concrete in reality the modulus of elasticity for concrete is not constant and decreases considerably at the breaking strength. The assumed $n = \frac{E_{St}}{E_B}$ differs more or less from the real value. Therefore it has no sence to exaggerate the accuracy of the calculation.

The presented design table is set up according to the following derivation. Similar tables for other steel stresses or other n-values can easily be computed.

---

a. Proc. Paper 1509, January, 1958, by Panagiotis D. Moliotis.

1. Asst. Design Engr., Richardson, Gordon and Associates, Pittsburgh, Pa.

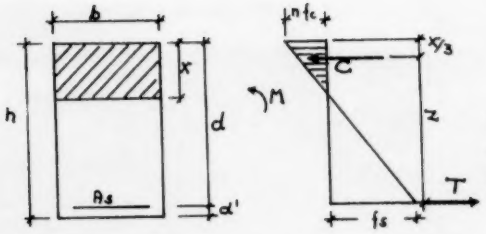

defined:

$x = k \cdot d$ (1)

$z = j \cdot d$ (2)

from (1) and stress strain diagram:

$$x = d \frac{n \cdot f_c}{n \cdot f_c + f_s} = k \cdot d \tag{3}$$

from (2) and stress diagram:

$$z = (d - x/3) = d(1 - k/3) = j \cdot d \tag{2'}$$

it is:

$$M = C \cdot z \tag{4}$$

$$M = T \cdot z \tag{5}$$

from (4) with (2'):

$$M = \tfrac{1}{2} \cdot f_c \cdot b \cdot x(d - x/3) = \tfrac{1}{2} \cdot k(1 - k/3) f_c b \cdot d^2$$

$$d = \sqrt{\frac{2}{k(1-k/3)f_c}} \sqrt{\frac{M}{b}} = r\sqrt{\frac{M}{b}} \tag{6}$$

from (5) with (2'):

$$M = A_s \cdot f_s (d - x/3) = A_s \cdot f_s \cdot d(1 - k/3) \tag{5'}$$

$$A_s = \frac{1}{(1-k/3)f_s} \cdot \frac{M}{d} = \frac{M}{d} \cdot \frac{1}{a} \tag{7}$$

from (5') with (6):

$$M = A_s \cdot f_s (1 - k/3) r \sqrt{\frac{M}{b}}$$

$$A_s = \frac{1}{(1-k/3) f_s \cdot r} \sqrt{M \cdot b} = t\sqrt{M \cdot b} \tag{8}$$

from (8) with (6):

$$A_s = t \cdot b \sqrt{\frac{M}{b}} = \frac{t}{r} \cdot b \cdot d = p \cdot b \cdot d \tag{9}$$

The examples show how to use the tables for various purposes.

If a given unusual flexural member is to be designed, the neutral axis can be determined for the allowable stresses from the lineary stress diagram

$x = \frac{n \times f_c = d}{n \times f_c + f_s}$. The table can be used for this purpose $x = k \times d$. Then for each section element the resultant C_i of the compression stresses and its moment $M_i = C_i \times z_i$ about the center of gravity of the tensile reinforcement can be computed. ΣM_i is the resisting moment of the concrete stresses, and $\Sigma C_i = T^C$ is the force in the tensile reinforcement. If the external moment M exceeds the resisting moment of the concrete stresses, the residual moment $\Delta M = M - \Sigma M_i$ must be resisted by additional compressive and tensile reinforcement $T^{St} = C^{St} = \frac{\Delta M}{z_{St}}$; z_{St} is the distance between the centers of gravities of the compression and tensile reinforcement. Then the necessary amount of reinforcement can be determined because the stresses at the center of gravity of the tensile as well as of the compressive are known from the stress diagram.

If bending and axial load are combined the same procedure is used when $\frac{M'}{N} > z$. The external moment will be taken about the center of gravity of the tensile reinforcement; therefore, the line of acting of the normal force coincides with the center of gravity of the tensile reinforcement. The stress diagram is the same as for bending alone. The amount of the resultant tensile force will be reduced, if N is a compressive force, and increased if N is a tension force: $T = T^C + T^{St} \pm N$. If the resisting moment of the concrete stresses exceeds the external moment $M < \Sigma M_i$ the cross section or the concrete fiber stress may be reduced. By interpolation between two computed values of A_c or f_c the accuracy of the calculation is usually sufficient.

Resultant of the Stresses for any Section or Section Element:

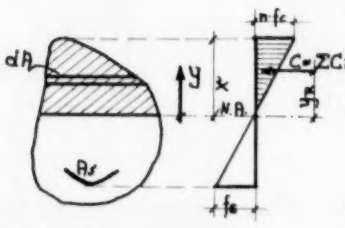

$$C_i = \int \frac{f_c}{x} \cdot y \cdot dA$$

$$C_i = \frac{f_c}{x} \cdot A_i \cdot \frac{\int y \cdot dA}{A_i}$$

$$C_i = A_i \cdot \frac{f_c}{x} \cdot y_{i,C.G.} \qquad (10)$$

$$y_{i,C.G.} = \frac{\int y \cdot dA}{A_i} = \frac{S_{i,N.A.}}{A_i}$$

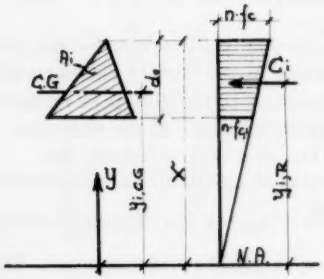

Element - i

Location of the resultant:

$$y_{i,R} = \frac{\int \frac{f_c \cdot y}{x} \cdot y \cdot dA}{\int \frac{f_c}{x} \cdot y \cdot dA} = \frac{\int y^2 \cdot dA}{\int y \cdot dA}$$

$$y_{i,R} = \frac{J_{i,N.A.}}{S_{i,N.A.}} \qquad (11)$$

Special Cases:

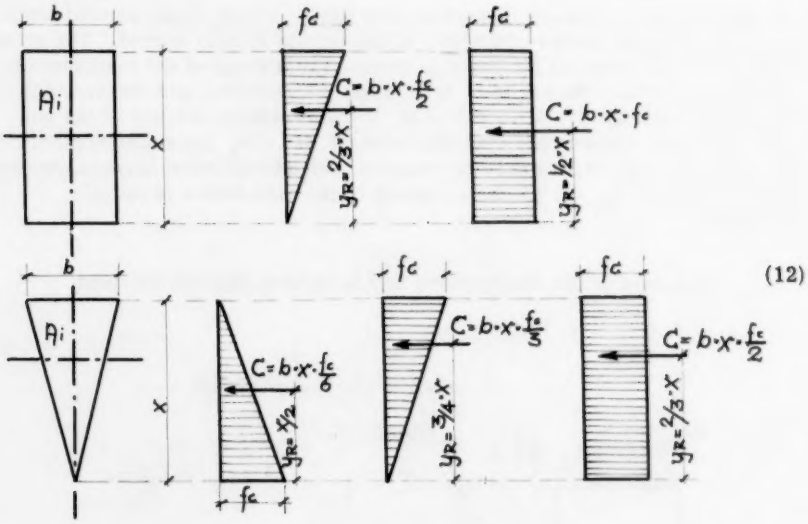

(12)

From equation (10) is seen that for any section or section element the resultant of the internal forces is equal to the area of the section multiplied by the stress at the center of gravity of the section $C_i = A_i = f_{c,i,C.G.}$. The distance of the resultant from the neutral axis can quickly be determined by dividing the moment of inertia by the section modulus, both in respect to the neutral axis. See equation (11). In most cases it is possible to set together the elements of the area and of the stresses diagram out of rectangular and triangular elements, - the location of the resultant is then known, see (12).

f_s = 20,000 lb/in^2 n = 15

fc	r	1/a	p	k	j
300	21.540	0.639	0.00138	0.184	0.939
330	19.813	0.642	0.00164	0.198	0.934
360	18.371	0.646	0.00191	0.213	0.929
390	17.150	0.649	0.00221	0.226	0.924
420	16.101	0.652	0.00251	0.239	0.920
450	15.191	0.655	0.00284	0.252	0.916
480	14.393	0.658	0.00318	0.265	0.912
510	13.688	0.661	0.00353	0.277	0.908
540	13.060	0.664	0.00389	0.288	0.904
570	12.498	0.666	0.00427	0.299	0.900
600	11.990	0.669	0.00465	0.310	0.896
630	11.530	0.672	0.00505	0.321	0.893
660	11.111	0.674	0.00546	0.331	0.890
690	10.727	0.677	0.00588	0.341	0.886
720	10.375	0.679	0.00631	0.351	0.883
750	10.050	0.682	0.00675	0.360	0.880
780	9.750	0.684	0.00720	0.369	0.877
810	9.471	0.686	0.00765	0.378	0.874
840	9.212	0.689	0.00812	0.386	0.871
870	8.970	0.691	0.00859	0.395	0.868
900	8.743	0.693	0.00907	0.403	0.866
930	8.530	0.695	0.00955	0.411	0.863
960	8.331	0.697	0.01004	0.419	0.860
990	8.143	0.699	0.01054	0.426	0.858
1020	7.966	0.701	0.01105	0.433	0.855
1050	7.798	0.703	0.01156	0.440	0.853
1080	7.640	0.705	0.01208	0.447	0.851
1110	7.489	0.707	0.01261	0.454	0.848
1140	7.346	0.709	0.01314	0.461	0.846
1170	7.210	0.711	0.01367	0.467	0.844
1200	7.080	0.712	0.01421	0.474	0.842
1230	6.957	0.714	0.01475	0.480	0.840
1260	6.840	0.716	0.01530	0.486	0.838
1290	6.727	0.718	0.01586	0.492	0.836
1320	6.619	0.719	0.01642	0.497	0.834
1350	6.516	0.721	0.01698	0.503	0.832
1380	6.417	0.722	0.01755	0.509	0.830
1410	6.321	0.724	0.01812	0.514	0.829
1440	6.230	0.725	0.01869	0.519	0.827
1470	6.142	0.727	0.01927	0.524	0.825
1500	6.058	0.728	0.01985	0.529	0.823
1530	5.976	0.730	0.02044	0.534	0.822
1560	5.899	0.731	0.02103	0.539	0.820
1590	5.822	0.733	0.02162	0.544	0.819
1620	5.749	0.734	0.02221	0.548	0.817
1650	5.678	0.736	0.02281	0.553	0.816
1680	5.610	0.737	0.02342	0.557	0.814
1710	5.544	0.738	0.02402	0.562	0.813
1740	5.480	0.739	0.02463	0.566	0.811
1770	5.418	0.741	0.02524	0.570	0.809
1800	5.358	0.742	0.02585	0.574	0.808

M [K ft]
b [in]
d [in]
A_s [in^2]

$d = r\sqrt{\frac{M}{b}}$

$A_s = \frac{M}{d}\frac{1}{a}$

$p = \frac{A_s}{b\,d}$

$x = K\,d$

$z = j\,d$

Example 1:

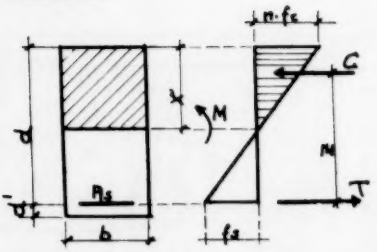

given: $M = 320$ Kft
$b = 17$ in
$f_{S,all.} = 20{,}000$ lb/in^2
$f_{C,all.} = 1{,}200$ lb/in^2
$n = 15$

determine: d ; A_S ; z

from table find for $f_S = 20{,}000$ lb/in^2 and $f_c = 1{,}200$ lb/in^2:

$r = 7.080$; $1/a = 0.712$; $j = 0.842$

$$d = r\sqrt{\frac{M}{b}} = 7.08\sqrt{\frac{320}{17}} = 30.7 \text{ in}$$

$$A_S = \frac{M}{d}\cdot\frac{1}{a} = \frac{320}{30.7}\,0.712 = 7.45 \text{ in}^2$$

$$z = 0.842 \cdot 30.7 = 25.9 \text{ in}$$

Often it may be more economical to use a f_c smaller than $f_{c,all.}$; this particular if the width is large.

Example 2:

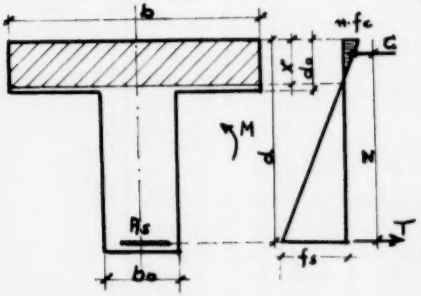

given: $M = 300$ Kft
$b = 50$ in
$b_o = 15$ in
$d_o = 10$ in
$f_{c,all.} = 1{,}200$ lb/in^2
$f_{S,all.} = 20{,}000$ lb/in^2
$n = 15$

determine: d ; A_S ; z

used: $f_c = 420$ lb/in^2 1/3 $f_{c,all.}$

$r = 16.101$; $1/a = 0.652$; $k = 0.239$; $j = 0.920$

$$d = 16.101\sqrt{\frac{300}{50}} = 39.4 \text{ in} \quad ; \quad x = 0.239 \cdot 39.4 = 9.44 < 10$$

$$A_S = \frac{300}{39.4}\,0.652 = 4.97 \text{ in}^2 \quad ; \quad z = 0.920 \cdot 39.4 = 36.3 \text{ in}$$

$z \approx d - d_o/3$

Example 3:

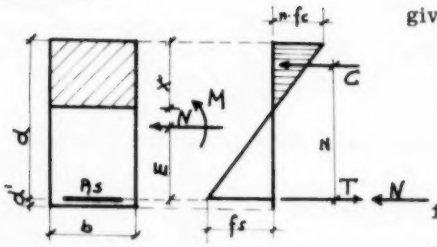

given: M = 140 Kft
N = 100 K
E = 14 in
b = 17 in
d = 31 in
d' = 2 in
$f_{s,all.}$ = 20,000 lb/in^2
$f_{c,all.}$ = 1200 lb/in^2
n = 15

determine: A_s ; f_c

Moment about the tensile reinforcement: $M' = M + N \cdot E$

$$M' = 140 + 100 \cdot 14/12 = 256.5 \text{ Kft}$$

$$r = \frac{d}{\sqrt{\frac{M}{b}}} = \frac{31}{\sqrt{\frac{256.5}{17}}} = 7.97$$

$$f_c = 1020 \text{ lb/in}^2$$

$$A_s = \frac{M'}{d} \cdot \frac{1}{a} - \frac{N}{f_s} = \frac{256.5}{31} 0.701 - \frac{100}{20} = 0.7 \text{ in}^2$$

Example 4:

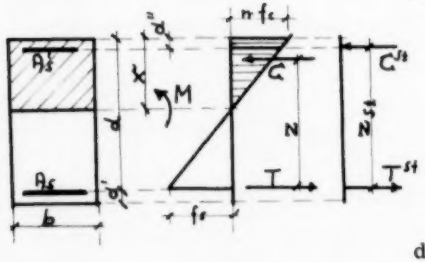

given:
M = 500 Kft
b = 17 in
d = 31 in
d' = d'' = 2 in
$f_{s,all.}$ = 20,000 lb/in^2
$f_{c,all.}$ = 1200 lb/in^2
n = 15

determine: A_s ; A'_s ; f'_s

with $f_{c,all.}$ and $f_{s,all.}$ find from table the resisting moment of the concrete stresses:

$$r = 7.080 \quad ; \quad 1/a = 0.712 \quad ; \quad k = 0.474$$

$$M_c = \left(\frac{d}{r}\right)^2 b = \left(\frac{31}{7.080}\right)^2 \cdot 17 = 326 \text{ Kft}$$

to M_c belongs the tensile reinforcement $A_{s,1} = \frac{M_c}{d} \cdot \frac{1}{a}$

$$A_{s,1} = \frac{326}{31} \cdot 0.712 = 7.5 \text{ in}^2$$

$$x = k \cdot d = 0.474 \cdot 31 = 14.7 \text{ in}$$

the residual moment $\Delta M = (M - M_c)$ must be resisted by additional tensile and compression reinforcement:

$$\Delta M = 500 - 326 = 174 \text{ Kft}$$

$$z_{St} = d - d' = \frac{31 - 2}{12} = 2.42 \text{ ft}$$

$$T_{St} = \frac{\Delta M}{z_{St}} = \frac{174}{2.42} = 72 \text{ K}$$

$$A_{s,2} = \frac{T_{St}}{f_{s,all.}} = \frac{72}{20.0} = 3.60 \text{ in}^2$$

total tensile reinforcement: $A_s = A_{s,1} + A_{s,2}$

$$A_s = 7.5 + 3.60 = 11.10 \text{ in}^2$$

compression reinforcement:
from statical moment about the neutral axis find A'_s:

$$A'_s \cdot (x - d') - A_{s,2} \cdot (d - x) = 0$$

$$A'_s = A_{s,2} \cdot \frac{(d - x)}{(x - d')}$$

$$A'_s = 3.60 \cdot \frac{(31.0 - 14.7)}{(14.7 - 2)} = 4.62 \text{ in}^2$$

because: $A_{s,2} \cdot f_s = A'_s \cdot f'_s$

$$f'_s = \frac{A_{s,2} \cdot f_s}{A'_s} = \frac{T_{St}}{A'_s}$$

$$f'_s = \frac{72}{4.62} = 15.55 \text{ K/in}^2$$

If moment and normal force are combined the same procedure is used. The moment about the tensile reinforcement will be determined: $M' = M \pm N{=}E$. The tensile reinforcement is found from:

$$A_S = A_{s,1} + A_{s,2} \mp A_{s,3}; \text{ where } A_{s,3} = \frac{N}{f_{s,all.}}$$

Example 5:

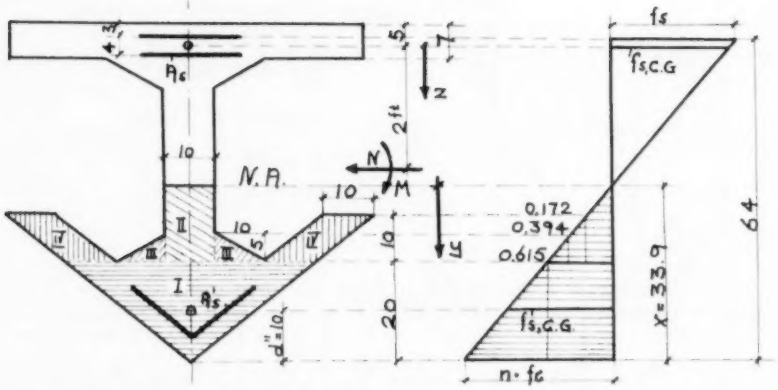

given: cross section as shown above,

f_c = 1,500 lb/in^2 ; M = 1,800 Kft

f_s = 20,000 lb/in^2 ; N = 500 K

n = 15 ; E = 2 ft

determine: A_s ; A'_s ; f'_s

assume: d' = 5 in ; d'' = 10 in

it is: M' = M + N·E = 1,800 + 500·2 = 2,800 Kft

$$x = \frac{64 \cdot 15 \cdot 1.5}{20.0 + 15 \cdot 1.5} = 33.9 \text{ in}$$

z_{St} = 67 - 15 = 52 in = 4.32 ft

	A_i [in^2]	$y_{i,C.G.}$ [in]	$f_{i,C.G.}$ [K/in^2]	C_i [K]	$y_{i,R}$ [in]	z_i [in]	M_i [Kft]
I	½·50·20=500	20.57	0.615	307	20.57	48.67	1245
			0.295	148	23.90	52.00	640
II	13.9·10=139	6.95	0.308	43	9.25	37.35	133
III	2·½·5·10= 50	12.23	0.394	20	12.23	40.33	66
			0.148	7	12.65	40.75	25
IV	2·10·10=200	8.90	0.172	34	8.90	37.00	106
			0.221	44	10.57	38.67	143
			$\sum C_i$ = 603		;	$\sum M_i$ = 2358	

ΔM = 2,800 - 2,358 = 442 Kft ; $C_{St} = T_{St}$ = 442/4.32 =102 K

$\sum T$ = 603 + 102 - 500 = 205 K

$f_{s,C.G.}$ = 20.0·28.1/30.1 = 18.65 K/in^2

$f'_{s,C.G.}$ = 15·1.5·23.9/33.9 = 15.8 K/in^2

A_s = 205/18.65 = 11 in^2 ; A'_s = 102/15.8 = 6.45 in^2

Second example from Mr. Moliotis:

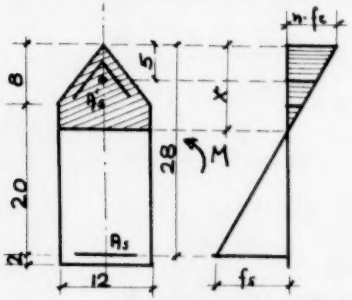

given: cross section as shown

$M = 850{,}000$ lb in

$f_c = 900$ lb/in^2

$f_s = 20{,}000$ lb/in^2

$n = 15$

determine: A_s ; A'_s

$x = k \cdot d = 0.403 \cdot 28 = 11.3$ in

i	A_i in^2	$y_{i,C.G.}$ in	$f_{i,C.G.}$ K/in^2	C_i K	$y_{i,R}$ in	z_i in	M_i K ft
△	$12 \cdot 8 \cdot \frac{1}{2} = 48$	5.96	0.476	22.9	6.56	23.26	45.2
□	$3.3 \cdot 12 = 39.6$	1.65	0.132	5.2	2.20	18.90	8.2
			$\sum C_i = 28.1$			$\sum M_i = 53.4$	

$$\Delta M = \frac{850{,}000}{12{,}000} - 53.4 = 17.6 \text{ Kft}$$

$$T^{St} = C^{St} = \frac{17.6}{23} \cdot 12 = 9.2 \text{ K}$$

$$A_s = \frac{28.1 + 9.2}{20.0} = 1.40 + 0.46 = 1.86 \text{ in}^2$$

$$A'_s = \frac{0.46\,(28 - 11.3)}{(11.3 - 5)} = 1.22 \text{ in}^2$$

Mr. Moliotis gives a revised value: $A'_s = 1.22$ in^2; the above method can be used for the remaining examples given by Mr. Moliotis.

REFERENCE

1. "Bemessung der Stahlbetonquerschnitte" Prof. Dr.-Ing. Dischinger Technische Universitaet Berlin-Charlottenburg, 1948.

PANAGIOTIS D. MOLIOTIS,[1] M. ASCE.— Corrections:

Page 2: Equation (2) should read:

$$f'_s = n f_c \left(1 - \frac{1}{K} \cdot \frac{d'}{d}\right)$$

Page 4: Equation (9) should read:

$$\rho' = 1 - \frac{1}{K} \cdot \frac{e'_o}{d} \frac{1}{\left(1 - \frac{1}{K}\frac{d'}{d}\right)}$$

1. Dr. Civ. Eng., Asst. National Technical Univ., Athens, Greece.

Page 7: Equation (33) should read:

$$p_t = \frac{1}{\frac{2f_s}{f_c}\left(1+\frac{f_s}{f_c}\right)}$$

Page 17: Lines 5, 6 and 7 should read:

$$\rho' = 1 - \frac{1}{0.403} \cdot \frac{3}{28} \cdot \frac{1}{\left(1 - \frac{1}{0.403} \cdot \frac{2}{28}\right)} = 0.677$$

$$A_s' = \frac{1\,663\,000 - 1\,270\,000}{28 \times 11\,150\left(1 - \frac{5}{28}\right)} \cdot \frac{0.542}{0.677} = 1.22\,in^2$$

$$A_s = 0.542 \times 0.0091 \times 103 \times 28 + \frac{11\,150}{20\,000} \times 1.22 \times 0.677 = 1.88\,in^2$$

ANALYSIS OF BRACED FRAMES[a]

Discussion by I.M. Nelidov

I. M. NELIDOV,[1] M. ASCE.— In this paper the author has presented a method of analysing frames with hinged connections of the braces, based on the principles of H. Cross and deflection stiffness. A sample problem was given of a portal assymmetrical frame with hinged braces, loaded with a uniform load over the top member.

The writer has done some work on similar frames with braces with rigid connections, where he used Cross' method and potential deformations of the frame, for more visual understanding of the deformed shape of the frame. In this discussion, the writer will repeat the example given by the author, using his own approach.

There are two steps in this analysis, one with lateral sway prevented, and another, with lateral sway. Referring to the figure showing the frame on p. 1560-8, the joints B and C and the joints at the lower end of knee braces, which we will call B' and C', are held from lateral displacement, while the uniform load of one k/ft. is applied to the top beam.

In this case, the intermediate supports of the top beam between joints B and C are also immovable and the top beam acts as a continuous beam of three spans and four supports. The fixed-end moments and end shears are respectively, for span 10.ft. $M = 1. \frac{10.^2}{12} = 8.33$ 'k and $V = 5.$k.; for span 20.ft., $M = 1. \frac{20.^2}{12} = 33.33$ 'k and $V = 10.$k. The balancing of the moments is shown below, with stiffness values for end spans .75 and for the center span .50, giving distribution factors respectively .60 and .40.

FEM.	−8.33	+8.33	−33.33	+33.33	−8.33	+8.33
	+8.33	+4.17			−4.17	−8.33
	0.00	+12.80	+ 8.53	−8.53	−12.80	0.00
			−4.26	+4.26		
		+2.55	+1.71	−1.71	−2.55	
			− .86	+ .86		
		+ .52	+ .34	− .34	− .52	
			− .17	+ .17		
		+ .10	+ .07	− .07	− .10	
			− .04	+ .04		
		+ .02	+ .02	− .02	− .02	
		+27.99	−27.99	+27.99	−27.99	

a. Proc. Paper 1560, March, 1958, by K. H. Gerstle.
1. Structural Engr., San Francisco, Calif.

The shears resulting from these moments are respectively for left and right supports of the end span at left: $V_1 = -2.80k$ and $V_2 = +2.80k$, the sign plus indicating upward direction; for center span: $V_1 = V_2 = 0$; for right hand span: $V_1 = +2.80k$ and $V_2 = -2.80k$. The reactions of the beam at consecutive supports starting from left are $R_1 = +2.20k$, $= R_4$, $R_2 = 17.80k = R_3$, positive for upward direction. The lateral horizontal forces induced by these reactions thru the braces and applied at points B' and C' are: -11.86k and 17.80k, at minus sign -, acting to the left, and with plus sign -to the right. Actually, when the joints B and C are held immovable, the joints B' and C' move laterally due to the action of the uniform load transferred thru the braces; therefore, we will deflect arbitrarily the joints B' and C' firstly outward, i.e. joint B' to the left and joint C' to the right an amount Δ; this will displace the intermediate supports of the top beam an amount $.667\Delta$ at left knee-brace and Δ at right knee brace. If we assume an arbitrary fixed-end moments in the right-hand column DC', M = -10.'k., then at the upper part of the same column the moment will be with one end hinged M = +5.'k, at the lower end of column C'C. For the left -hand column, since its height is 1.5 times that of column DC, the fixed-end moments in AB' will be M = +4.44'k, and the moment at the lower part of B'B will be M = -2.22'k. The fixed-end moments in the left span of the top beam BC will be M = -6.67'k; in its center span M = -.83'k, taking into account that this span is twice the height of column DC'; in the right -hand span M = +10.'k. Signs of the moments are positive when clockwise.

The rigidities of the top beam BC being previously computed, the balancing of the moments is as given below.

-6.67	-6.67	-.83	-.83	+10.00	+10.00
+6.67	+3.33			- 5.00	-10.00
	+2.50	+1.67	-1.67	- 2.50	
0.00					0.00
		- .83	+ .83		
	+.50	+ .33	- .33	- .50	
		- .16	+ .16		
	+.10	+ .06	- .06	- .10	
		- .03	+ .03		
	+.02	+ .01	- .01	- .02	
	-.22	+ .22	-1.88	+1.88	

The shears resulting from these moments are, for left span: $V_1 = +.02$ and $V_2 = -.02k.$; for center span: $V_1 = +.08k$ and $V_2 = -.08k$; for right span; $V_1 = -.19k$ and $V_2 = +.19k$. The respective reactions respectively from the left supports are: $R_1 = +.02k.$, $R_2 = +.06k$, $R_3 = -.27k$ and $R_4 = +.19k$. The horizontal forces exerted thru the knee-braces at their lower ends due to these reactions are, at the left joint B': -.04k and at C' -.27k. The moments in column AB due to the fixed-end moments resulting from the displacement Δ are obtained thru the balancing shown below, with stiffness of AB' taken as 1.00 and of B'B as .75, giving the distribution factors respectively .57 for AB' and .43 for B'B; the column is laid horizontally for convenience. For column DC' the balancing is shown below at right.

+4.44	+4.44	-2.22	0.00	-10.00	-10.00	+ 5.00	0.00
-. 63	-1.26	- .96		+ 1.43	+ 2.85	+ 2.15	
+3.81	+3.18	-3.18		- 8.57	- 7.15	+ 7.15	

The shears for the left column are, for AB': V_1 = +.46 and V_2 = -.46k, positive acting to the right, considering vertical column; for part B'B: V_1 = -.21k. and V_2 = +.21k. The respective reactions in the column are: at A R_1 = +.46k, at B' R_2 = -.67k and at B R_3 = +.21k., positive acting to the right.

For the column DC, we will have: for DC', V_1 = -1.57k. and V_2 = 1.57k; for C'C, V_1 = +.72k. and V_2 = -.72, at C' and C respectively; the resulting reactions are: at D R_1 = -1.57k, at C' R_2 = + 2.29k and at C R_3 = -.72k.

Since the lateral deflections at joints B' and C' are not equal, these points should be deflected both in one direction, so as finally to achieve the inequality. We arbitarily deflect these points to the left an amount Δ; this will induce an upward displacement of the upper end of the right-hand knee brace of the amount Δ; at the upper end of the left-hand knee-brace the displacement will be downward to the amount .667Δ. If, as before, the fixed-end moments in the right -hand column DC' are taken arbitrarily at +10.00'k, the moments in the left-hand column AB' will be +4.44'k.; the moments in the lower end of the upper half of the columns respectively will be, in C'C M = - 5.00'k. and in B'B M = - 2.22'k. The moments in the top beam in its left-hand span will be: M = -6.67'k, in its center part M = + 4.17'k and in the right-hand span M = -10.00'k, all fixed-end moments. The balancing of these moments in the beam BC is as given below.

-6.67	-6.67	+4.17	+4.17	-10.00	-10.00
+6.67	+3.33			+ 5.00	+10.00
	- .50	- .33	+ .33	+ .50	
		+ .16	- .16		
	- .10	- .06	+ .06	- .10	
		+ .03	- 03		
	- .02	- .01	+.01	+ .02	
	-3.96	+3.96	+4.38	-4.38	

The resultant shears are, in the left -hand span: V_1 = +.40k and V_2 = -.40k; in center span: V_1 = -.42k and V_2 = +.42k; in right -hand span: V_1 = +.44 k and V_2 = -.44k. The respective reactions are R_1 = +.40k, R_2 = -.82k, R_3 = .86k and R_4 = -.44k. The forces induced thru these reactions horizontally at points B' and C' at lower ends of the braces are: at B': +.55k and at C' + .86k.

Since the lateral deflection of the column AB in this case is the same as in the previous case, the moments, shears and reactions in this column are the same as were obtained then. For the right -hand column the deflection was taken to the left or in opposite direction compared with the previous case; therefore, the signs for the moments, shears and reactions should be reversed. In order to determine the unbalanced force of reactions at the bases of the columns due to the imposed restraints of the joints, we will write the equations from which the coefficients can be determined, multiplying by which the data obtained in this step, the unbalanced force could be found. These equations are:

$-11.86 - .04\ C_1 + .55\ C_2 = -.67\ C_1 - .67\ C_2$ - for the left-hand column, and

$+17.80 - .27\ C_1 + .86\ C_2 = + 2.29\ C_1 - 2.29\ C_2$ - for the right -hand column.

By solving these, it is found that $C_1 = 11.58$ and $C_2 = 3.75$
The unbalanced force is therefore: $H = .46\ (11.58 + 3.75) - 1.57(11.58-3.75) = -5.25$, acting to the left; which means that the frame is acted upon with the excess force acting to the right, and therefore, we must deflect it primarily to the left, for equilibrium.

In achieving this, we must firstly to deflect the lower parts of columns to the left, so that the upper portion of the frame would remain undistorted; then, to deflect the upper parts of the columns, with the inevitable distortion of the beam; and then, deflect the columns outwardly, as was done in the second part of step one.

By deflecting the lower part of column AB, namely AB', to the left, the fixed-end moments induced there are M = +4.44 'k, if the moments in the right-hand column DC' for the same deflection are taken at M = + 10.00'k. In the upper part of both columns the fixed-end moments are zero. Below is shown the balancing of the moments for both columns.

+4.44	+4.44	0.00	0.00	+10.00	+10.00	0.00	0.00
-1.26	-2.53	-1.91		- 2.85	- 5.70	-4.30	
+3.18	+1.91	-1.91		+7.15	+ 4.30	-4.30	

The corresponding shears in the left hand column are: in AB' $V_1 = +.34k$ and $V_2 = -.34k$; in B'B $V_1 = -13k$ and $V_2 = +.13k$. The reactions are, at A $R_1 = +.34k$, at B' $R_2 = -.47k$, and at B $R_3 = +.13$ k.

The shears in the column DC are: in DC' $V_1 = +1.15k$ and $V_2 = -1.15k$; in C'C $V_1 = -.43k$ and $V_2 = +.43k$. The reactions are, at D $R_1 = +1.15k$, at C' $R_2 = 1.58k$. and at C $R_3 = +.43k$.

In deflecting the upper portion of the columns to the left an amount Δ, the top of the left brace will rise .667 Δ, while the top of the right brace will go down an amount Δ. This will produce the moments, shears and reactions similar to those obtained for the beam BC in the second part of step one but with opposite signs. The moments in the upper parts of the columns with fixed end condition will be correspondingly for the right and left columns M = +10.00'k and M = +4.44'k. The balancing of these moments is given below, for the left and right columns respectively.

0.00	0.00	+4.44	+4.44	0.00	0.00	+10.00	+10.00
		-2.22	-4.44			- 5.00	-10.00
- .63	-1.26	- .96		-1.43	- 2.85	- 2.15	
			0.00				0.00
-.63	-1.26	+1.26		-1.43	- 2.85	+ 2.85	

The shears in the left-hand column are: in AB' $V_1 = +13k$, and $V_2 = -.13k$; in B'B $V_1 = +.08k$. and $V_2 = -.08k$. The reactions are: at A $R_1 = -.13k$., at B' $R_2 = +.21k$. and at B $R_3 = -.08k$. The shears in the right hand column are: in DC' $V_1 = -.43k$. and $V_2 = +.43k$.; in C'C $V_1 = +.29k$ and $V_2 = -.29k$; The reactions are: at D $R_1 = -.43k$, at C' $R_2 = +.72k$. and at C $R_3 = -.29k$. In deflecting the columns outwardly, the same data are obtained as were listed in 2nd part of step one. The equations necessary for determination of coefficients C_3, C_4 and C_5 are given below.

$-.55\ C_4 - .04\ C_5 = -.47\ C_3 + .21\ C_4 - .67\ C_5$ - for the lower end of left-hand column, and

$-.86\ C_4 - .27\ C_5 = -1.58\ C_3 + .72\ C_4 + 2.29\ C_5$ - for the lower end of right hand column and

$.34\ C_3 - .13\ C_4 + .46\ C_5 + 1.15\ C_3 - .43\ C_4 - 1.57\ C_5 = 5.25$

The solution of these equations renders the values of coefficients C as follows:

$$C_3 = 5.88, \quad C_4 = 4.38 \quad \text{and } C_5 = .91.$$

After substituting these coefficients in the last of previous equations, it was found that the equation is satisfied.

In order to demonstrate how moments and reactions are obtained with the aid of the above coefficients, a sample computation will be given for joint A. Thus $M_a = 3.81\ (11.58 + 3.75) + 3.18x5.88 - .63x4.38 + 3.81x.91 = 58.5 + 18.70 - 2.76 + 3.46 = 77.9$ 'k.

$R_a = .08x11.58 - .42x3.75 + 0.00 + .42x4.38 + .08x.91 = .93 - 1.58 + 0.00 + 1.84 + .07 \pm 20.00 = 21.26$ k.

Other moments and reactions can be obtained in a similar way, and they check the values given by the author in his figure on p. 1560-11 within 1%.

In concluding, the writer wishes to say that while the method of analysing braced frames by following their deformations may by not as short as that offered by the author, in the estimation of the writer it gives a visual process of realizing the deformed shape of the frame.

NUMERICAL SOLUTIONS FOR BEAMS ON ELASTIC FOUNDATIONS[a]

Discussion by Victor R. Bergman and N. J. Ryker, Jr.

VICTOR R. BERGMAN,[1] A.M. ASCE.—Mr. Malter has chosen to deal exclusively with the mathematical manipulations involved in the solutions, and with this decision there can be no argument. Still, in view of Mr. Malter's own statement that the phase covered in his work is only one aspect of a tripartite problem, it may be admissible to recommend for the benefit of designing engineers who must fact the problem in its entirety, a paper by Karl Terzaghi, published in 1955.[2]

In his laudably concise presentation of the application of numerical methods to the solution of beams on the so-called "Winkler foundation," Prof. Malter has furnished his readers with two references[6, 7] for further study of the finite-difference method. This technique, as applied to the problem considered, is of such beautiful simplicity that consultation of references is unnecessary. The only feature of the procedure that may prove unfamiliar to the structural analyst is the replacement of the second derivative in the familiar beam equation, $\frac{d^2y}{dx^2} = \frac{M}{EI}$, by its finite-difference approximation, $\frac{y_r - 2y_i + y_l}{h^2}$. A simple derivation of this approximate expression is offered in Fig. 1.

N. J. RYKER, JR.[3].— In this paper Professor Malter has outlined in excellent detail two numerical methods for solution of beams on elastic foundation. The paper will undoubtedly increase the popularity of the powerful successive approximation methods for the solution of these problems. The earlier work of Professor Popov[1] dealt primarily with the graphical solutions and therefore may have had limited acceptance by those who abhor graphics (an attitude apparently growing in popularity). Professor Popov did mention that his calculations could be set up in tabular form.

The second innovation by Professor Malter and one which can contribute greatly to rapid convergence for long flexible beams, is the initial assumption of an approximate deflected shape rather than the rigid shape. Contrary to the authors statement, however, the successive approximation method using the Newmark type solution is not restricted to relatively short beams. It is the purpose of this discussion to present a method[2] that will assure

a. Proc. Paper 1562, March, 1958, by Henry Malter.

1. Vice-Pres., Godwin Constr. Co., New York, N. Y.
2. "Evaluation of Coefficients of Subgrade Reaction" (Geotechnique, Dec., 1955).
3. Preliminary Design Engr., Missile Division, North American Aviation, Inc., Downey, Calif.

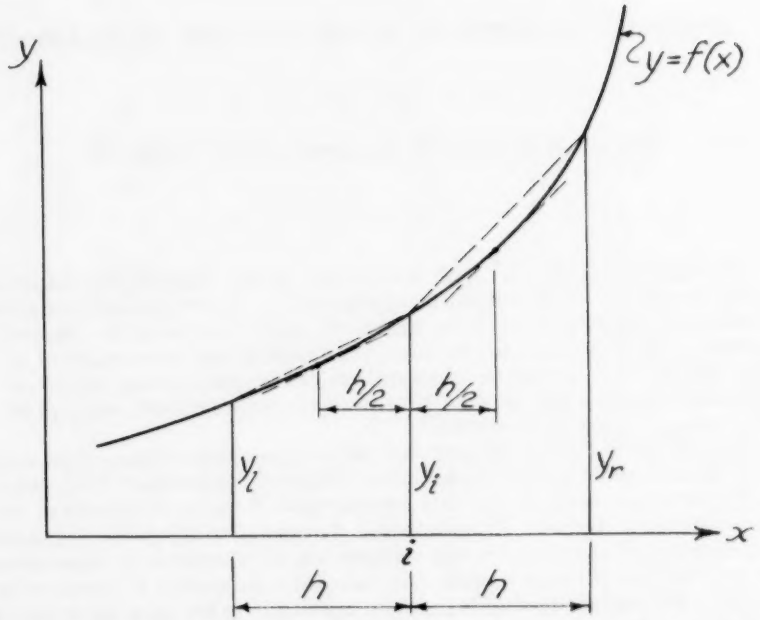

Required: An approximate expression for $\frac{d^2y}{dx^2}$ at $x=i$, in terms of the ordinates y_l, y_i, and y_r.

Derivation:

At $x=i-\frac{h}{2}$, $\quad \frac{dy}{dx} \cong \frac{y_i - y_l}{h}$

At $x=i+\frac{h}{2}$, $\quad \frac{dy}{dx} \cong \frac{y_r - y_i}{h}$

The change of slope between $x = i-\frac{h}{2}$ and $x=i+\frac{h}{2} \cong \frac{y_r-y_i}{h} - \frac{y_i-y_l}{h} \cong \frac{y_r-2y_i+y_l}{h}$, and the rate of change of slope at $x=i$ is

$$\frac{d^2y}{dx^2} \cong \left(\frac{y_r-2y_i+y_l}{h}\right)/h \cong \frac{y_r-2y_i+y_l}{h^2}$$

Fig. 1 Derivation of Finite Difference Expression for $\frac{d^2y}{dx^2}$.

convergent solutions for very long beams on elastic foundations.

In general, the method proposed by Professor Malter will provide a convergent solution as long as $\lambda L = 3$, where L is the length of the beam and $\lambda 4 = k/4EI$. For beams of greater length a convergence factor may be used to obtain a convergent solution. The general procedure is as follows:

1. Assume an original deflected shape and place the beam in equilibrium with the applied loads and moments by rigid beam deflection and rotation. Let the balanced beam shape be denoted by y_o.

2. Using the resulting foundation pressures and the applied loads, calculate the new deflected shape by any convenient method. Add rigid beam deflections and rotations so that there is no net load or moment on the beam (remove all applied loads). Let this deflected shape be denoted by δ_1.

3. Calculate the deflected shape due to the foundation pressures of δ_1 and adjust as in step 2. Let this shape be denoted by δ_2.

4. Calculate the quantity $r = \dfrac{\delta_1}{\delta_1 - \delta_2}$ at each panel point of the beam, and average for the entire beam.

5. The final shape is then:

$$y = y_o + \delta_1 + r\,\delta_2$$

6. If the quantity $r\,\delta_2$ is large or if the convergence factor r varies greatly along the beam repeat steps 1-5.

The development of this procedure is quite simple. In successive approximation methods the solution can be represented as:

$$y = y_o + \delta_1 + \delta_2 + \cdots$$

where y_o, the original assumed shape, balances all applied loads and δ_1, δ_2, etc., which are corrections to this shape, are in static equilibrium without applied loads. As long as δ_n and all successive δ_n's are similar in shape, then

$$r\,\delta_n = \delta_n + \delta_{n+1} + \delta_{n+2} + \cdots$$

and

$$y = y_o + \delta_1 + \cdots + r\,\delta_n$$

The quantity r can be calculated from two successive cycles; to minimize calculations it is proposed that only the first and second cycles be used even though these shapes generally are not similar.

$$y = y_o + r\delta_1$$

$$y = y_o + \delta_1 + r\,\delta_2$$

Equating these two quantities, the convergence factor in step 4 is obtained.

The validity of this procedure is dependent upon the similarity of δ_1 and δ_2; since in general they will not be similar, the second of the two equations above will more closely approximate the true shape.

Mr. Karol[3] in his discussion of Professor Popov's paper suggested using:

$$r = \frac{P_1}{P_1 + P_2}$$

where P_1 = total reaction under δ_1, if the ends of the shape δ_1 are placed at the surface of the foundation.

P_2 = total reaction under δ_2, if the ends of the shape δ_2 are placed at the surface of the foundation.

This equation is based upon the end pressures of δ_1 and δ_2 because for a constant foundation modulus

$$P_1 = \left[\frac{(q_1)_{x=0} + (q_1)_{x=L}}{2}\right] L$$

where q_1 is the foundation pressure for δ_1. Because it is based solely upon the end values, it fails to give a convergent solution in some cases that the suggested method does.

Mr. Plumb,(4) also in a concurrent development of a convergence factor similar to Mr. Karol's continued his successive approximation process until the ratios of successive differences were a constant. However, in the case of beams of $\lambda L = 6$ the procedure must be repeated for at least four cycles and requires the use of 6-10 significant figures because the answer is on the order of 10^{-4} δ_4.

The general procedure outlined above can be applied directly to the procedures outlined by Professor Malter. The principal difference being that δ_1 and δ_2 are not obtained directly.

1. Follow Malter's steps (a) through (m) and then using M_o calculated in (m) repeat steps (i) through (l).
2. Correct the original deflected shape y_a and the two successive values y to place them in equilibrium with the applied loads using Malter's correction configurations. Let these successive values be y_o, y_1, and y_2.
3. Calculate $\delta_1 = y_1 - y_o$ and $\delta_2 = y_2 - y_1$.

To illustrate this procedure consider the first problem presented by Professor Malter. The first cycle remains as shown. However, the actual calculated values of M_o must be used to initiate the second cycle from which the deflection, shears and moments shown in Table I were calculated.

After the moment and shear at the end of the beam, rows 3 and 4, were calculated, equal and opposite moments and shears were applied to balance the deflected beam, rows 5 and 6. The rigid deflections of Malter's correction configurations for shear (y_B) and moment (y_A) were added to y', row 2, producing y_2. Similar corrections were computed for y_A and y' in the first cycle producing y_o and y_1 respectively. From the differences, the convergence factor r was computed. The variation of r along the beam indicates that δ_1 and δ_2 are not similar, but the average value of r = .788 produces better agreement with Hetenyi's solution than does y_2. It is apparent from the values of y_2 and y_1, that, because of the idealization of the beam, the solution will never exactly coincide with Hetenyi's solution.

A better example of the rapid convergence is supplied by Malter's second example, table II. In this case using one cycle of the general procedure (which is equivalent to two cycles of Malter's procedure) and an average

TABLE I - Example 1

Second Cycle	Point A	B	C	D
M_o, $h^2/12$ lb-in.	0	-14.81	-17.69	0
y', 10^{-2} inches	+0.819	0	0	+0.947
V, h/12 lbs	-9.90	-4.17	-3.22	-29.9
M, $h^2/12$ lb-in.	0	-9.90	-14.07	-17.29
$y'_{c1} = (-\frac{29.9}{93.6})\, y_B$	-0.512	+0.128	+0.769	+1.281
$y'_{c2} = (\frac{17.29}{175.5})\, y_A$	+0.221	+0.025	-0.172	-0.369
Balanced Deflections				
$y_2 = y + y'_{c1} + y'_{c2}$	+0.528	+0.153	+0.597	+1.859
y_1	+0.580	+0.123	+0.594	+1.982
y_o	+ .454	+0.193	+0.629	+1.393
$\delta_1 = y_1 - y_o$	+0.126	-0.070	-0.035	+0.589
$\delta_2 = y_2 - y_1$	-0.052	+0.030	+0.003	-1.23
r	+0.708	+0.700	+0.920	+0.826
Results				
y	0.539	0.147	0.596	+1.885
y (Malter corrected)*	0.528	0.153	0.597	+1.859
y (Hetenyi)	0.517	0.114	0.53	+1.89

*A numerical error in Malter's analysis has been corrected producing these results.

TABLE II - Example 2, Foundation Pressures (lb/ft)

	Point A	B	C	D
Popov	2.7	4.5	5.9	6.5
Malter (3 cycles)	2.5	4.4	5.9	6.7
Ryker (2 cycles)	2.5	4.4	5.9	6.63
r	.797	.842	.859	.666

convergence factor of 0.710 results were obtained which were equivalent to Malter's three cycles.

In Malter's third example convergence was less rapid because of the extreme flexibility of the beam. An original shape was assumed which seemed consistent with the applied loading and this was balanced producing the original shape y_o. After two cycles the convergence factor was computed and a resulting shape computed. Another cycle was computed because the wide variation in the factor, and the result produced a maximum deflection of .057 inches which is comparable to the value of 0.056 shown by Malter. It is interesting to note that Malter could only obtain the solution to the problem by averaging the results; this is equivalent to using a convergence factor of 0.5 and in this case after two cycles the computed average convergence factor was 0.55.

In extending the method to very long beams,(2) a comparison was made between this numerical procedure and the exact solution for centrally loaded beams of $\lambda L = 8$. In this comparison the maximum error in deflection at the end of the beam after 2 cycles of the general procedure (equivalent to 4 cycles of actual deflection calculation) was less than 5 percent of the maximum deflection. The maximum moment was identical to the moment calculated by Hetenyi's method. Without the use of the convergent factor the successive approximation solution was rapidly divergent. The calculated value of the convergence factor was .083 indicating that an averaging technique would also be unsatisfactory.

The purpose of this discussion was to show that the use of a convergence factor(2,3, or 4) enables one to obtain convergent solutions by successive approximations for beams lengths of all practical interest. That is beams with a free length beyond the applied load or restraint of not more than $\lambda L = 4$. As shown by Hetenyi(5) there is no appreciable effect on the beam at greater distance. Longer beams can be handled by assuming free beam length of $\lambda L = 4$ for analysis and assuming the rest of the beam is unstressed and undeflected. This will generally result in errors no greater than 5 percent of the maximum values.

REFERENCES

1. "Successive Approximations for Beams on an Elastic Foundation," by E.P. Popov, Transactions, ASCE, Vol. 116, pp. 1083-1095.

2. "An Approximate Numerical Method for Analysis of Stiffened Cylinders, Conical Shells and Domes," by N.J. Ryker, Jr., submitted in partial fulfillment for a degree of Master of Science in Civil Engineering at the University of California, Berkeley, Calif., August 1951.

3. "Discussion of Successive Approximations for Beams on an Elastic Foundation," by Jacob Karol, Transactions, ASCE, Vol. 116.

4. "Approximate Methods of Analysis of Beams and Circular Plates on an Elastic Foundation," by V. A. Plumb, submitted in partial fulfillment for a degree of Master of Science in Civil Engineering at University of California, Berkeley, Calif.

5. "Beams on Elastic Foundation," by Miklos Hetenyi, The University of Michigan Press, Ann Arbor, Michigan, 1946.

DEFLECTION LIMITATIONS OF BRIDGES[a]

Progress Report of the Committee on Deflection Limitations of Bridges of the Structural Division

---

Discussion by A. Kabaila

A. KABAILA,[1].—This report is a very timely one. The engineering profession holds A.A.S.H.O. Bridge Specifications in high esteem not only in U.S.A., but also in other parts of the world. For instance, in 1953 the Conference of the State Road Authorities of Australia have adopted A.A.S.H.O. Bridge Specifications almost without modification. The Committee therefore should be congratulated in their effort to rationalize clause 3.6.10. of this Specification.

One part of clause 3.6.10., which is open to some criticism, seems to have been treated by the Committee as a matter of minor importance only:

> "When bridges have cross bracing or diaphragms sufficient in depth and strength to insure lateral distribution of loads, the deflection may be computed for the standard loading, considering all beams or girders as acting together and having equal deflection."

Usually plate girder bridges have cross bracing of the same depth as the girders. If the bracing members are of little heavier size than the minimum specified, then almost all moderate width bridges, except those of rather short spans, do fall under the category of "bridges with sufficiently rigid and strong cross bracing." When high strength steel is used and the girder depth is somewhat restricted, stiffness considerations are often the critical design factor. However, the deflection of all girders is not anywhere nearly the same, provided that the live load is placed towards one side of the bridge. A numerical example below demonstrates this aspect:

Figure 1-1 symbolically shows a general arrangement of a bridge, Figure 1-2 -a typical cross section. All girders are identical. The permissible live load deflection at point "C" is 41 x 12 / 300 = 1.64 ins. Live load deflection computed on the assumption that all girders deflect equally is equal to 1.15 ins. (see step 2. below).

If the deformations compatible with the restraint conditions and statics are considered, then the computed live load deflection is 1.72 ins. (see step 4. below). In the latter case the following assumptions are made:

1. Cross frame at "C" is rigid. In this example, this approximation has an effect on maximum deflection of approx. 3%.

---

a. Proc. Paper 1633, May, 1958.

1. Lecturer in Civ. Eng., Royal Melbourne Technical College, Victoria, Australia.

2. Ignore other cross frames. Because of the first assumption this is of no consequence on the deflections at point "C."

3. Torsional rigidity of the deck and the girders is neglected. The torsional effect is negligible in this case.

Following are the steps of the computation:

1. Consider an imaginary vertical restraint (a fictitious "jack") at point "C." (Figure 2-1). The reaction of the "jack for one lane load, including the impact of 17.5%, is 95.7 kips.

2. Figure 2-2 shows the computed stiffness of one girder: a load of 41.6 k. at point "C" produces a deflection of 1. ins. Since the bridge can accommodate 2 lanes of loading only, it follows immediately that, if in accordance with 3.6.10 equal deflection for all girders is assumed, the deflection is equal to: 95.7 x 2 / 41.6 x 4 = 1.15 ins.

3. When the "jacks" are removed, the effect is equal to applying a force of 95.7 k. per lane at point "C." Cross frame at "C" deflects downwards and simultaneously rotates into the position shown in figure 2-3. It follows from the geometrical considerations that the deflections of the girders from left to right are: $z + 3y$; $z + y$; $z - y$; and $z - 3y$ (ins.) respectively, where z and y are constants to be determined from the considerations of equilibrium.

4. Reactions in kip units on the cross frame from the girders are equal to the corresponding deflections in inches multiplied by 41.6. Hence, the condition that the sum of vertical forces is equal to zero, gives:
$4z \times 41.6 = 191.4$ k. Therefore $z = 1.15$ ins.
Sum of moments about the centre line gives:
$2 (12.75 \times 3y + 4.25y) \times 41.6 = 191.4 \times 3.5$ ft.k.; Hence $y = 0.19$ ins.
It follows that the maximum deflection of the outer girder is equal to:

$$z + 3y = 1.15 + 3 \times 0.19 = 1.72 \text{ ins.}$$

and that of the inner girder:

$$z + y = 1.15 + 0.19 = 1.34 \text{ ins.}$$

The difference between this computed deflection, which is consistent with the conditions of equilibrium, and the assumption that all girders deflect equally, is approx. 50%. Little consolation can be found in the argument that the live load is not likely to be on one side of the bridge: one truck overtaking another certainly would approach the condition assumed in this computation and in most cases the truck load is as severe as the lane load.

Incidentally, the computed deflection of the internal girder, assuming that each girder acts independently and using the fractional lane loads given by the Specification, is equal to 1.96 ins.

Where the designs are carried out by the consultants on a competitive basis, the main purpose of the specification is to provide the competitors with the minimum requirements of the responsible authority. Though the limiting values of maximum deflection are rather arbitrary, the variation of 50% between the deflections computed on a rational basis and those obtained by the procedure outlined by the Specification, is most undesirable. Rather than to encourage a competitor to use more accurate rational design methods, the Specification penalizes him for doing so.

The problem of load distribution is inseparable from the problem of deflections. The live loads transmitted to the girders are, of course, proportional to the deflections. Thus we find that the portion of one lane load carried by the outside girder is equal to:

$$1.72 \times 41.6 / 95.7 = 0.748;$$ or 1.50 of a wheel load.

And on the inner girder:

$$1.34 \times 41.6 / 95.7 = 0.583;$$ or 1.17 or a wheel load.

The fraction of the wheel load on each stringer in accordance with A.A.S.H.O. Specification is:

Outside girder: sixth edition of the Specification 1.00
seventh edition of the Specification 1.39
Inner girder: both editions of the Specification 1.70

In the latter case the live load on the inner girder is overestimated by approximately 45%. Undoubtedly, many bridge designing engineers are aware of the above conclusions and, in accordance with the general note of Division III*, they use fractional loads obtained in a similar manner to this numerical example.

A more definite statement by the Specification of the acceptable approach to this problem, however, would be desirable. When the flexibility of the cross bracing or the diaphragms is comparable to that of the stringers (either because of greater width of more flexible cross members), the problem of load distribution is more involved and the difference between the values given by the Specification and those computed by a more rigorous analysis may not be as great. However, satisfactory methods of analysis are readily available.[2,4] To simplify the designer's task, the specification could include design charts and an outline of the recommended solution. In the search for practicable, yet more rational design methods, the preparation of such charts can hardly be considered as an obstacle. Surely, there are many engineers who would consider it a privilege, if a responsible authority invited them to undertake such an investigation.

REFERENCES

1. "Huette, des Ingenieurs Taschenbuch III," Berlin, Verlag von Wilhelm Ernst & Sohn. 1956.
2. "The Analysis of Grid Frameworks of Negligible Torsional Stiffness by Means of Basic Functions" -L. G. Jaeger, Proceedings of the Institution of Civil Engineers, (London), April, 1957, Volume 6.
3. "Lateral Load Distribution Test on I-Bridge," A. White and B. Purnell. Proc. Paper No. 1255, Journal of the Structural Division, Proceedings of the American Society of Civil Engineers, Vol. 83, No ST. 3., May, 1957.

*This note reads: "In any case where the specifications provide for an empirical formula as a design convenience, a rational analysis based on a theory accepted by the Bridge Committee of the American Association of State Highway Officials, with stresses in accordance with the specifications will be considered as compliance with the specification."

4. "Die Vereinfachte Tragerrostberechnung" F. Leonhardt, und W. Andre. Julius Hoffman Press, Stuttgart, 1950.

5. "Distribution of Loads on Bridge Decks," Proc. Paper 1303, Journal of the Structural Division, Proc. A.S.C.E., Vol. 83, No. ST. 4, July, 1957.

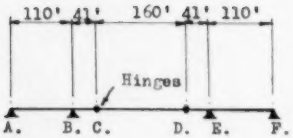

FIGURE 1-1

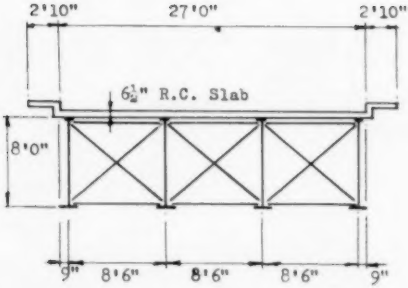

FIGURE 1-2

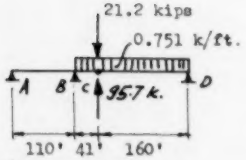

FIGURE 2-1

FIGURE 2-2

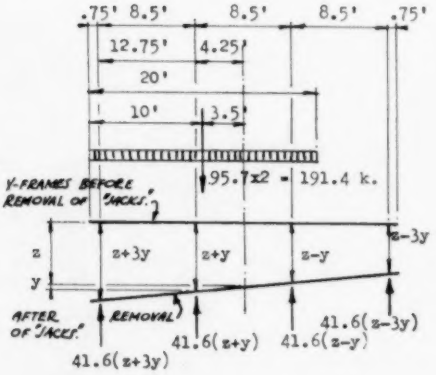

FIGURE 2-3

PROCEEDINGS PAPERS

The technical papers published in the past year are identified by number below. Technical-division sponsorship is indicated by an abbreviation at the end of each Paper Number, the symbols referring to: Air Transport (AT), City Planning (CP), Construction (CO), Engineering Mechanics (EM), Highway (HW), Hydraulics (HY), Irrigation and Drainage (IR), Pipeline (PL), Power (PO), Sanitary Engineering (SA), Soil Mechanics and Foundations (SM), Structural (ST), Surveying and Mapping (SU), and Waterways and Harbors (WW), divisions. Papers sponsored by the Board of Direction are identified by the symbols (BD). For titles and order coupons, refer to the appropriate issue of "Civil Engineering." Beginning with Volume 82 (January 1956) papers were published in Journals of the various Technical Divisions. To locate papers in the Journals, the symbols after the paper numbers are followed by a numeral designating the issue of a particular Journal in which the paper appeared. For example, Paper 1449 is identified as 1449 (HY 6) which indicates that the paper is contained in the sixth issue of the Journal of the Hydraulics Division during 1957.

VOLUME 83 (1957)

OCTOBER: 1387(CP2), 1388(CP2), 1389(EM4), 1390(EM4),1391(HY5), 1392(HY5), 1393(HY5), 1394(HY5), 1395 (HY5), 1396(PO5), 1397(PO5), 1398(PO5), 1399(EM4), 1400(SA5), 1401(HY5), 1402(HY5), 1403(HY5), 1404 (HY5), 1405(HY5), 1406(HY5), 1407(SA5), 1408(SA5), 1409(SA5), 1410(SA5), 1411(SA5), 1412(EM4), 1413 (EM4), 1414(PO5), 1415(EM4)[c], 1416(PO6)[c], 1417(HY5)[c], 1418(EM4), 1419(PO5), 1420(PO5), 1421(PO5), 1422(SA5)[c], 1423(SA5), 1424(EM4), 1425(CP2).

NOVEMBER: 1426(SM4), 1427(SM4), 1428(SM4), 1429(SM4), 1430(SM4)[c], 1431(ST6), 1432(ST6), 1433(ST6), 1434(ST6), 1435(ST6), 1436(ST6), 1437(ST6), 1438(SM4), 1439(SM4), 1440(ST6), 1441(ST6), 1442(ST6)[c], 1443(SU2), 1444(SU2), 1445(SU2), 1446(SU2), 1447(SU2), 1448(SU2)[c].

DECEMBER: 1449(HY6), 1450(HY6), 1451(HY6), 1452(HY6), 1453(HY6), 1454(HY6), 1455(HY6), 1456(HY6)[c], 1457(PO6), 1458(PO6), 1459(PO6), 1460(PO6)[c], 1461(SA6), 1462(SA6), 1463(SA6), 1464(SA6), 1465(SA6), 1466(SA6)[c], 1467(AT2), 1468(AT2), 1469(AT2), 1470(AT2), 1471(AT2), 1472(AT2), 1473(AT2), 1474(AT2), 1475(AT2), 1476(AT2), 1477(AT2), 1478(AT2), 1479(AT2), 1480(AT2), 1481(AT2), 1482(AT2), 1483(AT2), 1484(AT2), 1485(AT2)[c], 1486(BD2), 1487(BD2), 1488(PO6), 1489(PO6), 1490(BD2), 1491(BD2), 1492(HY6), 1493(BD2).

VOLUME 84 (1958)

JANUARY: 1494(EM1), 1495(EM1), 1496(EM1), 1497(IR1), 1498(IR1), 1499(IR1), 1500(IR1), 1501(IR1), 1502 (IR1), 1503(IR1), 1504(IR1), 1505(IR1), 1506(IR1), 1507(IR1), 1508(ST1), 1509(ST1), 1510(ST1), 1511(ST1), 1512(ST1), 1513(WW1), 1514(WW1), 1515(WW1), 1516(WW1), 1517(WW1), 1518(WW1), 1519(ST1), 1520 (EM1)[c], 1521(IR1)[c], 1522(ST1)[c], 1523(WW1)[c], 1524(HW1), 1525(HW1), 1526(HW1)[c], 1527(HW1).

FEBRUARY: 1528(HY1), 1529(PO1), 1530(HY1), 1531(HY1), 1532(HY1), 1533(SA1), 1534(SA1), 1535(SM1), 1536(SM1), 1537(SM1), 1538(PO1)[c], 1539(SA1), 1540(SA1), 1541(SA1), 1542(SA1), 1543(SA1), 1544(SM1), 1545(SM1), 1546(SM1), 1547(SM1), 1548(SM1), 1549(SM1), 1550(SM1), 1551(SM1), 1552(SM1), 1553(PO1), 1554(PO1), 1555(PO1), 1556(PO1), 1557(SA1)[c], 1558(HY1)[c], 1559(SM1)[c].

MARCH: 1560(ST2), 1561(ST2), 1562(ST2), 1563(ST2), 1564(ST2), 1565(ST2), 1566(ST2), 1567(ST2), 1568 (WW2), 1569(WW2), 1570(WW2), 1571(WW2), 1572(WW2), 1573(WW2), 1574(PL1), 1575(PL1), 1576(ST2)[c], 1577(PL1), 1578(PL1)[c], 1579(WW2)[c].

APRIL: 1580(EM2), 1581(EM2), 1582(HY2), 1583(HY2), 1584(HY2), 1585(HY2), 1586(HY2), 1587(HY2), 1588 (HY2), 1589(IR2), 1590(IR2), 1591(IR2), 1592(SA2), 1593(SU1), 1594(SU1), 1595(SU1), 1596(EM2), 1597(PO2), 1598(PO2), 1599(PO2), 1600(PO2), 1601(PO2), 1602(PO2), 1603(HY2), 1604(EM2), 1605(SU1)[c],1606(SA2), 1607(SA2), 1608(SA2), 1609(SA2), 1610(SA2), 1611(SA2), 1612(SA2), 1613(SA2), 1614(SA2)[c], 1615(IR2)[c], 1616 (HY2)[c], 1617(SU1), 1618(PO2)[c], 1619(EM2)[c], 1620(CP1).

MAY: 1621(HW2), 1622(HW2), 1623(HW2), 1624(HW2), 1625(HW2), 1626(HW2), 1627(HW2), 1628(HW2), 1629 (ST3), 1630(ST3), 1631(ST3), 1632(ST3), 1633(ST3), 1634(ST3), 1635(ST3), 1636(ST3), 1637(ST3), 1638(ST3), 1639(WW3), 1640(WW3), 1641(WW3), 1642(WW3), 1643(WW3), 1644(WW3), 1645(SM2), 1646(SM2), 1647 (SM2), 1648(SM2), 1649(SM2), 1650(SM2), 1651(HW2), 1652(HW2)[c], 1653(WW3)[c], 1654(SM2), 1655(SM2), 1656(ST3)[c], 1657(SM2)[c].

JUNE: 1658(AT1), 1659(AT1), 1660(HY3), 1661(HY3), 1662(HY3), 1663(HY3), 1664(HY3), 1665(SA3), 1666 (PL2), 1667(PL2), 1668(PL2), 1669(AT1), 1670(PO3), 1671(PO3), 1672(PO3), 1673(PL2), 1674(PL2), 1675 (PO3), 1676(PO3), 1677(SA3), 1678(SA3), 1679(SA3), 1680(SA3), 1681(SA3), 1682(SA3), 1683(PO3), 1684 (HY3), 1685(SA3), 1686(SA3), 1687(PO3), 1688(SA3)[c], 1689(PO3)[c], 1690(HY3)[c], 1691(PL2)[c].

JULY: 1692(EM3), 1693(EM3), 1694(ST4), 1695(ST4), 1696(ST4), 1697(SU2), 1698(SU2), 1699(SU2), 1700(SU2), 1701(SA4), 1702(SA4), 1703(SA4), 1704(SA4), 1705(SA4), 1706(EM3), 1707(ST4), 1708(ST4), 1709(ST4), 1710 (ST4), 1711(ST4), 1712(ST4), 1713(SU2), 1714(SA4), 1715(SA4), 1716(SU2), 1717(SA4), 1718(EM3), 1719 (EM3), 1720(SU2), 1721(ST4)[c], 1722(ST4), 1723(ST4), 1724(EM3)[c].

AUGUST: 1725(HY4), 1726(HY4), 1727(SM3), 1728(SM3), 1729(SM3), 1730(SM3), 1731(SM3), 1732(SM3), 1733 (PO4), 1734(PO4), 1735(PO4), 1736(PO4), 1737(PO4), 1738(PO4), 1739(PO4), 1740(PO4), 1741(PO4), 1742 (PO4), 1743(PO4), 1744(PO4), 1745(PO4), 1746(PO4), 1747(PO4), 1748(PO4), 1749(PO4).

SEPTEMBER: 1750(IR3), 1751(IR3), 1752(IR3), 1753(IR3), 1754(IR3), 1755(ST5), 1756(ST5), 1757(ST5), 1758(ST5), 1759(ST5), 1760(ST5), 1761(ST5), 1762(ST5), 1763(ST5), 1764(ST5), 1765(WW4), 1766(WW4), 1767(WW4), 1768(WW4), 1769(WW4), 1770(WW4), 1771(WW4), 1772(WW4), 1773(WW4), 1774(IR3), 1775 (IR3), 1776(SA5), 1777(SA5), 1778(SA5), 1779(SA5), 1780(SA5), 1781(WW4), 1782(SA5), 1783(SA5), 1784 (IR3)[c], 1785(WW4)[c], 1786(SA5)[c], 1787(ST5)[c], 1788(IR3), 1789(WW4).

OCTOBER: 1790(EM4), 1791(EM4), 1792(EM4), 1793(EM4), 1794(EM4), 1795(HW3), 1796(HW3), 1797(HW3), 1798(HW3), 1799(HW3), 1800(HW3), 1801(HW3), 1802(HW3), 1803(HW3), 1804(HW3), 1805(HW3), 1806 (HY5), 1807(HY5), 1808(HY5), 1809(HY5), 1810(HY5), 1811(HY5), 1812(SM4), 1813(SM4), 1814(ST6), 1815 (ST6), 1816(ST6), 1817(ST6), 1818(ST6), 1819(ST6), 1820(ST6), 1821(ST6), 1822(EM4), 1823(PO5), 1824 (SM4), 1825(SM4), 1826(SM4), 1827(ST6)[c], 1828(SM4)[c], 1829(HW3)[c], 1830(PO5)[c], 1831(EM4)[c], 1832(HY5)[c]

c. Discussion of several papers, grouped by divisions.

AMERICAN SOCIETY OF CIVIL ENGINEERS

OFFICERS FOR 1958

PRESIDENT

LOUIS R. HOWSON

VICE-PRESIDENTS

Term expires October, 1958:
FRANCIS S. FRIEL
NORMAN R. MOORE

Term expires October, 1959:
WALDO G. BOWMAN
SAMUEL B. MORRIS

DIRECTORS

Term expires October, 1958:
JOHN P. RILEY
CAREY H. BROWN
MASON C. PRICHARD
ROBERT H. SHERLOCK
R. ROBINSON ROWE
LOUIS E. RYDELL
CLARENCE L. ECKEL

Term expires October, 1959:
CLINTON D. HANOVER, Jr.
E. LELAND DURKEE
HOWARD F. PECKWORTH
FINLEY B. LAVERTY
WILLIAM J. HEDLEY
RANDLE B. ALEXANDER

Term expires October, 1960:
PHILIP C. RUTLEDGE
WESTON S. EVANS
TILTON E. SHELBURNE
CRAIG P. HAZELET
DONALD H. MATTERN
JOHN E. RINNE

PAST PRESIDENTS

Members of the Board

ENOCH R. NEEDLES

MASON G. LOCKWOOD

EXECUTIVE SECRETARY

WILLIAM H. WISELY

TREASURER

CHARLES E. TROUT

ASSISTANT SECRETARY

E. LAWRENCE CHANDLER

ASSISTANT TREASURER

CARLTON S. PROCTOR

PROCEEDINGS OF THE SOCIETY

HAROLD T. LARSEN
Manager of Technical Publications

PAUL A. PARISI
Editor of Technical Publications

MARVIN SCHECHTER
Assistant Editor of Technical Publications

COMMITTEE ON PUBLICATIONS

HOWARD F. PECKWORTH, *Chairman*

PHILIP C. RUTLEDGE, *Vice-Chairman*

E. LELAND DURKEE
TILTON E. SHELBURNE
R. ROBINSON ROWE
LOUIS E. RYDELL